Neurometabolic Implications of Coenzyme Q_{10} Deficiency: Pathogenesis, Detection and Treatment

Submitted By:

Kate Duberley

Department of Molecular Neuroscience

UCL Institute of Neurology

Queen Square, London

Submitted July 2013

Funded by Ataxia UK

Thesis submitted for the degree of Doctor of Philosophy, University College London (UCL)

I, Kate Duberley confirm that the work presented in this thesis is my own. Where information has been derived from other sources, I confirm that this has been indicated in the thesis.

Signed……Date…….

Abstract

Disorders of Coenzyme Q_{10} (CoQ_{10}) biosynthesis represent the most treatable subgroup of mitochondrial diseases. Neurological involvement is frequently observed in CoQ_{10} deficiency, typically presenting as cerebellar ataxia and/or seizures. The aetiology of the neurological presentation of CoQ_{10} deficiency has yet to be fully elucidated and therefore in order to investigate these phenomena we have established a neuronal cell model of CoQ_{10} deficiency by treatment of the neuronal SH-SY5Y cell line with Para-AminoBenzoic Acid (PABA). This neuronal cell model provides insights into the effects of CoQ_{10} deficiency on neuronal mitochondrial function and oxidative stress. A marginal decrease in CoQ_{10} status (76% residual CoQ_{10}) appears to be sufficient to impair Electron Transport Chain (ETC) function and increase mitochondrial oxidative stress, highlighting the vulnerability of neurons to a small deficit in CoQ_{10} status. In contrast to CoQ_{10} deficient fibroblasts, a CoQ_{10} deficiency (46% residual CoQ_{10}) in neuronal cells appears to result in reversal of Complex V activity. This phenomenon has not been reported in previous studies of CoQ_{10} deficiency and may be a unique characteristic of neuronal cells.

This neuronal cell model was subsequently utilised in the evaluation of candidate therapies for neurological conditions associated with CoQ_{10} deficiency. The efficacy of CoQ_{10} supplementation and methylene blue (MB) treatment were evaluated. CoQ_{10} supplementation proved effective at preventing mitochondrial oxidative stress and partially restoring neuronal mitochondrial function. However ETC complex activities were still compromised, suggesting an explanation for the refractory nature of neurological CoQ_{10} deficiency to treatment.

Muscle is considered the “gold standard” for CoQ_{10} quantification; however neurological CoQ_{10} deficiency does not always present with a significant decrease in muscle CoQ_{10} status, despite a genetic diagnosis of CoQ_{10} deficiency. Cerebrospinal Fluid (CSF) CoQ_{10} quantification offers a more direct measurement of cerebellar CoQ_{10} levels. A tandem mass spectrometry (MS/MS) method capable of quantifying nanomolar (nM) levels of CoQ_{10} was therefore developed.

In conclusion this PhD thesis has been successful in expanding our understanding of the pathophysiology of neuronal CoQ_{10} deficiency and subsequently suggesting why neurological CoQ_{10} deficiency might be refractory to CoQ_{10} treatment. This thesis has also led to the development of a new technique for quantification of CSF CoQ_{10} concentration, opening up many possibilities for future studies and applications. This project is funded by Ataxia UK (www.ataxiauk.org.uk).

Table of Contents

Table of Figures

List of Tables

List of Abbreviations

Acetyl-CoA ..... Acetyl-Coenzyme A
AD ..... Alzheimer's disease
ADCK3 ..... aarF domain containing kinase 3
ADP ..... Adenosine diphosphate
AMR ..... ATP monitoring reagent
ANOVA ..... Analysis of Variance
APTX ..... Aprataxin
ALS ..... Amyotrophic lateral sclerosis
AOA-1 ..... Ataxia-oculomotor-apraxia 1
ATP ..... Adensine triphosphate
BODIPY 581/591 ..... 4,4-difluoro-3a,4a-diaza-s-indacene 581/591
BN-PAGE ..... Blue Native-polyacrylamide gel electrophoresis
BSA ..... Bovine serum albumin
Coq ..... Coenzyme Q biosynthetic enzyme (non-human)
COQ ..... Coenzyme Q biosynthetic enzyme (human)
CoQ ..... Coenzyme Q (ubiquinone)
CoQH ..... Semi-reduced CoQ (ubisemiquinone)
$CoQH_2$ ..... Reduced CoQ (ubiquinol)
CS ..... Citrate synthase
CSF ..... Cerebrospinal fluid
CV ..... Coefficient of Variation
DHE ..... Dihydroethidium
DHO ..... Dihydroorotate
DHODH ..... Dihydroorotate Dehydrogenase
DMEM ..... Dulbecco's modified Eagle's medium
DMSO ..... Dimethyl sulfoxide
DNA ..... Deoxyribonucleic acid
dsDNA ..... Double stranded DNA
DTNB ..... 5, 5'-dithio-bis (2-nitrobenzoic acid)
EC ..... Eletrochemical
ER ..... Endoplasmic reticulum
ETC ..... Electron transport chain

ETF ..... Electron-transferring-flavoprotein

ETFDH ..... Electron-transferring-flavoprotein dehydrogenase

ETF-QO ..... Electron-transferring-flavoprotein quinone oxidase

FA ..... Friedreich's Ataxia

FAD ..... Flavin adenosine dinucleotide

$FADH_2$ ..... Flavin adenosine dinucleotide (reduced)

FBS ..... Fetal Bovine Serum

FCCP ..... trifluoromethoxy)phenylhydrazone

FPP ..... Farnesyl pyrophosphate

GPP ..... Geranyl pyrophosphate

GTP ..... Guanosine triphosphate

GSH ..... Glutathione (reduced)

GSSG ..... Glutathione (oxidized dimeric form)

4-HB 4-hydroxybenzoate

HBSS ..... Hank's balanced salt solution

HEPES ..... 4-(2-hydroxyethyl)-1-piperazineethanesulfonic acid

HMG-CoA ..... 3-hydroxy-3-methylglutaryl-coenzyme A

HPLC ..... High performance liquid chromatography

HD ..... Huntington Disease

ICARS ..... International Cooperative Ataxia Rating Scale

IPP ..... Isopentenyl pyrophosphate

iPS ..... Induced Pluripotency Stem

IS ..... Internal standard

k ..... Rate order constant

KCN ..... Potassium cyanide

LC-MS/MS ..... Tandem (liquid chromatography) mass spectrometry

LDL ..... Low Density Lipoprotein

LOD ..... Limit of Detection

LOQ ..... Limit of Quantification

MCAD ..... Medium-chain acyl-CoA dehydrogenase

MDH ..... Malate dehydrogenase

MtDNA ..... Mitochondrial Deoxyribonucleic acid

MMA ..... Methyl Malonic Acidaemia

MS ..... Mass Spectrometry

MVA ..... Mevalonic aciduria

NAD+ ..... Nicotinomide adenine dinucleotide (oxidised)
NADH..... Nicotinomide adenine dinucleotide (reduced)
NADPH ..... Nicotinomide adenine dinucleotide phosphate (reduced)
NMR..... Nucleotide Monitoring Reagent
NO ..... Nitric Oxide
NOX ..... Nicotinomide adenine dinucleotide oxidase
NRR ..... Nucleotide Releasing Reagent
OA..... Orotic acid
OAA ..... Oxaloacetic acid
OCR ..... oxygen consumption rate
PABA ..... Para-aminobenzoic acid
PD..... Parkinson's Disease
PDSS1/2 ..... Prenyl (decaprenyl) diphosphate synthase, subunit 1
PKU ..... Phenylketonuria
PTP..... Permeability transition pore
RNA ..... Ribonucleic acid
ROS ..... Reactive oxygen species
SAM ..... S-adenosyl-methionine
SD..... Standard Deviation
SEDDS ..... Self-emulsifying drug delivery system
SEM ..... Standard error of the mean
SRM..... Selection reaction monitoring
tRNA ..... Transfer ribonucleic acid
TMRM ..... Tetramethylrhodamine methyl ester
TPT ..... Trans-prenyl-transferase
UCP ..... Uncoupling proteins
UPDRS ..... Universal Parkinson's Disease Rating Scale
UV..... Ultraviolet
Vitamin B2 ..... Riboflavin
Vitamin E ..... γ-tocopherol
Vitamin C ..... Ascobate
Δp ..... Protonmotive force
$\Delta\Psi_m$..... Mitochondrial membrane potential

Acknowledgements

This thesis is dedicated to everyone that has contributed to my development as a scientist and as a person. First and foremost I would like to thank my parents (Paul and Dawn Duberley) for their invaluable support and wisdom. They taught me that if you work hard you can achieve anything you set your mind to. A perfect parenting team, with my Dad's continual encouragement and hard working values, in addition to my Mum's considerate and selfless nature; I am indebted to them. I would also like to thank my sister for always being there when I need her and my grandparents for their support, be it cutting out "interesting" articles from the Daily Mail or showing genuine concern for my "cells".

I am also forever thankful to my PhD supervisors; Iain Hargreaves, Shamima Rahman and Simon Heales, for sharing their diversity and wealth of knowledge with me, for their support and their kindness; as Shamima put it they are "my PhD family". Shamima truly is an inspirational woman. She has taught me a great deal about mitochondrial genetics and has been a driving force behind my PhD. I would especially like to thank her for helping me prepare publications and my thesis, her keen attention to detail and writing finesse is phenomenal. I would also like to thank Prof. Simon Heales. His passion for biochemistry has been infectious. Iain has been a fantastic supervisor and friend over the past 4 years. I thank him for introducing me to the intricacies of CoQ_{10} biochemistry, for which I have been told he is "famous" (Euromit 2011). I also thank him for encouraging me and helping me overcome the challenges that I faced in my PhD, and life. I will remember his patience, kindness and fascinating inquisitive mind.

I would also like to thank all of the people that contributed to this work in some way, large or small. To the Neurometabolic unit (NMU) most importantly; John Land, Anu Chalasani, Viruna Neergheen, Simon Pope and Marcus Oppenheim for always being helpful and friendly. I will miss the NMUs interesting conversation and eccentricity. I would also like to thank Simon Eaton and Kevin Mills for sharing their expertise in mass spectrometry (MS), especially to Simon Eaton for his patience during the MS method development and publication. I

would also like to thank the ICH students/staff for being so welcoming and helpful on my collaborative visits.

Additionally, I would like to thank all of my amazing friends, new and old for putting up with my constant moaning about “cells”. Primarily Lucianne Dobson, Philip Smethurst, Helen Crehan and Sarah Morgan, for supplying me with tea, chocolate and wine, also my “roomies” Pippa Smith and Stephanie Dare for always lending an ear. My friends and family often found it hard to understand that sometimes my “cells” need to come before shopping.

Finally, I would like to thank Ataxia UK for funding this research project. Ataxia UK is a fantastic little charity that has a big research vision; to aim for a cure by 2020. I have had the opportunity to get to know a number of the staff at Ataxia UK over the course of my PhD. They are an amazing team with a real passion for Ataxia research and advocacy.

Chapter 1

Introduction

1.1. Coenzyme Q_{10} Structure

Coenzyme Qs (CoQs), also known as ubiquinones are a group of homologous quinones that are widely distributed in animals, plants and microorganisms. CoQ was first characterised by Morton and associates in Liverpool in 1955 (Festenstein et al. 1955). It was initially described as the “275 mμ substance”, due to the sizable absorbance at 275 nm. Wolf et al then determined the complex structure of CoQ via NMR in 1958 (Wolf et al. 1958; Figure 1.1). As the new compound was a quinone and due to its ubiquitous nature the official name was established as ubiquinone (Braunstein et al. 1975). CoQ is known chemically as 2,3-dimethoxy, 5-methyl, 6-polyisoprene parabenzoquinone. The polyisoprenoid chain can vary in length between 6 and 10 isoprene units between different species. In humans the main species of ubiquinone is CoQ_{10}, with small amounts of CoQ_9 (2-7%; Turunen et al. 2004). The distribution of CoQ_{10} is variable between tissue types, ranging from 8μg/g in lung to 114μg/g in heart (Turunen et al. 2004; Table 1.1). Such extensive variation is likely to reflect differences in tissue energy requirements. Variation in CoQ_{10} content is also observed in the brain (Table 1.2). Forebrain regions, particularly the striatum have high CoQ_{10} content. The cerebellum also has a relatively high level of CoQ_{10}. The white matter has the lowest CoQ_{10} content. It is hypothesised that the distribution of CoQ_{10} in the brain may reflect the variation in energy requirements.

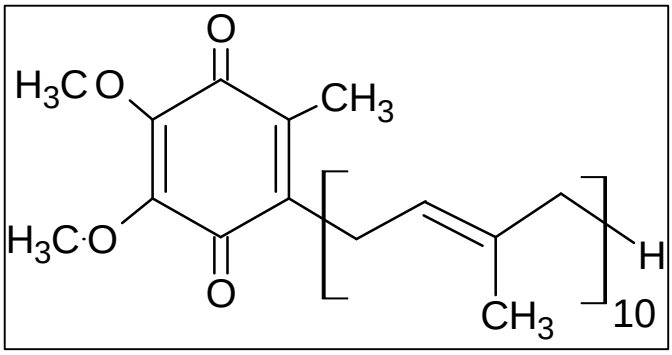

Figure 1.1 The Chemical Structure of Coenzyme Q_{10} (CoQ_{10})

The oxidised structure of CoQ_{10}; consisting of an isopreniod tail attached to a benzene ring. The isopreniod tail is species specific and can vary from 6-10 isopreniod units. The most common form in humans is the 10 isoprenoid form CoQ_{10}.

Tissue	Human CoQ_{10} content (µg/g tissue)
Heart	114
Kidney	67
Liver	55
Muscle	40
Brain	13
Pancreas	33
Spleen	25
Lung	8
Thyroid	25
Testis	11
Intestine	12
Colon	11
Ventricle	12

Table 1.1 CoQ_{10} Content in Human Tissues

Brain Region	Human CoQ_{10} content (µg/g tissue)
Striatum	25
Cerebellum	16
Parietal cortex	15
Temporal cortex	10
Hippocampus	6
Medulla oblongata	5
White matter	3

Table 1.2 CoQ_{10} Content in Brain Regions of Humans

Data for both tables taken from Turunen et al. 2004*. CoQ_{10} was quantified in tissue using a HPLC method with UV detection. The data in this paper was taken from* Aberg et al. 1992 and Runquist et al. 1995*.*

1.2. Coenzyme Q_{10} Function

1.2.1. The Mitochondrial Electron Transport Chain (ETC)

The main function of CoQ_{10} is in the mitochondrial electron transport chain (ETC). First proposed by Crane and colleagues in 1957, interest grew throughout the 1960's where this proposed role of CoQ_{10} was further elucidated (Ernster et al. 1969). Dr Peter Mitchell revolutionised the field by introducing the concept of oxidative phosphorylation, where the presence of a proton gradient across the mitochondrial inner membrane leads to the production of ATP (Mitchell 1961; Mitchell 1966). Mitchell later described this phenomenon as the protonmotive Q cycle (Mitchell 1975). In humans CoQ_{10} is well recognised as a fundamental component of the mitochondrial ETC where it acts as an electron carrier. CoQ_{10} accepts electrons derived from Complex I (NADH ubiquinone oxidoreductase; EC 1.6.5.3) and Complex II (succinate ubiquinone reductase; EC 1.3.5.1) and transporting them to Complex III (ubiquinol cytochrome *c* reductase; EC 1.10.2.2) (Ernster & Dallner 1995). The electrons are then transported via cytochrome *c* to their terminal electron acceptor Complex IV (cytochrome *c* oxidase; EC 1.9.3.1). The energy from the proton gradient produced by the ETC is then utilised in the production of ATP by Complex V (ATP synthase; EC 3.6.3.14).

An often forgotten esoteric component of the ETC is Electron Transfer Flavoprotein Quinone Oxidoreductase (ETF-QO; also called Electron Transfer Flavoprotein Dehydrogenase; EC 1.5.5.1). The ETF/ ETF-QO system serves as a short electron transfer pathway forming part of the mitochondrial ETC; catalysing the reduction of CoQ by ETF, linking fatty acid (and amino acid) metabolism to the ETC (Figure 1.2).

Historically, the ETC and ATP synthase were thought to be arranged in a fluid mosaic composition, whereby integral protein complexes of the mitochondrial inner membrane are randomly dispersed in the phospholipid bilayers (Green & Tzagoloff 1966). In this model electron transfer would occur via random collision (Hackenbrock et al. 1986). In 1973, the two-enzyme oxidation and reduction of CoQ was quantified in beef heart submitochondrial particles suggesting CoQ pool behaviour (Kröger & Klingenberg 1973). Thus CoQ would behave kinetically as a freely diffusing pool; shuttling electrons between Complexes I/II and Complex III.

The use of mild detergents in Blue Native Poly-Acrylamide Gel Electrophoresis (BN-PAGE) experiments allow the structural and functional integrity of the multi-complex units to be preserved (Schägger & Pfeiffer 2000). Thus numerous super-complexes or respirasomes have been described in yeast and mammalian mitochondria. Complexes I, III and IV all appear to form super-complexes with each other in varying stoichiometric ratios. 70% of Complex I is associated with super-complexes (7%: I_1III_2, 54%: $I_1III_2IV_1$, 9%: $I_1III_2IV_2$). The super-complex would allow direct transfer of electrons via the electron carriers (CoQ and cytochrome *c*) i.e. channelling (Schägger & Pfeiffer 2000). Consequently the ETC would behave a single enzyme unit, and inhibition of any of the enzymes components would result in a global influence (flux control; Kholodenko et al. 1994).

Although there is evidence of association between Complexes II and III (Tisdale 1961) this study used bile acids in enzyme preparation which may have led to protein aggregation (Schägger & Pfeiffer 2000). There is extensive evidence that Complex II exhibits pool behaviour (Kröger & Klingenberg 1973) and thus does not form part of a super-complex (Schägger & Pfeiffer 2000).

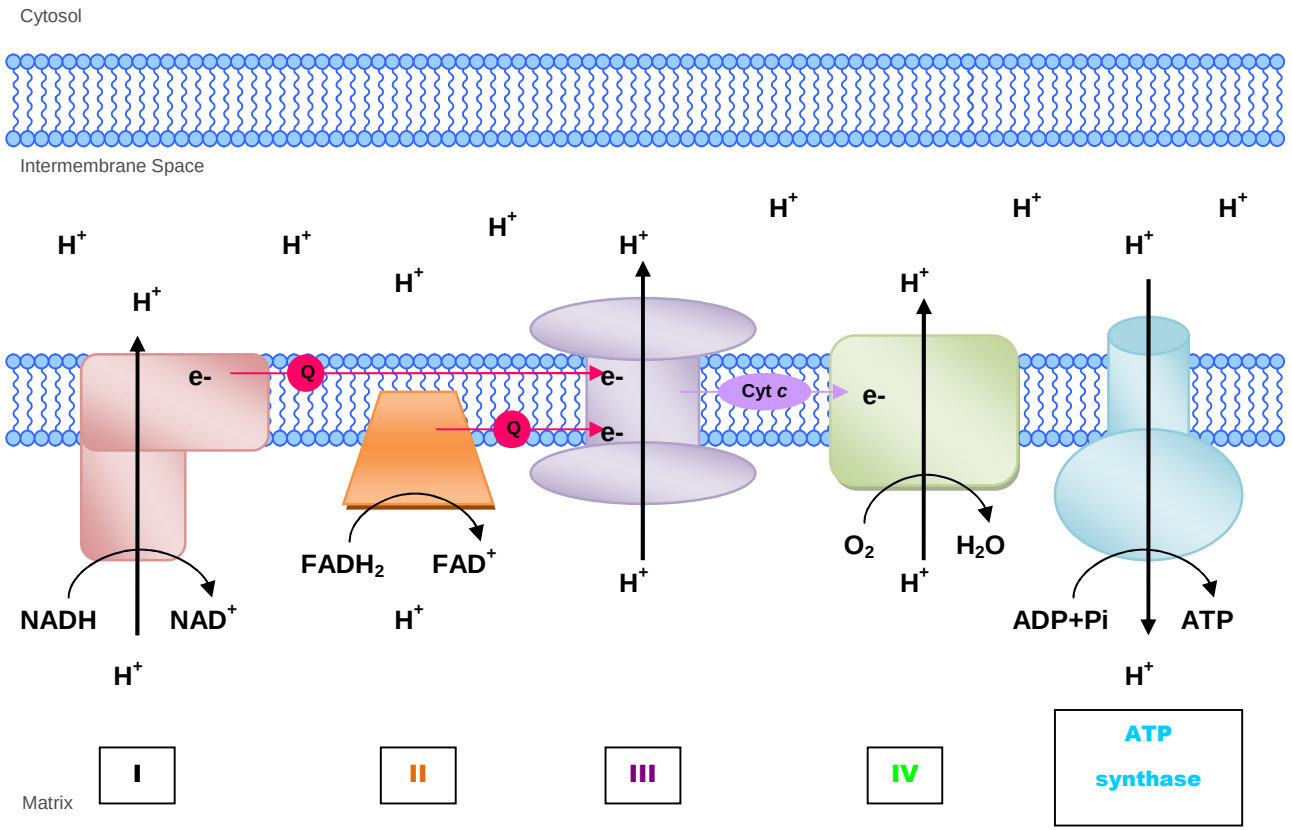

Figure 1.2 The Mitochondrial Electron Transport Chain (ETC) + Complex V (ATP Synthase)

Coenzyme Q_{10} (denoted as Q) transports electrons from Complex I and Complex II to Complex III. Cytochrome c (denoted as Cyt c) then transports electrons from Complex III to Complex IV. The proton gradient created in this process facilitates the phosphorylation of ADP to ATP by Complex V (ATP synthase)

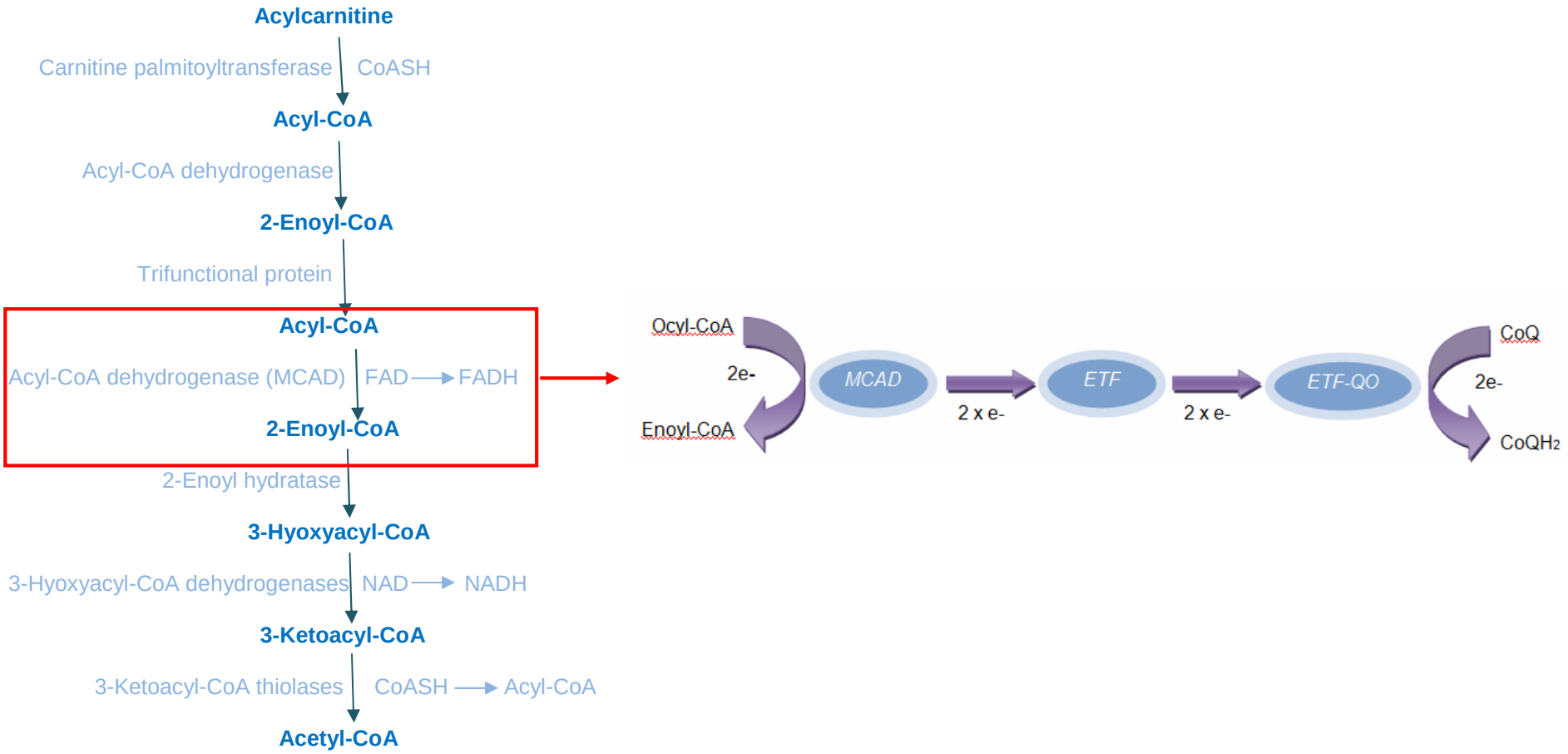

Figure 1.3 Fatty acid oxidation pathway and the ETF/ETF-QO System

Ocyl-CoA is oxidised to enoyl-CoA by medium-chain acyl-CoA dehydrogenase (MCAD). This is a step in the fatty acid oxidation pathway. MCAD (specifically the $FADH_2$) is re-oxidised by two electron-transfer flavoproteins (ETF). The semiquinone is then re-oxidised by ETF-quinone oxidase (QO) which in turn transfers electrons to ubiquinone.

1.2.1.1. Complex I

Complex I is the largest enzyme in the ETC; containing 45 subunits with a molecular mass of 980kDa. The L-shaped structure of Complex I was initially revealed by electron microscopy; further detail was subsequently provided by x-ray crystallography studies of the enzyme in the bacterium *Thermus thermophilus* and the fungus *Yarrowia lipolytica* (Fassone & Rahman 2012).

Complex I catalyses the two-electron oxidation of NADH, and the consequent reduction of CoQ, facilitating proton pumping across the inner mitochondrial membrane (reviewed in Hirst 2010). The potential energy from three sequential steps of rapid electron transfer, from a flavin mononucleotide along a series of iron-sulphur clusters, is utilised to produce a protonmotive force (Δp) enabling ATP synthesis via Complex V (Dutton et al. 1998). NADH is produced predominantly by the Krebs cycle and by the β-oxidation of fatty acids. Complex I oxidises NADH, thus replenishing the NAD+ pool in the mitochondrial matrix. The 2 electrons produced by this process are then utilised to reduce CoQ to $CoQH_2$ in the inner mitochondrial membrane. $CoQH_2$ is then re-oxidised by Complex III further adding to the Δp (Hirst 2010).

Complex I is well recognised as a major contributor to Reactive Oxygen Species (ROS) generation within the cell (Murphy 2009). Complex I ROS production was first demonstrated through the uncoupler sensitive H_2O_2 production by submitochondrial particles following CoQ reduction (Hinkle et al. 1967) and subsequently through the production of $O_2^{\bullet-}$ by isolated Complex I in the presence of NADH. $O_2^{\bullet-}$ production is increased after addition of rotenone, a Complex I non-competitive inhibitor (Cadenas et al. 1977). ROS production in this instance occurs when the NADH/NAD+ ratio is high and ATP production is low. ROS is also produced by Complex I in reverse electron transfer. This occurs when the Δp and the $CoQH_2$/CoQ ratio are high and ATP production is low (Chance & Hollunger 1961).

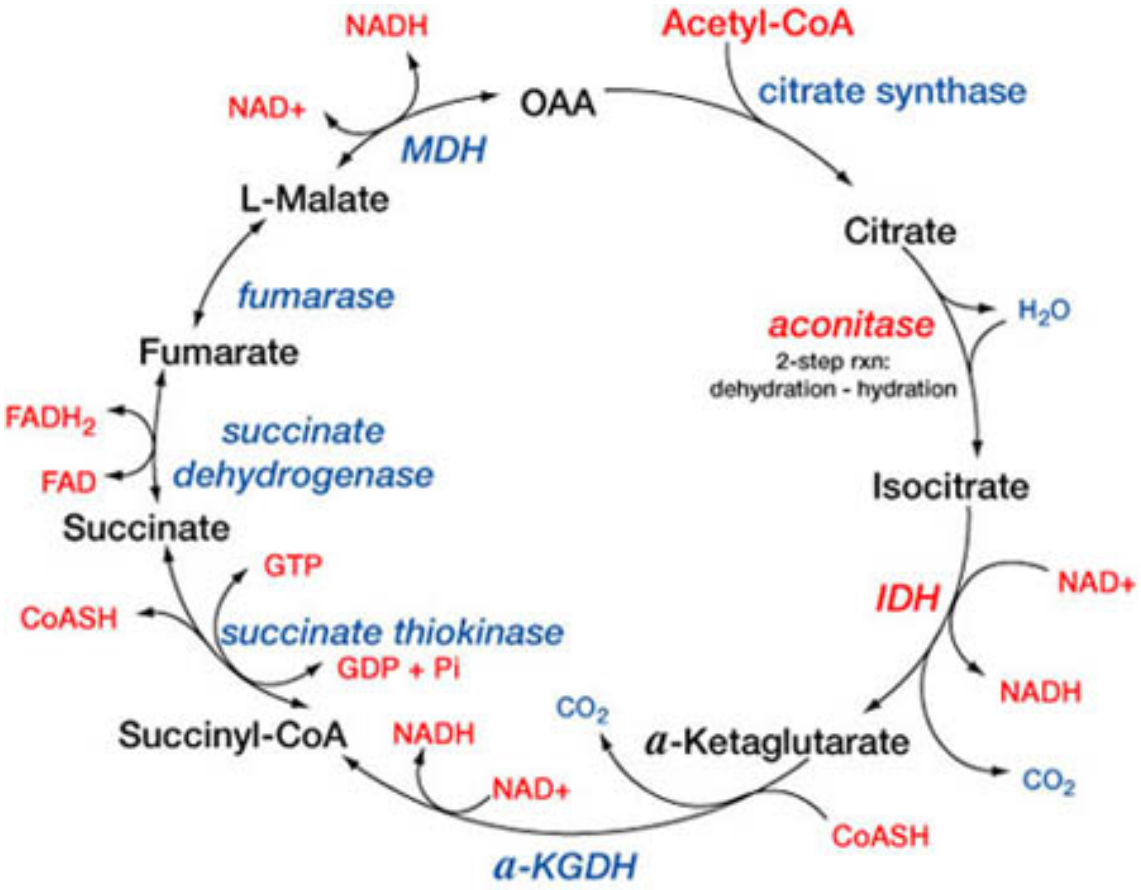

Figure 1.4 The Krebs cycle

The Krebs cycle begins with the transfer of a two-carbon acetyl group from acetyl-CoA to the oxaloacetate (OAA) to form citrate; a six-carbon compound. The citrate then goes through a series of chemical transformations, losing two carboxyl groups as CO_2. Most of the energy made available by the oxidative steps of the cycle is transferred as energy-rich electrons to NAD^+, forming NADH. For each acetyl group that enters the citric acid cycle, three molecules of NADH are produced. *The conversion of succinate to fumarate is catalysed by succinate dehydrogenase/ubiquinone reductase (Complex II) consequently reducing FAD to $FADH_2$.* At the end of each cycle OAA has been regenerated and the cycle continues.

Taken from: http://themedicalbiochemistrypage.org/tca-cycle.php

1.2.1.2. Complex II

Complex II is the only enzyme that participates in both the Krebs cycle (Figure 1.4) and the ETC. The oxidation of succinate to fumarate in the Krebs cycle is catalysed by Complex II. CoQ is subsequently reduced to $CoQH_2$ replenishing the $CoQH_2$ pool.

A flavoprotein (SDHA) and an iron-sulfur protein (SDHB) form a hydrophilic domain that projects out into the matrix and two hydrophobic transmembrane subunits (SDHC and SDHD) anchor the complex to the membrane (Ackrell 2000). The transmembrane subunits are composed of a cytochrome *b*, haem *b* group and a CoQ binding site. These subunits also contain two phospholipid molecules; cardiolipin and phosphatidylethanolamine (Ackrell 2000). The flavoprotein domain contains a FAD cofactor and a succinate binding site. Interestingly, in humans and in the majority of eukaryotes Complex II is the only complex that is completely nuclear encoded (Hirawake et al. 1999; Bourgeron et al. 1995).

During succinate oxidation the covalently bonded FAD cofactor accepts a hydride group forming $FADH_2$. Electrons from the $FADH_2$ are then transferred along the iron-sulphur clusters [2Fe-2S],[4Fe-4S] to the terminal [3Fe-4S]. An awaiting CoQ molecule is then reduced within the active site. This two electron reduction involves the intermediate production of semi-ubiquinone (Cecchini 2003). It has been suggested that the haem acts as an electron buffer to prevent ROS production (Yankovskaya et al. 2003), however further investigation is needed.

1.2.1.3. Complex III

Complex III, sometimes called the cytochrome *bc*1 complex is the third complex in the ETC. Complex III is synthesised by both the mitochondria (cytochrome *b*) and the nucleus (all other subunits). It contains 11 subunits, 3 respiratory subunits (cytochrome *b*, cytochrome c_1, Rieske protein), 2 core proteins and 6 low-molecular weight proteins (Crofts 2004). Ubiquinol cytochrome-c reductase catalyses the chemical reaction:

$$QH_2 + 2\ Fe^{3+}\text{-cytochrome c} + 2H^+_{in} \leftrightarrow Q + 2\ Fe^{2+}\text{-cytochrome c} + 4H^+_{out}$$

The above reaction is a modified version of the Q cycle, first proposed by Mitchell (1975). The Q cycle involves the release of four protons into the inter

membrane space, whilst only two protons are utilised from the matrix; resulting in a proton gradient across the membrane. The overall reaction facilitates the oxidation of two ubiquinols to ubiquinones, the reduction of a ubiquinone to a ubiquinol. Subsequently two electrons are transferred from ubiquinol to ubiquinone, via two cytochrome c intermediates (Figure 1.5)

Proton transfer is dependent on the simultaneous movement of electrons (from ubiquinol) via two routes. The [2Fe-2S] cluster of the Rieske iron sulfur protein (ISP) is the first electron acceptor. The electrons are subsequently passed via the bound cytochrome c_1 onto the mobile cytochrome c_2. The electrons then flow onto Complex IV (Crofts 2004).

The second path for the flow of electrons is via cytochrome b_L and cytochrome b_H to the Q_i-site (Crofts 2004). The Q_i-site catalyses the reduction of one CoQ to $CoQH_2$ through a two electron gate. The two electrons required are supplied by the oxidation of two ubiquinol molecules at the Q_o-site, thus releasing four H^+, delivering two electrons to each chain.

The Q_o-site of Complex III is an important site for superoxide production (Turrens et al. 1985). This is largely attributable to the production of semiubiquinone when the second electron path (described above) is blocked. Superoxide production occurs when the transfer of electrons from the intermediate semiubiquinone to cytochrome b_L becomes limited.

Under physiological conditions a low mitochondrial membrane potential and a low Δp lead to superoxide production; maximal superoxide production occurs at ~2% of normal turnover (Crofts 2004). Although Complex III superoxide production can be significantly increased by the addition of antimycin, a Complex III inhibitor, under physiological conditions production is far lower compared to Complex I superoxide production (Chance & Hollunger 1961).

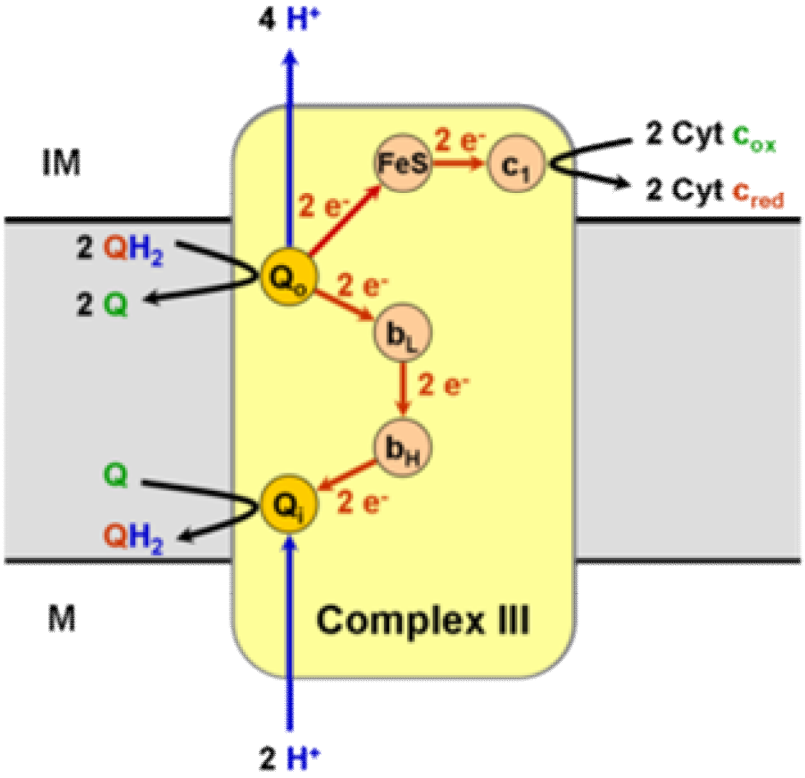

Figure 1.5 Complex III/ Q cycle

The modified Q cycle in Complex III: Ubiquinone (Q) binds the Q_i site of complex III. Ubiquinol (QH2) binds to the Q_o site of complex III and is oxidised in a two step process (Ubiqionol-semiubiquinone-ubiquinone). Ubiquinol is then oxidized (gives up one electron each) to the Rieske iron-sulfur '(FeS) protein' and to the b_L heme. This oxidation reaction produces a transient semiquinone before complete oxidation to ubiquinone, which then leaves the Q_o site of complex III. The 'FeS protein' then donates an electron to Cytochrome c_1.

Image taken from: http://en.wikipedia.org/wiki/File:Complex_III.png

1.2.1.4. Complex IV

Complex IV is the last enzyme in the mitochondrial ETC located in the mitochondrial membrane. The enzyme is composed of several metal prosthetic sites and 14 protein subunits. 11 subunits are synthesised by the nucleus and 3 originate from the mitochondria. The metal prosthetic sites include two haems, cytochrome *a* and a_3, and two copper centres (Cu_A and $Cu_{B;}$ Brzezinski and Gennis 2008).

Complex IV receives four electrons from the intermembrane space via four cytochrome *c* molecules. Protons are utilised from the mitochondrial matrix to convert one oxygen molecule to two water molecules. The haem-copper active site (cytochrome aa_3) of the enzyme is located deep within the protein, thus oxygen enters via a channel into the hydrophobic core of the membrane. The reaction displayed below illustrates the 4 electron reduction of water catalysed by cytochrome *c* oxidase (Brzezinski & Gennis 2008).

$$4\ Fe^{2+}\text{-cytochrome } c + 8\ H^{+}_{in} + O_2 \leftrightarrow 4\ Fe^{3+}\text{-cytochrome } c + 2\ H_2O + 4\ H^{+}_{out}$$

Complex IV is the only true proton pump in the ETC. The existence of a proton pump in Complex IV was first established by Wikstrom in 1977 (Wikstrom 1977). The protonmotive force in the mitochondria is driven by the mitochondrial membrane potential ($\Delta\Psi_m$). The Complex IV is very efficient at converting chemical energy into the Δp. As demonstrated in the above reaction two charges cross the membrane for every electron that passes through the enzyme complex. The $\Delta\Psi_m$ is then utilised by ATP synthase (Complex V) to synthesise ATP.

1.2.1.5. Complex V

Complex V (F_1 F_o ATP synthase; EC 3.6.3.14) consists of 2 regions; F_1 and F_o (Figure 1.6). The F_1 region is water soluble and catalyses the synthesis (or hydrolysis in the reverse mode) of ATP. The F_0 lies within the membrane that catalyses the ion translocation across the membrane (von Ballmoos et al. 2008).

The mechanism of action of Complex V was first proposed by Paul Boyer in 1997 (Boyer 1997); for which he won the Nobel Prize alongside John Walker. Boyer proposed a binding change model whereby the internal rotation of the γ subunit leads to a binding change in the catalytic β subunits. Crystallography

studies of the F_1 region revealed alternating alpha and beta subunits (3 of each), arranged around a central gamma subunit ($\alpha_3\beta_3\gamma\delta\varepsilon$). The Δp across the inner mitochondrial membrane drives the flow of protons through the F_o region of ATP synthase. The F_o region is composed of a ring of c subunits (c-ring). As a proton passes through the ring, via an arginine controlled mechanism, rotation of the c- ring ensues. The c-ring is tightly attached to the asymmetric central stalk, consisting primarily of the γ subunit of the F_1 region. The γ subunit rotates within the $\alpha_3\beta_3$ subunits of F_1 region initiating a series of conformational changes at the three catalytic nucleotide binding sites (von Ballmoos et al. 2008). Further rotation in line with the central stalk is prevented by a peripheral stalk that joins the $\alpha_3\beta_3$ subunits to the non-rotating portion of F_o (Wang & Oster 1998).

Under certain physiological conditions Complex V can work in the reverse mode, thus hydrolysing ATP and pumping protons against the proton gradient. Work by Boyer showed that when the $\Delta\Psi_m$ is reduced by the addition of an uncoupler in the presence of ATP, ATP hydrolysis occurs (Boyer 2002).

1.2.1.6. Electron Transfer Flavoprotein Quinone Oxidoreductase

β-oxidation of long chain fatty acids is an essential process for energy provision; particularly in cardiac and skeletal muscle. The products of β-oxidation can be utilised in the formation of ketone bodies, that in turn can be used for energy (Bartlett & Eaton 2004). During the β-oxidation process the two carbon units are removed from long-chain acyl-CoA esters by repeated cycles of oxidation, hydration, oxidation and thiolysis by chain length specific acyl-CoA dehydrogenases. Medium-chain acyl-CoA dehydrogenase (MCAD) oxidises acyl-CoA to enoyl-CoA. MCAD (specifically the $FADH_2$ component) is re-oxidised by two ETF. The ETF flavin semiquinone is in turn re-oxidised by ETF-QO which catalyses the transfer of the electrons to the mitochondrial CoQ pool (Figure 1.3; Watmough & Frerman 2010).

The ETF/ETF-QO system serves as a short electron transfer pathway connecting fatty acid β-oxidation and amino acid catabolism to the CoQ pool of the main respiratory chain.

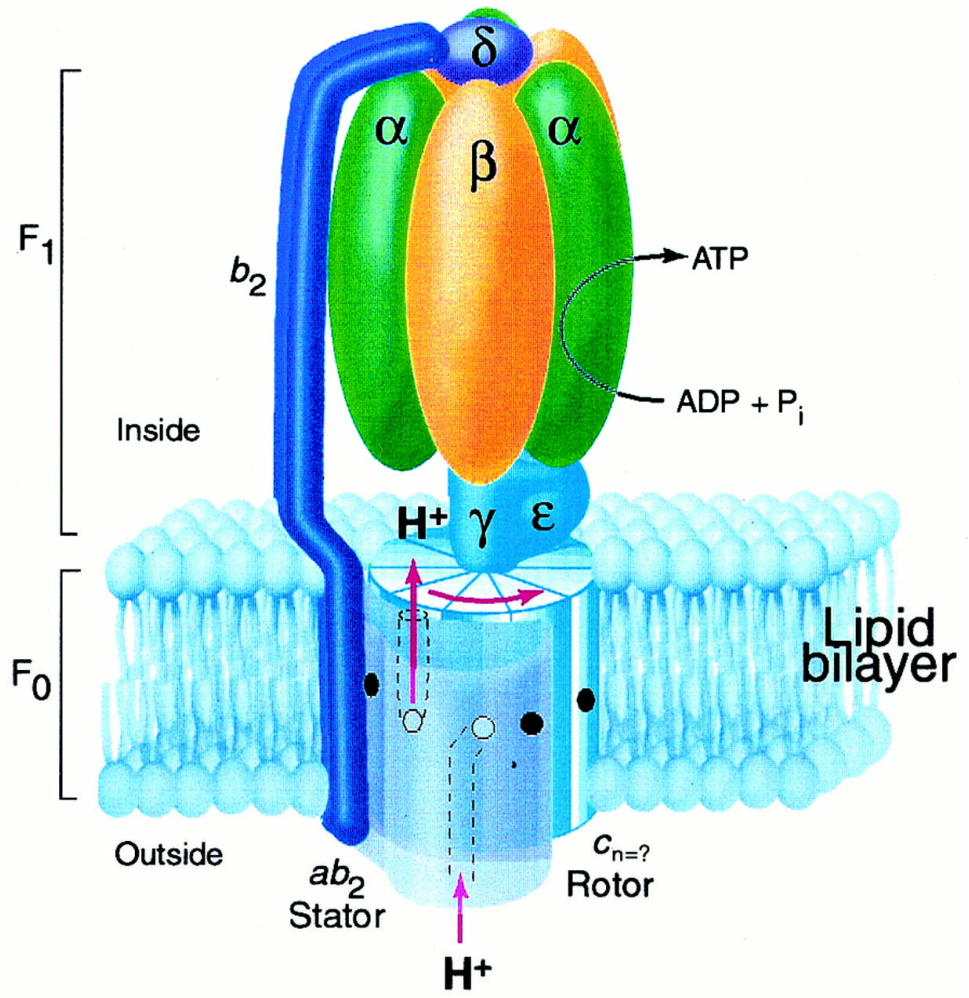

Figure 1.6 The Structure of Complex V (ATP Synthase) consists of F_1 and F_o Regions

Complex V (F_1 F_o ATP synthase; EC 3.6.3.14) consists of 2 regions; F_1 and F_o. The F_1 region is water soluble and catalyses the synthesis (or hydrolysis in the reverse mode) of ATP. The F_0 lies within the membrane that catalyses the ion translocation across the membrane.

Taken from: http://www.pnas.org/content/98/9/4966/F1

1.2.2. Mitochondrial Oxidative Stress and the Antioxidant Role of Coenzyme Q_{10}

1.2.2.1. Mitochondrial Oxidative Stress

Approximately 90% of normal mammalian oxygen consumption is mitochondrial, the majority of which is coupled to ATP synthesis. However ~1-2% is uncoupled by mitochondrial proton leak (Rolfe & Brown 1997). In line with the proportion of proton leakage ROS production accounts for 1–2% of the oxygen consumed by mitochondria. Mitochondria are considered to be the major source of $O_2^{\bullet-}$ free radicals and H_2O_2 production in the cell (Papa & Skulachev 1997; Skulachev 1998). The mitochondrial ETC is very efficient at producing ATP; however the alternating one-electron oxidation-reduction reactions predispose the mitochondria to elevated ROS production. There is a 5–10 fold higher concentration of $O_2^{\bullet-}$ free radicals in the mitochondrial matrix than in other subcellular compartments (Enrique Cadenas & Davies 2000).

The formation of mitochondrial ROS is dependent on the state of respiration. The 5 states of respiration were first proposed by Chance & Williams (1956). Resting or state 4 of respiration is characterised by a slow rate of respiration, a high mitochondrial membrane potential, no availability of ADP and a relatively high rate of $O_2^{\bullet-}$ and H_2O_2 production. Conversely, active or state 3 has a high rate of respiration, a lower mitochondrial membrane potential, high levels of ADP and a slow rate of $O_2^{\bullet-}$ and H_2O_2 production, most likely due to the oxidized state of the components of the respiratory chain. Finally, in anoxic state 5 respiration a limited supply of O_2 supply and a lack of ADP leads to only a partial reduction of O_2 leading to ROS production.

Nitric oxide (NO) also plays an important role in ROS production through various mechanisms including; reversible binding to Complex IV, inhibition of electron transfer at the *bc1* segment (Complex III), partial oxidation of mitochondrial ubiquinol to ubisemiquinone and generation of superoxide. NO is produced by endothelial nitric oxide synthase or by the mitochondrial isozyme (Poderoso et al. 1999; Poderoso et al. 1998; Cadenas & Davies 2000).

Free radicals are capable of causing substantial cellular damage to lipids, proteins and DNA, or oxidative stress. Lipid peroxidation is by far the most studied process resulting from oxidative stress. It is the process in which free radicals remove electrons from the lipids in cellular membranes (Niki 1987).

Phospholipids found in cellular membranes are highly vulnerable to lipid peroxidation. Polyunsaturated side chains e.g. arachidionic acid are particularly susceptible to free radical attack, forming lipid hydroperoxides and leading to changes in membrane permeability and fluidity and altered lipid-protein interactions. Initiation of lipid peroxidation occurs when a free radical of sufficient reactivity (for examples see Table 1.3) extracts a hydrogen atom from the methylene group of an unsaturated fatty acid. The initiating species then undergoes conjugated diene bond rearrangement. The lipid radical formed reacts with oxygen forming a peroxyl radical (Table 1.3). These peroxyl radicals can react with each, other forming detergents capable of damaging cellular membranes. These unstable molecules can also react with macromolecules and thus further contribute to the damage caused. A single initiation event can be amplified many times as long as oxygen and subsequent un-oxidised fatty acids are available (Rice-Evans & Burdon 1993).

During protein oxidation certain amino acids are more prone to oxidation than others. However it is the protein-bound transition metals that are the greatest risk factor. They react with ROS and form hydroxyl radicals at the metal-binding site (Stadtman & Berlett 1991; Stadtman 1990). Oxidised proteins are digested to amino acids by specific proteases, making replacement via synthesis of proteins the only repair mechanism (Grune et al. 1997; Ullrich et al. 1999). DNA oxidation by ROS is also believed to be dependent on transition metals (Halliwell & Aruom 1991). Due to the relatively high concentration of ROS in mitochondria, and because of the lack of protective histones and limited repair mechanisms, mitochondrial DNA is exposed to 10-fold higher oxidative damage than nuclear DNA (Ozawa 1997). Once damaged oxidized DNA may be repaired by either replacement or removal of the affected nucleic acids (Wood 1996).

Superoxide radical	$O_2^{\bullet -}$
Hydroxyl radical	$^{\bullet}OH$
Peroxyl radical	$ROO^{\bullet}$
Perhydroxyl radical	$HOO^{\bullet}$
Alkoxyl radical	$RO^{\bullet}$
Nitric oxide	$NO^{\bullet}$
Hydrogen peroxide	H_2O_2

Table 1.3 Examples of Reactive Oxygen Species (ROS)

ROS has the potential to alter the normal functioning of the cell. To protect the cell from further damage there are a number of defense mechanisms in place, which include antioxidants and non-enzymatic agents. Antioxidant enzymes include superoxide dismutase and various peroxidases such as glutathione peroxidase, catalase, thioredoxin reductase and peroxiredoxin (Holmgren & Bjornstedt, 1995; Wood, Poole, & Karplus, 2003). Nonenzymatic agents include vitamins C and E, carotenoids, glutathione, α-lipoic acid, flavinoids and CoQ.

Glutathione (GSH) is a ubiquitous tripeptide that, like CoQ, is known to participate in a number of important cellular processes. The thiol group present in reduced GSH acts as a reducing agent where it can directly neutralise free radicals and reactive oxygen compounds as well as maintaining exogenous antioxidants such as vitamins C and E in their reduced (active) forms (Meister & Anderson 1983). After donating an electron GSH is very reactive. It is able to react with other GSH compounds to form its dimeric oxidised form glutathione disulphide (GSSG). GSH can then be regenerated in a NADPH dependant process. The ratio of reduced glutathione to oxidized glutathione within cells is often used as a measure of cellular toxicity (Anderson 1985).

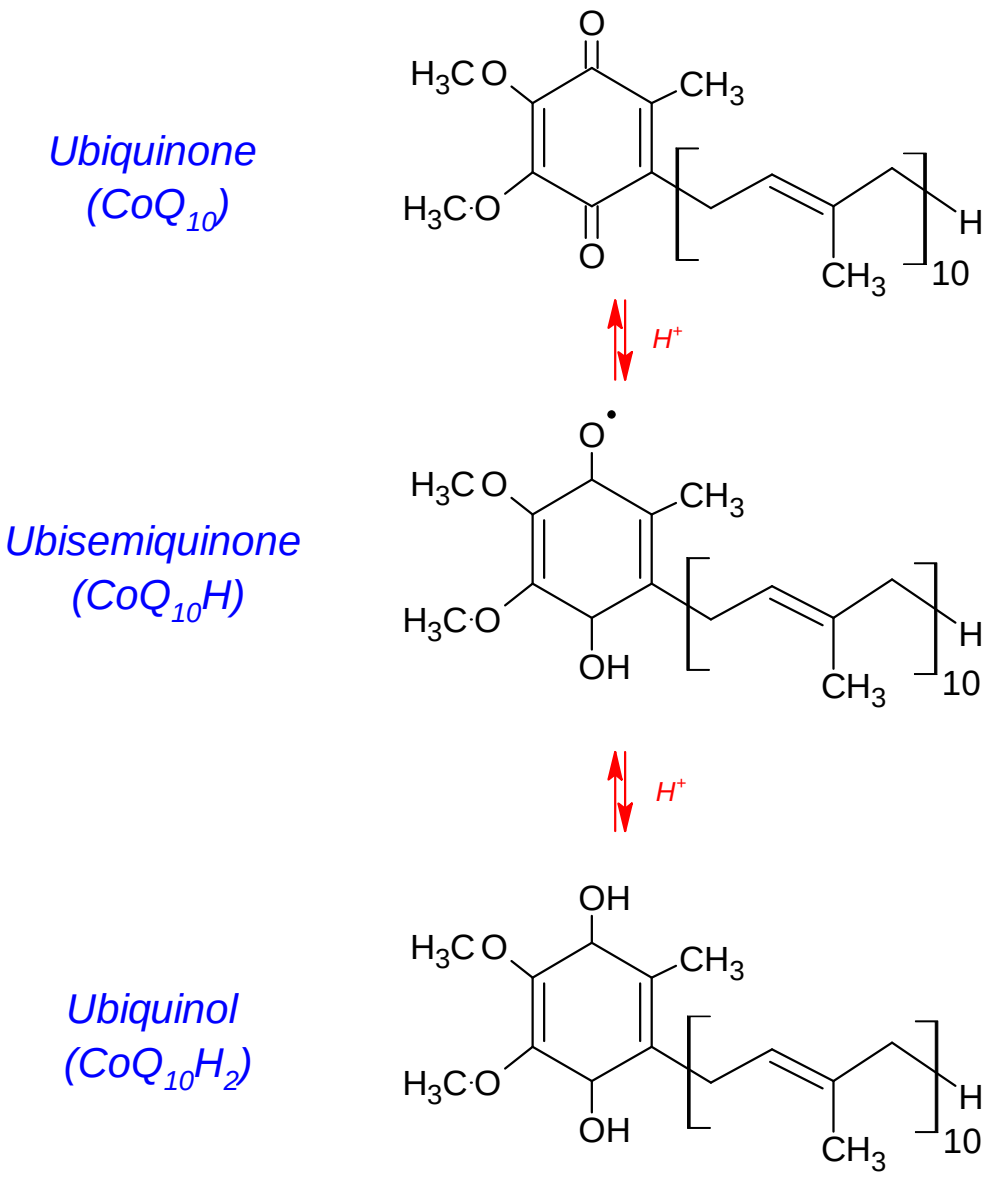

Figure 1.7 Redox States of CoQ_{10}

Ubiquinone, Ubisemiquinone and Ubiquinol: the fully oxidized ubiquinone form (CoQ_{10}); the radical semiquinone intermediate ($CoQ_{10}H\cdot$), and the fully reduced ubiquinol form ($CoQ_{10}H_2$).

1.2.2.2. Antioxidant Function of Coenzyme Q_{10}

CoQ is located in all cellular lipid membranes at an abundance approximately 3-30 times greater than that of vitamin E. Consequently, due to its close proximity to unsaturated lipids which are prone to lipid peroxidation, CoQ is the primary scavenger of free radicals. In its reduced form, ubiquinol, CoQ is a potent antioxidant and is considered more efficient than vitamin E (Frei et al. 1990). It has been suggested that ubiquinol acts earlier in the prevention of lipid peroxidation than vitamin E (Ernster & Forsmark-Andree 1993) and ubiquinol is also able to regenerate vitamin E from the α-tocopheroxyl radical. Ubiquinol is able to inhibit lipid peroxidation in most subcellular membranes (Ernster et al. 1992; Ernster & Dallner 1995) and plays an important role as an antioxidant in the circulation (Romagnoli et al. 1994; Alleva et al. 1995). Reductive regeneration of ubiquinol is vital to maintain its antioxidative function. The ETC ensures that mitochondrial ubiquinol is kept in a highly reduced state (Aberg et al. 1992). In the plasma and endomembranes there are at least three enzymes that are known to maintain CoQ in its reduced state. These enzymes are NADH cytochrome b5 reductase, NADH/NADPH oxidoreductase and NADPH coenzyme Q reductase (Villalba & Navas 2000; Takahashi et al. 1996). NADH cytochrome b5 reductase and NADPH coenzyme Q reductase are able to facilitate a one electron transfer and are important in the neutralisation of semiubiquinone to ubiquinol. DT diaphorase is able to reduce CoQ via a 2 electron transfer, consequently eliminating the intermediate production of ubisemiquinone (Figure 1.7). Interestingly under conditions of oxidative stress (such as lack of selenium and vitamin E) the CoQ content in membranes is increased in conjunction with the amount of DT diaphorase (Navarro et al. 1999).

The potency of CoQ as an antioxidant can be demonstrated using CoQ deficient yeast models (Poon et al. 1997) and patient fibroblasts (Quinzii et al. 2010). Yeast mutants deficient in CoQ show more lipid peroxide formation than normal yeast (Poon et al. 1997). In patient fibroblasts middle range CoQ_{10} deficiency (30-50% of normal) was associated with increased ROS, including an increase in lipid peroxidation (Quinzii et al. 2010).

Ubiquinol is also able to reduce vitamin E back its active form (Arroyo et al. 2000). Regeneration of vitamin E is also evident in low density lipoproteins.

Here a relatively small amount of CoQ is capable of direct reduction of vitamin E back to its reduced active form (Schneider & Elstner 2000; Thomas et al. 1999). Vitamin C is regenerated by glutathione within the cell, however there is evidence that electron transport (via CoQ) in the plasma membrane can be used to regenerate vitamin C (Crane 2001).

1.2.3. The Plasma Membrane Redox System

As in the mitochondrial ETC, CoQ is also able to facilitate electron transport across the plasma membrane. The plasma membrane of eukaryotic cells contains an NADH oxidase (NOX) that is implicated in the transfer of electrons across the membrane. The NOX protein is located on the external surface of the plasma membrane. Hormones and growth factors are both able to stimulate activity of the NOX (Brightman et al. 1992). A quinone reductase is bound to the internal cytosolic surface of the plasma membrane. This catalyses the reduction of CoQ in the presence of NADH (Kishi et al. 1999), thus enabling the regeneration of the cellular reduced CoQ pool. There are several proposed functions of NOX including control of cell growth and differentiation and regenerating extracellular reduced ascorbate (Crane et al. 1985; Burón et al. 1993).

It is also possible that NOX is involved in the regulation of the cytosolic NAD^+/NADH ratio (Gómez-Díaz et al. 1997). Larm et al (1994) demonstrated that in the absence of mitochondrial DNA the cell is able to regenerate NADH via the plasma membrane. Crane et al. (1994) proposed that the CoQ_{10} plasma membrane electron transfer system may function as a signaling molecule. It was discovered that in *Escherichia coli* the redox state of CoQ acts as a control of tyrosine kinase activity (Iuchi & Lin 1991). Semiquinone may also play a role; oxidation of semiquinone in the plasma membrane could generate peroxide, activation of peroxide generation induces tyrosine kinase and gene expression (Shibanuma et al. 1990; Stirpe 1991).

1.2.4. Lysosomal Electron Transfer

It was also suggested that lysosomes contain an NADH-dependent CoQ reductase involved in translocation of protons into the lysosomal lumen (Gille & Nohl 2000), thus allowing the regulation of lysosomal pH. It is thought that the reduction of CoQ occurs in two subsequent one-electron transfer steps involving FAD and cytochrome *b5* with molecular oxygen as the terminal

electron acceptor. Though intriguing, further research will be necessary to define the function of this CoQ-dependent lysosomal reductase.

1.2.5. The Mitochondrial Permeability Transition Pore (PTP)

The mitochondrial inner membrane has an extremely low permeability to ions and solutes. To facilitate trans-membrane transport, the inner membrane contains numerous macromolecule transporters and ion channels. However during in vitro Ca^{2+} accumulation the mitochondrial inner membrane undergoes permeabilisation, known as permeability transition, via the PTP. This causes interruption of the ETC, disruption of ionic status, and hydrolysis of ATP (Fontaine & Bernardi 1999).

The PTP is effectively a voltage-dependent channel, favoring a closed conformation at high membrane potentials and an open conformation at low membrane potentials. Permeability transition is thought to be regulated by many factors including the mitochondrial membrane potential, the matrix pH, cyclosporin A, phosphate, oxidized glutathione and pyrimidine nucleotides derived from oxidative stress. It has been suggested that the permeability transition is a key event in apoptosis (Green & Reed 1998). Several analogues of CoQ have been shown to affect the PTP (E Fontaine et al. 1998; Walter et al. 2000; Walter et al. 2002). It has been suggested that the quinones' benzoquinone rings share a common binding site, acting as either inhibitors or inducers of PTP. CoQ_{10} seems to prevent PTP opening (Papucci et al. 2003). This mechanism may go some way to explain the relationship between apoptosis and CoQ_{10} (López-Lluch et al., 1999). However, the PTP opening and the mechanism of action by CoQ_{10} were not investigated in this study.

1.2.6. Uncoupling Proteins (UCPs)

UCPs are able to transport H^+ from the outside to the inside of the mitochondrial inner membrane, thus counteracting the proton gradient built by the ETC (Nicholls & Locke 1984). UCPs are ubiquitous throughout animal and plant cells. Five UCPs (1–5 in humans) are known and they form a subfamily of the mitochondrial carrier family. UCP3 is the most common subtype in human skeletal muscle (Pecqueur et al. 2001). UCPs are important in thermogenesis but may also be involved in suppression of oxygen radicals. Echtay et al (2000; 2001) showed that CoQ is a vital cofactor in UCP function in bacterial liposomes which is inhibited by the addition of ATP. It has been suggested that CoQ

interact with UCP within the hydrophobic bilayer given that short chain CoQs were ineffective in activating UCPs (Echtay et al. 2001).

1.2.7. Cofactor in Pyrimidine Biosynthesis

The pyrimidine derivatives: cytosine, thymine, and uracil are components of nucleic acids (DNA and RNA). Pyrimidines are therefore important for protein synthesis and cell growth. CoQ_{10} is a cofactor in the conversion of dihydroorotate (DHO) to orotic acid (OA) (Malmquist et al. 2008). Dihydroorotate dehydrogenase (DHODH) is a flavin containing protein that catalyses this conversion in the *de novo* synthesis of pyrimidine. DHODH is classified into two families. Most eukaryotes, including humans, have family 2 enzymes. Family 2 enzymes are bound to the inner membrane of the mitochondria and transfer electrons to CoQ_{10}, chemically coupling pyrimidine to the respiratory chain. Human DHODH appears to have two distinct CoQ-substrate binding sites on either side of the flavin mononucleotide (FMN) (Malmquist et al. 2008).

De novo pyrimidine synthesis has been studied in CoQ_{10} deficient patient fibroblasts (López-Martín et al. 2007). The fibroblasts showed slow growth rates compared to control fibroblasts. Growth was increased after incubation with uridine, indicating that a defect in pyrimidine biosynthesis and not a defect in ETC function is responsible for the slow growth rates.

1.2.8. Regulation of Cellular Membranes

All organelles isolated through subfractionation of the liver contain varying amounts of CoQ. CoQ is a major component as expected, in both the outer and inner membranes of the mitochondria. It is also found in high concentrations in the lysosome and in the Golgi vesicles (Löw et al. 1992; Zhang 1996; Ericsson & Dallner 1993). The distribution of CoQ, as well as that of other mevalonate lipids, is able to considerably alter membrane properties. It is the structural organisation of these lipids that may explain the differences between organelle membrane type and possibly perturbation during disease. CoQ, dolichol and dolichyl-P have long isoprenoid chains that would remain in the hydrophobic region between the bilayer. This is likely to increase membrane thickness and could de-stabilise the membrane, thereby increasing fluidity and permeability. Cholesterol acts in a converse manner. Due to cholesterols short chain length it does not protrude into the intermembrane space and therefore stabilises the

membrane leading to decreased fluidity and permeability (Van Dijck et al. 1976). From this we can come to two conclusions: firstly that for optimal function of subcellular membranes the distribution of mevalonate lipids must be appropriate to that membrane and secondly if this balance fluctuates in any way the effect may be deleterious to organelle function.

1.3. CoQ Biosynthesis

CoQ biosynthesis has been comprehensively investigated in bacteria and yeast but little is known about the pathway in mammals. CoQ biosynthesis begins with acetyl-coenzyme A (acetyl-CoA) which enters the mevalonate pathway producing farnesyl pyrophosphate (FPP; Figure 1.8). FPP is then condensed to the tyrosine derived 4-hydroxybenzoate. The terminal stages of CoQ biosynthesis involve a series of ring modifications to the benzoquinone core of the molecule (Figure 1.9). The terminal portion of bacterial and yeast CoQ biosynthesis differ in the order of synthetic events in the terminal portion of the pathway, i.e. in prokaryotes (yeast) the ring modifications occur in the order of decarboxylation, hydroxylation and methylation, whereas in eukaryotes (bacteria) decarboxylation precedes hydroxylation and methylation. COQ biosynthetic genes isolated from yeast (coq1–8) have a putative mitochondrial targeting signal (Belogrudov et al. 2001), however CoQ is found in all subcellular compartments. This suggests that there must be a transport mechanism from the mitochondria to other subcellular membranes. Interestingly it appears that in yeast, CoQ synthesizing enzymes (Coq3-9) are organised in a multi-subunit complex (Hsu et al. 2000; Hsieh et al. 2007), and thus accumulate 3-hexaprenyl-4-hydroxybenzoic acid (product regulated by the Coq2 gene) regardless of the gene defect.

1.3.1. The Mevalonate Pathway

The mevalonate pathway encompasses the formation of FPP from acetyl-CoA to FPP (Figure 1.8). FPP is a common substrate for the biosynthesis of CoQ, as well as cholesterol, dolichol and isoprenylated proteins (Grünler et al. 1994; Brown & Goldstein 1986), making the mevalonate pathway universal to all end-products. Interestingly the mevalonate pathway lipids are synthesised in exceptionally different concentrations. The most likely point of regulation is at the FPP branch point. The initial stages of the mevalonate pathway involve the condensation of three acetyl-CoA to 3-hydroxy-3-methylglutaryl- coenzyme A

(HMG-CoA). This is mediated by two enzymes, acetoacetyl-CoA thiolase and HMG-CoA synthase. HMG-CoA reductase then converts HMG-CoA to mevalonate. This enzyme is considered to be the central regulatory enzyme in cholesterol biosynthesis and consequently CoQ biosynthesis.

Mevalonate is consequently phosphorylated by two enzymes, mevalonate kinase and phosphomevalonate kinase. Mevalonate pyrophosphate then undergoes decarboxylation producing isopentenyl pyrophosphate (IPP). IPP is a precursor of FPP and the main component of dolichol. Isomerisation of IPP gives dimethylallyl pyrophosphate which participates in the synthesis of isopentenyl tRNA at the position six of an adenosine (Warner et al. 2000). FPP synthase catalyses the fusion of IPP and its isomer dimethylallyl pyrophosphate to FPP forming an intermediate product, geranyl pyrophosphate (GPP) (Rilling 1985). FPP is then converted into cholesterol, dolichol, CoQ or isoprenylated proteins by one of 4 enzymes: squalene synthase, cis-prenyltransferase, trans-prenyltransferase and farnesyl-protein transferase. These are considered to be the rate limiting enzymes in the terminal part of the lipids biosynthetic pathway.

1.3.2. CoQ Biosynthesis

The biosynthesis of CoQ has been studied extensively in Escherichia coli and Saccharomyces cerevisiae and Schizosaccharomyces pombe (Tran & Clarke 2007; Kawamukai 2009). The polyprenyl tail of CoQ is produced in a species specific manner by trans-prenyl-transferase (TPT; also called decaprenyl transferase; encoded for by coq1). The number of isoprenoid units varies between species. Saccharomyces species predominantly produce CoQ_6, mice and rats predominantly produce CoQ_9 and humans predominantly produce CoQ_{10}. In humans, TPT is encoded by the *PDSS1* and *PDSS2* genes.

The ring precursor in coenzyme Q biosynthesis is 4-hydroxy benzoate (4HB). Bacteria can produce 4HB via de novo synthesis (Siebert et al. 1994) however animals rely on a dietary source of essential amino acids. Thus tyrosine and phenylalanine are used to generate 4HB (Tran & Clarke 2007).

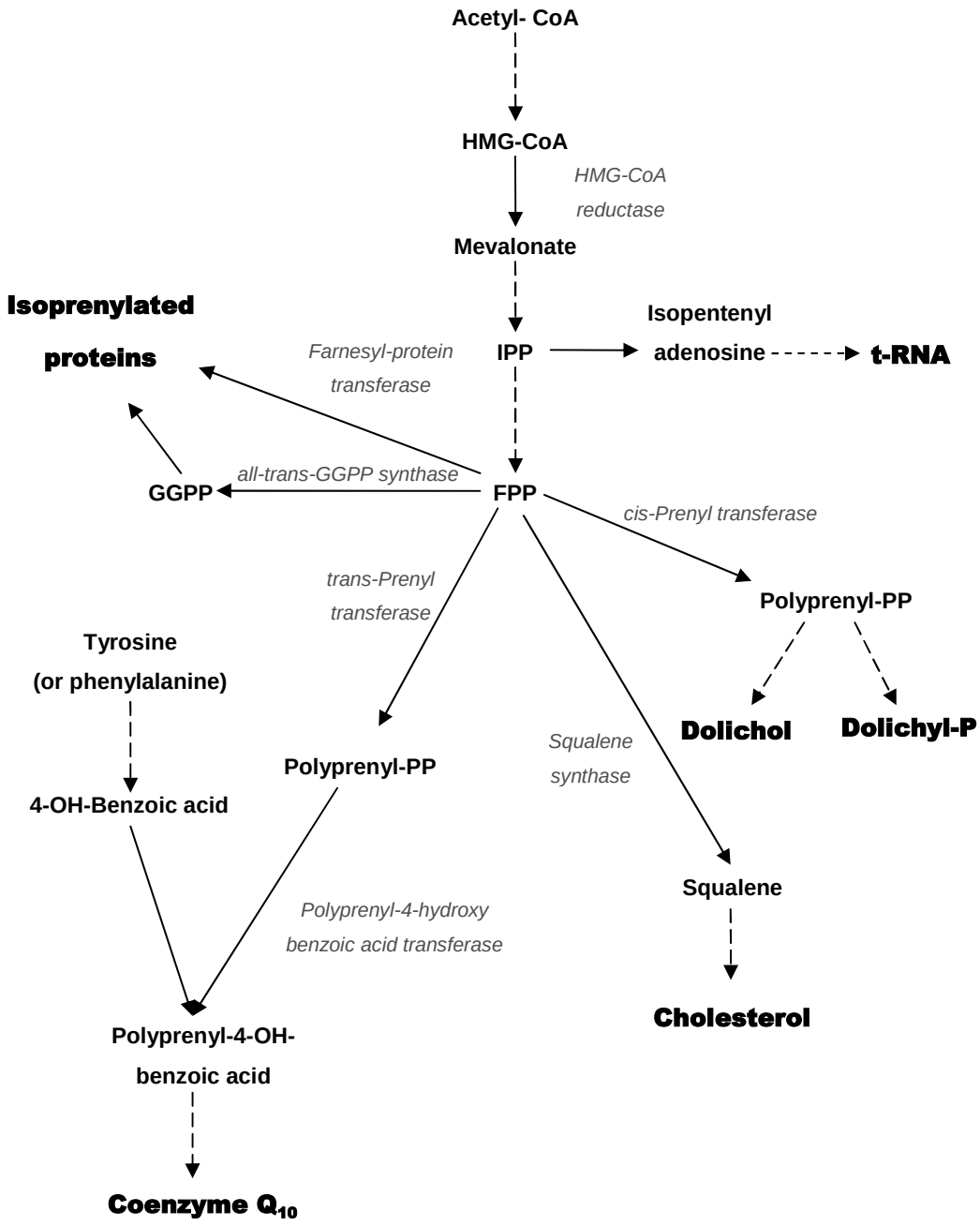

Figure 1.8 The Mevalonate Pathway-illustrating the synthesis of CoQ_{10}

Acetyl CoA is converted via a complex pathway into Coenzyme Q_{10} (CoQ_{10}), cholesterol, dolichol (and Dolichol-P), t-RNA and Isoprenylated proteins via the mevalonate pathway. *3-hydroxy-3-methyl-glutaryl-CoA reductase (HMG CoA reductase) is the main rate controlling enzyme of the mevalonate pathway.* The Farnesyl diphosphate (FPP) branch point enzymes also appear to regulate the synthesis of these compounds. *IPP: isopentenyl diphosphate; GPP: geranyl diphosphate; FPP: farnesyl diphosphate*

Human homologues of the yeast genes have been shown to restore CoQ biosynthesis in yeast mutants (reviewed in Tran & Clarke 2007). In yeast, coq polypeptides (enzymes responsible for CoQ biosynthesis) are located on the matrix side of the inner mitochondrial membrane (Tran & Clarke 2007). Many lines of evidence suggest that the coq polypeptides are conjoined in one or more multi-subunit complexes, similar to the ETC complexes (explained in Section 1.2.1).

Yeast mutants with deletions in *coq3, coq4, coq5, coq6, coq7, coq8*, or *coq9* genes accumulate only the first CoQ-intermediate, 3-hexaprenyl-4- hydroxy-benzoic acid (Poon et al. 1995; Poon et al. 1997; Johnson et al. 2005). Subsequently, levels of the Coq polypeptides are substantially decreased in yeast mutants with deletions in any of the *COQ* biosynthetic genes (Hsieh et al. 2007; Gin & Clarke 2005). This is hypothesised to be caused by the destabilisation of the CoQ multisubunit complex. Further publications add to these lines of evidence, suggesting a direct interaction of the complexes. Gel filtration and BN-PAGE analysis of yeast digitonin extracts revealed that several of the coq polypeptides co-migrate at a high molecular mass (Hsieh et al. 2007; Marbois et al. 2005; Tran et al. 2006). It was also noted that demethoxy-CoQ, the penultimate intermediate in Q biosynthesis, co-migrates with the Coq polypeptide complex suggesting that it is still attached to the complex post-synthesis (Marbois et al. 2005).

Phenotype	No. of cases	Clinical features (*responsible gene*)	CoQ_{10} level
Encephalomyopathy	4	Juvenile-onset mitochondrial myopathy, recurrent myoglobinuria, encephalopathy (***No known gene***)	3.7%-39% of normal in muscle, normal in fibroblasts in 1 patient
Isolated myopathy	18	Juvenile- or adult-onset muscle weakness, myoglobinuria, exercise intolerance, cramps, myalgias, elevated creatine kinase level (***ETFDH***)	12.4%-49% of normal in muscle, normal in fibroblasts in 1 patient
Nephropathy	11	Infantile- or early childhood-onset steroid-resistant nephrotic syndrome (***COQ2***); Infantile- or juvenile-onset steroid-resistant nephrotic syndrome typically with congenital sensorineural deafness (***COQ6***)	38% of normal in muscle in 1 patient, 17% of normal in fibroblasts in 1 patient
Infantile multisystemic disease	18	Infantile-onset psychomotor regression, encephalopathy, optic atrophy, retinopathy, hearing loss, renal dysfunction (mainly nephrotic syndrome) (***COQ2, PDSS2, COQ9, PDSS1, COQ6***)	2.5%-37% of normal in muscle, reduced in fibroblasts: 10/11 patients
Cerebellar ataxia	117	Typically juvenile-onset cerebellar ataxia, additional manifestations may occur (**ADCK3, APTX**)	4%-66% of normal in muscle, reduced in fibroblasts: 18/30 patients

Table 1.4 Table Illustrating the Phenotypes Associated with CoQ_{10} Deficiency

Data taken from (Emmanuele et al, 2012)

1.4. Human CoQ_{10} Deficiency

CoQ_{10} deficiency was first reported by Ogasahara in 1989 in siblings with progressive muscle weakness, fatigability and central nervous system dysfunction (Ogasahara et al. 1989). Primary CoQ_{10} deficiency is usually inherited in an autosomal recessive manner, with recessive mutations reported in 7 CoQ_{10} biosynthetic genes (6 biosynthetic enzymes) to date: *PDSS1* (Mollet et al. 2007) and *PDSS2* (Rötig et al. 2000; López et al. 2006), *ADCK3* (Mollet et al. 2008; Lagier-Tourenne et al. 2008), *COQ9* (Duncan et al. 2009), *COQ6* (Heeringa et al. 2011), *COQ4* (Salviati et al. 2012) and *COQ2* (Mollet et al. 2007; Quinzii et al. 2006; Diomedi-Camassei et al. 2007). CoQ_{10} deficiency can be broadly divided into five major phenotypes: 1) Encephalomyopathy; 2) infantile multisystemic disease; 3) isolated cerebellar ataxia; 4) a pure myopathic form; and 5) nephropathy (Table 1.4). Leigh syndrome has been reported in 3 patients and can be considered a separate phenotype (Van Maldergem et al. 2002; López et al. 2006).

Numerous genes have been associated with these phenotypes (Table 1.4). The encephalomyopathic and the multisystemic phenotypes demonstrated the most severe defect in CoQ_{10} level (Encephalomyopathy: 3.7%-39% of normal in muscle; Infantile multisystemic: 2.5%-37% of normal in muscle). The 4 cases of the encephalomyopathic phenotype are not associated with any particular gene defect. However the Infantile multisystemic phenotype (18 reported cases) is associated with defects in 5 different genes: *COQ2, PDSS2, COQ9, PDSS1, COQ6* (Emmanuele et al, 2012).

There are 18 reported cases of the isolated myopathic phenotype which is associated with defects in the ETFDH gene. CoQ_{10} levels are 12.4%-49% of normal in the muscle of these patients. Defects in the *ADCK3* and the *APTX* gene are associated with the cerebellar phenotype. There are currently 117 cases that report varying effects on CoQ_{10} biosynthesis (4%-66% of normal CoQ_{10} in muscle). However in fibroblasts only 60% of patients have CoQ_{10} levels lower than normal.

The nephritic phenotype is associated with defects in two genes: COQ2 and COQ6. Patients with a defect in the *COQ2* gene present with an earlier onset (inflantile or early childhood) steroid resistant nephrotic disease; whereas

patient with a defect in the *COQ6* gene present later and also have sensorineural hearing loss. CoQ_{10} was not quantified in the majority of these patients however 1 patient had a CoQ_{10} level that was 38% of normal in muscle.

1.4.1. COQ2 (encoding PHB-polyprenyl transferase)

In 2006 Quinzii and colleagues discovered a homozygous missense mutation in the *COQ2* gene in two siblings with infantile steroid resistant nephropathy, and subsequent encephalomyopathy in the eldest child (Quinzii et al. 2006). Both patients had CoQ_{10} deficiency in muscle and fibroblasts, with a consequent decrease in Complex I/III (nicotinamide adenine dinucleotide–cytochrome c oxidoreduc- tase) and II/III (succinate–cytochrome c oxidoreductase) activity. The other ETC complexes had normal activity. In 2007, Mollet and colleagues reported a homozygous base pair deletion in exon 7 of the *COQ2* gene. This patient presented with neonatal neurological distress, liver failure, nephrotic syndrome, diabetes mellitus, pancytopenia, seizures, lactatemia and died at 12 days of multisystem failure. CoQ_{10} quantification revealed a decrease in fibroblasts and enzymological studies of liver homogenate revealed a decrease in Complex I/III and Complex II/III activities. Combined Complex I/III and II/III activities are dependent upon CoQ_{10} thus we would expect the activities to be low in a CoQ_{10} deficient patient. Diomedi-Camassei et al (2007) reported a *COQ2* mutation in two patients with early onset glomerular lesions. The first had steroid resistant nephrotic syndrome, with no extra-renal symptoms. The second patient presented with olioguria which rapidly developed into end stage renal disease and died at 6 months of epileptic encephalopathy complications. Both patients had decreased levels of CoQ_{10} and Complex II/III activity in muscle (Complex I/III not measured). Complex I activity was also decreased and Complex II, III and IV were at the lower limit of the reference range. Thus to date six patients have been identified as having *COQ2* gene mutations.

The *COQ2* gene encodes a protein called 4HB-polyprenyl transferase. This enzyme catalyses a polyprenyl transfer reaction whereby the tyrosine (or phenylanaline) derived 4-HB is condensed with the mevalonate pathway derived FPP (Figure 1.9).

1.4.2. PDSS1 and 2 (encoding transprenyl transferase)

The *PDSS2* gene encodes a subunit of the TPT enzyme. This heterotetramer is composed of two different subunits; PDSS1 and PDSS2. TPT catalyses the formation of CoQ_{10}'s decaprenyl side chain. In 2006 Lopez et al described a male infant with compound heterozygous mutations in the *PDSS2* subunit gene (López et al. 2006). The patient had severe Leigh syndrome, nephrotic syndrome and epilepsy. ETC activity determination revealed decreased ETC Complex II/III activity and Complex I activity in fibroblasts. Complex II, III and IV activities were normal. CoQ_{10} content was severely reduced in muscle and fibroblasts. A homozygous missense mutation in *PDSS1* was discovered in a single patient from a family with a history of consanguinity. The patient presented with a multisystem disease with early-onset deafness, encephaloneuropathy, obesity, livedo reticularis and valvulopathy. Assessment of ETC complexes revealed low levels of Complex III and Complex II/III, as well as CoQ_{10} deficiency in fibroblasts. Muscle analysis revealed ETC activities within the normal range for all the complexes (Mollet et al. 2007).

Rotig and collegues (2000) performed a radio-labelling study whereby patient fibroblasts were grown in the presence of ^{3}H-Mevalonate. The CoQ_{10} deficient patient was unable to convert ^{3}H-Mevalonate into ^{3}H-CoQ_{10}. This patient was later discovered to have a *PDSS2* gene defect (Rahman et al. 2012 [personal communication]).

1.4.3. ADCK3 (or CABC1)

ADCK3 (or *CABC1*) was originally isolated in yeast in 2002 by Iiizumi et al as a protein found within the mitochondria that was able to reduce apoptotic processes. The role of ADCK3 is unknown. ADCK proteins in general possess conserved protein-kinase motifs for ATP binding and phosphotransfer. It has been suggested that it may function in the distal portion of the biosynthetic pathway, possibly through phosphorylation of the coq3 protein (Tauche et al. 2008).

In 2008 two studies identified patients with *ADCK3* gene mutations (Mollet et al. 2008; Lagier-Tourenne et al. 2008). To date mutations in the *ADCK3* gene have been found in 22 patients from 15 different families (Emmanuele et al. 2012). All of the patients in this literature review presented with childhood onset ataxia

with slow progression. Two patients had concurrent epilepsy. Assessment of ETC activities often showed a mild decrease in Complex I/III and Complex II/III activities and CoQ_{10} deficiency in muscle. But in fact many of the patients had CoQ_{10} and ETC complex activities within the normal range, especially in fibroblasts. A paper published in 2012 described four patients with *ADCK3* gene mutations that presented with an adult onset cerebellar ataxia (Horvath et al. 2012). Similarly half of the patients had a muscle CoQ_{10} status and ETC complex activities within the normal range. Consequently to date there are 26 patients from 17 different families with a confirmed *ADCK3* gene mutation, making this the most common form of CoQ_{10} deficiency.

1.4.4. COQ9

The mutation in the *COQ9* gene was discovered in 2009 by Duncan and colleagues (Duncan et al. 2009). The patient in question developed a multi-systemic disease including intractable seizures, global developmental delay, hypertrophic cardiomyopathy, and renal tubular dysfunction (Rahman et al. 2001). Assessment of skeletal muscle revealed a profound decrease in CoQ_{10}. ETC Complex II/III activity was undetectable and the other ETC complexes had normal activities (Complex I/III was not measured). The exact function of the protein that *COQ9* encodes remains to be elucidated. Yeast studies of the coq9 protein indicate that it is localised in the inner mitochondrial membrane as part of a multi-subunit complex with other peptides involved in the biosynthesis of CoQ_{10} (Hsieh et al. 2007; Hsu et al. 2000). It is hypothesised that COQ9 protein acts distally to the prenylation step since yeast *coq9* mutants are capable of producing 3-hexaprenyl-4-hydroxybenzoic acid (Johnson et al. 2005). It is also interesting to note that Duncan and associates (2009) observed an un-identified peak on HPLC analysis of CoQ_{10} possibly representing an accumulating biosynthetic intermediate from the distal portion of the pathway in *COQ9* patient fibroblasts.

1.4.5. COQ6

Recently mutations in the *COQ6* gene has been reported in 11 patients from five families (Heeringa et al. 2011) making this the second most common phenotype of primary CoQ_{10} deficiency. These patients presented with a nephrotic syndrome associated with sensorineural hearing loss, similar to that

observed in patients with *PDSS1* and *COQ2* gene mutations. The *COQ6* gene consists of 13.2 kb and 12 exons. The protein that the *COQ6* gene encodes is highly conserved throughout evolution and is required for one or more ring hydroxylation steps in the biosythesis of CoQ_{10}.

In four of these cases central nervous system involvement including seizures and ataxia was reported. $\Delta\Psi_m$ was decreased in podocyte clones isolated from patients, suggesting a defect in the ETC function (Heeringa et al. 2011). However ETC activities were not measured in this study.

1.4.6. COQ4

COQ4 encodes a protein that organises the multienzyme complex for the synthesis of CoQ_{10}. The protein does not appear to possess a specific enzymatic activity but plays rather a structural role (Marbois et al. 2009; Casarin et al. 2008). A 3.9 Mb deletion of chromosome 9q34.13 was identified in a 3-year-old boy with mental retardation, encephalomyopathy and dysmorphic features. ETC Complex II/III activity and CoQ_{10} was reduced in fibroblasts (Salviati et al. 2012). This deletion also leads to the deletion of 80 other neighbouring genes; which may contribute the complexity of the clinical phenotype seen here.

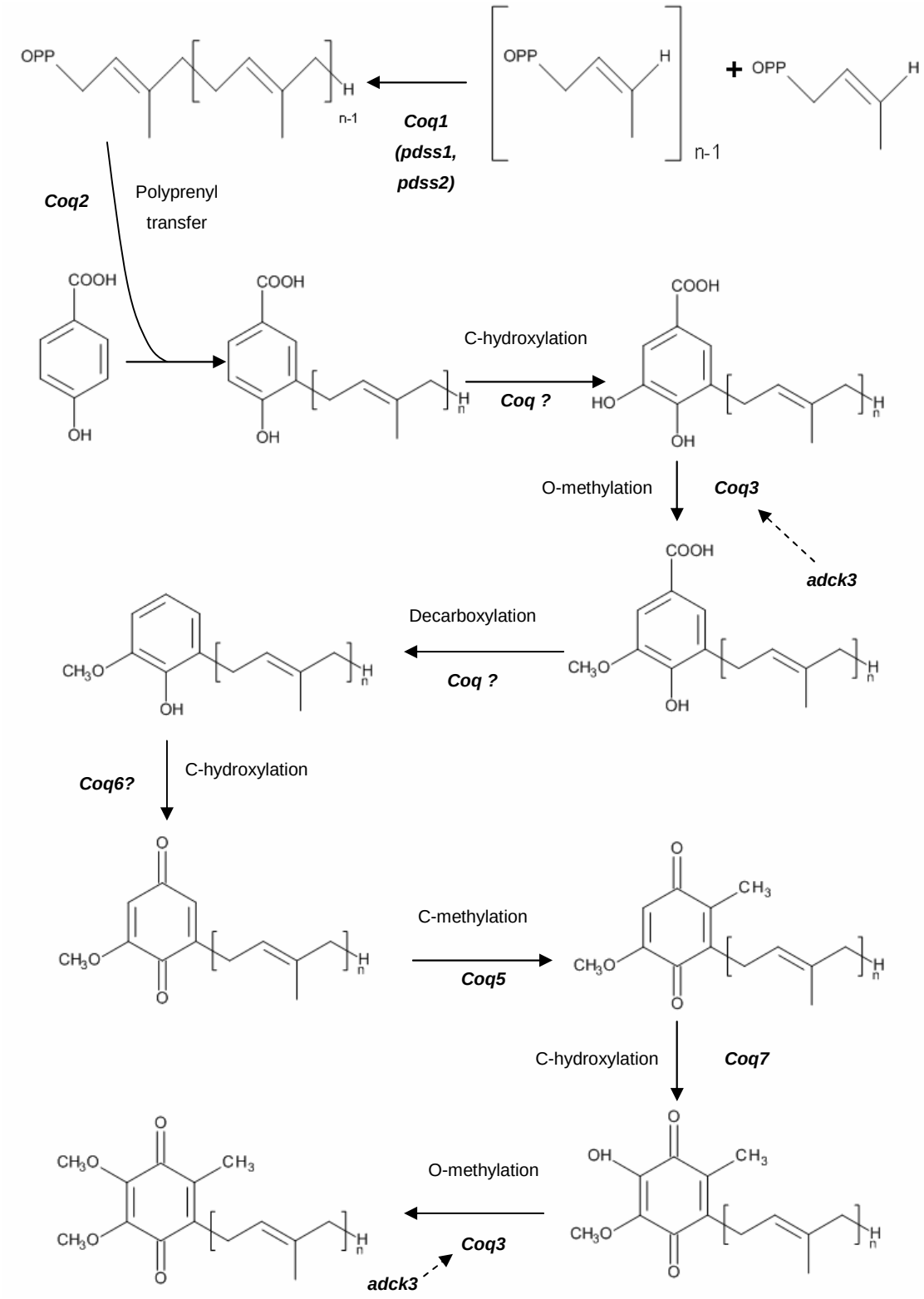

Figure 1.9 CoQ Biosynthesis

Characterised in yeast, demonstrates the proposed biosynthetic pathway of CoQ. Adck3 is thought to act as a kinase in the phosphorylation of coq3 (Tauche et al. 2008)

1.4.7. Secondary CoQ10 Deficiency

Mutations in genes not directly associated with the CoQ_{10} biosynthetic pathway have been detected in patients presenting with the cerebellar and myopathic forms of CoQ_{10} deficiency. Musumeci et al (2008) reported six patients with cerebellar ataxia, pyramidal signs and seizures, who were responsive to CoQ_{10} supplementation. Patients had a muscle CoQ_{10} deficiency with decreased Complex I/III and II/III activities, and a marginal decrease in separate Complex I and Complex II activities. Later studies revealed a homozygous mutation in the *APTX* gene, encoding aprataxin, which is a known cause of ataxia-oculomotor-apraxia 1 (AOA1; Moreira et al. 2001). In 2007, Le Ber et al. further established AOA1 as a cause of secondary CoQ_{10} deficiency (Le Ber et al. 2007). These authors noted decreased CoQ_{10} levels in five unrelated patients with genetically confirmed AOA1 with a more severe deficiency in patients with a homozygous W279X mutation. Again these patients improved after CoQ_{10} supplementation (Quinzii et al. 2005). The W279X gene mutation leads to a truncated protein and possibly to a complete loss of protein which may explain the greater decrease in CoQ_{10} content versus other gene defects in the APTX gene. There is no obvious link between aprataxin and CoQ_{10} biosynthesis. However it is intriguing that to note that hypercholesterolaemia is a common feature of AOA1, suggesting an interaction with the mevalonate pathway.

The myopathic phenotype is now associated with *ETFDH* (electron-transferring-flavoprotein dehydrogenase) gene mutation (see Section 1.2.2 for details on the biochemistry). Gempel and associates (2007) reported seven patients (five families) with exercise intolerance, fatigue and proximal myopathy. All patients had a severe CoQ_{10} deficiency, with a concurrent decrease in ETC Complex I and II/III activities and showed dramatic improvement following CoQ_{10} supplementation (Gempel et al. 2007). CoQ_{10} is a direct acceptor of electrons from the ETC/ETC-QO system and thus it is possible that an inhibitory feedback mechanism may be responsible for the down-regulation of CoQ_{10} seen in these patients.

CoQ_{10} deficiency has also been documented in Cardiofaciocutaneous syndrome due to a *BRAF* mutation (Aeby et al. 2007). However the cause of the CoQ_{10} deficiency associated with the *BRAF* mutation is yet to be elucidated.

1.4.7.1. Pharmacological Inhibition of CoQ_{10}

Statins are reversible inhibitors of the enzyme HMG CoA-reductase. They are the most widely used and effective drugs used to reduce low density lipoprotein (LDL) cholesterol, thus reducing the likelihood of cardiovascular events (Harper & Jacobson 2010). Statin myopathy occurs in 10-15% of statin users (Harper & Jacobson 2010). It is widely speculated that this is caused by a secondary CoQ_{10} deficiency (Hargreaves & Heales 2002). HMG CoA-reductase is a major regulatory enzyme in the mevalonate pathway, which is common to both CoQ_{10} and cholesterol (Alberts 1988). Thus a concurrent decrease in CoQ_{10} and cholesterol is plausible following statin therapy.

The majority of studies investigating CoQ_{10} deficiency in relation to statin therapy have been conducted on serum (Hargreaves et al. 2005). It has been suggested that serum is not the ideal tissue for CoQ_{10} quantification. Consequently the deficiencies highlighted may not be demonstrating a cellular CoQ_{10} deficiency. Serum/plasma CoQ_{10} levels are subject to dietary intake and hepatic synthesis; not *de novo* synthesis. Additionally CoQ_{10} levels are also dependant on blood lipids thus quantification of serum CoQ_{10} could be improved through standardising results against lipoprotein levels. However studies that use muscle for quantification of CoQ_{10} levels also variably find a deficiency in relation to statin therapy (Harper & Jacobson 2010). Subsequently CoQ_{10} supplementation also has variable efficacy in preventing myopathy when taken in conjunction with statin therapy (Harper & Jacobson 2010).

1.4.7.2. Mitochondrial Disorders

Secondary CoQ_{10} deficiency has been reported in a number of patients with mitochondrial diseases. In 1989, Zierz et al. reported a patient with Kearns-Sayre syndrome who had CoQ_{10} deficiency in plasma and muscle (Zierz et al. 1989). Subsequently in 1991, Matsuoka et al. reported 25 patients with mitochondrial encephalomyopathies that had low levels of CoQ_{10} in muscle (Matsuoka et al. 1991). Additionally Montero and colleagues published two papers outlining two patients, one with mtDNA (mitochondrial DNA) depletion and the other with a confirmed mitochondrial disease, who both presented with CoQ_{10} deficiency in muscle. Miles et al. investigated a large cohort of paediatric patients with suspected mitochondrial myopathy. This study found that muscle

CoQ_{10} content correlated with a decrease in ETC activity in these patients (Miles et al. 2008). A recent study of 76 patients with mitochondrial disorders of a hetrogeneous nature found that 37% of patients had a CoQ_{10} lower than normal (Sacconi et al. 2010). A possible explanation for the observed CoQ_{10} deficiency in patients with mitochondrial disorders could be an increase in oxidative stress. Mitochondria are the primary site of ROS production (Cadenas & Davies 2000) and thus mitochondrial dysfunction is commonly associated with increased ROS production. Synthesis/consumption of cellular antioxidants, such as CoQ_{10} may be perturbed during periods of high ROS production.

The observed CoQ_{10} deficiency appears to quantitatively be most severe in mtDNA depletion syndromes (Sacconi et al. 2010). In view of the involvement of CoQ_{10} in pyrimidine biosynthesis it is possible that a deficiency in CoQ_{10} further contributes to the mtDNA depletion syndrome.

1.4.7.3. Metabolic Disorders

Secondary CoQ_{10} deficiency has been reported in Mevalonic Aciduria (MVA), Methyl Malonic Acidaemia (MMA) and Phenylketonuria (PKU). In MVA a decrease in mevalonate kinase activity, an enzyme common to both CoQ_{10} and cholesterol synthesis, may lead to a decrease in CoQ_{10} production (Hargreaves 2007). Although decreased levels have been reported in plasma, Haas et al. (2009) did not find a significant decrease in the CoQ_{10} status in MVA patient fibroblasts.

However Haas et al did find CoQ_{10} deficiency in patients with MMA. MMA is caused by an inherited deficiency of the mitochondrial enzyme methylmalonyl-CoA mutase (EC 5.4.99.2) or by defects in the synthesis of 5-deoxyadenosylcobalamin, the cofactor of methylmalonyl-CoA mutase, resulting in an accumulation of MMA in tissues and body fluids. The authors suggest that the CoQ_{10} deficiency observed in the MMA patients is due to an increase in oxidative stress (Haas et al. 2009).

In PKU patients elevated phenylalanine levels have been reported to result in a decrease in plasma CoQ_{10} levels. Decreased levels of CoQ_{10} in plasma in PKU patients could possibly be due to phenylalanine inhibiting two enzymes required for cholesterol and CoQ_{10} biosynthesis, 3-hydroxy-3-methylglutaryl-CoA reductase and mevalonate-5-pyrophosphate decarboxylase (Hargreaves,

2007). However studies performed in blood mononuclear cells did not show a deficiency of CoQ_{10} (Hargreaves 2007).

1.4.7.4. Neurodegenerative Disorders

Mitochondrial dysfunction has long been implicated in the pathogenesis of neurodegenerative diseases. This is particularly evident in Parkinson's disease (PD). PD has historically been associated with a decrease in mitochondrial Complex I activity (Shults et al. 1997). Developments in genetics have led to the discovery of several familial PD genes that are associated with the mitochondria: *PINK1, DJ-1, Omi/HtrA2* (Gandhi et al. 2009). Low levels of CoQ_{10} have been reported in platelets (Shults et al. 1997), with concurrent decreases in ETC Complex I and II/III activities, and in the brain cortex (Hargreaves et al. 2008).

Patients with Friedreich's Ataxia (FA) also have mitochondrial dysfunction. Deficiencies in ETC Complex I, II and III have been described in cardiac and skeletal muscle (Lodi et al. 2002). CoQ_{10} deficiency in plasma has been associated with the efficacy of CoQ_{10} supplementation in FA patients.

Although mitochondrial dysfunction has also been implicated in other neurodegenerative diseases, serum CoQ_{10} levels are not significantly different from controls in Huntington Disease (HD), Amyotrophic lateral sclerosis (ALS) and Alzheimer's disease (AD) (Spindler et al. 2009).

1.5. CoQ_{10} Supplementation

Patients with primary and secondary CoQ_{10} deficiency showed variable responses to CoQ_{10} treatment. There is currently no recommended dose for CoQ_{10} supplementation. In fact the doses administered differ substantially; 30-3000mg/day. However, in general a dose of 10-30mg/kg/day for children and 1200-3000 mg/day in adults appear to be effective in patients with *COQ2* mutations (Rahman et al. 2012).

CoQ_{10} is available in many different forms with variable bioavailablity, including powder, suspension, oil solution, solubilised forms (All-Q and Q-Gel), as well as creams, tablets, wafers, and hard-shell or softgel capsules. Most recently a self-emulsifying drug delivery system (SEDDS) composed of oil and surfactant (Onoue et al. 2012) and a lipid-based formulation that self-assembles on

contact with an aqueous phase into a colloid delivery system (VESIsorb, colloidal-Q10) (Liu & Artmann 2009), have been developed in an effort to increase bioavailability. Various formulations of ubiquinol are also available (Hosoe et al. 2007).

1.5.1. Primary CoQ_{10} Deficiency

In patients with encephalomyopathy, muscle symptoms improved after therapy (Ogasahara et al. 1989; Sobreira et al. 1997; Giovanni et al. 2001), however one patient developed cerebellar ataxia (Sobreira et al. 1997).

Six patients with pure myopathy (Lalani et al. 2005; Horvath et al. 2012) improved after CoQ_{10} supplementation. Riboflavin (vitamin B2) is the co-factor shared by ETF, ETFDH and all acyl-CoA dehydrogenases. Two patients with *ETFDH* mutations only improved after additional treatment with riboflavin, 100 mg daily (Gempel et al. 2007). Therapy with riboflavin, carnitine and low-fat, low-protein diet is beneficial to patients with *ETFDH* mutations; however addition of CoQ_{10} supplementation may also be beneficial to therapy.

In patients with the infantile multisystemic phenotype, CoQ_{10} supplementation halted neurological disease progression and improved myopathy (Rötig et al. 2000). Another patient with a *COQ2* gene mutation improved dramatically after CoQ_{10} supplementation, particularly the neurological symptoms. Interestingly this patient's sister (who had isolated nephropathy) improved upon CoQ_{10} supplementation and did not go on to develop any neurological symptoms (Quinzii et al. 2006). A patient with the *COQ9* mutation who received CoQ_{10} supplementation had a reduction in blood lactate levels, but showed no sign of clinical improvement and died at 2 years (Rahman et al. 2001). A patient with the *PDSS2* gene mutation also failed to respond to CoQ_{10} supplementation and died at 8 months (López et al. 2006).

Two patients with the *COQ6* gene mutation showed improved renal function with decreased levels of proteinuria, however hearing loss did not improve (Heeringa et al. 2011).

Response to CoQ_{10} supplementation in patients with the ataxic phenotype is also variable. 46% of patients with the *ADCK3* gene mutation showed improvement of their ataxic symptoms (Lagier-Tourenne et al. 2008; Pineda et

al. 2010), however many patients were refractory to treatment (Horvath et al. 2012; Mollet et al. 2008). One patient, despite improvement of muscle symptoms, developed a tremor, myoclonic jerks, and cerebellar atrophy (Mollet et al. 2008). A similar level of variability is found in patients with defects in the *APTX* gene. Three siblings with the mutation demonstrated resolved ataxic and epileptic symptoms (Quinzii et al. 2005). However another patient showed no improvement upon CoQ_{10} supplementation (D'Arrigo et al. 2008). In cases where no causative gene defect for the ataxia was identified response to CoQ_{10} supplementation was also variable. Two patients demonstrated an improvement in muscle symptoms but not ataxic symptoms (Boitier et al. 1998; Musumeci et al. 2001). Nine patients demonstrated a decrease in the International Cooperative Ataxia Rating Scale (ICARS) (Pineda et al. 2010; Artuch et al. 2006; Gironi et al. 2004). Furthermore eleven patients with an undefined defect were refractory to treatment (Lamperti et al. 2003; Terracciano et al. 2012).

Two patients with Leigh syndrome and one patient with cardiofaciocutaneous syndrome improved after treatment (Aeby et al. 2007; Van Maldergem et al. 2002) and a patient with hypotonia and infantile spasms did not show any sign of improvement (Huntsman et al. 2009).

1.5.2. Secondary CoQ_{10} Deficiency

Large scale clinical trials are not feasible for primary CoQ_{10} deficiency due to the small number of patients, however many clinical trials have taken place in relation to a number of neurogenerative diseases. Success has been seen in the treatment of FA with CoQ_{10} in conjunction with vitamin E, whereby 49% of patients demonstrated an improvement in the ICARS score (Cooper et al. 2008). However this study did not have a placebo/no treatment group for comparison and this was only a small scale study (n=50). Interestingly despite the initial success seen in CoQ_{10} supplementation for PD (Shults et al. 2002) the recent Phase III trial was terminated after it was deemed unlikely to yield significant results (Beale et al. 2011). Publication of further analysis is pending, however this abstract did outline a trend towards a worse Universal Parkinson's Disease Rating Scale (UPDRS) score.

Owing to the increasing evidence of CoQ_{10} deficiency in mitochondrial diseases a phase III clinical trial is also underway investigating CoQ_{10} supplementation in

mitochondrial disease (Hassani et al. 2010). This is a randomized placebo-controlled, double- blinded trial to assess the safety and efficacy of CoQ_{10} in patients with mitochondrial disease.

1.6. Aims

The overall objective of this thesis was to investigate the pathogenesis of neurological CoQ_{10} deficiency at a cellular, biochemical level and to utilise this knowledge to understand why CoQ_{10} supplementation may not be successful in treating neurological CoQ_{10} disease.

Another objective will be to develop an analytical method capable of quantifying CoQ_{10} in CSF. The diagnosis of CoQ_{10} deficiency is currently unreliable. Quantification of CoQ_{10} in fibroblasts and muscle does not always result in the diagnosis of a CoQ_{10} deficiency, despite confirmation of an *ADCK3* gene mutation. Consequently a test for CSF CoQ_{10} quantification would not only be useful diagnostically, but also in monitoring CoQ_{10} supplementation.

Chapter 2

Materials and Methods

2.1. Materials

The following were purchased from VWR International Ltd (Lutterworth, UK):

Potassium Phosphate (analar grade); Potassium dihydrogen phosphate (analar grade); Magnesium Chloride Hexahydrate (analar grade); Potassium Cyanide (analar grade); Ethanol (analar grade); EDTA K+ (analar grade); Perchloric acid 60% (Hipersolv for HPLC); Ethanol 96% (Hipersolv for HPLC); n-Hexane (Hipersolv for HPLC); Methanol (Hipersolv for HPLC); Potassium hydroxide pellets (analar grade); 85% Orthophosphoric acid (Hipersolv for HPLC)

The following were purchased from Sigma Aldrich (Poole, UK):

Triton X-100; SigmaUltra ≥ 99.5%; Sterile 0.4% Trypan blue; Dimethyl sulphoxide; Coenzyme Q_1~95%; β-Nicotinamide adenine dinucleotide, reduced disodium salt hydrate ≥ 97%; Rotenone ≥ 95%; BSA (Bovine Serum Albumin) ≥ 96%; Trizma-base (reagent garde); Cytochrome *c* from equine heart ≥ 95%; Antimycin A from *Steptomyces sp*.; Sodium succinate dibasic hexhydrate *ReagentPlus*®, ≥ 99%; 5,5'-Dithiobis(2-nitrobenzoic acid), ≥ 98%; Acetyl coenzyme A sodium salt, ≥ 93%; Oxaloacetic acid, ≥ 97%; L-Ascorbic acid, cell culture tested; Potassium hexacyanoferrate(III), *ReagentPlus*®, ~99%; Coenzyme Q_{10}, ≥ 98%; Sodium perchlorate, 98%; 1-Propanol, chromasolv® for HPLC, ≥ 99.9%; Oligomycin from *Streptomyces sp.*; Carbonyl cyanide-4-(trifluoromethoxy)phenylhydrazone, ≥ 98%;

Sterile cell culture products: Dulbecco's modified eagles medium/Ham's F-12 Nutrient Mixture (DMEM/F-12) (1:1) with No L-glutamine; L-glutamine; Fetal bovine serum, heat inactivated (EU approved origin); 0.25% Trypsin-EDTA were purchased from Invitrogen Ltd (Paisley, UK).

Microscopy probes were all purchased from Invitrogen Ltd (Paisley, UK).

Disposable PD-10 Desalting Columns were purchased from GE Healthcare Lifesciences (Amersham, UK).

HPLC vials and caps were purchased from Chromacol (Welwyn Garden City, UK).

Techsphere ODS 5µ, 150 x 4.6mm and Techsphere ODS C18, 250 x 4.6mm HPLC columns were purchased from HPLC technology (Welwyn Garden City, UK).

DC total protein assay Reagent A and Reagent B were purchased from Bio-Rad Laboratories Ltd (Hemel Hempstead, UK).

2.2. Tissue Culture

2.2.1. Cell Line

The SK-N-SH cell line was conceived from a bone-marrow biopsy of a four year old female patient with a neuroblastoma of the chest (Biedler et al. 1973). This line contained two distinct cell groups: a neuroblast-like cell and an epithelial-like cell. The neuroblast-like cell group was three times sub-cloned as SH-SY, SHSY5 and finally SH-SY5Y (Biedler et al. 1978). The SH-SY5Y cell line has a neuroblast-like morphology (Figure 2.2) and the SK-N-SH cell line that it was cloned has been shown to have various neurotransmitter activities: dopaminergic, acetylcholinergic and adenosinergic (Biedler et al. 1978).

2.2.2. Cell Passage

SH-SY5Y cells were acquired from the European Collection of Cell Cultures (Health Protection Agency, Salisbury, UK). Cells were seeded at a density of 1 x 10^4 cells/cm^2 into 75cm^2 tissue culture flasks and maintained in Dulbecco's modified Eagle's medium/ Ham's F-12 nutrient mixture (1:1; DMEM/F-12; Invitrogen) supplemented with 10% fetal bovine serum (FBS) and 2mM L-Glutamine. Cells were grown at +37°C in 95% air and 5% CO_2. The culture medium was replaced the day after seeding. Cells were passaged at 80-90% confluence, approximately every 5-6 days. Passaging was undertaken in sterile conditions and involved washing once with 5mL Hank's balanced salt solution (HBSS) at +20°C. Cells were then lifted with 1mL/flask of 0.25% trypsin-EDTA (Invitrogen) and incubated at +37°C for 3min. The cell surface of the flask was then washed with 5 ml of HBSS and cells were collected by centrifugation at 500xg for 5min at +25˚C. The supernatant was removed and the cells were re-suspended in DMEM/F-12+10% FBS. 100µL cell suspension was mixed 1:1 with 4g/L trypan blue and cells counted using a Neubauer improved haemocytometer. Live cells (colourless and bright) were counted in the 4 corner

squares (Figure 2.1) and an average was taken. The number of cells per ml was then calculated (average number of cells in corner squares x dilution factor x 10^4). To obtain reproducible results only cells of passage number 19 to 24 were used for experiments.

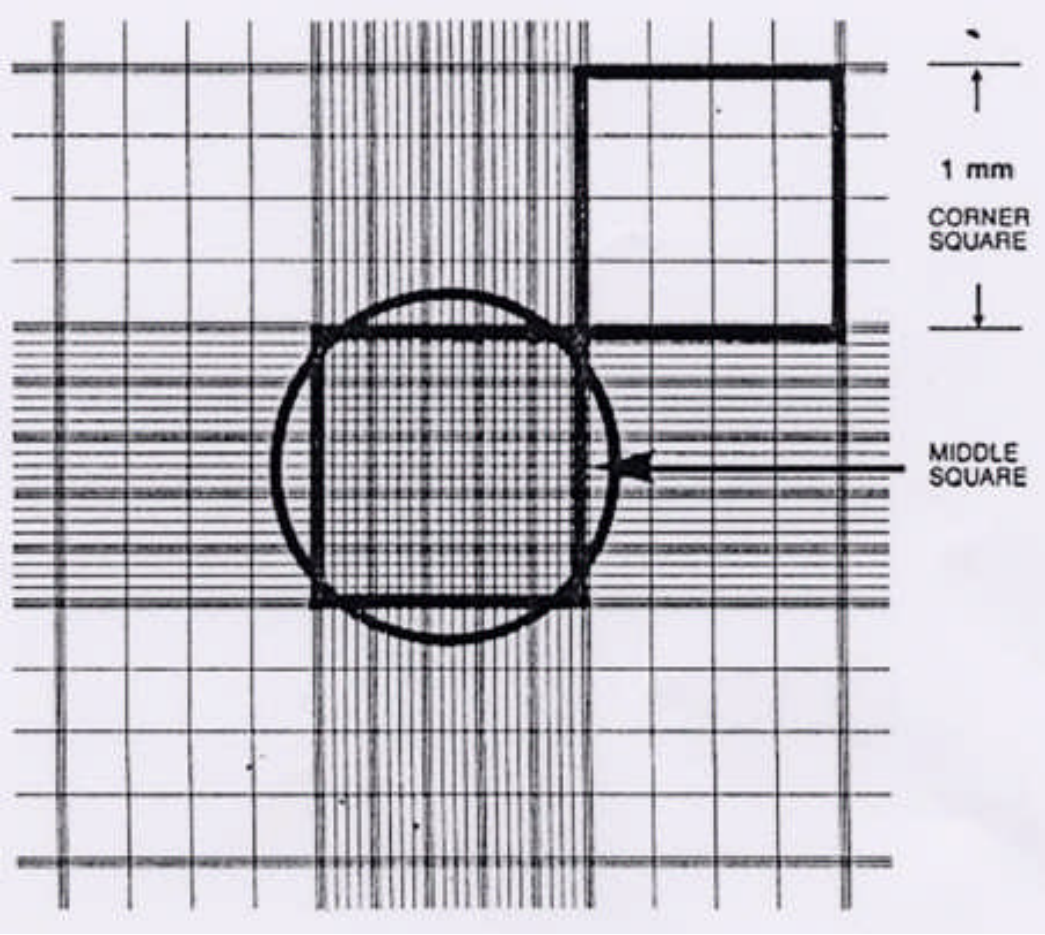

Figure 2.1 Haemocytometer

Used for counting cells as seen under a microscope

2.2.3. Cell Storage and Recovery

Cells were stored in liquid nitrogen at a density of 1 x 10^6 cells/mL in 40% FBS, 10% dimethyl sulphoxide (DMSO) and 50% DMEM/F-12 as 1mL aliquots. Cells were first frozen for 24hr in -80°C using an isopropanol freezing vessel and then transferred to liquid nitrogen for long term storage. Cells were recovered from liquid nitrogen and seeded at a density of 5 x 10^5 cells/cm^2 in 75cm^2 flasks.

2.2.4. Treatment of SH-SY5Y Cells

We set out to use a method previously described by González-Aragón et al in 2005. This study used 1mM Para-aminobenzoic acid (PABA) treatment over a 4 day time course on cultured HL-60 (Human promyelocytic leukemia cells) cells. This method originally used in 1975 by Alam, Nambidiri and Rudney works through competitively inhibiting the biosynthesis of CoQ_{10}. More specifically PABA competes with para-hydroxybenzoate for the active site of polyprenyl-4-hydroxybenzoate transferase (Alam et al. 1975).

Cells were treated with various concentrations of PABA: 0mM (no PABA treatment), 0.25mM, 0.5mM, 0.75mM and 1mM. Incubation of neuronal cells with a PABA concentration greater than 1mM did not induce a further decrease in cellular CoQ_{10} (see Section 3.4.1). Therefore 1mM PABA was selected as the upper limit of treatment. The cells were grown in the presence of the listed concentrations over a 5 day time course.

In Chapter 4 and Section 1.1.1 cells were subsequently treated with CoQ_{10} (Sigma) and methylene blue (MB; chapter 4; Sigma). Cells were treated with 2.5 and 5 µM CoQ_{10} for 5 days; as this is the approximate concentration reached in the plasma of patients undergoing CoQ_{10} supplementation (López et al. 2010; Miles 2007; Bhagavan & Chopra 2006).

Cells were also treated with MB in parallel with the CoQ_{10} supplementation. Here we chose to use a concentration range of: 0.1, 0.5 and 1 µM for 5 days. Cells treated with 2 µM MB and greater died after 24 hours.

As the CoQ_{10} formulation that we are using is suspended in ethanol and due to the lipophilic nature of CoQ_{10} is can be challenging to get into aqueous solution (this is discussed further in chapter 4). Thus, to ensure optimal absorption we

incubated the media plus CoQ_{10} at +37°C for 15 minutes prior to addition of the SH-SY-5Y cells.

2.2.5. SH-SY5Y Cell Harvesting for Biochemical Analysis

Cells were seeded at a density of 1 x 10^4 cells/cm^2 into 175/75cm^2 tissue culture flasks or 6 wells plates for the ATP assay. Following a 5 day treatment with various concentrations of PABA the cells were harvested for testing (see Section 2.2.4). Cells were washed once with HBSS and lifted with trypsin-EDTA at +37°C for 3 min. Trypsin was quenched by the addition of an equal volume of DMEM/F-12. The cell surface of the flask was then washed with 5 ml of HBSS and cells were collected by centrifugation at 500xg for 5min at +4˚C. The supernatant was removed and the cells washed by resuspension in HBSS and centrifugation at 500xg for 5min at +4˚C. The supernatant was removed and cells were resuspended in HBSS. The cells were then aliquoted into seven eppendorfs and stored at -80°C; one eppendorf to be used for the determination of: ETC Complex I,II+III and IV, citrate synthase (CS), CoQ_{10}, total GSH and total protein. The samples for assessment of ATP in the 6 well plates were assayed immediately.

2.2.6. SH-SY5Y Cell Harvesting for Microscopy

For live cell imaging microscopy analysis cells were required to be alive and adherent to 22mm cover slips. The cover slips were sterilized with 100% ethanol, left to dry for ~15 mins, then placed (one coverslip per well) into a 6 well plate. Cells were seeded at a density of 1 x 10^4 cells/cm^2 and were treated over a 5 day time-course (see Section 2.2.4).

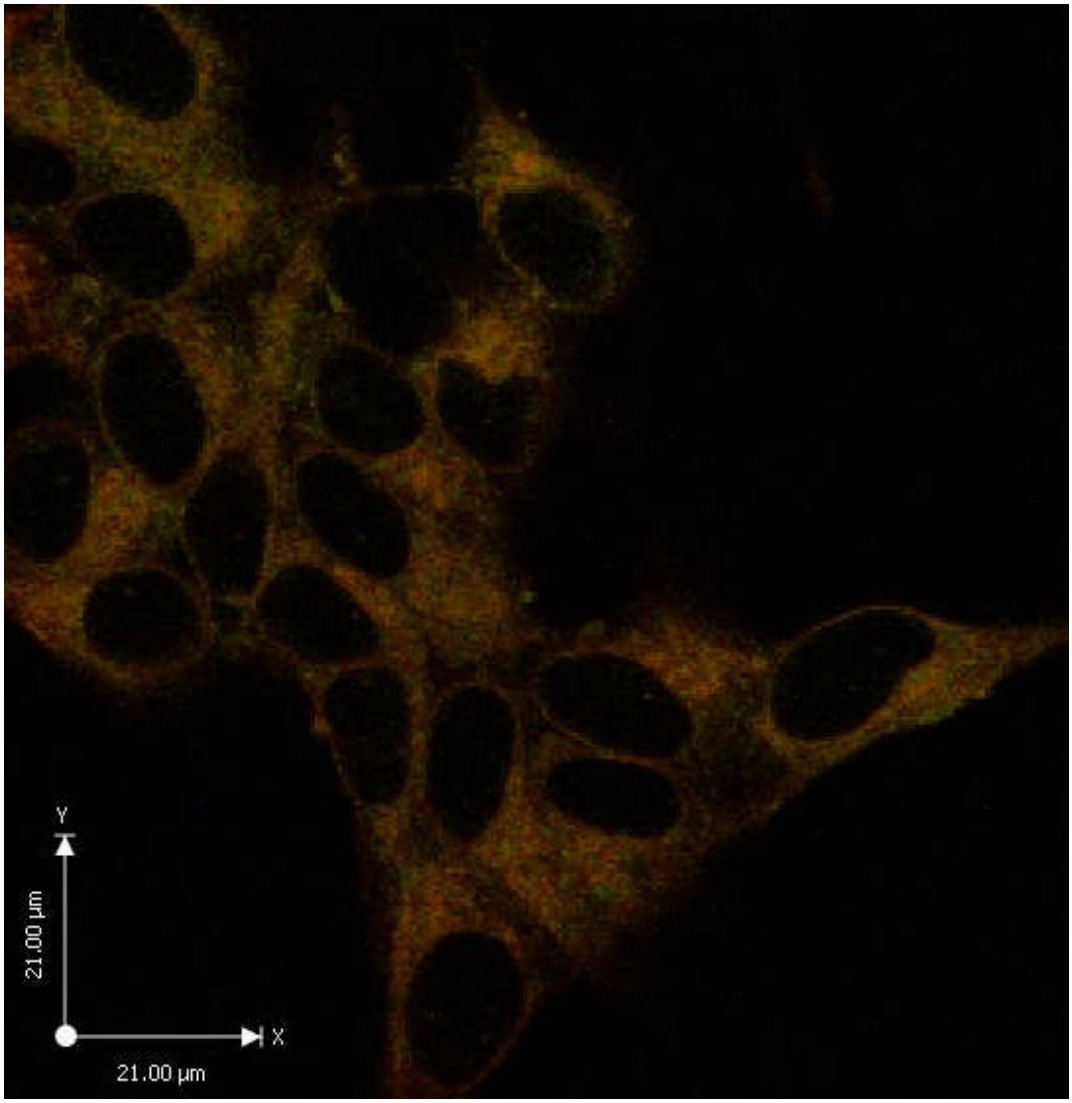

Figure 2.2 SH-SY5Y Neuroblastoma Cells stained with Bodipy 581/591, a Lipid Peroxidation Marker

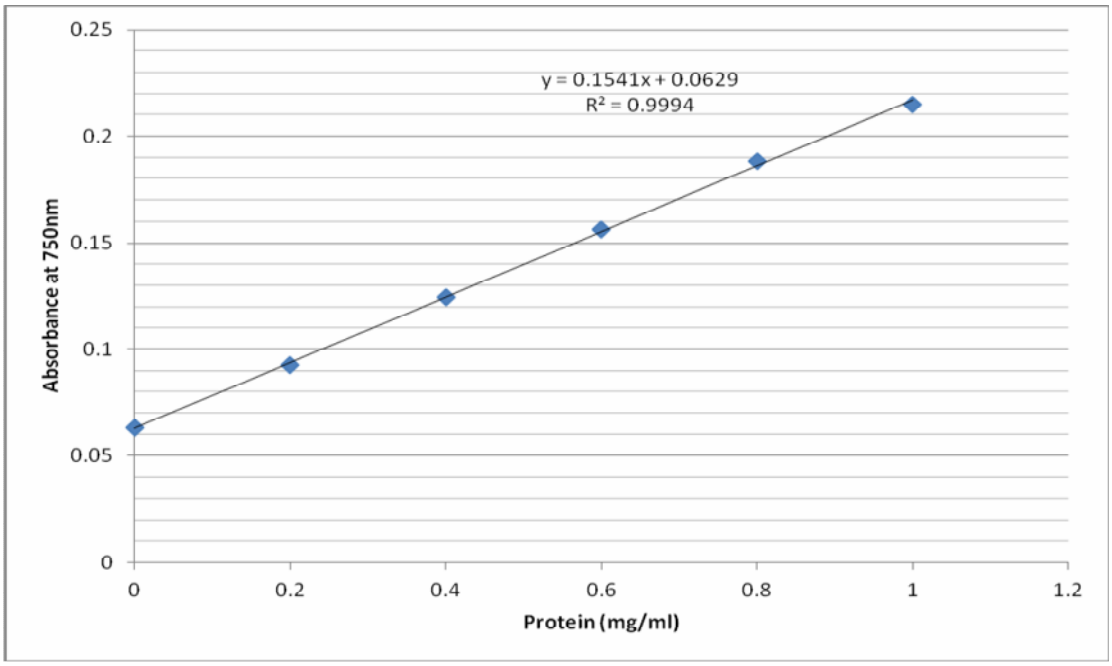

Figure 2.3 A typical Bovine Serum Albumin (BSA) standard line

A 6 point concentration curve (0-1mg/ml). The BSA standard line is used to determine the concentration of protein in a given solution. Absorbance values for a solution are read across to the standard line to determine the concentration of protein (e.g. If absorbance= 0.1, then protein concentrations=0.24mg/ml)

2.3. Total Protein Determination

Total protein was determined by the Bio-Rad DC-protein assay (Bio-Rad Laboratories Ltd, Hemel Hempstead, UK). This assay is a modified method based on that of Lowry et al. (1951). The assay was performed as per manufacturer's instructions. Briefly all samples were diluted in HPLC grade H_2O. A 6-point standard line was prepared with BSA in distilled water from 0 to 1mg/mL. 5µL of each standard and sample were added to 3 wells of a 96 well plate. 25µL reagent A (alkaline copper tartrate) and 200µL reagent B (Folin-Ciocalteau phenol) was added to each sample. Samples were incubated for 15 min at +25˚C, in the dark. After incubation absorbance of samples was measured at 750nm using a FLUOstar omega plate reader (BMG Labtech Ltd). Total protein was determined from linear regression of sample absorbance units against the BSA standard line (Figure 2.3).

2.4. Coenzyme Q_{10} Quantification

2.4.1. Equipment

PU-980 intelligent pump (Jasco); AS-950 intelligent autosampler (Jasco); Techsphere ODS 5µ, 150 x 4.6mm column; TSPChromojet SP4400 series integrator; PG-975-50 UV/VIS detector (Jasco).

2.4.2. Procedure

CoQ_{10} was measured using reversed-phase HPLC with Ultraviolet (UV) detection using a modified method of that described by Boitier et al (1998). The mobile phase was prepared by dissolving 7g of sodium perchlorate to Ethanol-Methanol-60% (v/v) perchloric acid (700:300:1.2). The flow rate was 0.7mL/min (see Figure 2.6 for HPLC schematic diagram).

To account for the loss of analyte during sample preparation an internal standard (IS) was added before the CoQ_{10} was extracted from each sample. Dipropoxy-CoQ_{10} was first proposed for use as an internal standard in 2005 by Duncan et al. Previously naturally occurring ubiquinones have been used as ISs, i.e. CoQ_9, however, contamination with both dietary sources and endogenous synthesis is possible. Dipropoxy-CoQ_{10} is advantageous because it is a chemically synthesised compound with very similar characteristics to

CoQ_{10}. The IS (200 nM) was added to the cell sample prior to extraction. Cellular membranes were disrupted by freeze thawing three times followed by vigorous mixing using a vortex. Extraction of CoQ_{10} involves the addition of 5:2 (v/v) hexane/ethanol. Samples were centrifuged at 15,000 rpm for 3 min at +25˚C and the top hexane layer was collected and stored on ice. The lower aqueous layer is re-extracted a further two times. Samples were evaporated using a rotary evaporator, resuspended in 300 µl ethanol and filtered (using a 4-SF-02 (PV) filter) prior to injection.

A working standard (200nM CoQ_{10} and 200nM dipropoxy-CoQ_{10}) was injected for calibration (Figure 2.5). 50µL of each sample was injected and separated on a C18 reversed phase Techsphere ODS 5µ, 150 x 4.6mm column (HPLC Technology, Welwyn Garden City, UK), maintained at +25˚C. CoQ_{10} is detected using an online UV detector (PG-975-50 UV/VIS detector) at a wavelength of 275nm (

Figure 2.4).

2.4.3. Data Analysis

CoQ_{10} was quantified using the following equation:

Conc CoQ_{10} (pmol/ml) =

(sample peak area /internal standard peak height) x internal standard conc. (µM)

Dilution factor:

Conc CoQ_{10} (pmol/ml) =

(Conc CoQ_{10} (pmol/ml) x resuspension volume) / volume of extracted sample

For intracellular determination of CoQ_{10} the concentration was divided by total protein (mg/mL) and expressed as pmol/mg of protein (see Section 2.3).

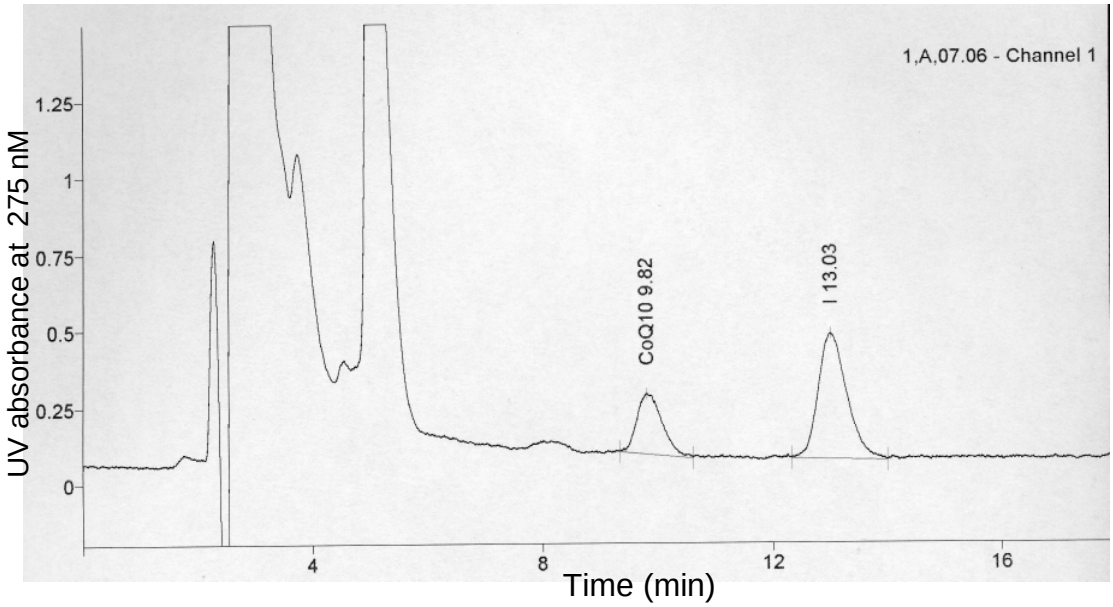

Figure 2.4 A Typical CoQ_{10} Chromatogram for a SH-SY5Y Cell Sample

Samples quantified using a UV detection method. CoQ_{10} elutes at ~9.5 minutes and I (Internal standard [di-propoxyCoQ_{10}]) elutes at ~13 minutes.

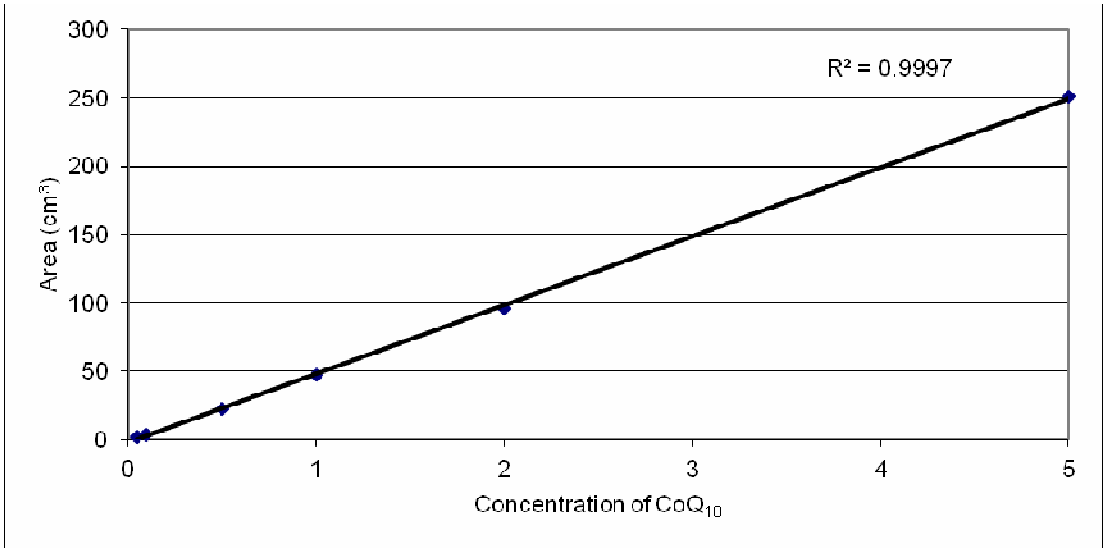

Figure 2.5 Concentration Curve for CoQ_{10} (HPLC-UV Detection Method)

The area (height x width) of the CoQ_{10} peak recorded on a using a HPLC with UV detection. 6 concentrations of CoQ_{10} (0-5uM) were used to determine the linearity of the method.

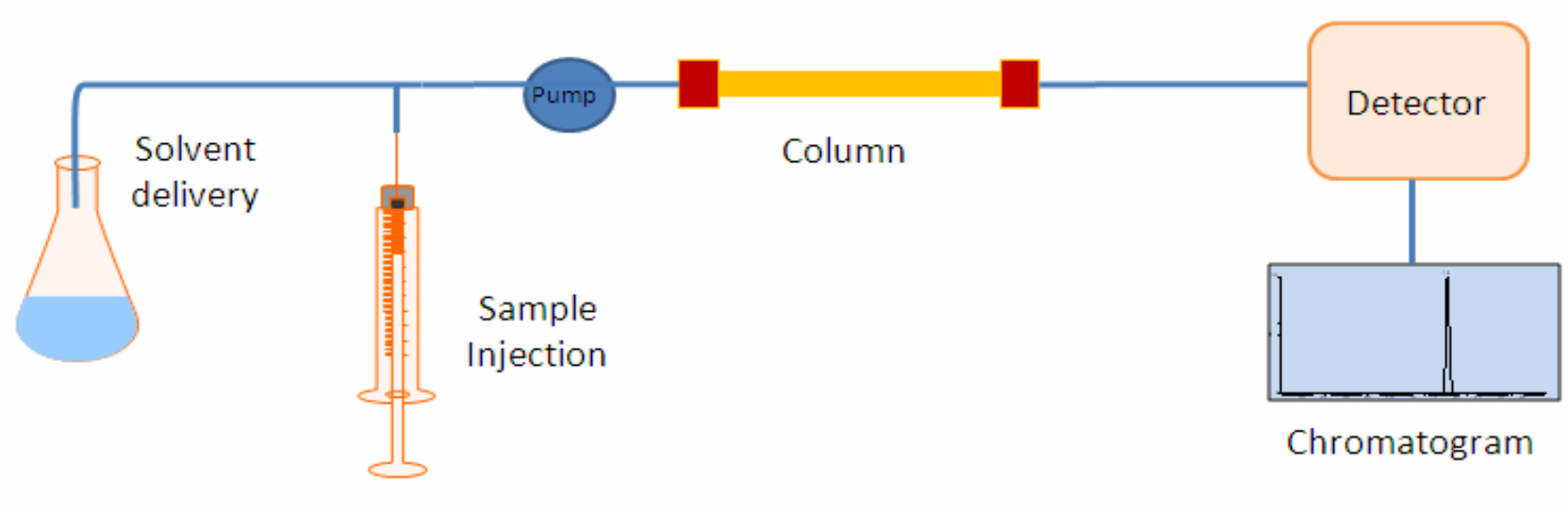

Figure 2.6 Schematic Diagram of a High Performance Liquid Chromatography (HPLC) System

The sample is delivered into the solvent via an injector and pumped around the HPLC system using a pump. The molecule of interest is then separated by the column and the detector displays a visual read out called a chromatogram that can be interpreted to determine the separation of the molecule of interest.

2.5. Reduced Glutathione (GSH) Quantification

2.5.1. Equipment

PU-1580 pump (Jasco); AS-2055 Plus autosampler (Jasco); Techsphere ODS C18, 250 x 4.6mm column; Coulochem II electrochemical detector (ESA); 5010 analytical cell (ESA); Thermo Finnigan Chromjet integrator (Thermo Fisher Scientific, Rockford, IL, USA); DG-980-50 inline degasser (Jasco).

2.5.2. Procedure

GSH was measured using reversed-phase high performance liquid chromatography (HPLC) with coulometric electrochemical detection using the method of Riederer et al (1989). The mobile phase consisted of 15mM orthophosphoric acid in HPLC grade H_2O. The flow rate was 0.5mL/min (see Figure 2.6 for HPLC schematic diagram).

Samples were subjected to three cycles of freeze-thawing to disrupt cellular membranes and subsequently diluted in 15mM orthophosphoric acid. They were then centrifuged at 15,000rpm for 5 minutes +5^{o}C, and the supernatant was removed for analysis. 50µL of each sample was injected and separated on a C18 reversed phase 250 x 4.6mm Techsphere ODS column (HPLC Technology, Welwyn Garden City, UK), maintained at +25˚C. The screening electrode (E1) was set to +50mV to oxidise analytes of low oxidation potential. Optimum potential for the detector electrode (E2) was determined via a voltamogram (Figure 2.7A). This involved monitoring the peak height of a 5µM glutathione standard between a range of detector electrode potentials (+300mV to +800mV). A maximum response was achieved with 750mV, and thus was used for analysis. Samples were quantified against an external standard of 5µM GSH diluted in 15mM orthophosphoric acid. A calibration curve confirmed linearity between 0.1µM and 25µM (r^2 = 0.995) (Figure 2.7B). Figure 2.8 shows a typical GSH chromatogram.

2.5.3. Data Analysis

GSH was identified using a Thermo Finnigan Chromjet integrator (Thermo Fisher Scientific) and quantified using the following equation:

Conc. (μM) =

(sample peak height /external standard peak height) x external standard conc. (μM)

For intracellular determination of GSH the conc. (μM) was divided by total protein (mg/mL) and expressed as nmol/mg of protein (see Section 2.3).

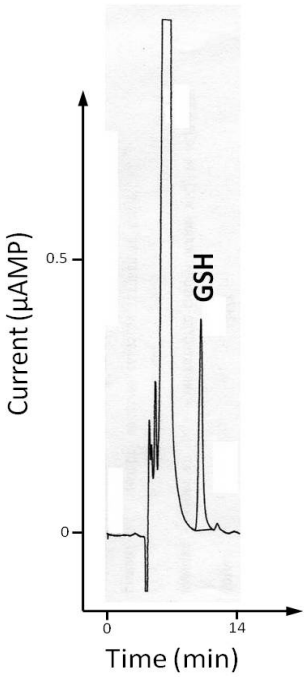

Figure 2.7 A Typical Reduced glutathione (GSH) Chromatogram for a SH-SY5Y Cell Sample

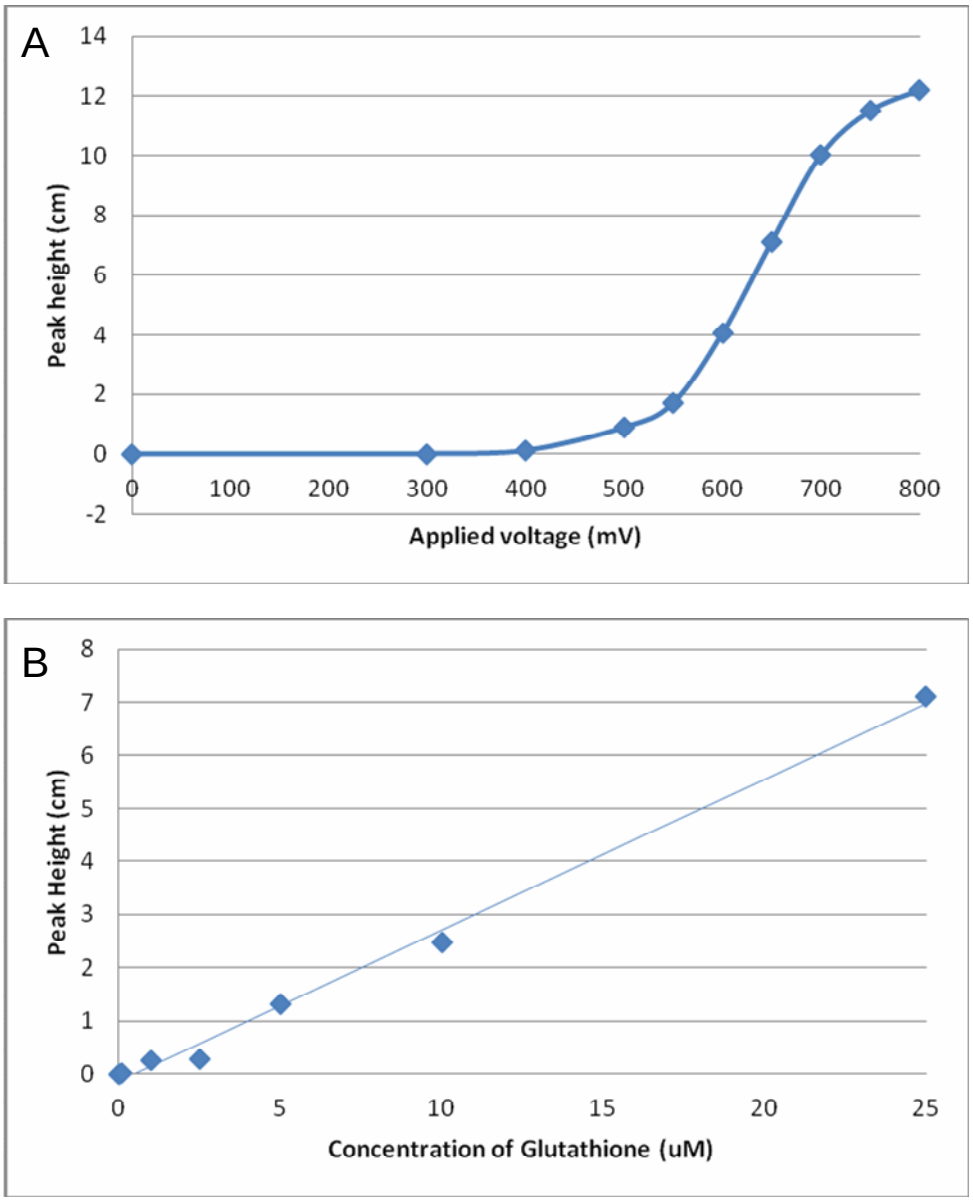

Figure 2.8 Reduced Glutathione (GSH) A) Voltamagram- utilised to find the optimum electrochemical detector (EC) electrode voltage. A voltage on the plateau of the voltamagram ensures detection of the entire compound of interest, B) Calibration Curve- increasing concentrations of GSH produce a proportional increase in chromatogram peak height, demonstrating linearity of the EC detector method

2.6. Enzyme Assays

2.6.1. Complex I Assay (NADH:ubiquinone reductase; EC 1.6.5.3)

This assay is based on that described by Reed & Ragan (1987). It measures the oxidation of NADH by Complex I, as the decrease in absorbance at 340nm. During this process electrons are transferred to exogenous ubiquinone (CoQ_1) forming ubiquinol. NADH oxidation also occurs in other cellular processes that are mainly anabolic e.g. gluconeogenesis. Rotenone (a specific Complex I inhibitor) is used to determine the level of Complex I independent NADH oxidation. Rotenone acts on the matrix embedded long arm of the complex arresting electron transfer from the Fe-S cluster to CoQ (Friedrich et al. 1994).

20µL of each sample was added to two analogous cuvettes containing at final concentration 2.5mg/mL bovine serum albumin (BSA), 0.15mM β-NADH, 1mM potassium cyanide (KCN) in a 20mM potassium phosphate buffer + 8mM magnesium chloride (pH 7.2). The final volume in each cuvette was 1mL. Samples were then gently mixed by double invertion and inserted into the Uvikon 941 spectrophotometer (Northstar Scientific, Potton, UK). Duplicate cuvettes were placed into either the reference or sample compartment. The reaction was started by the addition of 10µL 5mM CoQ_1 into the sample cuvette. The reaction was monitored at an absorbance of 340nm at 30sec intervals for 5min at +30˚C. 20µL 1mM rotenone was added to each sample cuvette and measurement was continued for 5min. Subtraction of the decrease before and after rotenone addition will produce a specific value for Complex I NADH oxidation. Absorbance was converted to molar concentration using the Beer-Lambert law:

$$c = \frac{\Delta A \times l}{\varepsilon}$$

Where ΔA is the specific change in absorbance; ε = extinction coefficient (6.81 x 10^3 M^{-1} cm^{-1}); l = path length (1cm) and c = mole/min/ml.

Results are expressed as nmol/min/mg of protein (for protein determination method see Section 2.3); then as a ratio of mitochondrial specific citrate synthase activity (see Section 2.6.4), to control for mitochondrial enrichment/depletion. Linearity of Complex I activity (R^2=0.999) with total protein was quantified to further validate the method Figure 2.9A.

2.6.2. Complex II/III Assay (succinate cytochrome c reductase; EC 1.8.1.3)

Complex II/III was measured by a method described by (Bhuvaneswaran & King 1967). Complex II (succinate dehydrogenase; EC 1.6.5.3) catalyses the oxidation of succinate to fumarate and in the process reduces ubiquinone to ubiquinol. Ubiquinol then acts as an electron donor facilitating the reduction of cytochrome *c* by Complex III (Cytochrome bc^1 complex; EC 1.10.2.2). This assay measures the reduction of cytochrome *c* by measuring an absorbance increase at 550nm. The Complex III inhibitor, antimycin A is used to discover the level of cytochrome *c* oxidation which is not dependant on Complex II/III activity. Antimycin A binds to the Qi site of cytochrome c reductase, thereby inhibiting the oxidation of ubiquinol.

20µL of each sample was added to a two analogous cuvettes containing at final concentration 0.3mM EDTA, 1mM KCN, 0.1mM cytochrome c in 100mM potassium phosphate buffer (pH 7.4). The final volume in each cuvette was 1mL. Samples were then gently mixed by double invertion and inserted into the Uvikon 941 spectrophotometer (Northstar Scientific, Potton, UK). Duplicate cuvettes were placed into either the reference or sample compartment. The reaction was started by the addition of 40µl of 0.5M succinate to the sample cuvette. The reaction was measured at an absorbance of 550nm at 30sec intervals for 5min at +30˚C. 10µL 1mM antimycin A was added to each sample cuvette and measurement was continued for 5min. Subtraction of the increase before and after antimycin A addition will produce a specific value for Complex II/III cytochrome *c* reduction. Absorbance was converted to molar concentration using the Beer-Lambert law as described earlier (see Section 2.6.1). The extinction coefficient of cytochrome *c* is 19.2×10^3 M^{-1} cm^{-1} (path length 1 cm, total volume 1mL). Results are expressed as nmol/min/mg of protein (see Section 2.3) or as a ratio to citrate synthase activity (see Section 2.6.4). Linearity of Complex II/III activity (R^2=0.996) with total protein was quantified to further validate the method Figure 2.9B.

2.6.3. Complex IV Assay (Cytochrome c oxidase; EC 1.9.3.1)

Complex IV was measured by the method of Tzagoloff & Wharton (1965). This assay measures the oxidation of cytochrome *c* catalysed by Complex IV.

0.8M oxidized cytochrome c is first reduced by the addition of a few crystals of ascorbic acid. A PD10 desalting column equilibrated with 10mM potassium phosphate buffer (pH 7.0) was used to remove ascorbate from the now reduced cytochrome *c.* To quantify the concentration of reduced cytochrome *c*, 50µL was added to 950µL H_2O in a sample and a reference cuvette and the sample cuvette was blanked against the reference at 550nm using a Uvikon 941 spectrophotometer (Northstar Scientific). Cytochrome *c* in the reference cuvette was then oxidsed by the addition of 10µL100mM ferricyanide. The absorbance was recorded after 1min and used to determine the concentration of reduced cytochrome *c* using Beer-Lambert law (see Section 2.6.1). The extinction coefficient for cytochrome *c* is 19.2 x 10^3 M^{-1} cm^{-1} (path length 1 cm, total volume 1mL).

Reduced Cytochrome c to a final concentration of 50µM was then added to sample and reference cuvettes containing 10mM potassium phosphate (pH 7.0) to a final volume of 1mL. The sample cuvette was blanked against the reference at 550nm using a Uvikon 941 spectrophotometer (Northstar Scientific).10µL 100mM ferricyanide was added to the reference cuvette. The reaction was started by the addition of 20µL sample to the sample cuvette and the change in absorbance at 550nm was recorded over 3min at +30˚C. The reaction of Complex IV with cytochrome c follows first-order kinetics as it is dependent on the concentration of cytochrome *c*. Activity is therefore expressed as a first order rate constant (k). k is calculated by plotting the natural log of absorbance against time and determining the slope. Results are expressed as k/min/mg of protein (see Section 2.3) or as a ratio to citrate synthase activity (see Section 2.6.4). Linearity of Complex IV activity (R^2=0.999) with total protein was quantified to further validate the method Figure 2.9C.

2.6.4. Citrate Synthase Assay (CS; EC 4.1.3.7)

CS is an enzyme in the citric acid cycle which catalyses the condensation of oxaloacetate and acetyl-coenzyme A to form citric acid and coenzyme A. It is found within the mitochondrial matrix and is commonly used as a measure of mitochondrial enrichment (Almeida et al. 1998; Hargreaves et al. 1999). The assay used was described by Shepherd & Garland in 1969. The assay measures the production of coenzyme A via a reaction with 5, 5'-dithio-bis (2-nitrobenzoic acid) (DTNB).

20µL of each sample was added to two analogous cuvettes containing at final concentration 0.1mM acetyl-coenzyme A, 0.2mM DNTB in 100mM tris buffer (pH 8.0) + 1g/L triton X-100. The final volume in each cuvette was 1mL. Samples were then gently mixed by double invertion and inserted into the Uvikon 941 spectrophotometer (Northstar Scientific, Potton, UK). Duplicate cuvettes were placed into either the reference or sample compartment. The reaction was started by the addition of 10µL 20mM oxaloacetate to the sample cuvette. The reaction measured at 412nm for 5min at 30sec intervals for 5min at +30˚C. Absorbance was converted to molar concentration was calculated using Beer-Lambert law (see Section 2.6.1). The extinction coefficient of DTNB is 13.6 x 10^3 M^{-1} cm^{-1} (path length 1 cm, total volume 1mL). Results are expressed as nmol/min/mg of protein (see Section 2.3). Linearity of CS activity (R^2=0.999) with total protein was quantified to further validate the method Figure 2.9D.

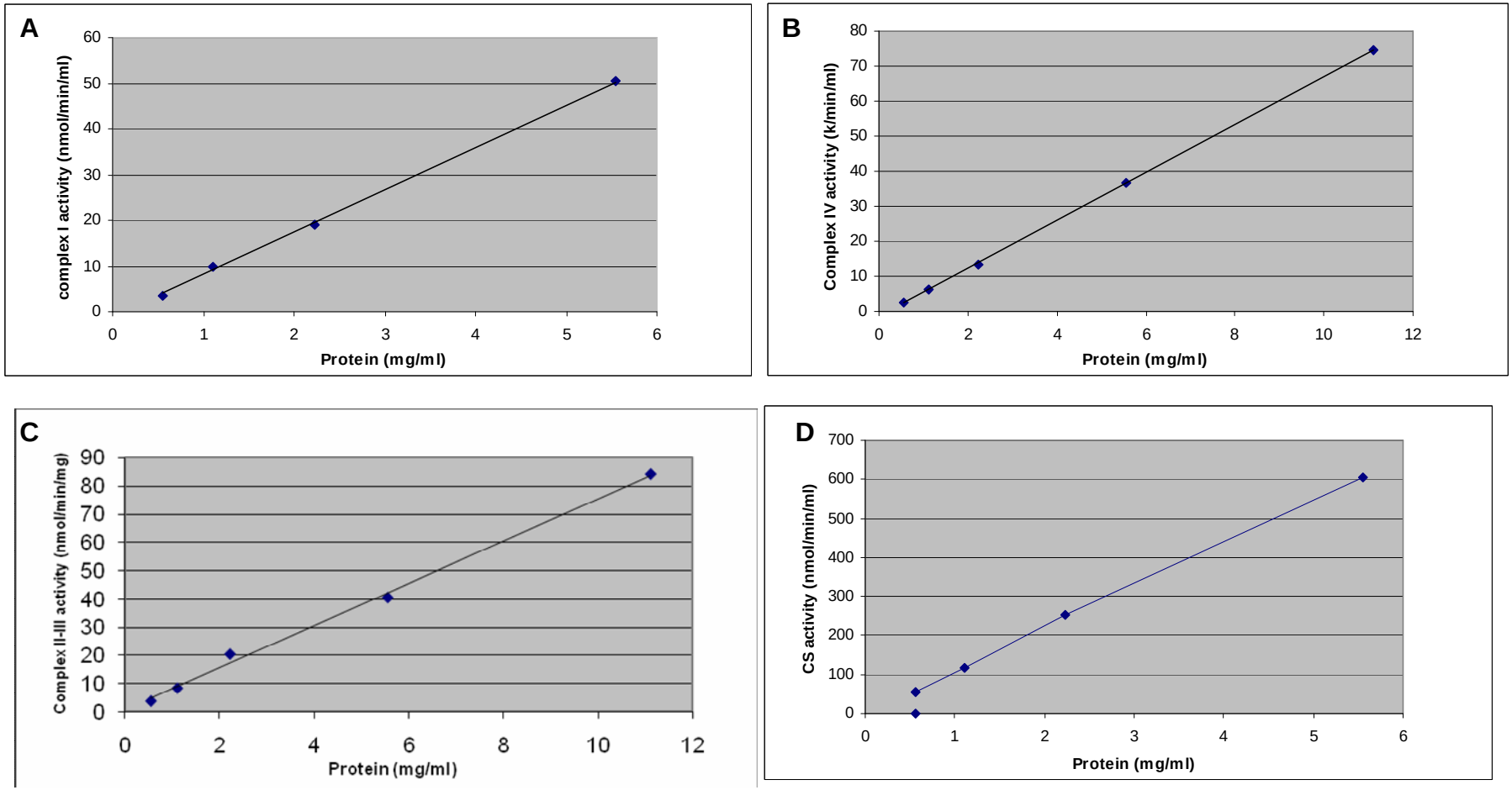

Figure 2.9 Linearity of Mitochondrial Complex Activities versus SH-SY5Y protein- demonstrating an increase in the level of SH-SY5Y protein produces a proportional increase in enzyme activity. A) Complex I: R^2=0.999, B) Complex II/III: R^2=0.996, C) Complex IV: R^2=0.999, D) Citrate Synthase: R^2=0.999

2.6.5. Complex V (EC 3.6.3.14) in Gel Assay

BN-PAGE can be used for one-step isolation of protein complexes from biological membranes and total cell and tissue homogenates. It can also be used to determine native protein masses and oligomeric states and to identify physiological protein–protein interactions. BN-PAGE was developed for the separation of mitochondrial membrane proteins and complexes in the mass range of 10 kDa to 10 Mda (Witting et al. 2000).

Nonionic detergents are used for solubilisation of biological membranes. One of the mildest detergents is digitonin Dodecylmaltoside may also be used and has stronger delipidating properties compared to digitonin. The anionic dye Coomassie blue G-250 is added to the supernatant. This dye binds to membrane proteins because of its hydrophobic properties. The dye imposes a charge shift on the proteins that causes even basic proteins to migrate to the anode at pH 7.5. During BN-PAGE proteins are separated according to size in acrylamide gradient gels.

Blue native gel electrophoresis was used to further examine the effect of CoQ_{10} deficiency on mitochondrial ETC protein levels, and on Complex V (ATP synthase) activity. A mitochondrial fraction was initially obtained from the SHSY-5Y cell pellet (7.5 $x10^5$ cells) using two low speed centrifugation steps (600g x 10min) at +4°C, separated by a homogenisation step (30 strokes). The supernatant from each spin was combined and a higher spin (14,000g x 10 min) was performed in order to eliminate nuclei and other subcellular membranes. The mitochondrial membranes were then solubilised using a 750mM amino hexanoic acid/50mM Bis Tris buffer + 4% n-dodecyl β-D maltoside detergent. Samples were left on ice for 30 minutes and a further high spin (14,000g x 10 min) was used to pellet insoluble material.

Mitochondrial protein was quantified via a Bradford protein assay (Bradford 1976). An equal quantity of mitochondrial protein (30µg) was loaded for each condition. The blue native gel was run using a 3-12% Bis-Tris gel (Invitrogen) to ensure discrete separation of Complex V. Blue native gel electrophoresis was performed according to an adaption of a previously reported method (Witting et al 2006). The in-gel Complex V activity staining involved incubation at +25°C overnight with the Complex V activity stain (34mM Tris, 270mM glycine, 14mM magnesium chloride, 6mM Lead (II) nitrate and 8mM ATP). The stain measures

Complex V activity in the reverse mode i.e. lysis of the ATP supplied. The inorganic phosphate produced by this process results in the accumulation of lead phosphate where the Complex V is present.

The complex protein levels and the Complex V activity bands were quantified by scanning with a Biorad Chemidoc™ XRS 170-8070 system densitometer (Bio-Rad Laboratories, UK). The Complex V activity reading was then divided by the protein reading, as the protein readings obtained for each condition were variable.

2.6.6. Adenosine Triphospate (ATP) Assay

ATP is a multifunctional coenzyme which is often referred to as the "molecular unit of currency" in intracellular energy transfer. ATP is the end product of respiration. In aerobic respiration the main source of ATP is from the ETC (8- glycolysis, 30- electron transport chain; Rich, 2003). ATP can be used to assess the functional integrity of living cells and to assess the functionality of the ETC. The kit used, ViaLight® HS Kit (Lonza Rockland Inc, USA) is based upon the bioluminescent measurement of ATP utilising the luciferase enzyme, which catalyses the formation of light from ATP and luciferin according to the following reaction (Holmsen et al. 1966):

$$ATP + Luciferin + O_2 \xrightarrow[Mg^{2+}]{Luciferase} Oxyluciferin + AMP + PPi + CO_2 + LIGHT$$

Initially all reagents are brought up to room temperature. The ATP monitoring reagent (AMR) is then reconstituted in the tris buffer provided (10mL of tris/vial). After 15 mins any surplus AMR not required for the current assay should be stored at -20˚C (stable for 2 months). A 6 point ATP standard line was freshly prepared for each experiment (diluted in distilled water) from 0-2µM (Figure 2.10). 300 µL of each sample is mixed with an equal volume of Nucleotide Releasing Reagent (NRR) and left to stand for 5 mins at +20˚C. 180 µL per well of each sample, in triplicate, should be transferred to the clear bottomed white walled illuminescence plate. 20 µL of the previously prepared AMR is added. The plate is read using a FLUOstar omega plate reader (BMG Labtech Ltd) with a specilised illuminescence head. Absorbance was then converted to molar concentration by linear regression of sample absorbance against the ATP standard curve.

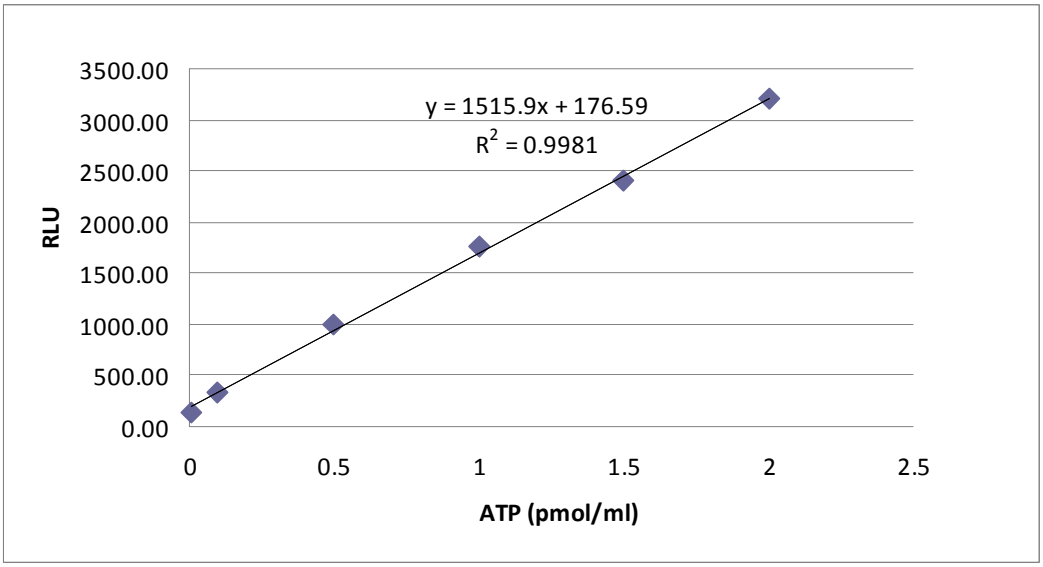

Figure 2.10 ATP Concentration curve

A 6 point concentration curve (0-2pmol/ml). The ATP concentration curve is used to determine the concentration of ATP in a given solution. Relative Luminesence units (RLU) values for a solution are read across to the standard line to determine the concentration of ATP (e.g. If RLU=1000, then protein concentrations=0.5pmol/ml)

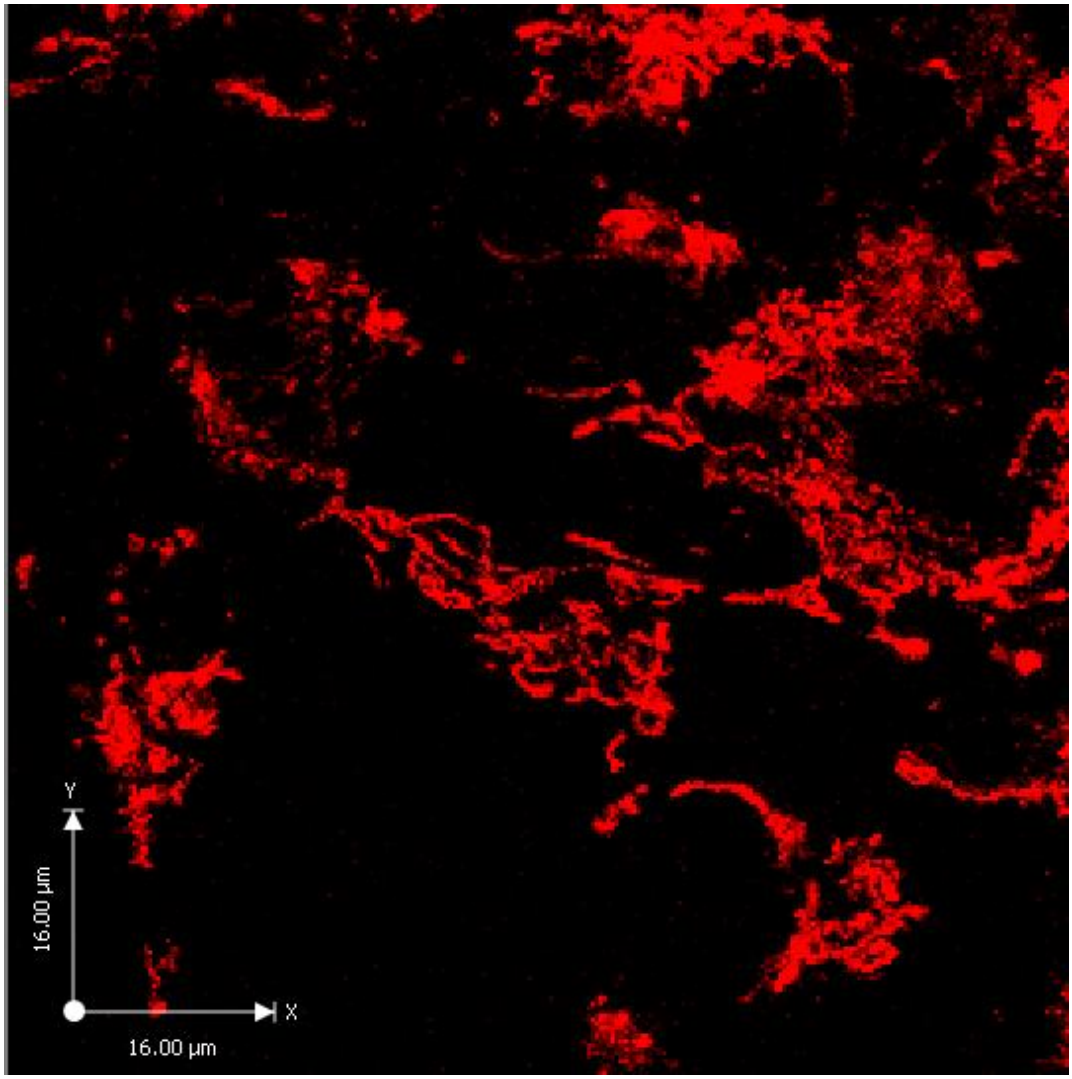

Figure 2.11 SH-SH5Y Cells Treated with 1mM Para-Aminobenzoic Acid (PABA) incubated with 25µM tetramethylrhodamine methyl ester (TMRM)

2.7. Confocal Microscopy

2.7.1. Preparation of Cells

SH-SY5Y cells were cultured in 6 well plates on 22 mm glass coverslips. Cells were seeded at a density of 1 x 10^4 cells/cm^2 and were treated over a 5 day time-course (see Section 2.2.6).

2.7.2. Confocal microscopy method

A Zeiss 710 VIS confocal laser scanning microscope equipped with a META detection system and a 63x oil immersion objective was used for all microscopy experiments. Analysis was performed using Velocity software (Perkin Elmer, Cambridge, UK). Analysis involved selecting 50-100 regions of interest using the stamp tool function (e.g. TMRM: areas of red fluorescence, picogreen: areas of green fluorescence that resembled mitochondria [not nuclear DNA]). An average fluorescence (AU) of the regions of interest for each view was taken. Results from each day of experimentation were expressed as a percentage of the average control fluorescence (AU) to control for variation between days. Averages were taken for views per day and subsequently taken between days.

e.g.

Day 1

100%=average of control views fluorescence per day (AU)

Treatment 1 (1mM PABA):

Treatment view 1 (fluorescence of treatment view 1 (AU)/average control fluorescence (AU) x 100), treatment view 2 (same as treatment view 1), treatment view 3 (same as treatment view 1) etc.

An average was then taken for views per day.

Average of treatment 1, day 1 (n=1) = 120% of control fluorescence

Averages were subsequently taken between days.

2.7.3. Mitochondrial Membrane Potential

$\Delta\Psi_m$ is a key indicator of mitochondrial function (Figure 2.11). The characterization of $\Delta\Psi_m$ in situ can also indicate mitochondrial bioenergetics and cellular metabolism. $\Delta\Psi_m$ can be monitored with monovalent cationic fluorescent dyes such as tetramethylrhodamine methyl ester (TMRM). The accumulation of TMRM in mitochondria is driven by their membrane potential.

Due to the probes Nernstian nature (Figure 2.15a), mathematical analysis can provide quantitative data for mitochondrial membrane potential (Ward et al. 2000; Abramov et al. 2010; Düssmann et al. 2003; Nicholls 2006).

The cells were initially loaded with 25nM TMRM for 20 min at +20°C. TMRM and all other microscopy probes were reconstituted in 4-(2-hydroxyethyl)-1-piperazineethanesulfonic acid (HEPES)-buffered salt solution composed of (mM): 156 NaCl, 3 KCl, $2MgSO_4$, 1.25 KH_2PO_4, 2 $CaCl_2$, 10 glucose and 10 HEPES, pH adjusted to 7.35 with NaOH. The dye was present at the same concentration in all solutions throughout the experiment. $\Delta\psi_m$ was monitored in single cells. TMRM was excited using the 565 nm laser line and fluorescence measured above 580nm. A Zeiss 710 VIS confocal laser scanning microscope equipped with a META detection system and a 63x oil immersion objective was used for all microscopy experiments. Illumination intensity was kept to a minimum to avoid phototoxicity and the pinhole set to give an optical slice of ~2 mm.All imaging data were collected and analysed using Volocity software (Perkin Elmer, Cambridge, UK). Three Z-stack measurements per cover slip were used to assess relative fluorescence intensity.

All conditions were compared to mean control intensity (100%) to control for experimental differences. One time series measurement was taken per cover slip. Data were acquired at intervals of 5–10 s. In these experiments TMRM is used in the 'redistribution mode' (Abramov et al. 2010) to assess $\Delta\psi_m$, and therefore a reduction in mitochondrial localised TMRM fluorescence represents mitochondrial depolarisation.

The rate of change before and after addition of oligomycin (2mg/ml; an established Complex V inhibitor), was used to assess the functionality of Complex V. Generally $\Delta\psi_m$ is maintained by the ETC (Complexes I-IV), however when the functionality of the ETC is compromised Complex V may be reversed to help maintain the $\Delta\psi_m$. Depolarisation after addition of oligomycin (a Complex V inhibitor) indicated a reversal of Complex V activity. Total depolarisation was induced by the mitochondrial uncoupler FCCP (1µM; Carbonyl cyanide 4-(trifluoromethoxy)phenylhydrazone). This method has been used in previous studies to establish reversal of Complex V activity (Yao et al. 2012; Gandhi et al. 2009).

2.7.4. Mitochondrial Superoxide

Mitosox™ Red is a mitochondrial superoxide indicator (Figure 2.15c). It is a cationic derivative of dihydroethidum designed for selective detection of superoxide in the mitochondria of live cells (Figure 2.12). This triphenylphosphonium cation is driven across the mitochondrial membrane depending on the membrane potential; oxidation by superoxide results in hydroxylation at the 2-position (2-hydroxyethidium).

For measurements, cells were loaded with 1μM Mitosox for 20 min at +20˚C. Slides were then washed once before being suspended in 1ml of HEPES buffer for measurement. One timeseries measurement was taken per well. The rate of probe oxidation was measured as increase in red fluorescence over a 5 min time course. All readings were expressed as a percentage compared to mean control rate of probe oxidation (100%) to control for experimental differences. Fluorescence excitation was at 560 nm and emission detection was at ~590 nm.

2.7.5. Cytosolic Superoxide

Cytosolic dihydroethidium (DHE) exhibits blue fluorescence; however, once this probe is oxidized to ethidium, it intercalates within DNA, staining the cell nucleus a bright fluorescent red (Figure 2.13). It is widely used as an indicator of cytosolic superoxide production (Abramov et al. 2010). Similar to MitoSOX™, dihydroethidium is oxidized by superoxide to 2-hydroxyethidium (Figure 2.15b).

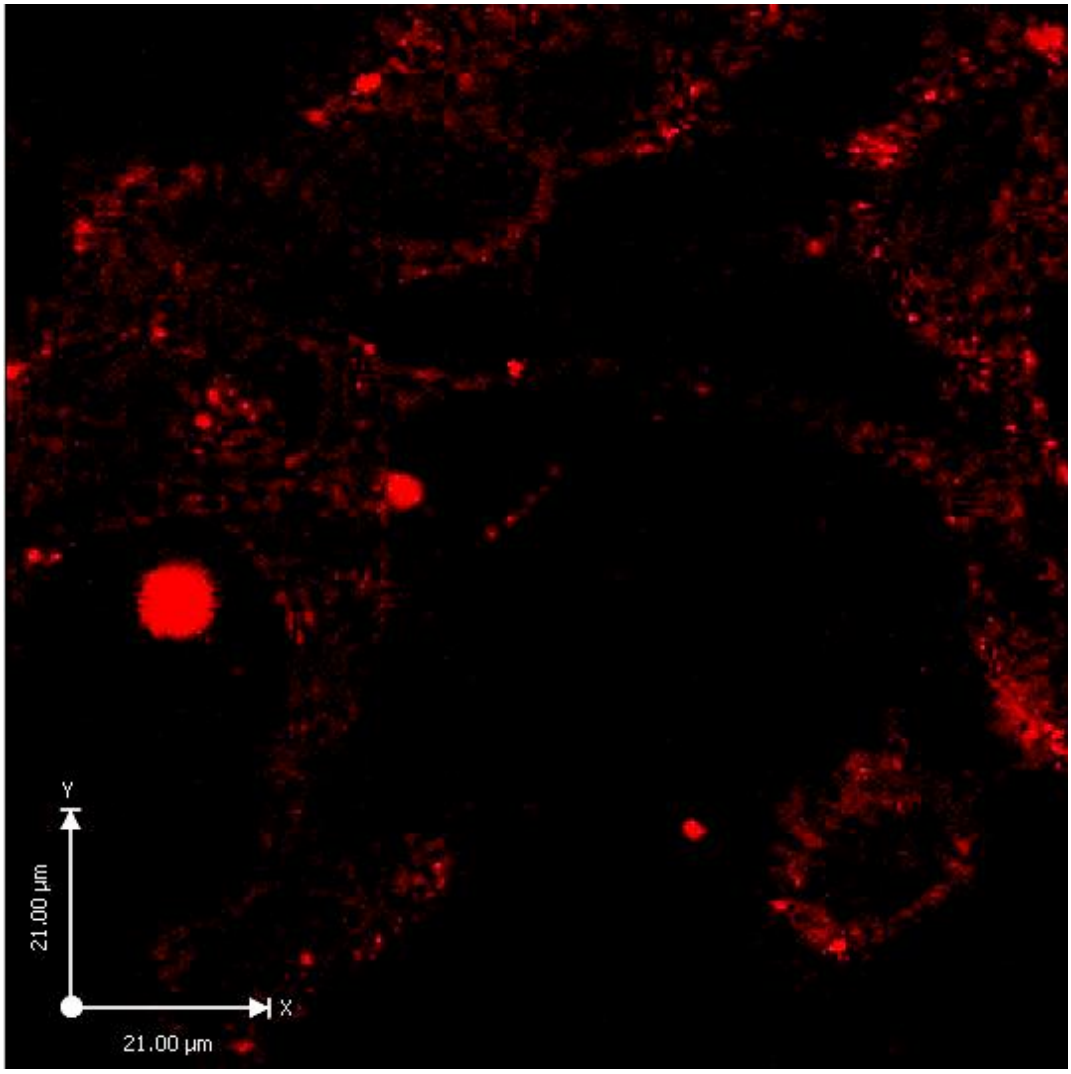

Figure 2.12 SH-SY5Y Cells Incubated with 1µM Mitosox

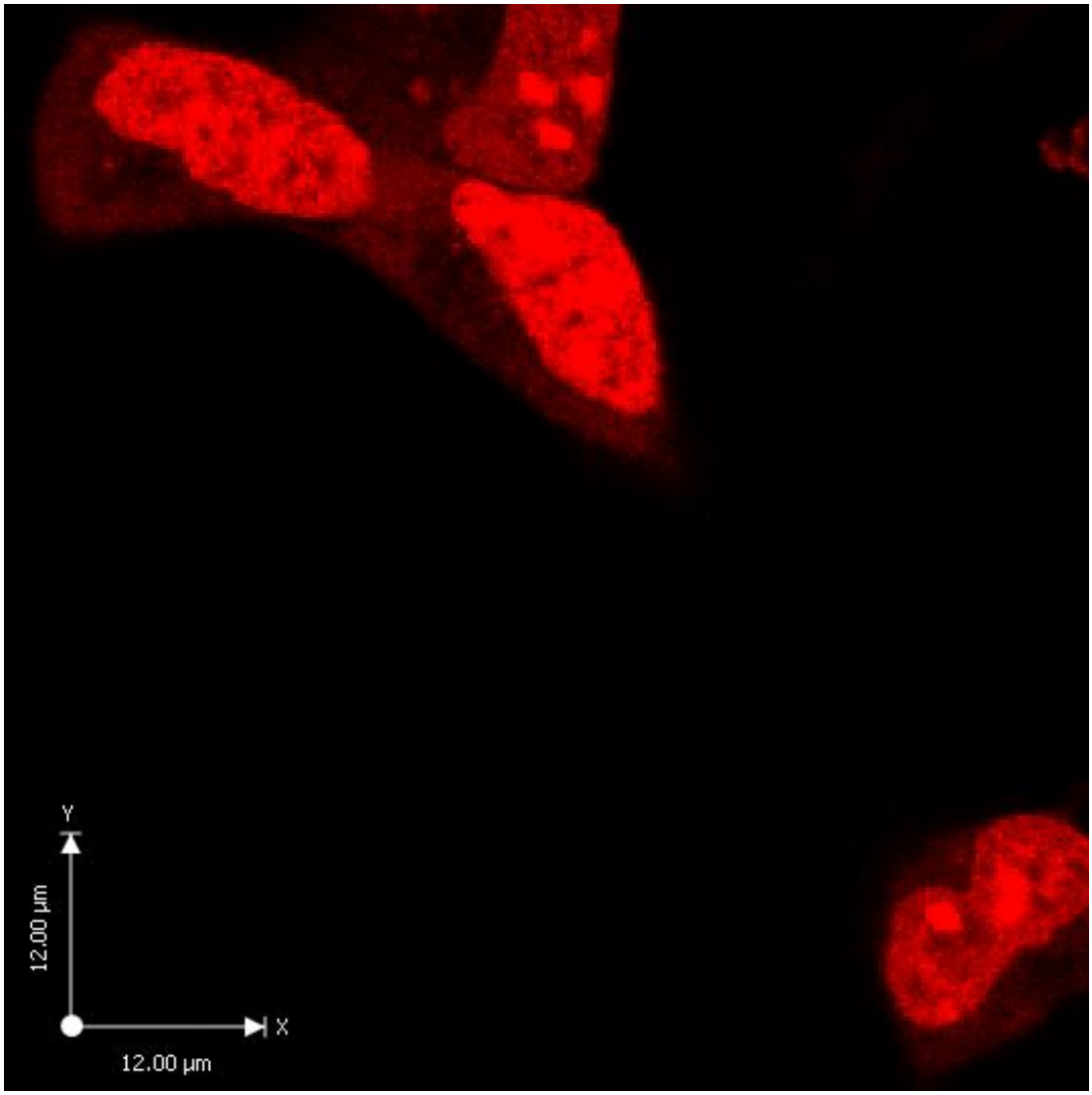

Figure 2.13 SH-SH5Y Cells Treated with 1mM Para-Aminobenzoic Acid (PABA) incubated with 5 µM dihydroethidium (DHE)

For measurements, cells were loaded with 5μM DHE for 10 min at +20˚C and the dye was present at the same concentration in all solutions throughout the experiment. Slides were then washed once before being suspended in 1ml of HEPES buffer for measurement. One timeseries measurement was taken per well. The rate of probe oxidation was measured as increase in red fluorescence over a 5 min time course. All readings were expressed as a percentage compared to mean control rate of probe oxidation (100%) to control for experimental differences. Fluorescence excitation was at 560 nm and emission detection was at ~590 nm.

2.7.6. Lipid Peroxidation

The BODIPY 581/591 C_{11} fatty acid is a sensitive fluorescent reporter for lipid peroxidation (Figure 2.15e), undergoing a shift from red to green fluorescence emission upon oxidation of the phenylbutadiene segment of the fluorophore (Figure 2.2). This oxidation-dependent emission shift enables fluorescence ratio imaging of lipid peroxidation in live cells.

For measurements, cells were loaded with 1μM DHE for 10 min at +25˚C. Slides were then washed once before being suspended in 1ml of HEPES buffer for measurement. One timeseries measurement was taken per well. The rate of probe oxidation was measured as increase in the ratio of red to green over a 5 min time course. All readings were expressed as a percentage compared to mean control ratio (100%) to control for experimental differences.

2.7.7. Mitochondrial DNA Quantification

Quant-iT™ Picogreen® (molecular probes, Invitrogen) is a fluorescent nucleic acid stain used to quantify double stranded DNA (dsDNA). Picogreen® is an asymmetrical cyanine dye (Figure 2.15d) that upon binding dsDNA emits fluorescence at ~530nm. Here we use it estimate the degree of mitochondrial DNA (mtDNA) depletion in the neuroblastoma cell model (Figure 2.14).

SH-SH5Y cells incubated with 3μg/ml of the Quant-iT™ Picogreen® stock solution for 30 mins at +25˚C. Coverslips were washed once and resuspended in 1ml of HEPES buffered salt solution. In this instance only mtDNA fluorescence was analysed i.e. fluorescence external to the nucleus with mitochondrial morphology; illustrated by the white arrows in Figure 2.14.

Relative fluorescence intensity was used as a measure of mtDNA depletion; compared to mean control intensity (100%). Fluorescence excitation was at 480nm and fluorescence emission was at 550nm.

2.8. Statistical Analysis

All results are expressed as mean ± standard error of the mean (SEM). One-way ANOVA (analysis of variance) was used for comparison of groups >2, with Bonferroni post-hoc analysis. In all cases $p < 0.05$ was considered significant. Expression of ratios (i.e. complex activities expressed as a ratio to citrate synthase activity) required the data to be transformed using the following equation: arcsin $\sqrt{}$enzyme activity/citrate synthase activity. This minimises the negative skew of distribution produced when expressing proportions, thus yielding a normal distribution prior to analysis (Gegg et al. 2004).

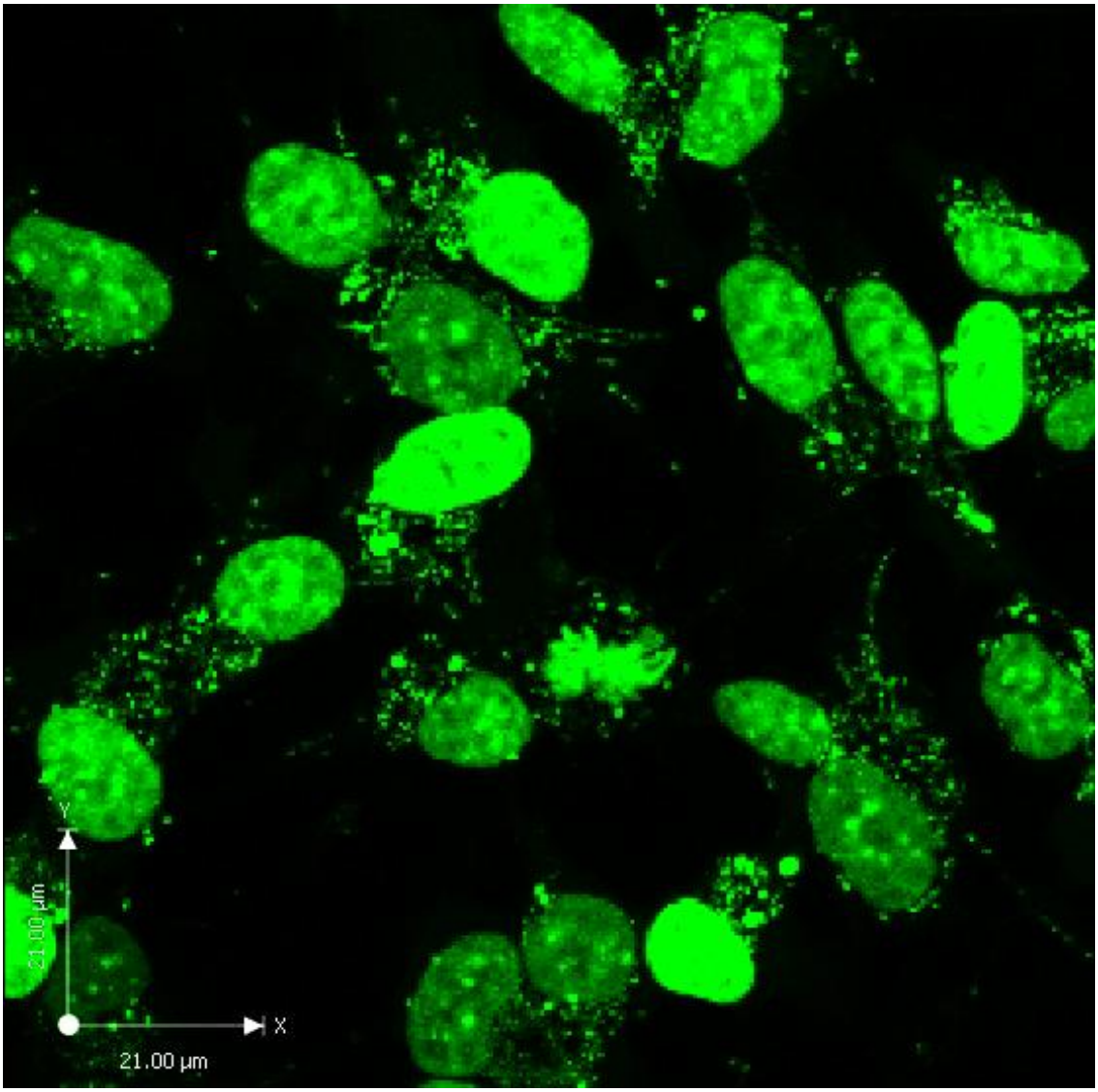

Figure 2.14 SH-SH5Y Cells Incubated with 3µg/ml of the Quant-iT™ Picogreen® Stock Solution

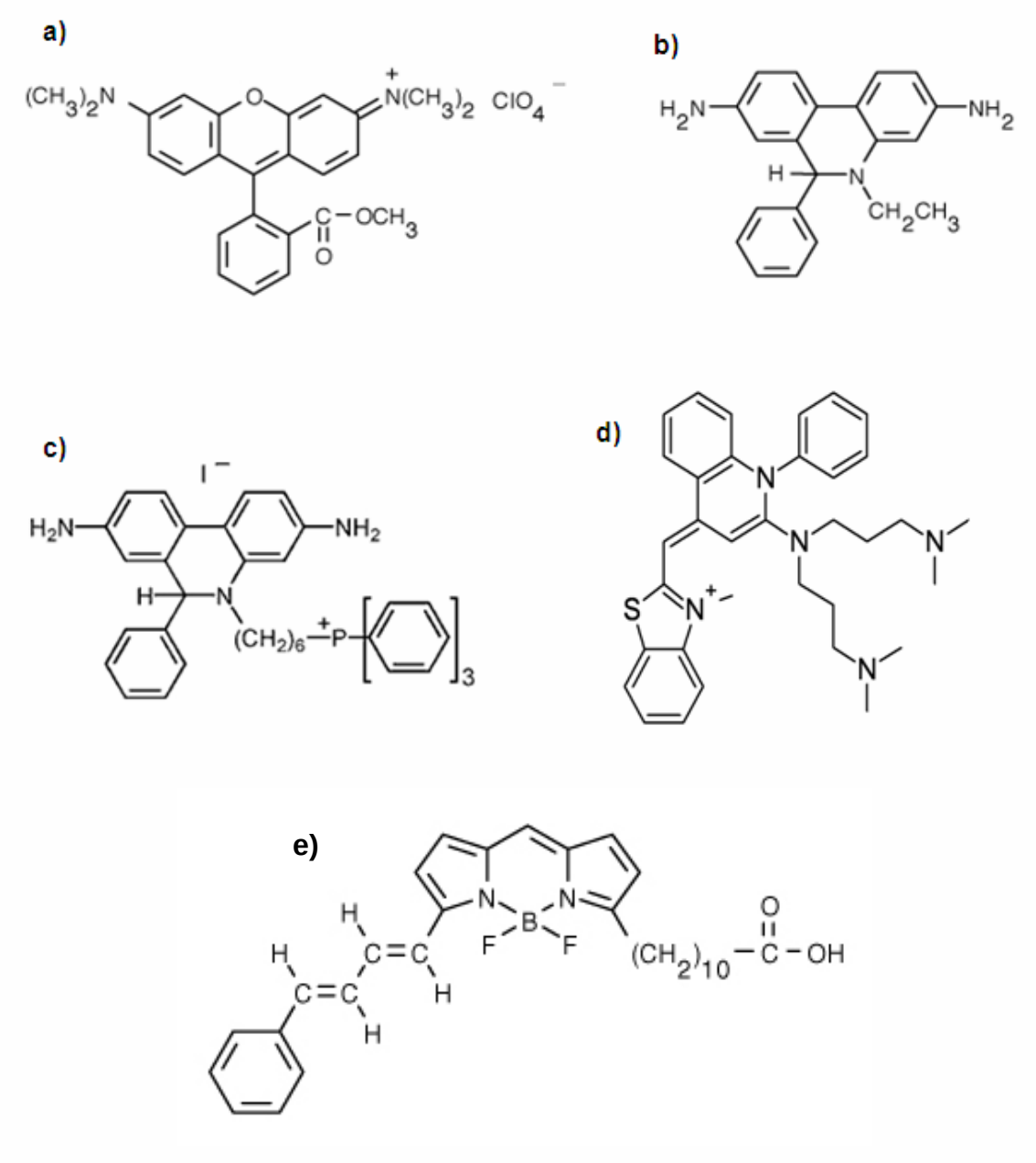

Figure 2.15 Chemical Structures of Microscopy Dyes a) TMRM, b) DHE, c) Mitosox, d) Picogreen, e) Bodipy 581/591

Chapter 3

Neuronal Cell Model of Coenzyme Q_{10} Deficiency

3.1. Introduction

The first clinical case of CoQ_{10} deficiency was reported by Ogasahara in 1989 in siblings with progressive muscle weakness, fatigability and central nervous system dysfunction (Ogasahara et al. 1989). Primary CoQ_{10} deficiency is usually inherited in an autosomal recessive manner, with recessive mutations reported in 7 CoQ_{10} biosynthetic genes (6 biosynthetic enzymes) to date: *PDSS1* (Mollet et al. 2007) and *PDSS2* (López et al. 2006), *ADCK3* (Mollet et al. 2008; Lagier-Tourenne et al. 2008), *COQ9* (Duncan et al. 2009), *COQ6* (Heeringa et al. 2011), *COQ4* (Salviati et al. 2012) and *COQ2* (Mollet et al. 2007; Figure 1.9). CoQ_{10} deficiency can be broadly divided into five major phenotypes: 1) Recurrent rhabdomyolysis with encephalopathy; 2) infantile-onset multisystem disease; 3) isolated cerebellar ataxia; 4) a pure myopathic form; and 5) steroid resistant nephropathy ± sensorineural hearing loss. Leigh syndrome can also be considered a separate phenotype (Rahman et al. 2012).

Neurological involvement is a common feature of CoQ_{10} deficiency. There have been 3 reported cases of Leigh syndrome, a severe neurological disease as the result of a CoQ_{10} deficiency caused by mutations in the *PDSS2* gene (Van Maldergem et al. 2002; CM Quinzii et al. 2006). Encephalopathy predominates the multisystematic neonatal phenotype and sensorineural hearing loss is variably present in the steroid resistant nephrotic syndrome (Rahman et al. 2012). The ataxic phenotype of CoQ_{10} deficiency is the most common clinical presentation of the disorder with 94 known cases reported to date (Emmanuele et al. 2012). The causative gene defect has been identified in 34 of these patients. In 22 of these patients ataxia is caused by a mutation in the *ADCK3* gene and in the remaining 12 patients ataxia is the result of a mutation in the *APTX* gene.

One of the original publications of the *ADCK3* gene mutation (Lagier-Tourenne et al. 2008) suggested that patients with the *ADCK3* gene defect can be distinguished from other recessive ataxias by the presence of cerebellar atrophy and childhood onset. However Horvath at al. discovered several patients with an adult onset form of the disease with mild cerebellar ataxia (Horvath et al. 2012). The *ADCK3* gene is a functional homolog of *coq8* (yeast) and UbiB (bacterial). *ADCK3* encodes a putative kinase which appears to indirectly modulate CoQ_{10} biosynthesis. Yeast studies have indicated that the *ADCK3*

encoded protein stabilises the COQ3 enzyme that catalyses the O-methylation steps in the terminal portion of CoQ biosynthesis (Tauche et al. 2008).

AOA1 is a recessive ataxia caused by a gene mutation in *APTX*. The *APTX* gene encodes a ubiquitously expressed protein that is thought to play a role in single stand DNA break repair (Moreira et al. 2001). The cause of CoQ_{10} deficiency in AOA1 as yet remains to be elucidated. Interestingly hypercholesterolemia is a common clinical presentation of AOA1. Cholesterol and CoQ_{10} share a common initial portion of their biosynthetic pathways; suggesting a possible interaction of aprataxin with this pathway resulting in up regulation of cholesterol biosynthesis and down-regulation of CoQ_{10} biosynthesis (Quinzii et al. 2005).

Patients with all phenotypes of CoQ_{10} deficiency have been reported to show some form of clinical improvement following CoQ_{10} supplementation. While muscle abnormalities improve clinically and biochemically, neurological symptoms associated with CoQ_{10} deficiency appear to be particularly refractory to treatment (Rahman et al. 2001; Auré et al. 2004). A recent literature review stated that CoQ_{10} supplementation is only effective in 46% of patients with the ataxic phenotype (Emmanuele et al. 2012). However when treatment was instigated for the other clinical phenotypes of CoQ_{10} deficiency 79% of patients were reported to show some clinical improvement upon CoQ_{10} supplementation (Emmanuele et al. 2012). At present the reasons for this variation remain unclear but possible explanations include: irreversible structural and/or biochemical neuronal dysfunction; poor penetration of CoQ_{10} supplements across the blood-brain barrier; and inability of neuronal cells with a CoQ_{10} deficiency to utilise exogenous CoQ_{10}.

3.2. Aims

In order to investigate the pathogenesis of neuronal CoQ_{10} deficiency we have established a pharmacologically induced SH-SY5Y neuroblastoma cellular model of this disorder using PABA treatment. PABA has previously been reported to competitively inhibit COQ2 activity (Alam, Nambudiri, et al. 1975; Figure 1.7) inducing a CoQ_{10} deficiency in HL-60 cells (González-Aragón et al. 2005). This cellular model will allow the effects of CoQ_{10} deficiency on neuronal ETC function and cellular oxidative stress to be evaluated.

3.3. Methods

3.3.1. Cell Culture

SH-SY5Y cells were cultured as described in Section 2.2.4 and treated with PABA and CoQ_{10} as described in Section 2.2.4 over a 5 day incubation period.

3.3.2. Quantification of CoQ_{10} Levels

CoQ_{10} content was analysed in SH-SY5Y cells by reverse phase HPLC as described in Section 2.3

3.3.3. Mitochondrial Bioenergetics Analysis

Complexes I, II+III and IV of the ETC, CS and ATP were assayed in SH-SY5Y cells as described in Section 2.6.

3.3.4. Blue Native in-Gel Complex V Assay

Complex V activity was determined in SH-SY5Y cell homogenates using blue native gel electrophoresis as described in Section 2.6.5

3.3.5. Oxidative Stress Assessment

Reduced glutathione (GSH) content was also quantified in SH-SY5Y cells as described in Section 2.5. Mitochondrial (Mitosox) and cytosolic (DHE) superoxide production and lipid peroxidation (Bodipy 581/591) in SH-SY5Y cells was determined by confocal microscopy as described in Section 2.7

3.3.6. Mitochondrial DNA Quantification

Quant-iT™ Picogreen® was used to quantify mitochondrial DNA (mtDNA) content as described in Section 2.7.7.

3.3.7. Mitochondrial Membrane Potential

TMRM was used to determine $\Delta\psi m$ in the SH-SY5Y cells as described in Section 2.7.3.

3.3.8. Total Protein Determination

The protein content of the SH-SH5Y cells was determined by the Lowry method as described in Section 2.3.

3.3.9. Statistical Analysis

Statistical analysis was performed as described in Section 2.8.

3.4. Results

3.4.1. Optimisation of PABA Treatment

CoQ_{10} levels were significantly decreased ($p < 0.0001$) compared to controls (untreated cells) after 5 days of PABA treatment. The effect was progressive and reproducible (0mM PABA =100%, 0.25mM=90%, 0.5mM=76%, 0.75mM=68% residual CoQ_{10} compared to control levels). Treatment of SH-SY5Y cells with 1mM PABA induced a maximal 54% decrease (46% residual CoQ_{10}; Figure 3.1) in cellular CoQ_{10} status. Treatment of SH-SY5Y cells with higher concentrations of PABA (2mM) did not induce a further decrease in cellular CoQ_{10} status (53% decrease; 47% residual CoQ_{10}); thus 1mM PABA was selected as the maximum treatment condition.

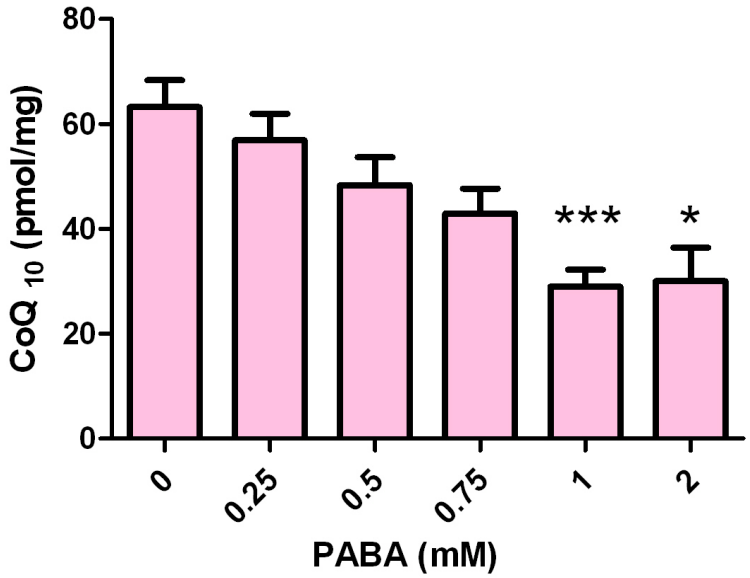

Figure 3.1 Effect of Para-Aminobenzoic Acid (PABA) Treatment on CoQ_{10} Concentration

Error bars represent standard error of the mean (SEM); statistical analysis was carried out using one-way ANOVA with Bonferroni post hoc analysis; levels of significance: *:p<0.05, **:p<0.005, ***:p<0.0005; n=15.

In view of the reported half-life of rat brain ubiquinone status (CoQ_9) of approximately 90 hours (3.75 days; Turunen et al. 2004) an incubation period of 5 days was selected for the present study. Furthermore, the neuronal CoQ_{10} status following PABA treatment for 10 days was found to be comparable to that of the 5 day treatment period (Figure 3.2) indicating that a longer period of treatment would not be necessary.

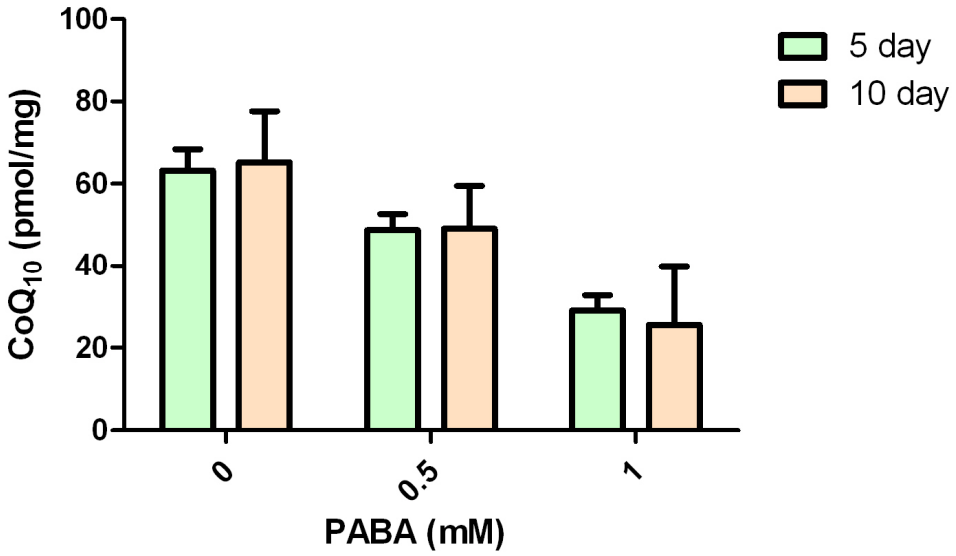

Figure 3.2 Effect of 5 day versus 10 day Treatment with 0 (control; no treatment), 0.5 and 1mM PABA

Error bars represent standard error of the mean (SEM).

We also evaluated the effect of PABA treatment on cell growth. To do so we used a trypan blue haemocytometer method to count the number of cells per ml; as described in Section 2.2.2. There was no significant difference in cell growth between conditions (Figure 3.3).

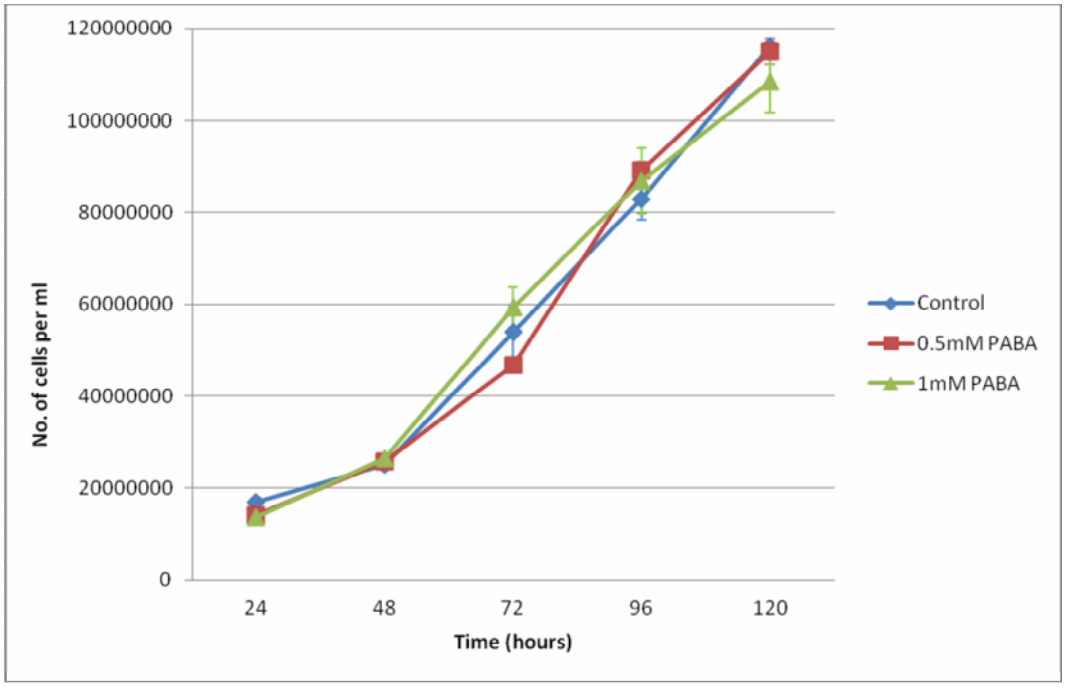

Figure 3.3 SH-SY5Y Cell Growth Curve

A cell count of control (no treatment) SH-SY5Y cells and SH-SY5Y cells treated with 0.5mM and 1mM PABA performed on a haemocytometer.

3.4.2. Electron Transport Chain Activities

All ETC complex activities are expressed as a ratio of CS. CS is used as a mitochondrial marker enzyme to allow differences in mitochondrial enrichment between samples to be taken into account. CS activity was not affected by the compromised CoQ_{10} status (Figure 3.4); however there is an insignificant trend towards an increase in mitochondrial content at 76% residual CoQ_{10}.

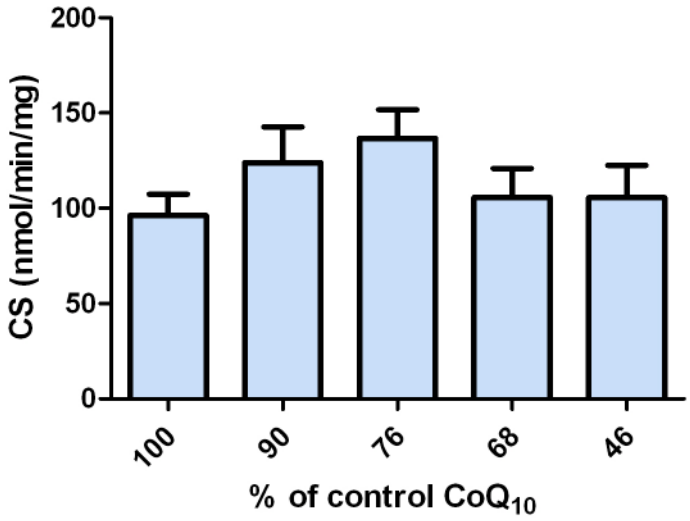

Figure 3.4 Effect of CoQ_{10} Deficiency on Citrate Synthase Activity

Error bars represent standard error of the mean (SEM); n=7

The effect of a decrease in neuronal CoQ_{10} status on ETC enzyme activity was assessed in the PABA-treated SH-SY5Y cells. All ETC complexes displayed a significant, progressive decrease in activity accompanying the diminution in cellular CoQ_{10} status. The decrease in Complex IV activity was the most pronounced following reduction of cellular CoQ_{10} levels, with a decrease of 69% compared to control (Figure 3.5C). Complex I (Figure 3.5A) and Complex II/III (Figure 3.5B) activities were decreased by 59%.

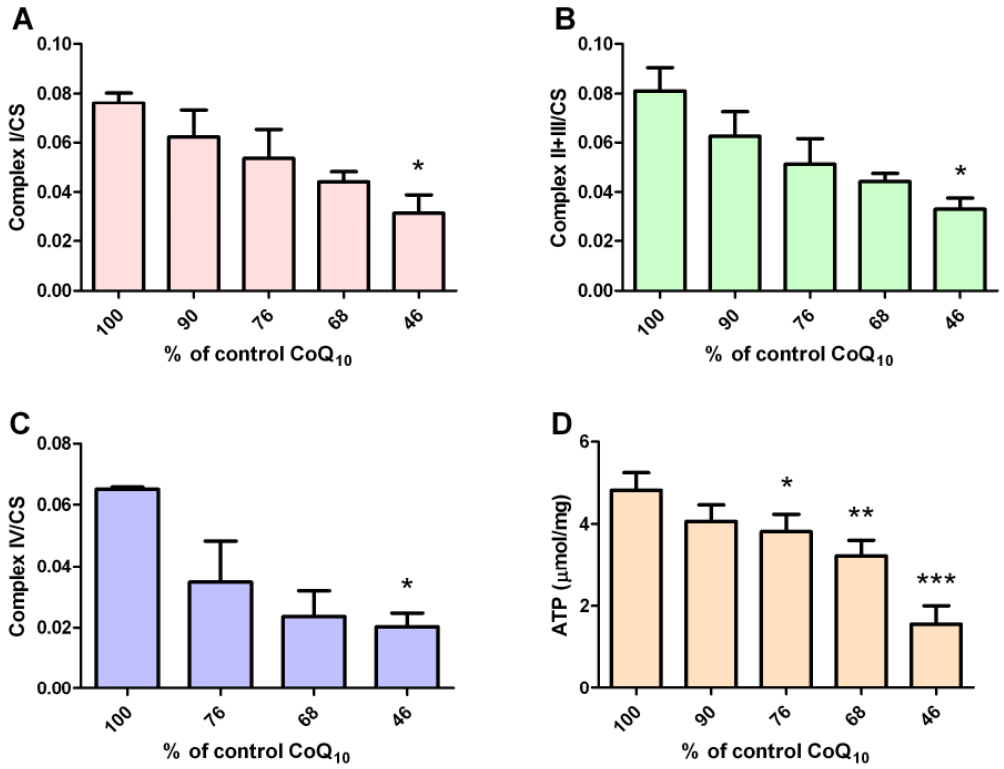

Figure 3.5 Effect of CoQ_{10} Deficiency on A) Complex I Activity (n=4), B) Complex II+III Activity (n=7), C) Complex IV Activity (n=3), D) Total Cellular ATP Concentration (n=5)

Error bars represent standard error of the mean (SEM); statistical analysis was carried out using one-way ANOVA with Bonferroni post hoc analysis; levels of significance: *:p<0.05, **:p<0.005, ***:p<0.0005.

3.4.3. Cellular ATP Status

A decrease in cellular CoQ_{10} status resulted in a significant and progressive decrease in the level of total cellular ATP (Figure 3.5D). A maximal 68% decrease in total cellular ATP levels (compared to control) was observed at 46% residual CoQ_{10} levels. This decrease did not appear to affect cell growth, since there was no difference in the growth curves between PABA treated and control cells (Figure 3.3).

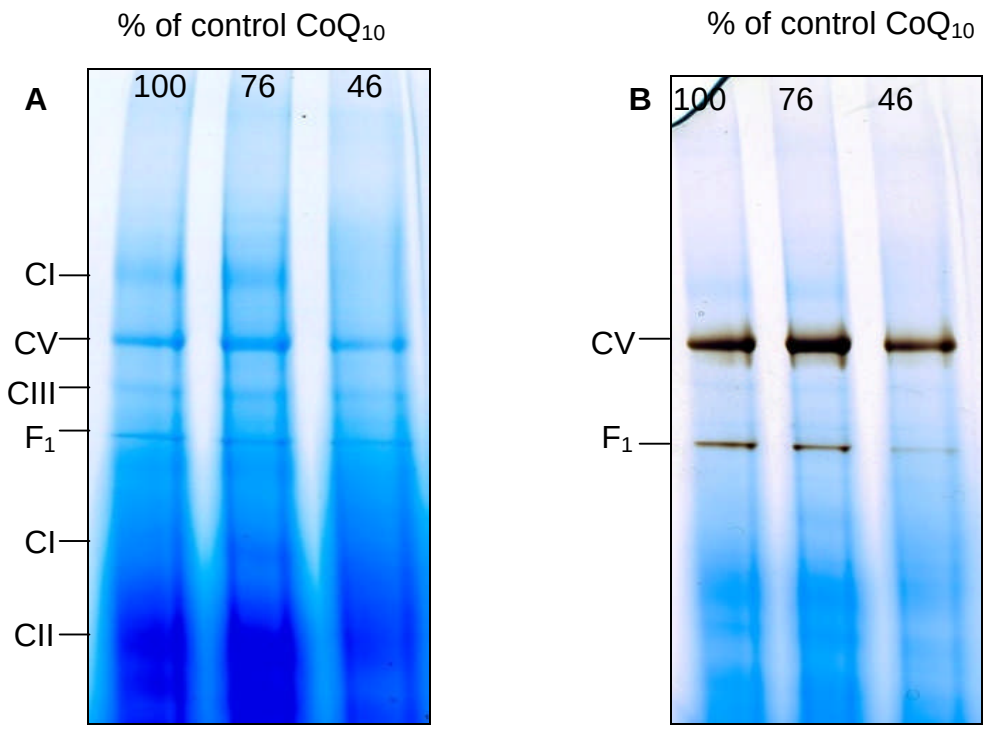

Figure 3.6 a) Blue native gel image of CoQ_{10} deficient neuroblastoma cells; 100%, 76% and 46% of control CoQ_{10} levels and b) Image of in-gel Complex V assay; n=3.

3.4.4. Blue Native Complex V Assay

Blue native gel electrophoresis studies revealed that the protein level of Complex V (holo-F_1-F_0) in CoQ_{10} deficient neuronal cells was comparable to control levels (Figure 3.6A). Complex V activity was decreased by 14% of the control level at 46% residual CoQ_{10} and the F_1 band activity was decreased by 59% (Figure 3.6B).

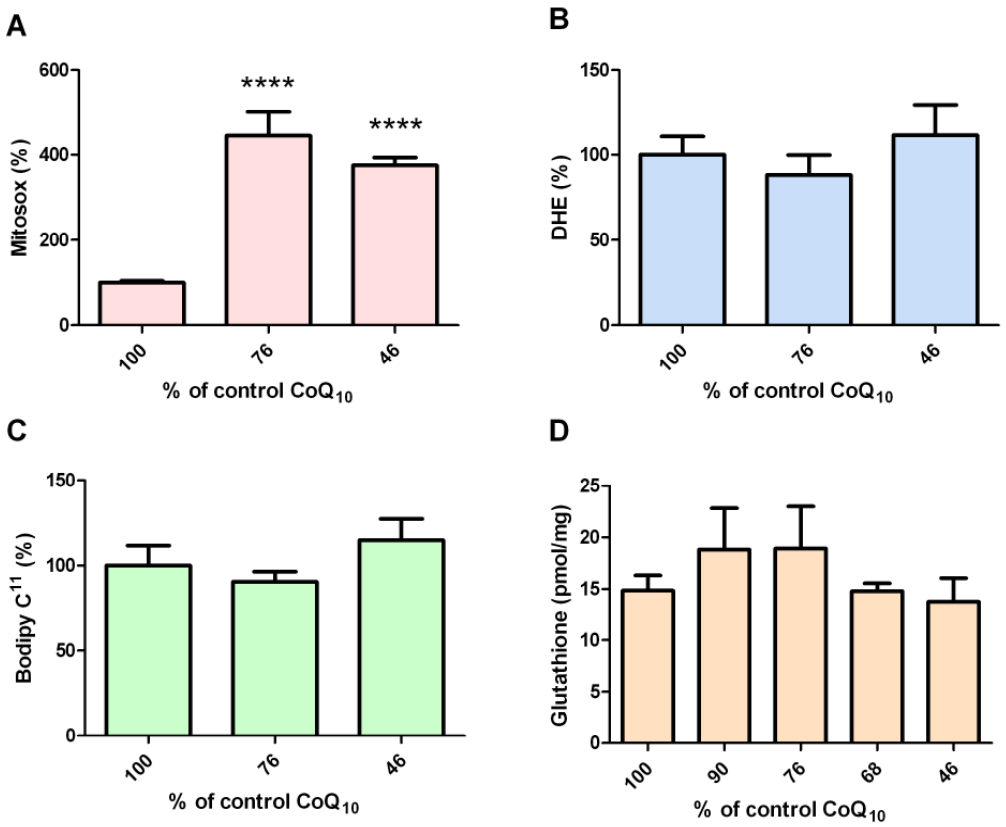

Figure 3.7 Effect of CoQ_{10} Deficiency on Oxidative Stress:

A) mitochondrial superoxide (n=4), B) cytosolic superoxide (n=3), C) lipid peroxidation (n=3), D) Glutathione (n=7)

Error bars represent standard error of the mean (SEM); statistical analysis was carried out using one-way ANOVA with Bonferroni post hoc analysis; levels of significance: *:p<0.05, **:p<0.005, ***:p<0.0005, ****:p<0.00005.

3.4.5. Oxidative Stress Analysis

Mitochondrial and cytosolic superoxide levels were determined in order to assess the distribution of oxidative stress. Results suggested a CoQ_{10}-dependent variable distribution of superoxide. At both 46% and 76% residual CoQ_{10}, the level of mitochondrial superoxide was significantly elevated increasing by approximately 4 times that in control cells (Figure 3.7A). However, mitochondrial superoxide production was marginally higher at 76% residual CoQ_{10} compared to 46% residual CoQ_{10}. There was no significant difference between conditions for cytosolic superoxide (Figure 3.7B); however there was a slightly lower level of cytosolic superoxide at 76% residual CoQ_{10}.

Lipid peroxidation varied between the different treatment conditions (Figure 3.7C), although not significantly. At 46% residual CoQ_{10} levels there was a 15% increase in lipid peroxidation. In contrast, a 10% decrease in lipid peroxidation was detected at 76% residual CoQ_{10} levels. The status of cellular GSH was also assessed. However following PABA induced CoQ_{10} deficiency no evidence of a decrease in glutathione status was observed (Figure 3.7D). Interestingly, glutathione levels appeared to increase although not significantly at 76% residual CoQ_{10} levels, coinciding with the decrease in both cytosolic superoxide and in lipid peroxidation.

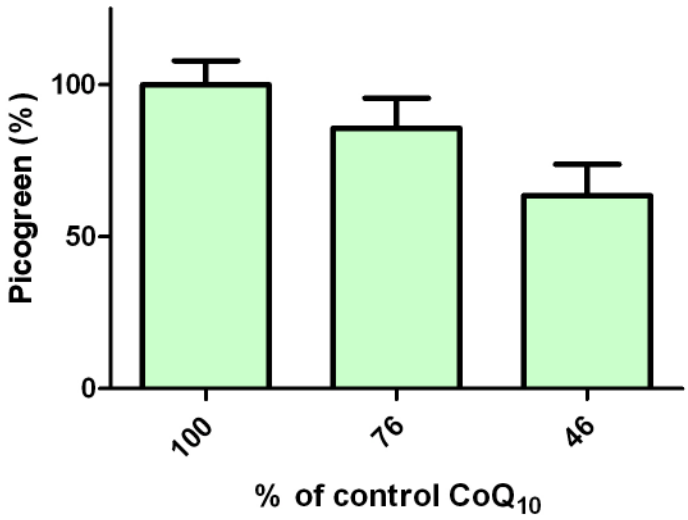

Figure 3.8 Effect of CoQ_{10} Deficiency on Mitochondrial DNA (Picogreen)

Error bars represent standard error of the mean (SEM); n=3

3.4.6. Mitochondrial DNA Quantification

In the CoQ_{10} deficient neuronal cell model a non-significant decrease in the level of mtDNA was observed. This decrease was maximal at 46% residual CoQ_{10} with a decrease in mtDNA levels of 26% compared to the control (Figure 3.8).

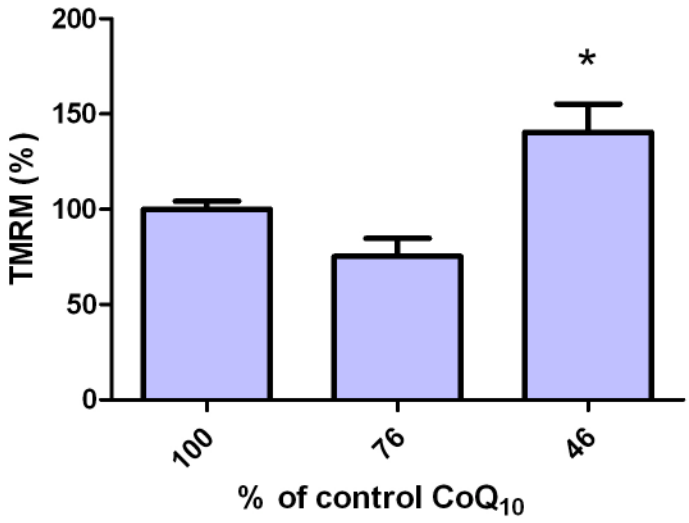

Figure 3.9 Effect of CoQ_{10} Deficiency on Mitochondrial Membrane Potential

Error bars represent standard error of the mean (SEM); statistical analysis was carried out using student t-tests; levels of significance: *:p<0.05, n=7

3.4.7. Mitochondrial Membrane Potential

Complex V is the final enzyme in the oxidative phosphorylation pathway. The preceding ETC complexes create a proton gradient across the inner mitochondrial membrane. Complex V utilises the energy from this process to convert ADP and P_i into ATP:

$$ADP + P_i + 4H^+ \rightleftharpoons ATP + H_2O + 4H^+$$

This reaction is in equilibrium and can be shifted depending on the proton-motive force. If the proton-motive force is decreased, for example if the ETC complex activities are substantially reduced, then Complex V can run in reverse mode (Gandhi et al. 2009). By running in the reverse mode Complex V is able

to pump protons across the mitochondrial membrane, thus maintaining the Δψm.

Assessment of Δψm revealed a 25% decrease at 76% residual CoQ_{10}. Conversely a significant 40% increase was observed at 46% residual CoQ_{10} (Figure 3.9).

Control cells (Figure 3.10A) and cells with 76% residual CoQ_{10} (Figure 3.10B) demonstrated either no response or a slight hyperpolarisation in response to Complex V inhibition by oligomycin (0.2 μg/ml). In these cells the Δψm is maintained by the activity of the ETC (100% = basal Δψm, 0 = FCCP Δψm at end). In contrast, oligomycin treatment caused a distinct and immediate mitochondrial depolarisation in cells with 46% residual CoQ_{10} (Figure 3.10C) indicating that at this level of CoQ_{10} deficiency Δψm is largely maintained by the reversal of Complex V activity rather than by mitochondrial respiration.

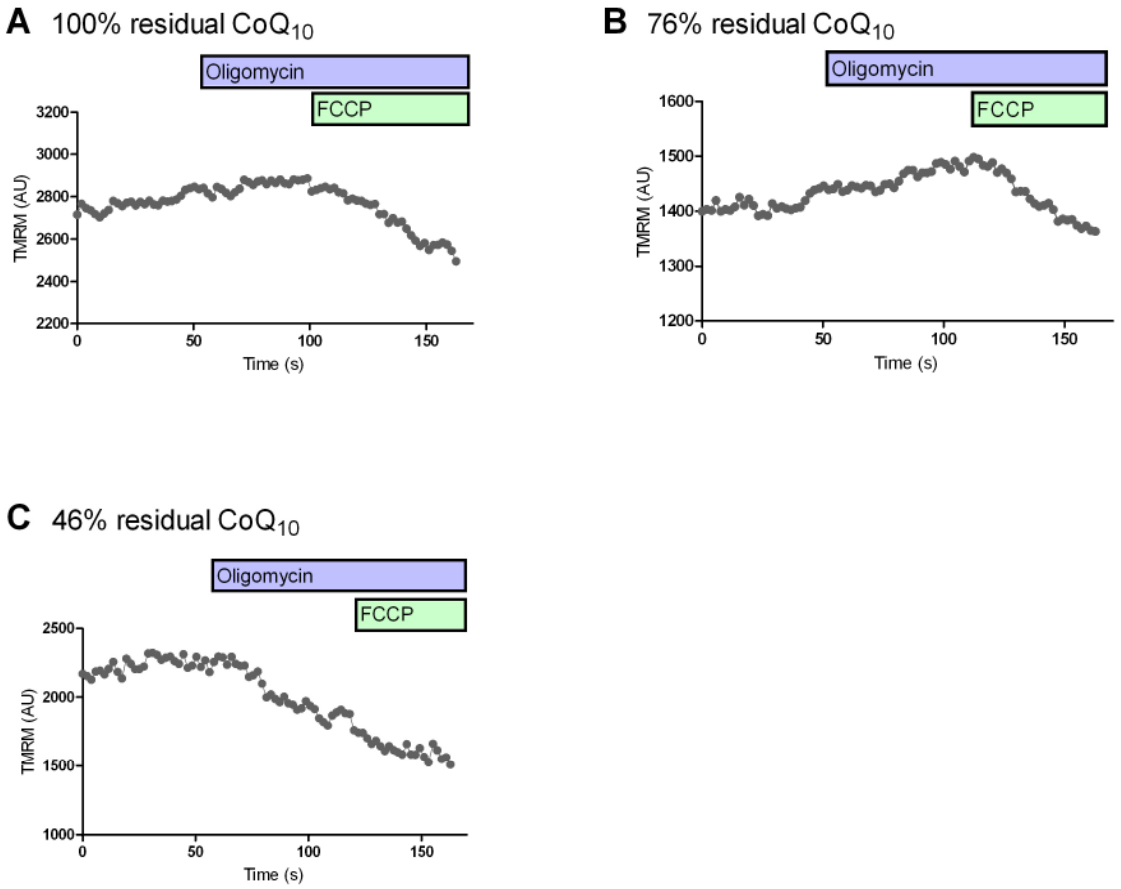

Figure 3.10 Representative Trace of a Time-Series Measurement of Mitochondrial Membrane Potential after the Addition of Oligomycin and FCCP: A) Control (100% CoQ_{10}), B) 76% of Control CoQ_{10} Level, C) 46% of Control CoQ_{10} Level;

Bars indicate the presence of oligomycin/FCCP; n=4

3.4.8. Co-incubation of PABA and CoQ_{10}

To ensure that the effect seen in the neuronal cell model is due to PABA induced CoQ_{10} deficiency and not an indirect effect of PABA we co-incubated cells with the maximal concentration of PABA (1mM) together with CoQ_{10} (5µM) to determine whether CoQ_{10} supplementation could reverse the CoQ_{10} defect . This concentration of CoQ_{10} (5µM) was selected because it is the approximate plasma concentration reached in patients undergoing oral CoQ_{10} supplementation (Miles 2007; Bhagavan & Chopra 2006; Shults et al. 2004) and subsequently because this concentration effectively normalised the bioenergetic status of CoQ_{10} deficient fibroblasts after a week time course (López et al. 2010).

Co-incubation of the SH-SY5Y cells with 1mM PABA together with 5µM CoQ_{10} effectively restores ETC enzyme activity. Co-incubation was most effective in restoring Complex II/III activity (90% of no treatment/control level; Figure 3.10B). No significant loss of ETC activity was observed between the cells co-incubated with PABA and CoQ_{10} and untreated cells (Figure 3.11A, B and C).

Mitochondrial oxidative stress was also evaluated (Figure 3.11D). Co-incubation of PABA and CoQ_{10} gave a 4% lower Mitosox reading compared to no treatment. Here both the co-incubation condition and the no treatment attained the same level of significance ($p<0.005$) when compared to isolated PABA treatment

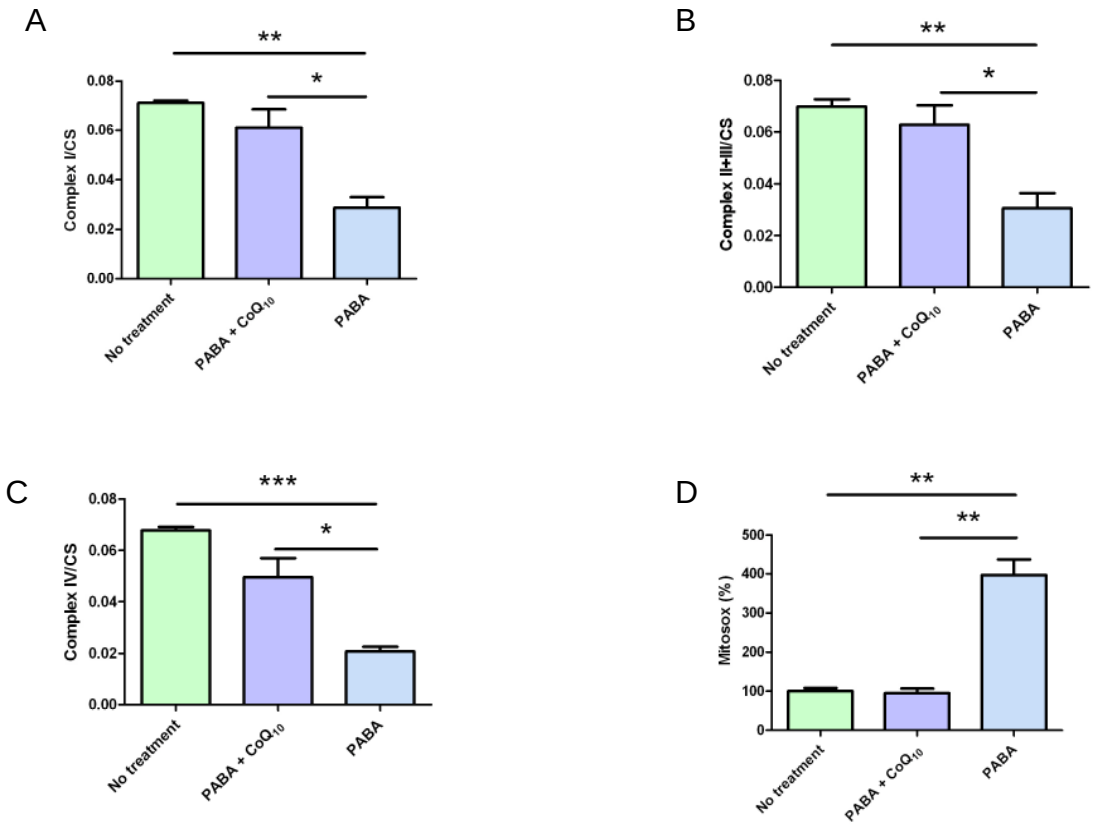

Figure 3.11 Effect of Co-incubation of PABA and 5 μM CoQ_{10} over a 5 day Time Course on: A) Complex I Activity (n=3), B) Complex II+III Activity (n=3), C) Complex IV Activity (n=3), D) Mitochondrial Oxidative Stress (n=3)

Error bars represent standard error of the mean (SEM); statistical analysis was carried out using one-way ANOVA with Bonferroni post hoc analysis; levels of significance: *:$p<0.05$, **:$p<0.005$

PABA (mM)	CoQ_{10} (% of control)	RC Activity	Mitochondrial Superoxide	Cytosolic Superoxide	Lipid Peroxidation	GSH	mt DNA	Δψm	Oligomycin induced depolarisation?
0	**100**	-	-	-	-	-	-	-	-
0.5	**76**	↓	↑*	↓	↓	↑	↓	↓	-
1	**46**	↓*	↑*	↑	↑	-	↓	↑*	Yes

CoQ_{10} levels are means ± SEM. Δψm, mitochondrial membrane potential; -, no effect/control; ↑*↓*, significant increase/decrease; ↑↓ insignificant increase/decrease.

Table 3.1 Summary of Results Obtained in Neuronal Cell Model of CoQ_{10} Deficiency induced by PABA Treatment: CoQ_{10} Defect, Mitochondrial Bioenergetics Analysis, Oxidative Stress Assessment.

3.5. Discussion

CoQ_{10} deficiency often results in neurological disease; however the lack of an appropriate cellular model has so far prevented the elucidation of the underlying pathogenic mechanisms. In this study we have established the first neuronal cell model of CoQ_{10} deficiency.

Using PABA treatment in neuroblastoma-derived SHSY-5Y cells, we have been able to induce a maximal 54% decrease (46% residual CoQ_{10}) in the level of cellular CoQ_{10}, which has enabled an evaluation of the effect of a deficit in CoQ_{10} status upon neuronal ETC function, oxidative stress, mtDNA and Δψm (Table 3.1). A decrease in neuronal CoQ_{10} status was found to result in a progressive decrease in the activities of ETC Complexes I, II/III and IV, with a concomitant decrease in the level of total cellular ATP. Mitochondrial oxidative stress was found to be significantly increased following a deficit in neuronal CoQ_{10}; however no significant effect was found on cytosolic oxidative stress, lipid peroxidation, GSH content or mtDNA. A variable effect was found on Δψm; whereby an insignificant decrease in Δψm was found in the middle range CoQ_{10} deficiency and a significant increase maintained by a reversal of Complex V (indicated by oligomycin induced depolarisation) was found with a more severe deficiency of CoQ_{10}.

Importantly we have also demonstrated that the observed aberrant mitochondrial function observed in this neuronal cell model is a result of CoQ_{10} deficiency and not a result of PABA treatment. All complex activities were restored to levels comparable to controls and a similar level of mitochondrial oxidative stress to controls was observed (Figure 3.11).

The increase in mitochondrial oxidative stress may be a possible explanation for the pattern of ETC dysfunction observed following a deficit in CoQ_{10} status. Loss of ETC function may result from oxidative damage to the membrane phospholipids, protein subunits and/or mtDNA (Kowaltowski 1999). In previous studies it has been suggested that Complex IV is the most susceptible ETC complex to oxidative stress-induced inactivation (Benzi et al. 1991; Heales, Davies & Bates. 1995). This may explain why Complex IV showed the largest decrease in activity compared to the other neuronal cell ETC complexes following a diminution of CoQ_{10} status. Susceptibility of Complex IV to oxidative

damage may in part arise from its dependence on cardiolipin for maximal activity. Cardiolipin is a mitochondrial inner membrane polyunsaturated phospholipid (Soussi et al. 1990), and due to its unusually high content of unsaturated bonds cardiolipin is prone to lipid peroxidation (Soussi et al. 1990). The non-significant decrease in the level of mtDNA detected in the neuronal cells following a diminution in cellular CoQ_{10} status may contribute to the global loss of ETC activity. MtDNA is particularly prone to oxidative damage due to the lack of protective histones and limited repair mechanisms (Ullrich et al. 1999). CoQ_{10} is a cofactor in the conversion of DHO to OA (Malmquist et al. 2008) and so is essential for *de novo* pyrimidine synthesis. Defects in nucleotide metabolism have been associated with mtDNA depletion (López-Martín et al. 2007). The decrease in the level of mtDNA observed in this study further supports a link between CoQ_{10} deficiency and mtDNA depletion (Montero et al. 2007).

A neuronal cell CoQ_{10} deficiency was found to have a variable effect upon Δψm. The Δψm decreased in the middle range of CoQ_{10} deficiency (76% of control level) but increased at the lowest residual CoQ_{10} level (46% of controls). The increase in Δψm in the presence of a concomitant decrease in ETC Complex I, II/III and IV activities indicates that a reversal of Complex V activity has occurred to maintain Δψm (Gandhi et al. 2009; Yao et al. 2012). Reversal of Complex V activity has been described in a limited number of mitochondrial diseases (Abramov et al. 2010; McKenzie et al. 2007); however this is the first study to report a reversal of Complex V activity in association with CoQ_{10} deficiency. When the ETC is fully functional, as is the case with the controls, Δψm is maintained by Complexes I, III and IV pumping protons across the inner mitochondrial membrane. A mild decrease in ETC function, as observed in the neuronal cells with 76% residual CoQ_{10} level, induces a decrease in Δψm. However, when ETC function is profoundly decreased, as in neurons with 46% residual CoQ_{10} levels, Complex V activity appears to reverse. This is indicated by the rapid decrease in Δψm on addition of the Complex V inhibitor oligomycin. Here, the reversed activity of Complex V is maintaining the Δψm. By blocking the translocation of protons across the inner mitochondrial membrane with oligomycin Δψm can no longer be maintained and hence decreases. This hypothesis is further supported by the significant decrease in cellular ATP observed at 46% residual CoQ_{10} level. This phenomenon has not been reported

in previous studies of CoQ_{10} deficient fibroblasts (Quinzii et al. 2008; Quinzii et al. 2010), leading to the possibility that the reversal of Complex V activity may be a unique characteristic of CoQ_{10} deficient neuronal cells.

Blue native gel electrophoresis assessment of Complex V revealed that a decrease in neuronal CoQ_{10} status (76% and 46% residual CoQ_{10}) did not result in a concomitant reduction in the protein level of the complex. Furthermore, only a minimal loss of Complex V activity (12% decrease compared to control) was detected at 46% residual CoQ_{10}. The detection of the F_1 band on the blue native gel is commonly observed with both muscle and cell samples. This results from some dissociation of the holo-F_0-F_1 complex by anionic detergents used in the blue native gel electrophoresis assay (Wittig et al. 2007). Once isolated from the mitochondrial environment of neuronal cells with 46% residual CoQ_{10}, evidence of a reversal of Complex V activity may not be detectable under *in vitro* conditions as observed in the blue native gel electrophoresis studies. This is because the requirement to maintain $\Delta\psi m$ will no longer be present.

The results of this study indicate that CoQ_{10} deficiency in neuronal cells may have different biochemical consequences than those previously reported for fibroblasts (Quinzii et al. 2010; Quinzii et al. 2008). One of the most profound differences is the effect of CoQ_{10} deficiency upon ETC complex activities. In general CoQ_{10} deficient patient fibroblasts only display a loss of Complex II/III and I/III activity. Not the universal loss of ETC complex activities observed in this neuronal cell model, even at cellular CoQ_{10} levels <20% of control levels. The reason for this disparity is uncertain. However, since all the enzymes of the ETC are susceptible to ROS induced oxidative damage (Zhang et al. 1990), ETC dysfunction may result from an imbalance between mitochondrial oxidative stress and antioxidant capacity. The higher degree of ETC dysfunction observed in CoQ_{10} deficient neuronal cells may reflect a lower cellular antioxidant status than observed in fibroblasts. However further studies are needed to verify this.

In agreement with studies in fibroblasts, an increase in oxidative stress confined to the mitochondrion was observed in the CoQ_{10} deficient neuronal cells. Quinzii et al (2008) suggested a variable effect of CoQ_{10} deficiency on mitochondrial oxidative stress; whereby severe (<20% of control CoQ_{10}) and moderate (>60% of control CoQ_{10}) defects demonstrate low levels of oxidative stress. However

an intermediate defect (30-40% of control CoQ_{10}) in patient fibroblasts resulted in an increase in the level of mitochondrial oxidative stress. However neuronal cells display mitochondrial oxidative stress at slightly higher CoQ_{10} levels than fibroblasts (76-46% of control levels). The reason for the disparity between the two cell types is as yet unknown but may again reflect variations in cellular antioxidant status.

The increase in mitochondrial oxidative stress following PABA-induced CoQ_{10} deficiency may result from inefficient transfer of electrons from ETC Complexes I, II and III. This results in increased electron leak and enhanced production of the unstable semiquinone isoform of CoQ_{10}, a major site of ROS production (Turrens et al. 1985). A decrease in CoQ_{10} status may also affect the organisation and assembly of Complex III and its association with Complex IV into respiratory supercomplexes, thus altering the composition and activity of these complexes. These alterations may result in an enhancement of ROS generation at these sites (Rodríguez-Hernández et al. 2009). Interestingly, the degree of mitochondrial oxidative stress in the CoQ_{10} deficient neuronal cells does not reflect the level of ETC deficiency. Complex I and III are the major sites of ROS generation in the ETC (Sugioka et al. 1988; Turrens & Boveris 1980). However, although the degree of Complex I and II/III inhibition is more pronounced at 46% residual CoQ_{10} level, mitochondrial oxidative stress is lower than at 76% residual CoQ_{10}. A possible reason for this discrepancy is the existence of energy thresholds. This happens once ETC complex activities are decreased beyond a certain threshold of inhibition. Then the rate of mitochondrial respiration and consequently ETC electron flow decreases with a concomitant fall in ATP synthesis (Davey et al. 1998). Therefore, the level of ETC inhibition at 46% residual CoQ_{10} may be sufficient to reduce ETC electron flow and consequently decrease mitochondrial ROS generation (Wallace 2000). The decrease in ETC activity at 46% residual CoQ_{10} may also contribute to the profound loss of cellular ATP occurring at this level of CoQ_{10} deficiency.

Here we have highlighted the vulnerability of neuronal mitochondrial metabolism to a small deficit in CoQ_{10} status (76% residual CoQ_{10} levels). This small deficit in CoQ_{10} status also resulted in a simultaneous loss of ETC function and increased mitochondrial oxidative stress. This could explain the prominent neurological dysfunction associated with CoQ_{10} deficiencies.

Although no evidence of a decrease in cellular GSH status was observed in the CoQ_{10} deficient neurons, a non-significant increase in the level of this tripeptide was observed at 76% control CoQ_{10} status. This increase in GSH status coincides with a decrease in lipid peroxidation and cytosolic superoxide at this level of CoQ_{10} deficiency. In agreement with these results, Zhu et al (2007) have also reported an up-regulation of GSH synthesis in response to an increase in cellular oxidative stress. The cause of this increase in cellular GSH status has yet to be elucidated but may result from an up-regulation in the expression of the antioxidant binding transcription factor *NRF2* (Zhu et al. 2005). Interestingly, a non-significant increase in the activity of glutathione reductase has been reported in fibroblasts from a patient with the COQ2 gene mutation which may explain the elevated and normal levels of GSH following a deficit in neuronal cell CoQ_{10}. However the activity of this enzyme has yet to be assessed in this cell model (Quinzii et al. 2008).

3.6. Conclusion

In conclusion, the results of this study have shown evidence that both ETC dysfunction and mitochondrial oxidative stress may be involved in the pathogenesis of neuronal cell CoQ_{10} deficiency. Interestingly, a marginal decrease in CoQ_{10} status (76% residual CoQ_{10}) appears to be sufficient to impair ETC function and increase mitochondrial oxidative stress, highlighting the vulnerability of neurons to a small deficit in CoQ_{10} status. In contrast to CoQ_{10} deficient fibroblasts, a CoQ_{10} deficiency (46% residual CoQ_{10}) in neuronal cells appears to result in reversal of Complex V activity. This phenomenon has not been reported in previous studies of CoQ_{10} deficiency and may be a unique characteristic of neuronal cells. This neuronal cell model provides insights into the effects of CoQ_{10} deficiency on neuronal mitochondrial function and oxidative stress, and will be an important tool to evaluate candidate therapies for neurological conditions associated with CoQ_{10} deficiency as discussed in the next chapter.

Chapter 4

Investigation of Coenzyme Q_{10} and Methylene Blue Treatment on the Neuronal Cell Model of Coenzyme Q_{10} Deficiency

4.1. Introduction

CoQ_{10} and its analogues have been used in the treatment of a number of diseases and conditions. These include various neurodegenerative diseases (FA, AD, PD, FA; Spindler et al. 2009), cardiovascular diseases (Greenberg & Frishman 1990; Langsjoen & Langsjoen 1999); and more tentatively dermatological (Inui et al. 2008) and fertility (Mancini et al. 2005) issues.

Clinical trials to assess the therapeutic potential of CoQ_{10} have been undertaken for a number of neurodegenerative disorders with varied success. Clinical improvement has been reported in the treatment of FA with CoQ_{10} in conjunction with vitamin E; whereby 49% of patients demonstrated an improvement in the ICARS score (Cooper et al. 2008). Interestingly despite the initial success reported for CoQ_{10} in the treatment of PD (Shults et al. 2002) the recent Phase III trial was terminated after it was deemed unlikely to yield significant results (Beale et al. 2011).

CoQ_{10} is available in many different forms with variable bioavailablity, including powder, suspension, oil solution, solubilised forms (All-Q and Q-Gel), as well as creams, tablets, wafers, and hard-shell or softgel capsules. Most recently a self-emulsifying drug delivery system (SEDDS) composed of oil and surfactant (Onoue et al. 2012) and a lipid-based formulation that self-assembles on contact with an aqueous phase into a colloid delivery system (VESIsorb, colloidal-Q10) (Liu & Artmann 2009), have been developed in an effort to increase bioavailability. Various formulations of ubiquinol are also available (Hosoe et al. 2007).

In the context of this chapter we are interested in the treatment of primary CoQ_{10} deficiency. A recent literature review assessed the efficacy of CoQ_{10} supplementation on the various phenotypes associated with primary CoQ_{10} deficiency (Emmanuele et al. 2012). 75% of patients with CoQ_{10} deficiency were reported to show some form of clinical improvement following CoQ_{10} supplementation (excluding the ataxic phenotype). However, only 49% of patients with the ataxic phenotype demonstrated improvement/stabilisation in their ataxic symptoms following CoQ_{10} supplementation. The refractory nature of neurological symptoms associated with CoQ_{10} deficiency to CoQ_{10} supplementation has also been reported for the encephalomyopathic phenotype of this condition (Ogasahara et al. 1989; Sobreira et al. 1997; Giovanni et al.

2001). The muscle symptoms associated with CoQ_{10} deficiency have been reported to improve upon supplementation, however encephalopathy is only resolved in 1 of 4 patients (Giovanni et al. 2001).

Furthermore although biochemical improvement was reported for the CoQ_{10} deficient patients with the *COQ9* and *PDSS2* mutation no improvement in their neurological symptoms was observed. (Rahman et al. 2001; López et al. 2006)

At present the reasons for the refractory nature of the neurological symptoms associated with CoQ_{10} deficiency to CoQ_{10} supplementation remain to be elucidated. However they could include; poor transfer of CoQ_{10} across the blood-brain barrier, irreversible structural and biochemical neuronal dysfunction or an inability of CoQ_{10} deficient neurones to utilise exogenous CoQ_{10}.

Methylene blue (MB) is a heterocyclic aromatic chemical compound with the molecular formula $C_{16}H_{18}N_3SCl$ (Figure 4.1). MB is a potent cationic dye with maximum absorption of light around 670 nm (Cenens & Schoonheydt 1988). However in recent years the investigation of the therapeutic potential of MB has been undertaken. MB has historically been used as an anti-malarial agent (Mandi et al. 2005) and has been investigated experimentally for a number of conditions including sepsis (Ramamoorthy et al. 2013), dermatological conditions (Riddle et al. 2009; Salah et al. 2009), and various viruses (Floyd et al. 2004). Interestingly MB has also been suggested as a potential treatment for a number of neurodegenerative diseases such as AD and PD. The university of Aberdeen and TauRx Therapeutics have been investigating the effects of MB, or as it is known commercially Rember, or LMTX. They have suggested that MB may inhibit Tau and α- synlucin aggregation through increasing proteasome activity. However, in vitro studies have indicated that MB may also have a beneficial effect on mitochondrial function, which is likely to contribute to its therapeutic potential (Oz et al. 2009). A placebo controlled phase IIB clinical trial on patient with mild AD found that through taking a 60mg dose of MB per day over a period of 50 weeks the progression of AD slowed down by 5.4 ADAS-Cog units (Galimberti & Scarpini 2011). A phase III trial of the drug in AD is currently undergoing recruitment.

A study by Wen et al. (2011) found that MB directly improves ETC I/III activity through the enhanced electron transfer from NADH to cyt c. They found that MB can act as a direct substrate of NADH dehydrogenase in mitochondrial complex

I and electrons gained in this reaction can then be delivered to cyt c. Allowing MB to form an independant redox cycle between NADH and Cyt c that reroutes electrons between Complex I and III.

MB may also delay senescence at nM levels; increase mitochondrial Complex IV by 30%; enhance cellular oxygen consumption by 37-70%, increase heme synthesis and induce phase-2 antioxidant enzymes in hepG2 cells (Atamna et al. 2008).

CoQ_{10} deficiency is a mitochondrial disorder whereby ETC complex activities and antioxidant status can be perturbed. MB is a unique compound that is not only able to act as an antioxidant but is also able to shuttle electrons down the ETC, bypassing the disrupted complexes allowing the $\Delta\Psi_m$ to be maintained (Lin et al. 2012). Consequently MB may have a potential therapeutic benefit in the treatment of CoQ_{10} deficiency.

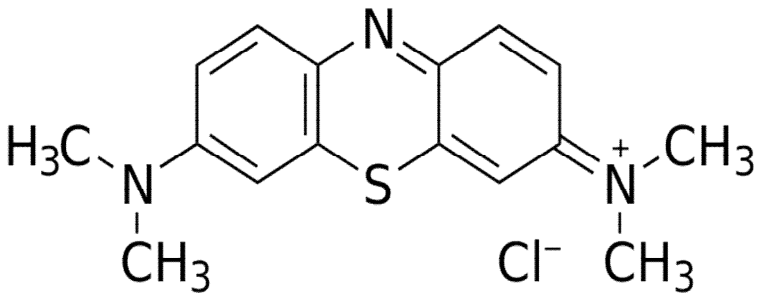

Figure 4.1 The Chemical Structure of Methylene Blue (Methylthioninium Chloride)

MB is a unique compound that is not only able to act as an antioxidant but is also able to shuttle electrons down the ETC, bypassing the disrupted complexes allowing the Δ□$_m$ to be maintained (Lin et al. 2012). The structure is stabilised by allowing the + charge to be distributed on the two nitrogens attached to the ring system (to become partial "ammonium ions"). When reduced, it forms leucomethylene blue which is colourless

4.2. Aims

In order to investigate the effect of CoQ_{10} supplementation on mitochondrial function in CoQ_{10} deficient neurones we administered varying amounts of CoQ_{10} (2.5, 5 and 10μM) to the previously established SH-SY5Y neuronal cell model of CoQ_{10} deficiency (see chapter 3). We also chose to investigate the effect of Methylene Blue (MB), an electron carrier that is a possible candidate therapy for mitochondrial disorders on mitochondrial function in CoQ_{10} deficient neuronal cells. Varying amounts of MB were administered to the neuronal cell model of CoQ_{10} deficiency (0.1 and 1μM). ETC Complex activities (I, II/III and IV), mitochondrial oxidative stress and mitochondrial membrane potential were evaluated in the CoQ_{10} supplementation experiments. ETC activities (I, II/III and IV) were investigated in MB experiments.

4.3. Methods

4.3.1. Cell Culture

SH-SY5Y cells were cultured as described in Section 2.2.4 and treated with PABA as described in Section 2.2.4 (1mM) over a 5 day incubation period. Following the 5 day treatment of the SH-SY5Y cells with PABA the cells were then treated with CoQ_{10} or MB (plus 1mM PABA) for a further 5 day period (see Section 4.4.1 for details).

4.3.2. Quantification of CoQ_{10} Levels

CoQ_{10} content was analysed in SH-SY5Y cells by reverse phase HPLC as described in Section 2.3

4.3.3. Mitochondrial Bioenergetics Analysis

Complexes I, II/III and IV of the ETC, CS and ATP were assayed in SH-SY5Y cells as described in Section 2.6.

4.3.4. Oxidative Stress Assessment

Microscopy analysis of mitochondrial oxidative stress (Mitosox) was performed on SH-SY5Y cells as described in Section 2.7.4.

4.3.5. Mitochondrial Membrane Potential

TMRM was used to determine Δψm in the SH-SY5Y cells as described in Section 2.7.3.

4.3.6. Total Protein Determination

The protein content of the SH-SH5Y cells was determined by the Lowry method as described in Section 2.3.

4.3.7. Statistical Analysis

Statistical analysis was performed as described in Section 2.8.

4.4. Results

4.4.1. Treatment Optimisation

4.4.1.1. Coenzyme Q_{10}

CoQ_{10} is a lipophilic molecule; thus solubilising this quinone in an aqueous solution is challenging. The media used to culture the SH-SY5Y cells (DMEM/F-12+10% FBS) is rich is lipids due to its high FBS content. Cells were passaged as previously described in Section 2.2.2. The CoQ_{10} (ethanol) stock solution was incubated in a water bath at +37°C for 10 minutes prior to use. A given concentration of the CoQ_{10} stock solution was added to the media in a 15/50ml falcon tube and incubated at +37°C for 20 minutes.

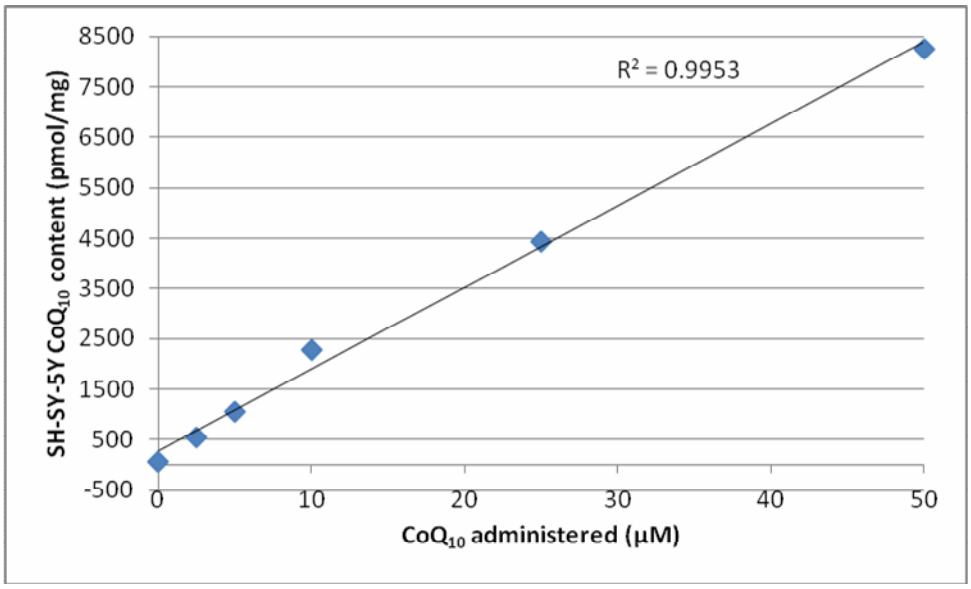

Figure 4.2 Concentration curve demonstrating the effect of CoQ_{10} supplementation on SH-SY5Y cell CoQ_{10} content; 0-50µM treatment.

In human plasma the approximate concentration reached during CoQ_{10} supplementation is ~1-5µM (Miles 2007; Bhagavan & Chopra 2006; Shults et al. 2004). A concentration of 5 µM was also used in a fibroblast CoQ_{10} supplementation study that effectively normalised the bioenergetic status of CoQ_{10} deficient fibroblasts following a treatment period of a week (López et al. 2010).

We subsequently constructed a dose response curve around this approximate value (Figure 4.2). Control cells were treated with a given dose (2.5-200µM) of CoQ_{10} for 5 days and then the CoQ_{10} status of the cells was assessed. A linear relationship between CoQ_{10} supplementation and SH-SY5Y CoQ_{10} content was established (0-50 µM CoQ_{10}). Cells treated with 100 and 200 µM CoQ_{10} died after 24 hours. Concentrations of 2.5, 5 and 10µM were selected for investigation in this study.

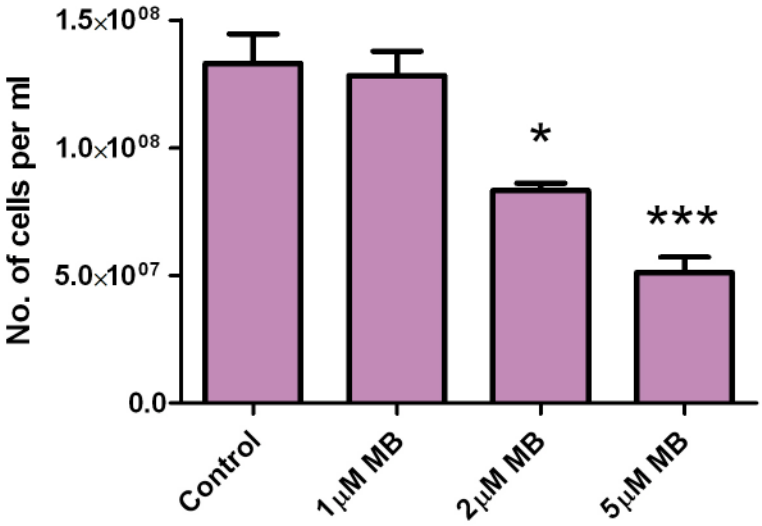

Figure 4.3 Cell count using a haemocytometer of SH-SY5Y cells treated with 0-5µM Methylene Blue (MB)

4.4.1.2. Methylene Blue

MB has been dubbed a “cerebral metabolic enhancer” (Lin et al. 2012). It is able to shuttle electrons directly from Complex I to Complex IV thus bypassing the other ETC complexes and the need for CoQ_{10} as an electron carrier; making it an ideal candidate as an alternative to CoQ_{10} supplementation. In HT-22 cells

(hippocampal cell line) 10 µM of MB was able to increase oxygen consumption rate (OCR) through enhancing Complex I/III activity (Lin et al. 2012). Initial attempts to use a concentration of 10 µM resulted in total cell death. Increased cell death was also observed between 1-5 µM (Figure 4.3). Thus we selected a concentration range between 0.1 and 1 µM for the present study.

4.4.2. Coenzyme Q_{10} Treated Cells

4.4.2.1. CoQ_{10} Content

1mM PABA treatment consistently resulted in a 54% decrease in cellular CoQ_{10} content (Figure 4.4A).

The CoQ_{10} intercellular content of the CoQ_{10} supplemented cells was assessed in PABA treated SH-SY5Y cells. Significant increases in CoQ_{10} intercellular content were noted in the PABA treated SH-SY5Y cells supplemented with 5 and 10µM CoQ_{10}. A maximal increase in CoQ_{10} content of 79 times (10 µM CoQ_{10} condition) was observed when compared to PABA treated SHSY-5Y cells (Figure 4.4A)

4.4.2.2. Mitochondrial Electron Transport Chain Activities

All ETC complex activities are expressed as a ratio of CS activity a mitochondrial marker enzyme (Hargreaves et al. 1999).

The effect of CoQ_{10} treatment on mitochondrial ETC complex activity was assessed in PABA-treated SH-SY5Y cells. Following treatment with 5 µM CoQ_{10} ETC Complex II/III activity was restored to 82% of control level (no PABA treatment condition (Figure 4.4C). However, increasing the concentration to 10µM did not further restore Complex II/III activity. 5µM CoQ_{10} and 10µM CoQ_{10} treatments significantly ($p<0.05$) increased Complex III/III activity compared to PABA treated cells (Figure 4.4C).

CoQ_{10} treatment resulted in a non-significant increase in Complex I activity compared to PABA treated cells. Interestingly it was noted that Complex I activity increased sequentially according to the dosage of CoQ_{10} administered with Complex I activity being restored to 71% of control levels at 10µM CoQ_{10} (Figure 4.4B). A similar non-significant progressive increase was noted for Complex IV activity following CoQ_{10} treatment. However, Complex IV activity was restored to 78% of control level at 10µM CoQ_{10} (Figure 4.4D).

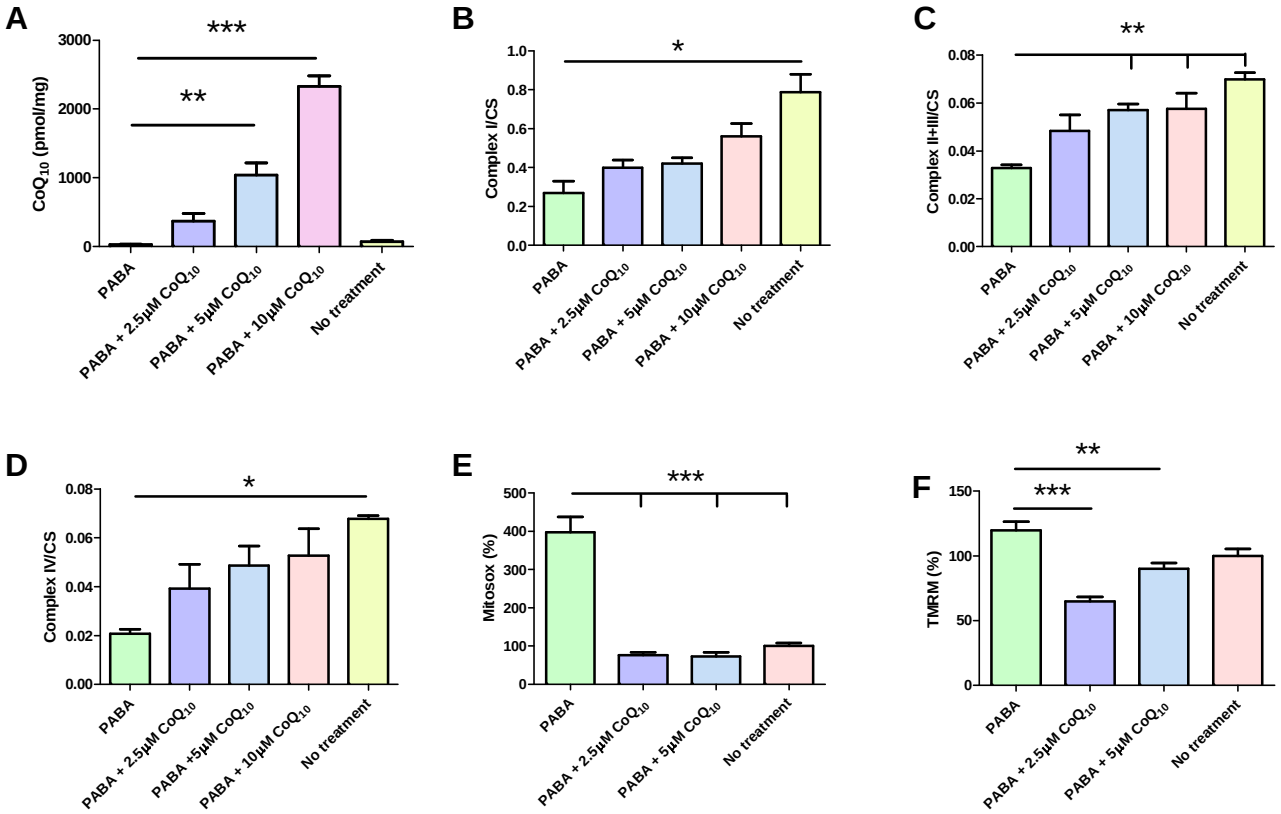

Figure 4.4 Effect of 5 day treatment with Coenzyme Q_{10} (CoQ_{10}) following PABA (1mM) induced CoQ_{10} deficiency in SH-SY5Y cells on a) CoQ_{10} (n=4), b) Complex I (n=3), c) Complex II+III (n=3), d) Complex IV (n=3), e) mitochondrial superoxide (Mitosox; n=4), f) mitochondrial membrane potential (TMRM; n=4)

Error bars represent standard error of the mean (SEM); statistical analysis was carried out using one-way ANOVA with Bonferroni post hoc analysis; levels of significance: *:p<0.05, **:p<0.005, ***:p<0.0005

4.4.2.3. Mitochondrial Oxidative Stress Analysis

Results suggest a significant decrease in the level of mitochondrial superoxide in cells treated with CoQ_{10} and PABA compared to PABA only treated cells (Figure 4.4E). There was no significant difference between treatments with 2.5 $CoQ_{10,}$ 5µM CoQ_{10} and controls.

4.4.2.4. Mitochondrial Membrane Potential

As stated in the previous chapter (Section 3.3.7) Δψm is differentially affected by neuronal CoQ_{10} deficiency. At the highest PABA induced CoQ_{10} deficiency, 1mM PABA, the Δψm is increased in comparison to normal levels. The middle range deficiency induced a decrease in Δψm (0.5mM PABA).

The results from the CoQ_{10} supplementation studies indicate that following treatment with 5µM CoQ_{10} Δψm was restored to 90% of control (no PABA treatment) levels (Figure 4.4F). Interestingly the Δψm observed in the 2.5µM CoQ_{10} (+1mM PABA) treatment condition was similar to that observed in the 0.5mM PABA treated cells (Section 3.3.7; 35% decrease: 2.5µM CoQ_{10}+1mM PABA v. 25% decrease: 0.5mM PABA).

It is also interesting to note that the punctuate structure of the mitochondria following PABA treatment (1mM) in the SH-SY5Y cells (Figure 4.5b). Increasing supplementation with CoQ_{10} produces a less punctuate mitochondrial structure and increases the fluorescence closer to control levels (Control: Figure 4.5a; PABA+ 2.5µM $CoQ_{10:}$ Figure 4.5c, PABA + 5µM $CoQ_{10:}$ Figure 4.5d).

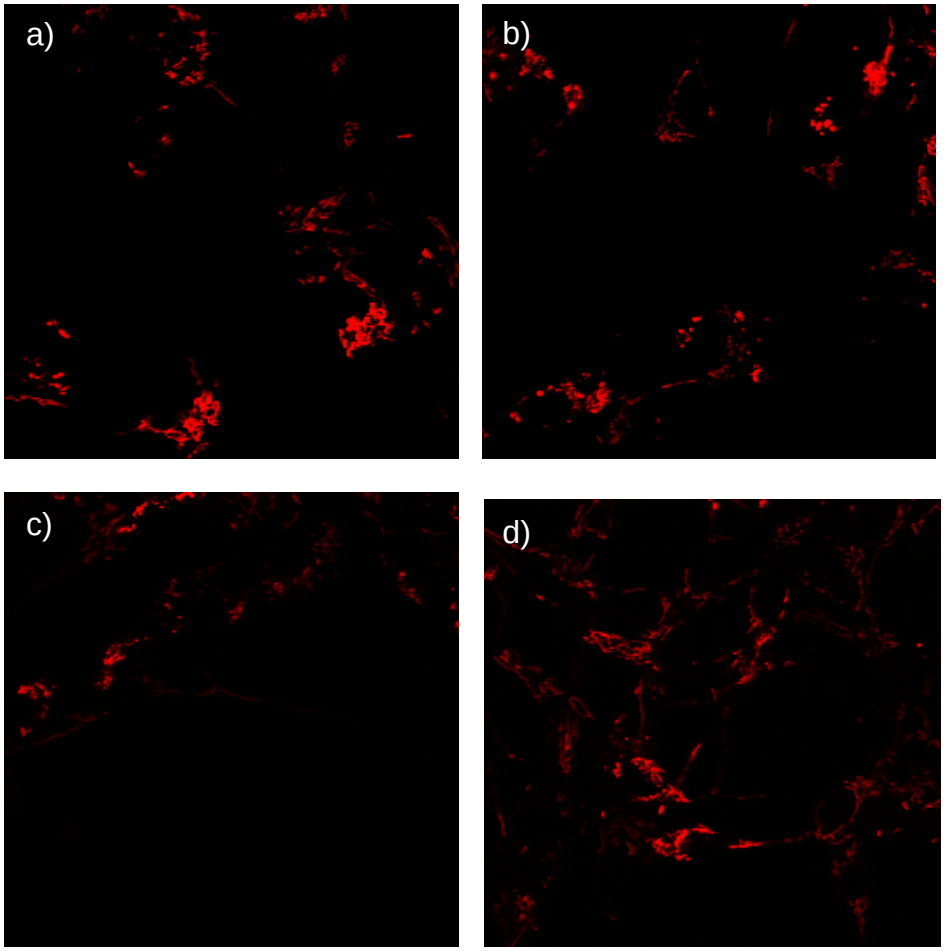

Figure 4.5 SH-SH5Y cells incubated with TMRM treated with a) no treatment, b) PABA, c) PABA+ 2.5µM CoQ_{10}, d) PABA + 5µM CoQ_{10}

Note the punctuate structure of the mitochondria following PABA treatment (1mM) in the SH-SY5Y cells (Figure 4.5b). Supplementation with CoQ_{10} produces a less punctuate mitochondrial structure and increases the fluorescence closer to control levels (Control: Figure 4.5a; PABA+ 2.5µM $CoQ_{10:}$ Figure 4.5c, PABA + 5µM $CoQ_{10:}$ Figure 4.5d).

4.4.3. Methylene Blue Treated Cells

4.4.3.1. CoQ_{10} Content

MB treatment did not appear to induce an increase in SH-SY5Y CoQ_{10} status. In contrast, inclusion of MB with the PABA treatment induced a progressive decrease in neuronal CoQ_{10} status compared to the PABA treated cells (Figure 4.6A). The addition of 0.5 and 1µM MB induced a significant decrease ($p<0.005$) compared to the PABA treated and 0.1µM MB and PABA treatment conditions ($p<0.05$).

4.4.3.2. Mitochondrial Electron Transport Chain Activities

The effect of MB treatment on mitochondrial ETC complex activity was assessed in PABA-treated SH-SY5Y cells. MB was not able to restore any of the ETC complex activities to control level (Figure 4.6). Complex II/III and IV activities in the MB treated cells (+PABA) were comparable to that of cells treated with PABA only (Figure 4.6 C and D; Complex II/III: ~54% decrease; Complex IV: ~71% decrease [compared to no treatment condition]). MB (+PABA) treated cells demonstrated a non-significant progressive increase in Complex I activity compared to PABA treated cells (Figure 4.6B). However there was still a significant difference in Complex I activity between the control and MB treatment conditions (Figure 4.6D).

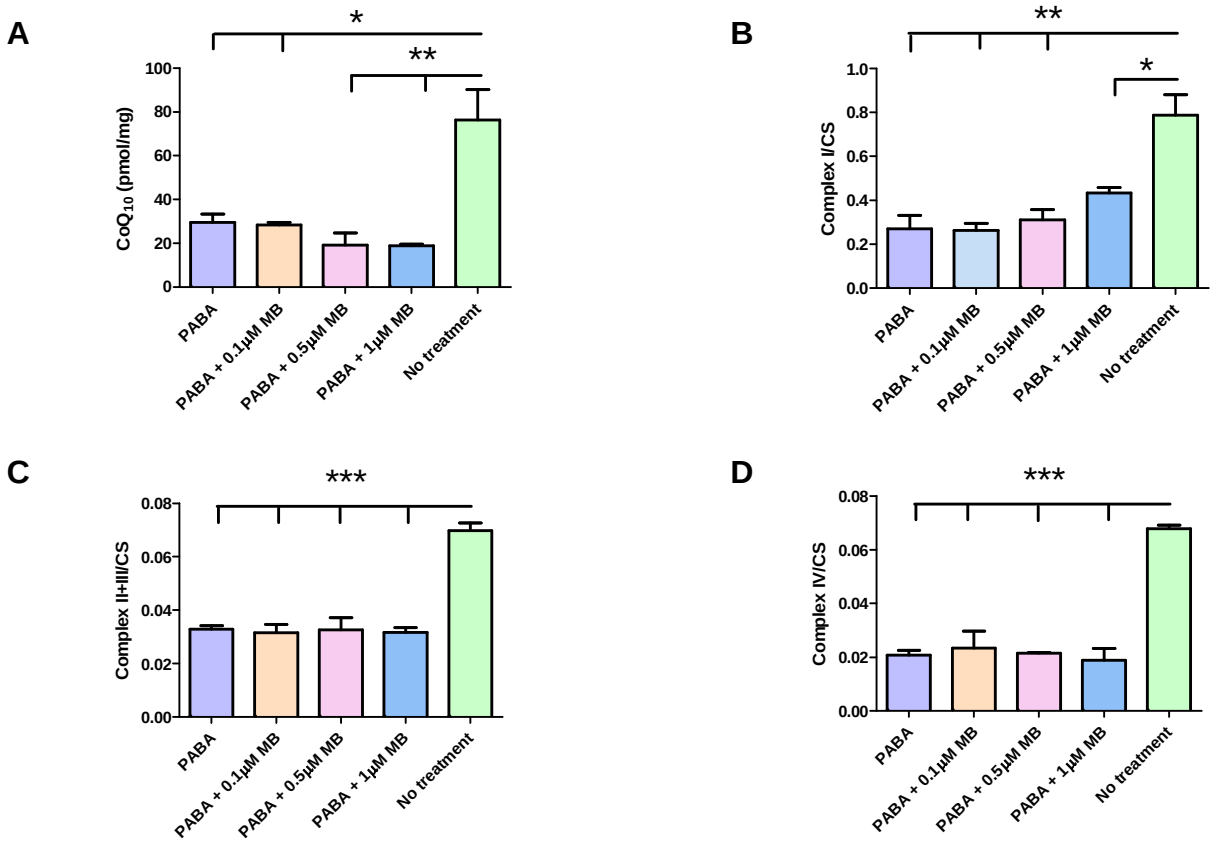

Figure 4.6 Effect of 5 day treatment with Methylene Blue (MB) following PABA induced Coenzyme Q_{10} (CoQ_{10}) deficiency in SH-SY5Y cells on a) CoQ_{10} (n=4), b) Complex I (n=3), c) Complex II+III (n=3), d) Complex IV (n=3)

Error bars represent standard error of the mean (SEM); statistical analysis was carried out using one-way ANOVA with Bonferroni post hoc analysis; levels of significance: *:p<0.05, **:p<0.005, ***:p<0.0005

Treatment	*Concentration (µM)*	*CoQ_{10} content*	*Complex I*	*Complex II/III*	*Complex IV*	*Mitochondrial superoxide*	*Δψm*
CoQ_{10}	**2.5**	↑	↑	↑	↑	↓***	↓**
	5	↑*	↑	↑*	↑	↓***	↓***
MB	**0.5**	↓	-	-	-		
	1	↓	↑	-	-		

Blank: not measured; -: no effect; ↑↓ insignificant increase/decrease; ↑*↓*, significant increase/decrease.

Table 4.1Summary of results obtained in neuronal cell model of CoQ_{10} deficiency induced by PABA treatment (1mM) treated with 2.5 and 5µM CoQ_{10} and 0.5 and 1µM methylene blue (MB): CoQ_{10} content, mitochondrial ETC complex activities, mitochondrial superoxide and Δψm.

4.5. Discussion

CoQ_{10} deficiency is a rare but often treatable disease. However the neurological symptoms associated with the disease are frequently refractory to treatment, for reasons as yet to be determined. In this chapter we have investigated the effect of CoQ_{10} and MB treatment on mitochondrial function in CoQ_{10} deficient neuronal cells.

Utilising our PABA induced neuronal cell model of CoQ_{10} deficiency we were able to investigate the effect of CoQ_{10} supplementation on ETC complex activities, mitochondrial superoxide and Δψm (Table 4.1). Following CoQ_{10} supplementation a significant increase in ETC Complex II/III activity was observed (>5μM CoQ_{10}) compared to the level of activity in the CoQ_{10} deficient cells. In addition, a progressive increase in Complex I and IV activities was also determined. However, CoQ_{10} treatment failed to restore ETC activity to control levels. This suggests the possibility that insufficient CoQ_{10} was reaching the inner mitochondrial membrane to restore ETC activity and therefore higher doses of CoQ_{10} supplementation may be required to ameliorate the deficit in ETC activity.

In addition, the significant decrease in mitochondrial oxidative stress (lower than controls) following CoQ_{10} treatment (5μM) indicates that oxidative damage to the ETC complexes may not be the primary mediator of this loss of ETC activity. Therefore following supplementation insufficient CoQ_{10} may still be present in the inner mitochondrial membrane to restore its electron carrier activity to normal levels. Furthermore, the persistent generalised loss of ETC following supplementation may be the result of an insufficient level of CoQ_{10} being present in the cell to restore pyrimidine synthesis to controls levels (López-Martín et al. 2007).

Following CoQ_{10} supplementation Δψm was restored to 90% of control levels indicating that the reversal of ETC Complex V activity, which was determined in the SH-SY5Y neuronal cells following 1mM PABA treatment (Chapter 3), had been ameliorated, and Complex V activity was working in the forward direction. Mitochondrial membrane potential has not previously been investigated at a cellular level in relation to CoQ supplementation.

The effect of MB treatment on ETC activity in CoQ_{10} deficient neuronal cells was investigated in this chapter. MB has been dubbed as a metabolic enhancer and thus would be a good candidate for restoring mitochondrial ETC activity in mitochondrial diseases. MB treatment induced a non-significant increase in Complex I activity, but was ineffective in restoring Complex II/III and Complex IV activity to control levels. This result is in agreement with the study of Lin et al (2012) which reported that Complex II/III activity was unaffected by MB treatment, but Complex I/III activity was enhanced following MB treatment as a possible consequence of increased electron donation from NADH to MB rat brain mitochondria.

Another interesting finding relating the Δψm studies was the punctuate nature of the mitochondria in the CoQ_{10} deficient neurones. Mitochondria are dynamic in structure and are capable of adapting their structure according to the energy demands of the cell; through fusion and division. The fused inter-mitochondrial system can decompose into small roundish mitochondria (punctuate structure) under some physiological conditions but also occurs in some pathology (Skulachev 2001). It has been suggested that this is a protective mechanism against oxidative stress (Skulachev 2001).

CoQ_{10} supplementation was effective in decreasing the level of mitochondrial oxidative stress observed in the CoQ_{10} deficient neuronal cells. This is in agreement with the result obtained in the fibroblast studies performed by Quinzii and colleagues (López et al. 2010). Mitochondrial oxidative stress has been implicated in contributing to the pathogenesis in a number of neurodegenerative diseases including CoQ_{10} deficiency. Ubiquinol is a potent antioxidant; due to CoQ_{10}'s high concentration in the mitochondria we would expect a deficiency in CoQ_{10} to increase mitochondrial oxidative stress which was observed in the CoQ_{10} deficient neuronal cells. Intriguingly, CoQ_{10} supplementation was found to reduce the level of mitochondrial oxidative stress below that of the control. Although ROS has been frequently associated with cellular damage; ROS are also important for cell signalling (Thannickal & Fanburg 2000). ROS generation by plasma membrane oxidases have been implicated in normal physiological signalling pathways involving growth factors and cytokines. Thus a decrease in ROS below control levels may actually be detrimental to cellular function.

Consequently decreased ROS signalling should be considered during CoQ_{10} supplementation.

CoQ_{10} supplementation was also partially effective at restoring mitochondrial ETC activity. Complex II/III activity was significantly restored to 82.5% [10µM CoQ_{10}] of the no treatment condition. CoQ_{10} supplementation was less effective at restoring Complex I and IV activity (Complex I: 71.1% restored [10µM CoQ_{10}]; Complex IV: 77.7% restored [10µM CoQ_{10}]). In contrast Quinzii and colleagues found a complete restoration of ETC activity in CoQ_{10} deficient fibroblasts, demonstrated through ATP quantification (López et al. 2010). The inability to restore ETC activity following CoQ_{10} treatment in the CoQ_{10} deficient neuronal cells may be an indication of why neurological CoQ_{10} deficiency has been reported to be refractory to treatment (Emmanuele et al. 2012). The ATP quantification used in the fibroblast study is a measure of the physiological output of the ETC. In the present study we have assessed the activity of the ETC complexes. It is possible that the ETC complex enzymes are compromised but are sufficient to perform oxidative phosphorylation at normal levels. Davey et al. (1998) reported that a deficiency in neuronal ETC Complex I activity by 25% of normal level may be sufficient to perturb oxidation phosphorylation. Therefore, a 29% decrease in ETC Complex I activity determined in the CoQ_{10} deficient neuronal cells following supplementation may indicate that oxidative phosphorylation is still compromised in these cells. However, quantification of cellular ATP levels would be required to confirm/refute this hypothesis.

MB is has demonstrated efficacy in treating a number of neurodegenerative disorders; including PD and AD (Lin et al. 2012). However the efficacy of MB has never been examined in CoQ_{10} deficiency. In this study we investigated the effect of MB treatment on the ETC complex activities in CoQ_{10} deficient neuronal cells. Following treatment with MB no significant increase in ETC activity was observed compared to the CoQ_{10} deficient neuronal cells. This suggests that MB was not effective at restoring the ETC deficiency associated with the perturbation in neuronal cell CoQ_{10} status. However further studies would be needed to investigate the effect on oxidative stress and physiological ETC function. Interestingly MB decreased the level of CoQ_{10} (not significant); implying that MB treatment of CoQ_{10} deficiency could further exacerbate the deficit in CoQ_{10} status.

Neurological CoQ_{10} deficiency is often refractory to treatment. Only 46% of patients with the ataxic phenotype showed a clinical improvement/stabilisation following CoQ_{10} supplementation; compared to 75% for other phenotypes (Emmanuele et al. 2012). It has been suggested that this may be a result of poor blood brain barrier penetration or irreversible structural brain alterations (López et al. 2010). The work in this chapter has indicated that CoQ_{10} supplementation to CoQ_{10} deficient neuronal cells results in a decrease in mitochondrial oxidative stress as well as an increase in Δψm, however it is unable to fully restore ETC activity to normal levels. Longer incubation periods and/or different formulations of CoQ_{10} may be required to improve ETC function.

Treatment regimens for CoQ_{10} are variable, between clinicians and for different conditions. Current formulations of CoQ_{10} demonstrate a plasma CoQ_{10} concentration of 1-5µM (oral dose: 90-3000mg; Miles 2007). There are many different formulations available and there is a great deal of variability in bioavailability between formulations. Newer more sophisticated formulations may be able to increase the plasma concentration in line with the 10µM target highlighted in this study.

However to date no studies have investigated the effect of CoQ_{10} supplementation of CSF levels of CoQ_{10}. The blood brain barrier may further widen the gap between achieving a therapeutic dose suitable for treatment of neuronal CoQ_{10} deficiency. A plasma CoQ_{10} concentration of 1-5µM may not translate to a similar concentration in the CSF. Therefore, CSF studies will be vital in developing treatment regimens for neurological CoQ_{10} deficiency.

4.6. Conclusion

In conclusion, the results in this chapter have indicated that CoQ_{10} supplementation has the ability to decrease mitochondrial oxidative stress and increase Δψm in neuronal CoQ_{10} deficiency. However higher doses of CoQ_{10} may be required to fully restore ETC activities to control levels. Studies have indicated that following CoQ_{10} supplementation a concentration of ~5µM is reached in the plasma. Here we demonstrate that a concentration of 5µM is capable for counteracting the reversal of Complex V activity and the increase in mitochondrial oxidative stress observed in CoQ_{10} deficient neuronal cells. However, the deficit in ETC activity could not be fully ameliorated by treatment even at higher doses of CoQ_{10} supplementation (10µM). This study highlights

the need for improved CoQ_{10} formulations to increase CoQ_{10} bioavailability in the treatment of neuronal CoQ_{10} deficiency.

We can also conclude that further work is needed to assess if MB is suitable for treatment of CoQ_{10} deficiency. Here we examine the effect on separate ETC enzyme assays, however the effect of MB treatment on oxidative stress and integrated ETC activity need to be investigated in relation to CoQ_{10} deficiency.

Chapter 5

Tandem Mass Spectrometry Method for Quantifying Coenzyme Q_{10} in CSF

5.1. Background

Currently, the most common analytical techniques employed to determine tissue levels of CoQ_{10} are high performance liquid chromatography (HPLC) with either UV or EC detection. UV detection utilises the ability of the benzoquinone core of CoQ_{10} to absorb UV light at 275 nm. This method has been widely used and is highly reliable. However it is time consuming, takes more than 15 minutes to analyse each sample, and has a detection limit of 6nM making it unsuitable for CSF CoQ_{10} assessment (Duncan et al. 2005). Similarly, HPLC EC detection methods are also widely described, and have been previously utilised for measurement of CoQ_{10} in CSF (Isobe et al. 2010; Isobe et al. 2009; Murata et al. 2008). However, both UV and EC detection can potentially be subject to interference, due to either electrical interference or mobile phase contamination when measurements are made close to the detection limit. A robust and sensitive tandem mass spectrometry (LC-MS/MS) method would ensure a fast, selective and highly sensitive method of ubiquinone quantification.

Various LC-MS/MS methods for measurement of CoQ_{10} have been described (Ruiz-Jiménez et al. 2007; Takamiya et al. 1999; Li et al. 2008; Schaefer et al. 2004). However, CoQ_{10} forms Na^+ and K^+ adducts which can be difficult to fragment, thus limiting sensitivity and utility of these methods. This has been overcome by use of methylamine to produce a dominant ion ($[M + CH_3NH_3]^+$) which fragments easily and this significantly increases sensitivity (Teshima & Kondo 2005).

A major problem with current mass spectrometric methods has been the selection of a suitable internal standard (IS). IS's currently used for CoQ_{10} analysis include ubiquinone analogues such as CoQ_9, which will be influenced by endogenous CoQ_9 in human tissue, and chemically synthesised analogues such as CoQ_{11}, di-ethoxy-CoQ_{10} and di-propoxy-CoQ_{10}. These are type 2 ISs, structurally related to CoQ_{10} with similar chemical properties. Type 1 ISs are preferred for MS. These compounds share the same chemical structure of the analyte but differ in mass owing to the incorporation of stable isotopes. This means the IS will fragment in an analogous way to the analyte to produce a characteristic product ion. Although isotopically-labelled CoQ_{10} has previously

been synthesised (Hamamura, Yamagishi, et al. 2002; Hamamura, Yamatsu, et al. 2002), the syntheses are difficult and none are commercially available.

5.2. Aims

The primary aim of this chapter is to develop a sensitive method capable of quantifying CoQ_{10} in CSF; the low nanomolar range. The UV detection method that is currently used to diagnose CoQ_{10} deficiency is not sensitive enough for the analysis of CSF CoQ_{10} content. However a method utilising MS may prove more sensitive. Hence we set out to establish a MS method suitable for the analysis of CoQ_{10} in skeletal muscle homogenates, fibroblasts and CSF.

A secondary aim is to develop an IS suitable for a MS method, consequently we synthesied a deuterated CoQ_{10} IS via an alcohol exchange method.

5.3. Synthesis of Deuterated CoQ_{10} (d_6-CoQ_{10})

Here we describe a novel and simple method for the synthesis of d_6-CoQ_{10} which is suitable for analysis of CoQ_{10} in skeletal muscle homogenates, fibroblasts and CSF.

The two methoxy groups of CoQ_{10} can be exchanged with other alcohols in alkaline solution. This has been exploited to synthesise other ISs such as diethoxy-CoQ_{10} (Edlund 1988) or dipropoxy-CoQ_{10} (Duncan et al. 2005) for HPLC. We used the same approach to replace the two CH_3O- groups of CoQ_{10} with two CD_3O- groups, yielding d_6-CoQ_{10}. Preliminary experiments attempting exchange of CH_3O- groups directly with a large excess of deuterated methanol in alkaline solution yielded a mixture of d_6-CoQ_{10} with a major contaminant of unexchanged CoQ_{10} (results not shown). In view of this we opted for a two-step synthesis, firstly synthesising and purifying diethoxy-CoQ_{10}, exchanging the two ethoxy groups with d_3-methoxy groups and re-purifying to yield d_6-CoQ_{10}. The d_6-CoQ_{10} synthesised had undetectable levels of unlabelled CoQ_{10} and is therefore suitable as an IS.

Initially a solution of di-ethoxy-CoQ_{10} was synthesised, as described by Edlund (1988): 100mg CoQ_{10} was dissolved in 1ml hexane and diluted in 4ml dry ethanol. 100µl sodium hydroxide in ethanol (40g/L) was added to the CoQ_{10} solution and was left for 30 mins. The reaction was then terminated by the

addition of 100µl glacial acetic acid. 10ml of hexane was added and the solution was centrifuged at 1000g for 5 mins at +25^{o}C. The top organic phase was removed and washed by adding 10ml H_2O and centrifuging at 1000g for 5 mins at +25^{o}C. This procedure was repeated twice. The organic phase was then dried down under nitrogen gas at 60^{o}C and reconstituted in 1ml methanol. Semi-preparative reverse phase HPLC was then used to purify the diethoxy-CoQ_{10} from unexchanged CoQ_{10} and the partially exchanged monoethoxy-CoQ_{10}. A Hypersil 250 x 10mm HyperPrep HS C18 column (Thermo-Hypersil, Runcorn, Cheshire, UK), plus a C18 guard column (Phenomenex, UK) were used at a flow rate of 3.2 ml/min at +25^{o}C. The mobile phase was isocratic and was composed of methanol and ethanol (25:75, v/v), containing 50mM ammonium acetate. The effluent was monitored at 275 nm and fractions were collected using 5ml glass tubes.

D$_6$-CoQ_{10} was then synthesised by utilising the backward version of this reaction, converting di-ethoxy-CoQ_{10} to *d*$_6$-CoQ_{10}. 200µl of purified di-ethoxy-CoQ_{10} was diluted in 800µl hexane. 4ml of *d*$_4$-methanol (CD_3OD) was then added to the mixture. 100µl sodium hydroxide (40g/L) dissolved in *d*$_4$-methanol was added to the solution which was incubated for 5 hours at +25^{o}C. The reaction was stopped by the addition of 100µl deuterium chloride. 10ml of hexane was added and the solution was centrifuged at 1000g for 5mins at +25^{o}C. The top organic phase was removed and washed by the addition of 10ml deuterium oxide and centrifuging at 1000g for 5 mins at +25^{o}C. This was repeated twice. The organic phase was then evaporated under nitrogen gas at +60^{o}C and reconstituted in 1ml methanol. The *d*$_6$-CoQ_{10} was then purified by semi-preparative HPLC as described above for di-ethoxy-CoQ_{10}.

5.4. Tandem Mass Spectrometry Method Development

5.4.1. Preparation of Standard Solutions

2µM Stock solutions for CoQ_{10} and *d*$_6$-CoQ_{10} were prepared in ethanol/methanol 1:1 (v/v). Samples were quantified spectrophotometrically at 275 nm using the molar extinction coefficient of 14.6 x 10^3 M^{-1} cm^{-1} of CoQ_{10} (Crane & Barr 1967). The CoQ_{10} stock solution was serially diluted in 50:50 (v/v) methanol:ethanol to construct a calibration curve. Samples were diluted to

concentrations of 200, 100, 50, 20, 10, 5, 2, 1, 0.5, 0 nM. 20nM d_6-CoQ_{10} was then added to each sample.

5.4.2. Subjects

5.4.2.1. Skeletal Muscle and Fibroblasts

The `disease control` group consisted of patients assigned retrospectively after no evidence of mitochondrial ETC deficiency was detected in their skeletal muscle biopsies or fibroblast cultures (muscle: mean [SE] age, 24.5 [3.9] years; range, 0.5–59 years; ratio of males to females, 7:6; fibroblasts: mean [SE] age, 11.33 [1.3] years; range, 0.03–55 years; ratio of males to females, 2:3)

5.4.2.2. CSF

The `disease control` group consisted of patients assigned retrospectively after demonstrating no evidence of a monoamine metabolite disorder (mean [SE] age, 6.15 [0.5] years; range, 0.1-22 years; ratio of males to females, 10:7).

Anonymised skeletal muscle homogenates and CSF samples were provided by the Neurometabolic Unit, National Hospital. Anonymised fibroblast cultures were provided by the Enzyme Laboratory, The Chemical Pathology Dept., Great Ormond Street Children`s Hospital. These samples were redundant samples retained by the lab for diagnostic test method development. Ethical consent from the patients was obtained for this purpose.

5.4.3. Preparation of Patient Samples

Skeletal muscle samples were prepared according to the method of Duncan *et al* (Duncan et al. 2005). Fibroblast samples were harvested in Hank's balanced salt solution ready for analysis. Protein content was analysed in skeletal muscle and fibroblast samples according the method described by Lowry *et al* (Lowry et al. 1951). Unfiltered CSF was used.

Due to its low level of protein it is often possible to analyse CSF by directly injecting it into the mass spectrometer. However due to observed ion suppression this was not possible. Ion suppression occurs when matrix components compete with the analyte for charge in the electrospray process. As a result the analyte of interest may not undergo complete ionisation and thus is not detected in an accurate quantity. To overcome this phenomenon the CoQ_{10} is extracted according to the method of Duncan et al (2005). This

removes the majority of competing matrix components leaving just the analyte of interest (plus other lipophilic components).

	No. of Hexane/Methanol Extractions (5:2, v/v, 700µl)	IS (nM)	Final volume (µl)
Muscle	2	200	300
Fibroblasts	2	50	300
CSF	3	10	70

Table 5.1 Extraction Procedure and Internal Standard (IS) Concentration

IS was added to the muscle, fibroblast and CSF samples (Table 5.1). ~100µl of each tissue, depending on the volume available, was extracted according to the method previously described in Section 2.4.2. Due to the low CoQ_{10} concentration in CSF (Isobe et al. 2009), samples were extracted a third time to increase recovery (Table 5.1). Samples were then evaporated to dryness using a rotary concentrator and re-suspended in 50:50 methanol/ethanol (final volume shown in Table 5.1).

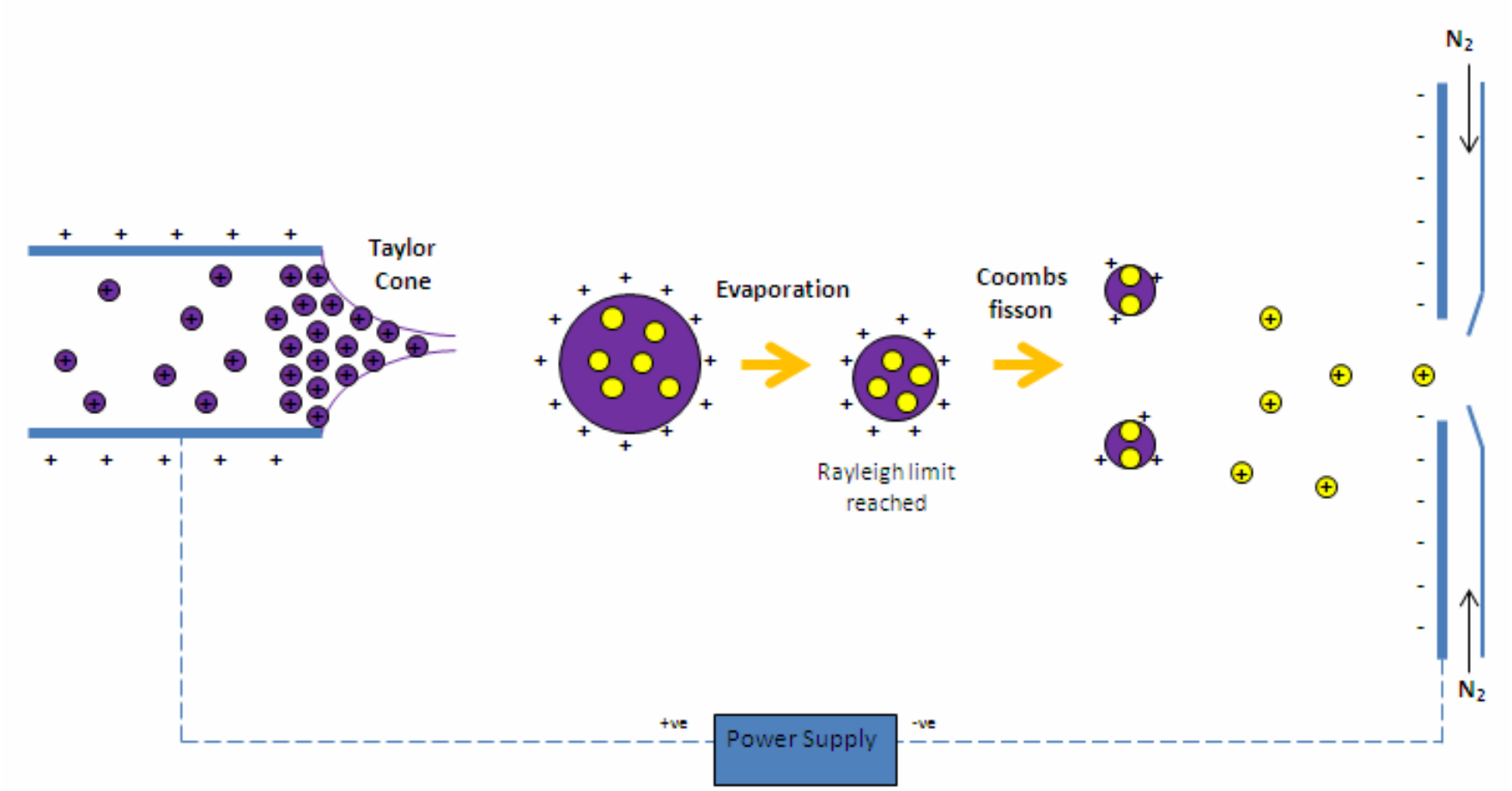

Figure 5.1 Schematic Diagram of the Electrospray Process

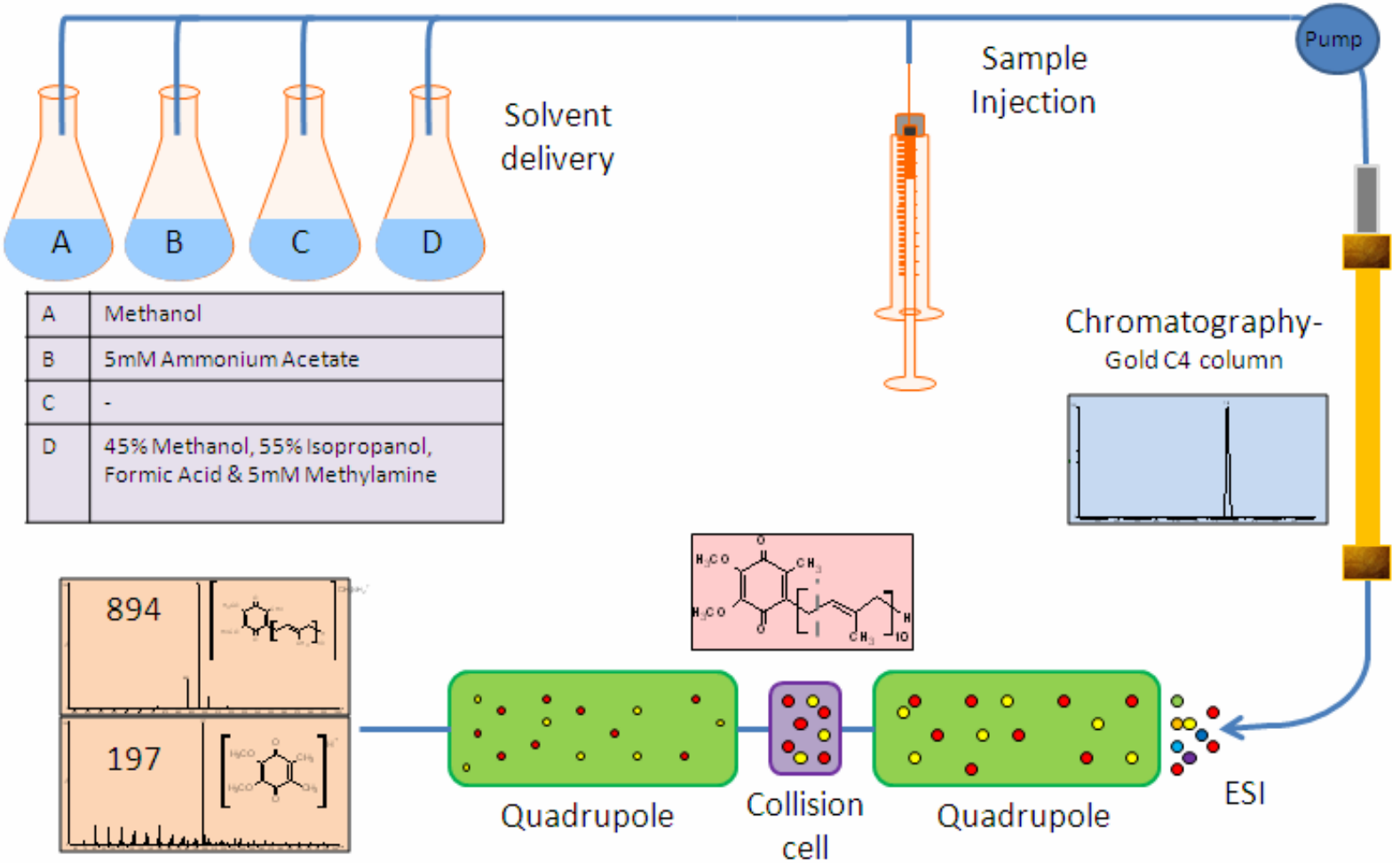

Figure 5.2 Schematic Diagram of Instrumentation Used in the Tandem Mass Spectrometry Method for Quantifying CoQ_{10}

5.4.4. Electrospray Ionisation-MS/MS (ESI-MS/MS)

The electrospray process first developed by John Bennett Fenn in 1989 (Fenn et al. 1989) is the interface between the HPLC and the MS; and importantly underpins the transformation of the liquid analyte into a gas phase ion (Figure 5.1). Developing a method for LC-MS/MS means considering optimal conditions for both chromatography and electrospray. ESI-MS/MS of CoQ_{10} and d_6-CoQ_{10} was carried out using a Quattro *micro* triple quadrupole mass spectrometer with a 2975 HPLC (Figure 5.2; Waters, Manchester, UK). To optimize analytical conditions, initially standards were directly infused into the electrospray source via a 25 μm (i.d.) fused silica transfer line by means of a syringe pump at a flow rate of 40 μl/ min. The instrument was operated in positive ionisation mode.

Since an extensive evaporation takes place in electrospray ionisation a volatile mobile phase is vital. In this case we used a largely alcohol based mobile phase (methanol/isopropanol) with an ammonium acetate additive. Formic acid was also used to aid positive ion formation (conductivity). The analyte is introduced into the MS from the HPLC system via a capillary. A voltage (3.38kV) is applied between the capillary and cone (end of capillary) within the source of the MS. Nitrogen is used as a nebulising gas to maintain a stable spray (flow rate of 950l/h [desolvation] and 50l/h [cone]). Heating aids solvent evaporation to charged droplets depending on flow rate. The source temperature was held constant at 150^{o}C and the desolvation at 350^{o}C. As solvent evaporation occurs the droplets become progressively smaller until the surface tension can no longer sustain the charge; the Rayleigh limit. Here, a process known as Coombs fisson occurs (Kebarle & Verkerk 2009) resulting in gas phase ions (Figure 5.1). The capillary voltage supplies excess charge to the analyte; as the capillary voltage remains at a constant high voltage (3.38kV) it is the cone voltage that is the important parameter in the electrospray process.

Thus the first parameter to be optimised was the cone voltage (V). A hydrodynamic cone was first observed by William Gilbert in the late 16th century (Gilbert, 1893; english translation). It wasn't until 1964 that Sir Geoffrey Ingram Taylor explained this phenomenon in relation to production of thunderstorms (Taylor 1964). The theory stated that when a small volume of conductive liquid is exposed to an electric field the surface tension of the liquid allows the formation of a cone structure. Above a threshold voltage a jet is emitted from

the apex of this cone structure allowing the beginning of the electrospray process. This process is now utilised in MS as a means of converting liquid samples into gaseous, highly charged molecules eligible for quantification.

A voltage of 30V was determined as the optimum voltage for CoQ_{10} electrospray (Figure 5.3a). At 60V the K^+ and Na^+ adducts predominated (Figure 5.3b), suggesting that this voltage is too high for spray formation of the methylamine adduct. Conversely at 5V the methylamine adduct was observed but at substantially lower levels, ~15% of the output at 30V (Figure 5.3c).

The extractor voltage (V) is the accelerating voltage that focuses ions toward the quadrapole. The optimal extractor voltage attained was 2V (Figure 5.4a). At 5V the methylamine adduct is ~65% of the output at 2V (Figure 5.4b); at 1V the methylamine adduct is at ~85% (Figure 5.4c).

The highly charged ions now pass into the triple quadrupole mass analyser. The first quadrupole mass analyser was developed by Prof James Douglas Morrison in LaTrobe University, Australia (Morrison et al. 1979). A triple quadrupole mass analyser consists of a linear series of three quadrupoles. The first (Q_1) and third (Q_3) quadrupoles act as mass filters, and the middle (Q_2) quadrupole is employed as a collision cell. After parent ion selection in Q_1 the collision cell uses an inert gas, in this case argon, to fragment the parent ion into characteristic daughter ion/s. The Q_3 is then used to select the daughter ions. It is the unique combination of parent and daughter ions that allow discrimination between molecules.

Each quadrupole consists of 4 parallel cylindrical rods. Its purpose is to filter sample ions according to their mass to charge ratio (m/z). Ions are separated according to their trajectories under the oscillating electric current that is applied to the rods. Each opposing rod pair is electrically connected. A radio frequency (RF) voltage is applied to each rod pair. The RF lens voltage (V) can be optimised to ensure accurate detection of a desired ion. In this case the optimal RF lens voltage for the Q_1 is 1.5V (Figure 5.5a). When a voltage of 3V was applied, the methylamine adduct of CoQ_{10} was found but peaks were 80% of 1.5V peak intensity (Figure 5.5b). Predictably peak height at 0.1V was substantially lower at 25% of optimal peak intensity (Figure 5.5c).

The ion energy also plays an important role in determining the trajectory of the ions. Here we selected a voltage of 1.5V as optimal (Figure 5.6a); a lesser voltage of 0.5V gave a read out of 80% compared to 1.5V (Figure 5.6b).

The Q_3 ion energy is optimal at 1.5V (Figure 5.7a); a higher voltage of 2V gave a read out 70% of the 1.5V intensity (Figure 5.7b).

The collision voltage (V) is an important aspect of MS. The aim is to fragment the parent ion into its characteristic daughter ion without causing further fragmentation. The optimal voltage for the methylamine adduct of CoQ_{10} was 27V (Figure 5.8a). At 30V the intensity of the daughter peak (m/z 197) was substantially less; ~35% compared to ~50% at 27V (Figure 5.8b). As the collision voltage decreases the fragmentation of the parent ion decreases leading to the appearance of the parent ion in the mass scan at 20V and a considerable decrease in the daughter ion peak intensity (Figure 5.8c). At 10V the daughter ion ceases and is replaced by the parent ion owing to a complete lack of fragmentation.

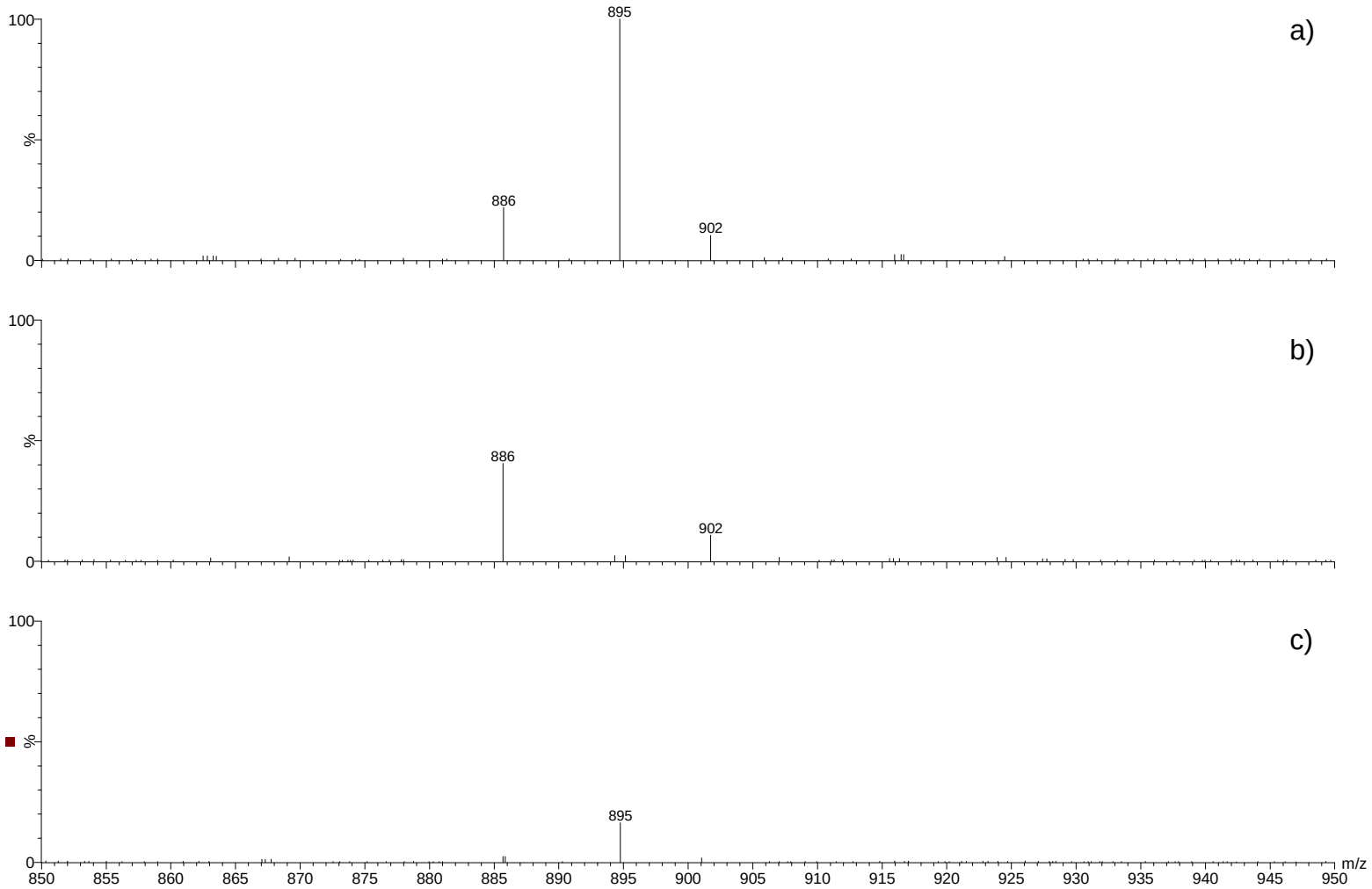

Figure 5.3 MS Scan for Optimisation of Cone Voltage (V)

a) 30V b) 60V, c) 5V (886m/z: Na^+ CoQ_{10} adduct; 895m/z: Methylamine CoQ_{10} adduct; 902m/z: K^+ CoQ_{10} adduct)

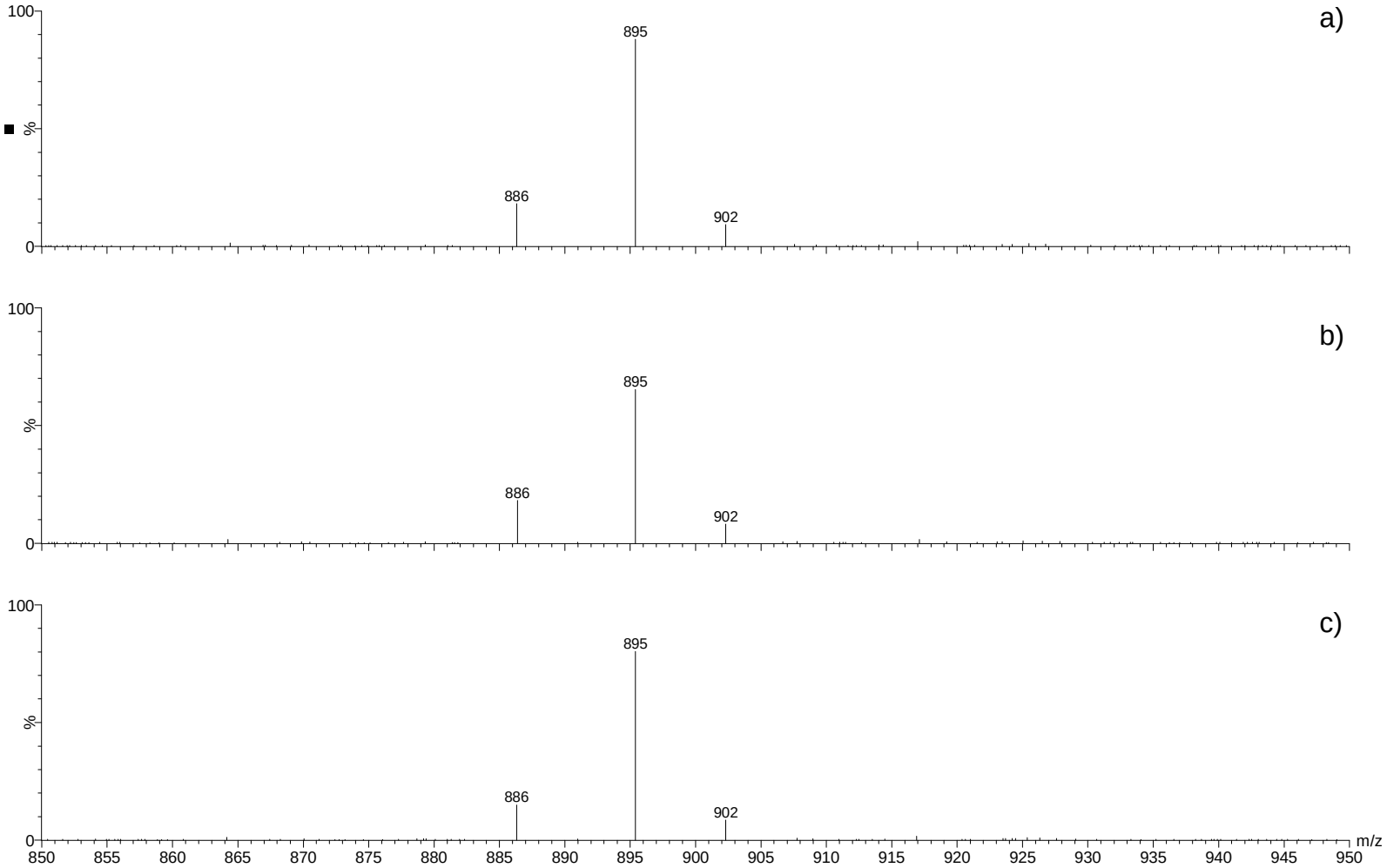

Figure 5.4 MS Scan of Extractor Voltage (V)

a) 2V, b) 5V, c) 1V (886m/z: Na^+ CoQ_{10} adduct; 895m/z: Methylamine CoQ_{10} adduct; 902m/z: K^+ CoQ_{10} adduct)

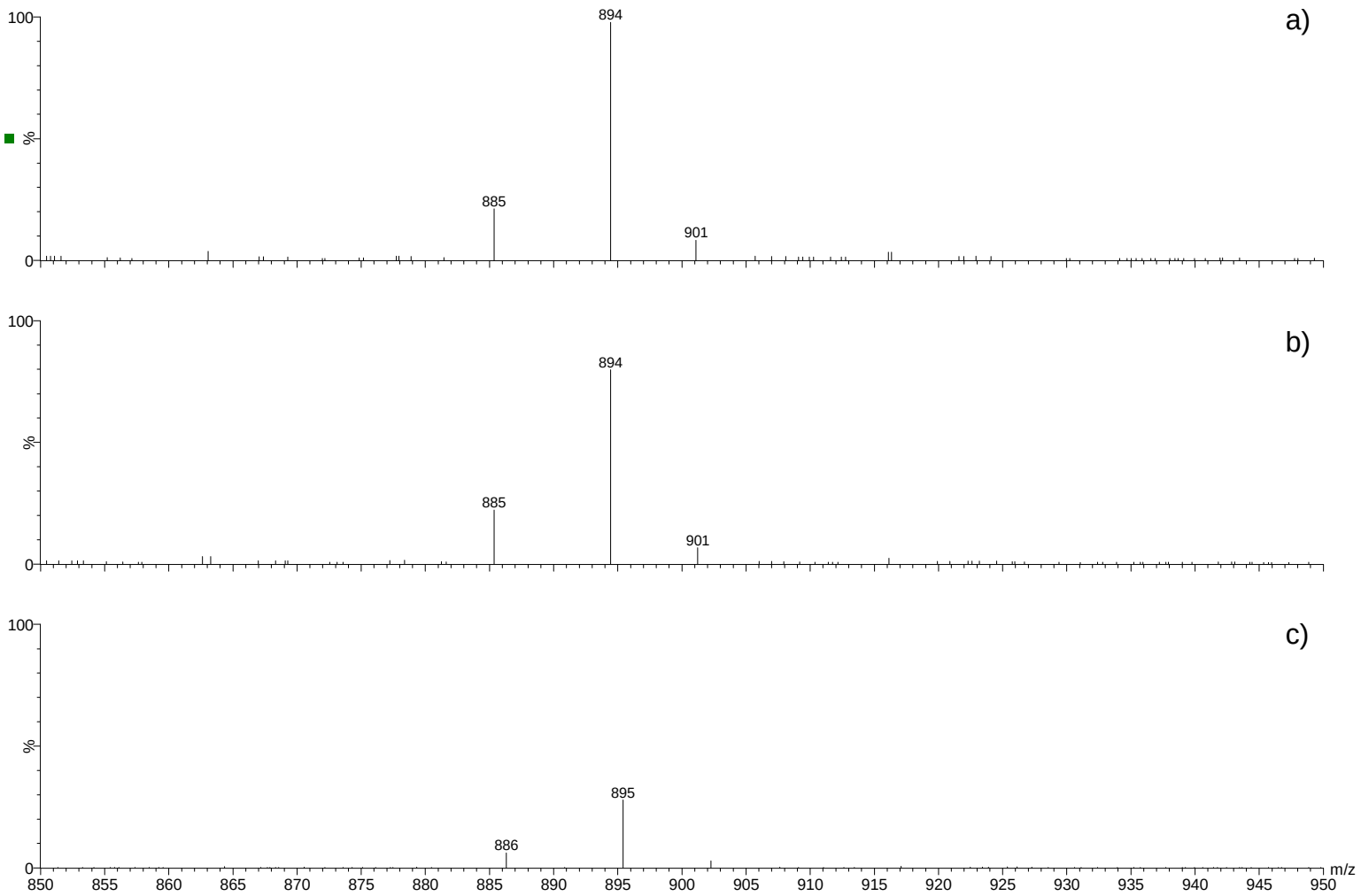

Figure 5.5 MS Scan of RF Lens Voltage (V)

a) 1.5V, b) 3V, c) 0.1V (885/6m/z: Na^+ CoQ_{10} adduct; 894/5m/z: Methylamine CoQ_{10} adduct; 901m/z: K^+ CoQ_{10} adduct)

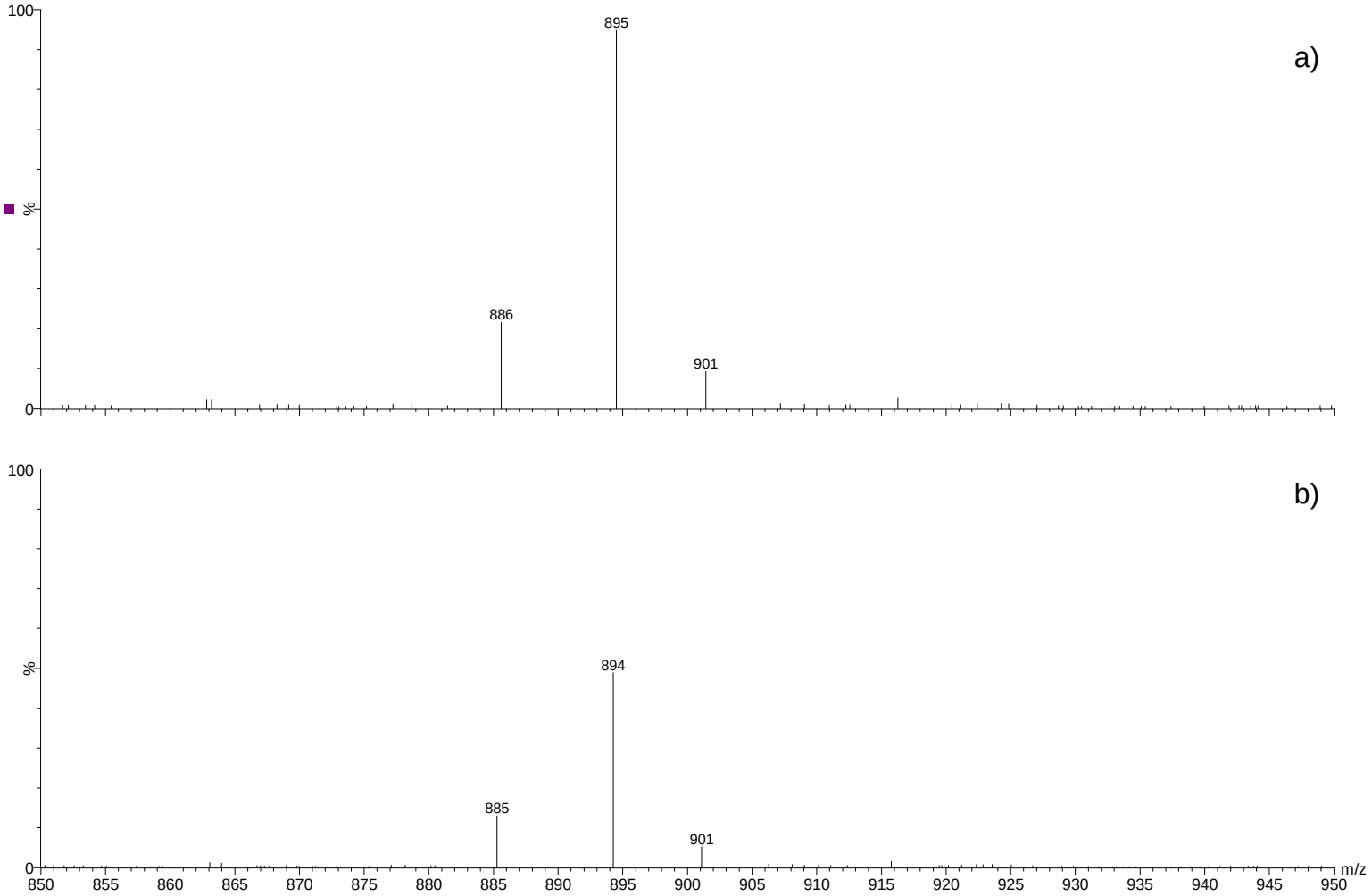

Figure 5.6 MS Scan of Ion Energy 1

a) 1.5V, b) 0.5V (885/6m/z: Na^+ CoQ_{10} adduct; 894/5m/z: Methylamine CoQ_{10} adduct; 901m/z: K^+ CoQ_{10} adduct)

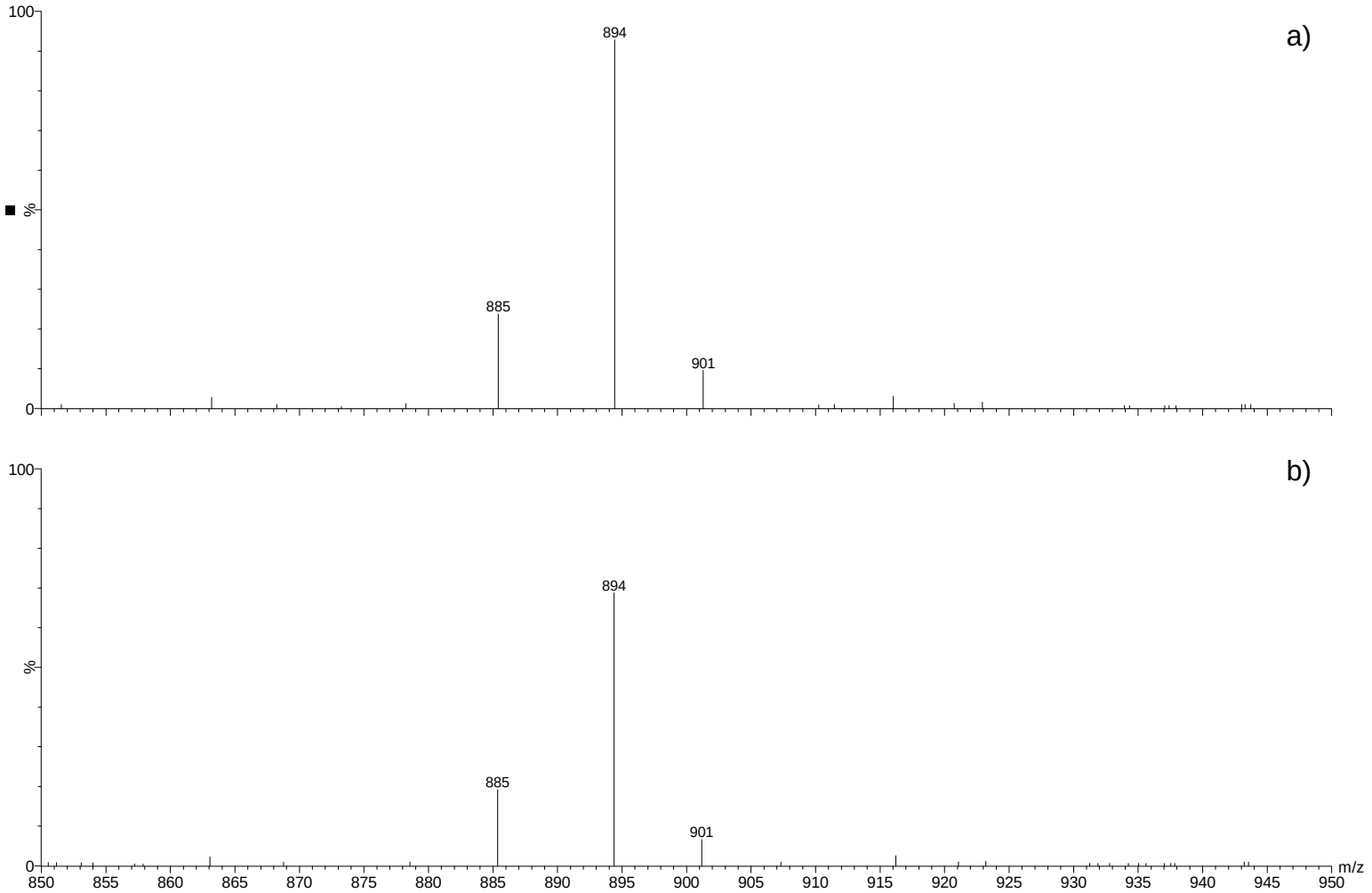

Figure 5.7 MS Scan of Ion Energy 2

a) 1.5V, b) 2V (885/6m/z: Na^+ CoQ_{10} adduct; 894/5m/z: Methylamine CoQ_{10} adduct; 901m/z: K^+ CoQ_{10} adduct)

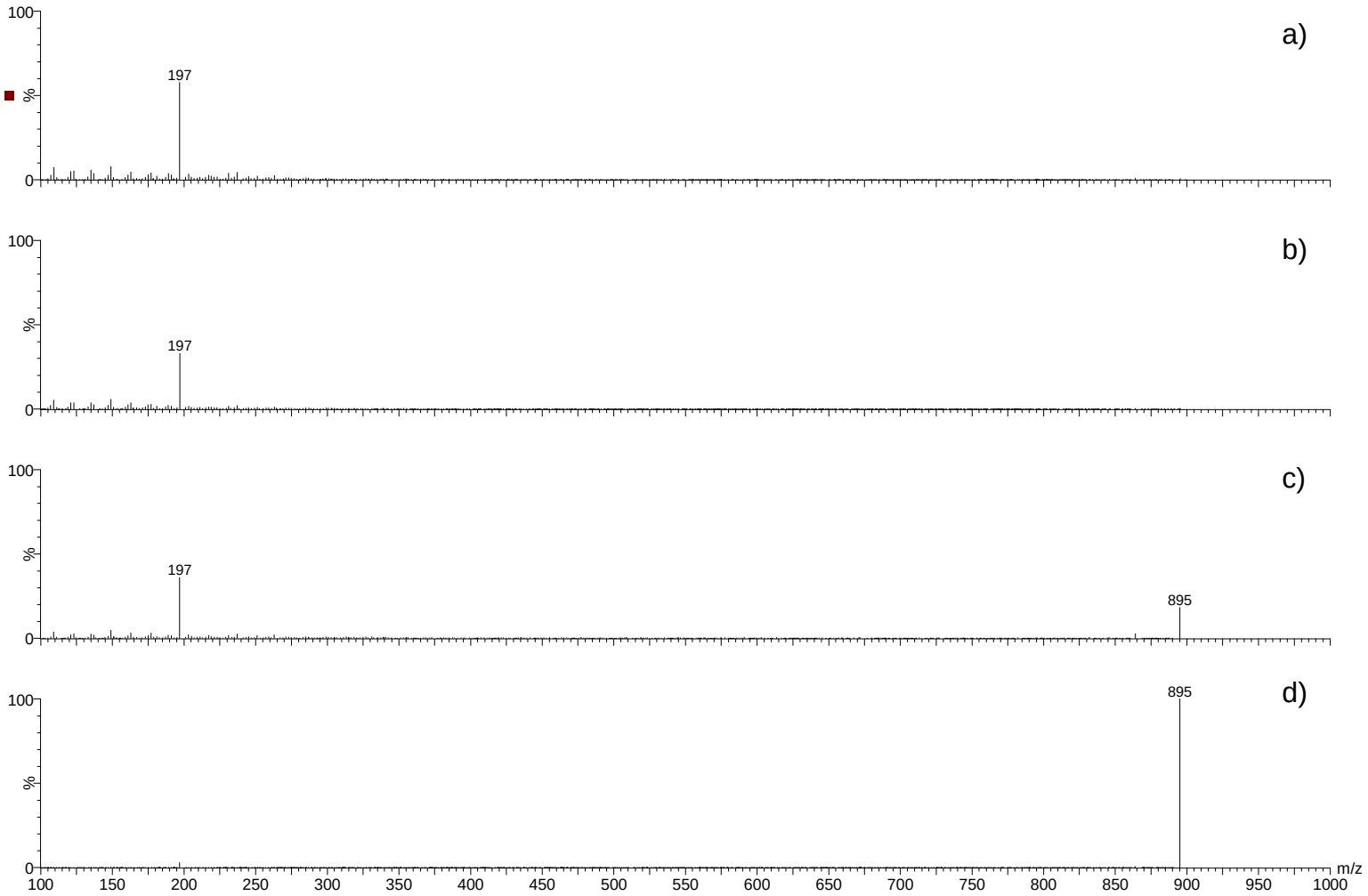

Figure 5.8 Daughter Scan of Collision Energy (V)

a) 27V, b) 30V, c) 20V, d) 10V (895m/z: Methylamine CoQ_{10} adduct parent ion; 197m/z: CoQ_{10} daughter

5.4.5. High Performance Liquid Chromatography (HPLC)

For quantitative analyses samples were separated using HPLC coupled to the mass spectrometer (Figure 5.2). The mobile phases consisted of (A) methanol (B) 4mM ammonium acetate 0.1% formic acid and (C) methanol:isopropanol:formic acid (45:55:0.5, v/v/v) containing 5mM methylamine as an ion pair reagent (Teshima & Kondo 2005). The column was a 3μM Hypersil Gold C4 (150mm x 3mm, 3μm) with a Gold C4 guard column (3mm, 10mm length, 3μm) operated at 40ºC at a flow rate of 0.4ml/min. The initial conditions were 50% A, 50% B for 2 minutes, followed by a switch to 50% B, 50% C at 4 minutes and a gradient to 100% C for a further 8 minutes, after which the column was re-equilibrated in the starting conditions for a further 5 minutes before the next injection.

50μl of sample was injected and CoQ_{10} and d_6-CoQ_{10} eluted at approximately 8 minutes (Figure 5.9). MS/MS detection was performed by selection reaction monitoring (SRM) from the methylammonium adduct molecule ($[M + CH_3NH_3]^+$).

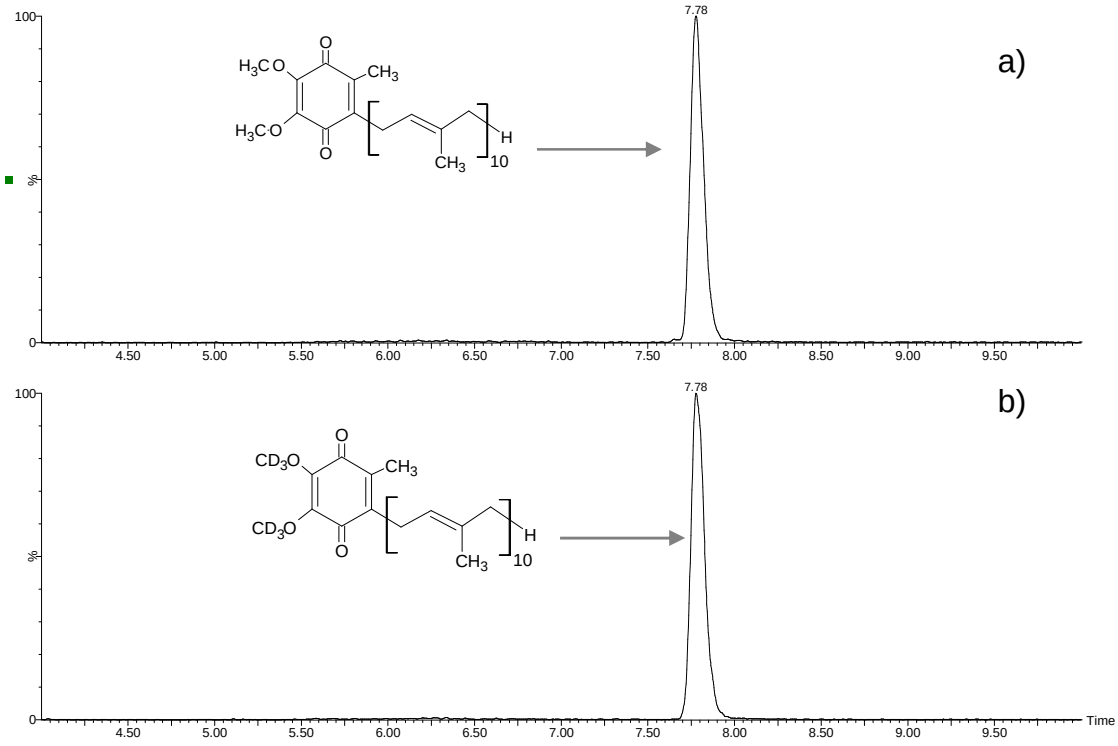

Figure 5.9 Chromatography of a Control Fibroblast Sample

a) CoQ10 – daughter ion: 197 m/z, parent ion: 865 m/z, and b) Deuterated CoQ10 -daughter ion: 203 m/z, parent ion: 901 m/z.

5.5. Results

5.5.1. Deuterated Internal Standard

As described by Teshima and Kondo (2005), use of a methylamine adduct yields a precursor ion of m/z 895 for CoQ_{10} (Figure 5.10a) and a product benzoquinone ring ion of m/z 197 (Figure 5.10a). D_6-CoQ_{10} gave similar ions with the expected 6Da difference (precursor m/z 901; Figure 5.10b and product m/z 203; Figure 5.10b), indicating that d_6-CoQ_{10} is an appropriate IS for the measurement of CoQ_{10}. D_6-CoQ_{10} was 99.5% isotopically pure, with only a 0.5% contamination with $CoQ_{10,}$ demonstrating the efficiency of the conversion and suitability for use as an IS.

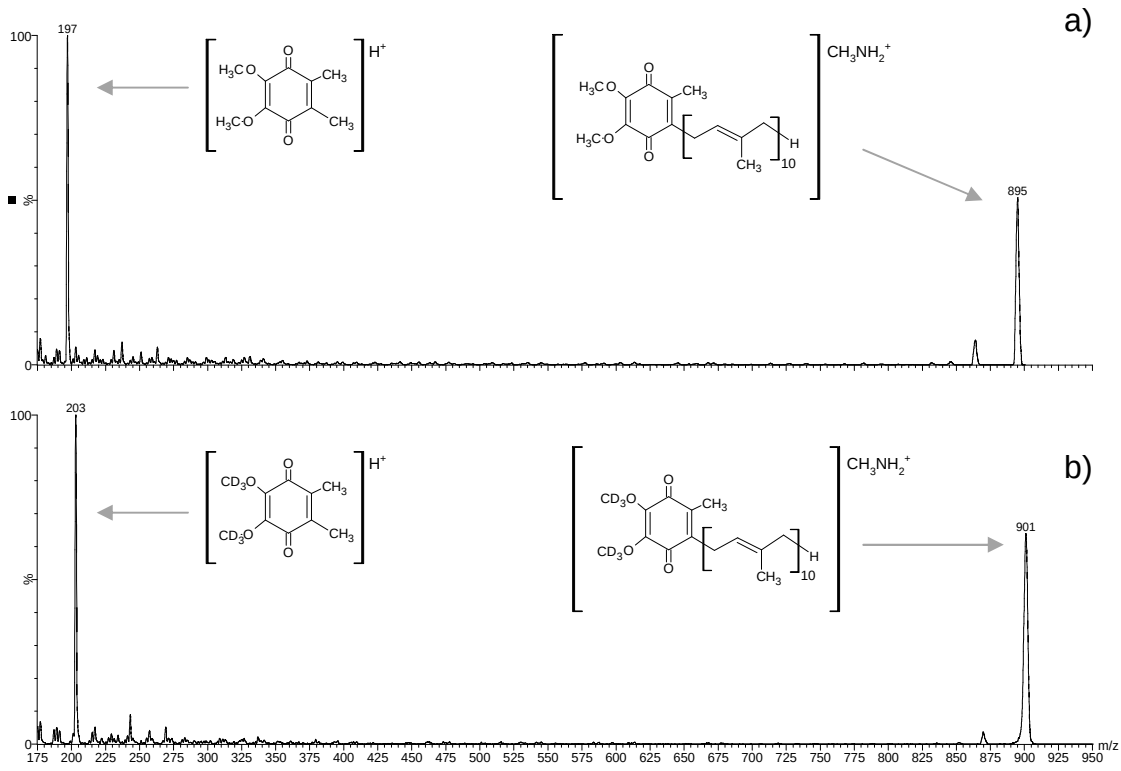

Figure 5.10 a) CoQ_{10} and b) d_6-CoQ_{10} Mass Spectra (895m/z: Methylamine CoQ_{10} adduct parent ion; 197m/z: CoQ_{10} daughter ion; 901 m/z: Methylamine d_6-CoQ_{10} adduct parent ion; 203 m/z: d_6-CoQ_{10} daughter ion)

5.5.2. Linearity, Precision, Recovery

Linearity is an important aspect of any analytical chemistry method and outlines the correlational relationship between concentration and response (Harvey 2009). A concentration curve over the range 0-200 nM CoQ_{10} (with a d_6-CoQ_{10} concentration of 20 nM) gave a linearity of $R^2 = 0.9995$ (Figure 5.11a). At lower concentrations (0-5 nM), linearity was less: $R^2 = 0.9886$ (Figure 5.11b).

The limit of detection (LOD) is defined as the lowest concentration or amount of an analyte that can be reliably identified as being qualitatively present in the sample. The limit of quantification (LOQ) is defined as the lowest concentration or amount of analyte that can be reproducibly quantified in a sample (Clinical Chemistry 2012). Thus the LOD in this method is 0.5nM and the LOQ is 2 nM (Figure 5.11b).

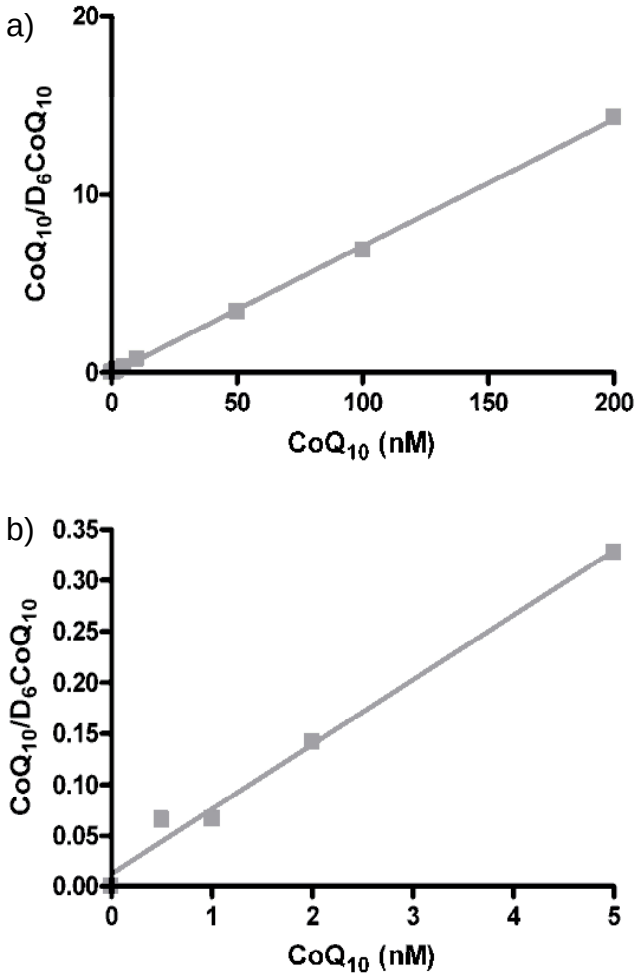

Figure 5.11 Concentration Curves for CoQ_{10} Standard
a) 0-200nM (R^2=0.9995), b) 0-5nM (R^2=0.9886)

The precision of an analytical method is a measure of variability. The closer the agreement between individual analyses the more precise the method (Harvey 2009). The precision of the MS method was assessed by examining the inter (between runs) and intra (within run) coefficient of variation (CV). CSF was pooled from 64 disease controls. The inter assay CV was calculated by comparing 10 pooled CSF repeats (1 run) over 5 separate days. The intra CV was calculated by comparing 10 repeats in the same run; an average was then calculated. The inter-assay CV was 3.6% when 10 nM CoQ_{10} was added to pooled CSF and 4.3% with addition of 20 nM CoQ_{10} (Table 5.2). Intra-assay CV was 3.4% (10 nM) and 3.6% (20 nM; Table 5.2).

	Average Intra-assay Coefficient of Variation (CV; %)	**Inter-assay Coefficient of Variation (CV; %)**	**Spike recovery**
Low Spike (10nM)	3.43	3.55	0.995
High Spike (20nM)	3.55	4.26	-

Table 5.2 Inter- and Intra-assay Coefficient of Variation (CV; %) and spiking accuracy of CoQ_{10} Tandem MS/MS method on pooled control CSF samples.

The accuracy of an analytical method is how closely the result of the experiment agrees with the “true” or expected result. The MS method was tested by measuring the concentration of a pooled CSF sample before and after addition of 10 nM CoQ_{10}. Pre-addition concentration was 4.09 nM +/- 0.03 (standard deviation; SD), post-addition was 14.04 nM +/- 0.61 (SD), giving a recovery of 99.5%.

5.5.3. Muscle Analysis

The CoQ_{10} status determined in muscle homogenates by the tandem MS method was compared with the results obtained from the analysis of the same samples by the HPLC UV detection method. This method is currently used to

determine the CoQ_{10} status of clinical samples in the Neurometabolic unit, National Hospital of Neurology and Neurosurgery and can therefore be considered to be the gold standard method for CoQ_{10} quantification. This method is described in Section 2.4.2 (Duncan et al. 2005). We compared 5 muscle biopsy samples previously analysed by the HPLC UV detection method with the tandem MS/MS method described. Correlation analysis revealed a R^2 value of 0.9914, indicating a strong positive correlation between methods.

We established a tentative reference range for skeletal muscle CoQ_{10} status of 187.3-430.1 pmol/mg (mean: 307.7pmol/mg; n = 15; Table 5.3; Figure 5.12A). The reference range for skeletal muscle CoQ_{10} using the UV detection method is 140-580 pmol/mg; thus the MS/MS method appears to have a tighter reference range. However substantially less samples were analysed suggesting this reference range will change upon analysing more samples.

	Reference range	Mean concentration
Muscle (pmol/mg; n=15)	187.3-430.1	307.7
Fibroblasts (pmol/mg; n=50)	57.0-121.6	89.3
CSF (nM; n=17)	5.697-8.681	7.39

Table 5.3 Reference Intervals for Skeletal Muscle, Fibroblasts and CSF

5.5.4. Fibroblast and CSF Analysis

The tandem MS/MS method was also employed to establish a tentative reference range for fibroblasts of 57.0-121.6 pmol/mg (Table 5.3; Figure 5.12B) with a mean concentration of 89.3 pmol/mg.

This compares to a reported value in the literature of 67.2±11.6 pmol/mg protein established from 5 control fibroblast lines, using HPLC with EC detection (Quinzii et al. 2010). This disparity may be due to differences in tissue culture media, fibroblast passage number and/or the protein assay used in determination. We have confirmed the potential application of our method to detect primary CoQ_{10} deficiency in fibroblasts by measurement of CoQ_{10} in fibroblasts from a patient with established CoQ_{10} deficiency due to a mutation in

COQ9 (Rahman et al. 2001; Duncan et al. 2009). The CoQ_{10} level determined for this patient was 13.17 pmol/mg; 12% of the mean control CoQ_{10} concentration for fibroblasts. This value is lower than that obtained by the UV detection method (Duncan et al. 2009; 25.3 pmol/mg).

The LOD for the UV detection method is 6 nM (Duncan et al. 2005), making it unsuitable for CSF analysis. The higher sensitivity seen with the tandem MS method has enabled the detection of the low levels of CoQ_{10} in CSF, allowing us to establish a tentative reference range of 5.70-8.68 nM (mean: 7.38 nM; Table 5.3; Figure 5.12C). No age (R^2=0.03; Spearman correlation: p=-0.17) or gender (t-test: p=0.98) effects on CSF CoQ_{10} concentration were detected

Isobe *et al.* (2009, 2010) measured CoQ_{10} (as oxidised and reduced CoQ_{10}) in CSF (filtered with a 10,000 MW cut off) of adults using HPLC with EC detection, a reference range was not reported. From the data reported in their papers the total CoQ_{10} concentration of CSF appears to be approximately 2.8nM (oxidised +reduced=total CoQ_{10}). It is possible that the difference between their data and our measured CSF CoQ_{10} concentration is due to their use of a 10,000 MW cutoff filter. In a preliminary experiment we found that filtered CSF had undetectable levels of CoQ_{10}, suggesting that CSF CoQ_{10} may be associated with lipoproteins or other CSF proteins, as in plasma (Eaton et al. 2000). In addition, the possibility arises that the differences in the mean CSF CoQ_{10} status between the present study and that of Isobe et al may be due to the differences in the mean age of the patients investigated. The average age of the controls in Isobe et al's study was 67 years whereas the subjects assessed in present study had a mean age of 6.15 years. However it is yet to be established whether age has an effect on CSF CoQ_{10} status and further work is required before this can be confirmed or refuted.

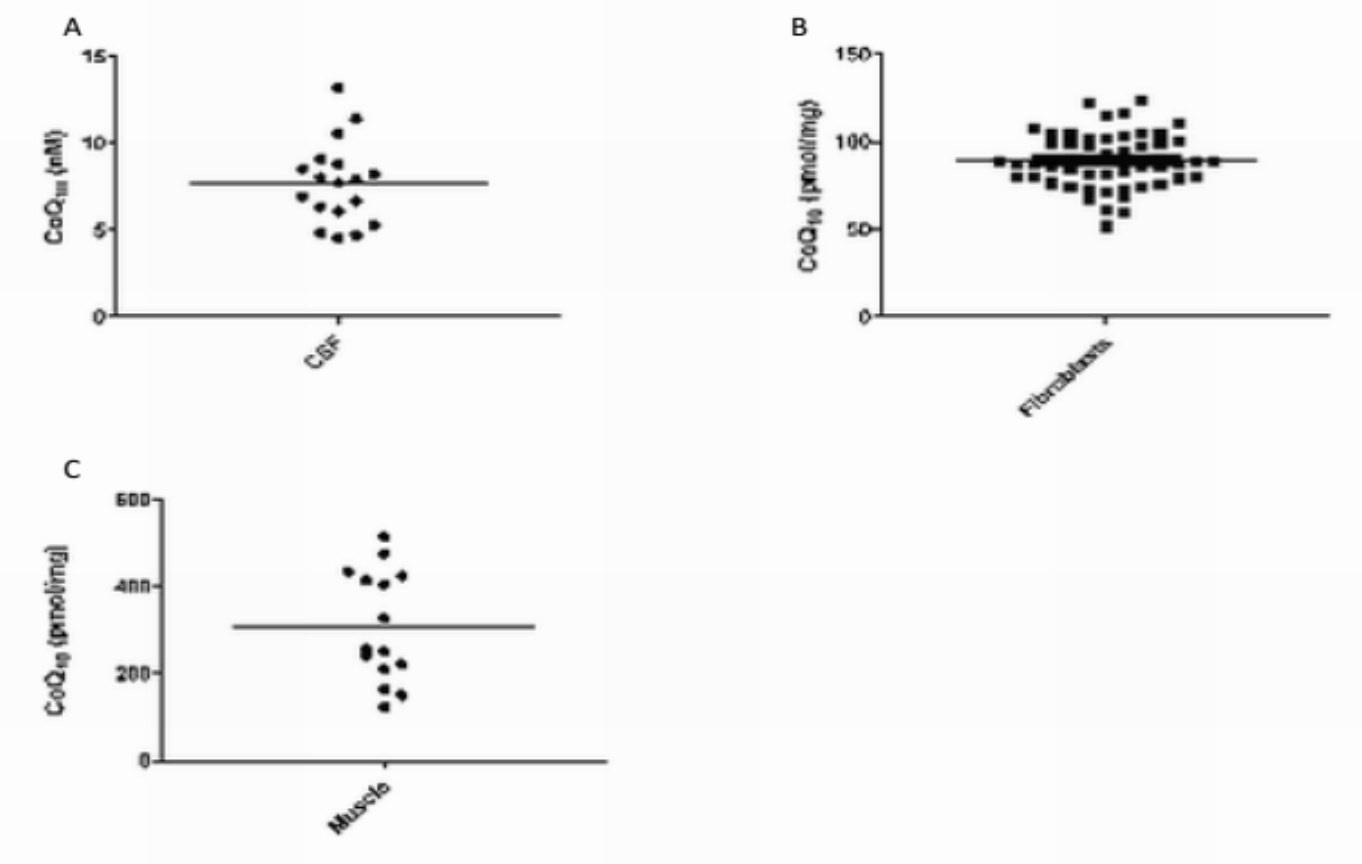

Figure 5.12 CoQ_{10} levels in a) skeletal muscle homogenate (n=15), b) fibroblasts (n=50), c) cerebrospinal fluid (CSF; n=17)

5.6. Discussion

HPLC linked to UV or EC detection are methods currently employed for the assessment of tissue CoQ_{10} status (Duncan et al. 2005; Isobe et al. 2010; Isobe et al. 2009). Although useful in the quantification of CoQ_{10} in skeletal muscle, mononuclear cells and plasma (Duncan et al. 2005), these methods are insufficiently sensitive to accurately determine CoQ_{10} in CSF and therefore in this study we utilised tandem MS/MS as a means to analyse CoQ_{10} status in view of the high level of sensitivity reported for this method (Ruiz-Jiménez et al. 2007; Takamiya et al. 1999; Li et al. 2008; Schaefer et al. 2004). In this chapter we have described the development of a highly sensitive method capable of accurately quantifying CoQ_{10} to low nM levels (LOQ: 2nM).

During the development of this MS method we also attempted tandem quantification of CoQ_{10} and $CoQ_{9.}$ Although it was possible to detect CoQ_9 we found that the sensitivity of the method was compromised with dual analysis, possibly due to ion suppression. This loss of sensitivity meant that CoQ_9 analysis was not viable during CSF quantification of CoQ_{10}. However this MS method could be employed to assess CoQ_9 status in mouse/rat models and also in other human tissue. It would be interesting to monitor CoQ_{10} and CoQ_9 concentrations in CoQ_{10} deficient patient fibroblasts to investigate the effect of a CoQ_{10} deficiency on CoQ_9 status and whether this impacts upon the disease phenotype. It is postulated that CoQ_9 present in human tissue is mainly of dietary origin; due to the high concentration found in plasma (Hargreaves & Heales 2002). However the possibility arises that CoQ_9 may have a functional role in human tissue. In rat the predominant form of ubiquinone is $CoQ_{9;}$ however in some tissues (brain, spleen, intestine) nearly a third of the total ubiquinone is $CoQ_{10;}$ suggesting differential expression and potentially different roles of the analogues (Aberg et al. 1992).

As part of this study we also attempted the analysis of the reduced form of CoQ_{10}, ubiquinol (CoQ_{10}-H_2). CoQ analogues are potent antioxidants and thus an alteration in the ratio of oxidized to reduced $CoQ_{10/9}$ maybe a potential marker of oxidative stress (Isobe et al. 2010; Isobe et al. 2009). However due to its propensity to oxidise it was not possible to determine ubiquinol using the MS method employed in the present study. Other groups have successfully analysed ubiquinol in mononuclear cells (Hahn et al. 2012) and serum (Ruiz-

Jiménez et al. 2007). Therefore although it may be possible to measure ubiquinol, the problems encountered maintaining it in its reduced state may present difficulties as encountered in this work. This inability to assess ubiquinol in the present work may be the result of; oxidation within the line, oxidation at the source, or oxidation during extraction/waiting for analysis. This will require further investigation to assess the viability of accurately measuring ubiquinol.

One of the most interesting applications of this method would be to investigate the terminal portion of the CoQ_{10} biosynthetic pathway. The biosynthetic pathway is best understood in several organisms; *Escherichia coli, Saccharomyces cerevisiae, and Schizosaccharomyces pombe* (Meganathan 2001; Kawamukai 2002); however very little is known about the human pathway. We currently know the function of two enzymes that are associated with human primary CoQ_{10} deficiency; *PDSS1/2* and COQ2. However there are four other genes associated with the primary CoQ_{10} deficiency (*ADCK3, COQ4, COQ6, COQ9*). We know that these genes are involved in the terminal portion of the CoQ_{10} biosynthetic pathway but we have yet to elucidate their function. In theory when CoQ_{10} biosynthesis is perturbed by the dysfunction of a particular enzyme there may be an accumulation of the respective enzyme substrate. There is evidence in yeast that the terminal enzymes involved in CoQ biosynthesis are held together in a multi-subunit complex stabilised by COQ4 (Marbois et al. 2009). Thus dysfunction at any point in the pathway may result in accumulation of the isoprenoid 3-hexaprenyl-4- hydroxy-benzoic acid (Marbois et al. 1994). Therefore, it would be of interest to investigate whether this phenomenon occurs in humans.

The ability to assess CoQ_{10} levels in CSF will be of potential clinical utility for the diagnosis of patients with neurological CoQ_{10} deficiency, both primary and secondary. A recent literature review revealed that only 60% of patients with the cerebellar phenotype of CoQ_{10} deficiency have a decreased level in fibroblasts, and decrease in muscle CoQ_{10} status may not always be significant (Emmanuele et al. 2012). However with many of these cases a reliable reference range for muscle and fibroblasts was not established. The ability to assess CSF CoQ_{10} status will enable a direct evaluation of cerebral CoQ_{10} levels in patients with the cerebellar ataxic presentation of CoQ_{10} deficiency. This may therefore improve the diagnostic yield of CoQ_{10} deficiency in this

clinical phenotype since the possibility arises that the CoQ_{10} deficiency may not be expressed or to a lesser degree in fibroblasts or skeletal muscle.

A similar story is observed with Complex II/III activity; only 53% of patients with the cerebellar ataxic presentation of CoQ_{10} deficiency presented with a decrease in Complex II/III activity in muscle (Emmanuele et al. 2012). A personal communication with Dr. Iain Hargreaves suggested that this is a common problem with diagnosis of CoQ_{10} deficiency. In the Neurometabolic unit (NHNN) patients with a skeletal muscle CoQ_{10} level that is 30% of the lower reference interval (~90 pmol/mg) may not present with a deficit in Complex II/III activity. Therefore, a decrease in CoQ_{10} status may not always result in a loss of Complex II/III activity. Furthermore, since it has been reported that approximately 45% of cellular CoQ_{10} is of mitochondrial origin (Ericsson & Dallner 1993) it is important to take into account the level of mitochondrial enrichment of a tissue sample when determining CoQ_{10} status.

This MS method would also be useful for monitoring therapeutic CSF CoQ_{10} levels following supplementation in mitochondrial and other neurodegenerative diseases. Currently CoQ_{10} supplementation is only effective in 46% of patients with the ataxic phenotype (Emmanuele et al. 2012). However we have proved in our model that CoQ_{10} supplementation is effective in recuperating CoQ_{10}, the ETC and also in reducing mitochondrial oxidative stress (see chapter 4). This raises the question: Why is CoQ_{10} supplementation effective at a cellular level but not in patients? (López et al. 2006; Rahman et al. 2001) A possibility is the poor penetration of CoQ_{10} across the blood brain barrier. To investigate this hypothesis CoQ_{10} levels could be monitored before and after treatment in the plasma and the CSF. If the CSF concentration is unaltered it is possible that CoQ_{10} is ineffective at crossing the blood-brain barrier. However time of lumbar puncture would be vital in this experiment. Further investigation into the pharmacokinetics of CoQ_{10} may need to be done before this experiment could be undertaken. Furthermore, the MS method developed in this chapter may also have utility in assessing the CSF levels of idebenone in the treatment of Friedreich's ataxia (Meier et al. 2012)

5.7. Conclusion

Deuterated ISs are the “gold” standard of MS; we have devised a simple synthesis of d_6-CoQ_{10}. Other deuterated ISs are available to purchase but this

method offers a relatively inexpensive method using chemicals that are readily available in most labs. This has enabled the establishment of a method suitable for CoQ_{10} quantification by tandem MS/MS of muscle, fibroblasts and CSF. This is advantageous over several published CoQ_{10} methods in which CoQ_9, an endogenous ubiquinone to human tissue, or non-endogenous chemically similar compounds are used as ISs. D_6-CoQ_{10} will fragment in the same way as CoQ_{10} and will prove to be a useful tool in CoQ_{10} analysis.

Chapter 6

General Discussion

CoQ_{10}, the predominant form of ubiquinone in humans, serves as an electron carrier in the ETC, a potent lipid soluble antioxidant and is involved in a number of other cellular functions. Therefore, a deficit in CoQ_{10} status could be a contributory factor to disease pathophysiology by causing a failure in oxidative phosphorylation and a diminution of cellular antioxidant function. Deficiency in CoQ_{10} status has been implicated in a number of diseases and conditions (Rahman et al. 2012; Spindler et al. 2009). Since the first reported cases of CoQ_{10} deficiency by Ogasahara and colleagues in 1989 of two sisters who presented with recurrent rhabdomyolysis with associated seizures and mental retardation a number of patients have been reported. Although the clinical presentation of CoQ_{10} deficiency is extremely heterogeneous there does appear to be five distinct clinical phenotypes (

Table 1.4). The most common clinical presentation of CoQ_{10} deficiency appears to be the ataxic phenotype and to date, 100 patients have been reported (Emmanuele et al. 2012). In addition, neurological dysfunction is also a common feature of the other clinical phenotypes associated with CoQ_{10} deficiency (

Table 1.4). Patients with all clinical phenotypes of CoQ_{10} deficiency have been reported to show some clinical improvement following supplementation (Rahman et al. 2012). Whilst muscle abnormalities have been reported to improve, neurological symptoms associated with CoQ_{10} deficiency appear particularly refractory to CoQ_{10} supplementation (Emmanuele et al. 2012). Furthermore, only 49% of patients with the ataxic phenotype of CoQ_{10} deficiency have been reported to respond to CoQ_{10} supplementation with clinical improvement in contrast to 75% of patients with the other clinical phenotypes of CoQ_{10} deficiency (Emmanuele et al. 2012).

At present, the reasons for the refractory nature of neurological dysfunction associated with CoQ_{10} deficiency to treatment have yet to be elucidated. They may result from irreversible structural and/or biochemical neuronal dysfunction prior to diagnosis, poor penetration of CoQ_{10} across the blood brain barrier and inability of CoQ_{10} deficient neurones to utilise supplemented exogenous CoQ_{10}. In view of the paucity of information about neuronal CoQ_{10} deficiency, the primary objective of this research project was to investigate the effect of CoQ_{10} deficiency upon neuronal cell mitochondrial metabolism and cellular oxidative

stress. In addition, the effect of CoQ_{10} supplementation was investigated on CoQ_{10} deficient neuronal cells to assess the ability of exogenous CoQ_{10} to correct neuronal cell CoQ_{10} deficiency and ameliorate ETC dysfunction and cellular oxidative stress.

In view of the refractory nature of neurological dysfunction associated with CoQ_{10} deficiency to treatment, coupled with the absence of existing analytical procedures to assess cerebral CoQ_{10} status, another aim of this project was to establish a liquid chromatography tandem mass spectrometry (LC-MS/MS) method to determine CSF CoQ_{10} status.

In order to assess the effect of a deficit in CoQ_{10} status on neuronal cell mitochondrial metabolism and oxidative stress we established a neuronal cell model of CoQ_{10} deficiency using pharmacological inhibition of CoQ_{10} synthesis. Utilising the ability of PABA to competitively inhibit the CoQ_{10} biosynthetic pathway enzyme, COQ2 we were able to induce up to a maximal 54% decrease in SHSY-5Y neuroblastoma cell CoQ_{10} status compared to control levels (46% residual CoQ_{10}). By treating SHSY-5Y cells with different concentrations of PABA (0.25 -1 mM) the neuronal cell CoQ_{10} status could be titrated to between 90% and 46% residual $CoQ_{10,}$ enabling an assessment of different levels of neuronal CoQ_{10} deficiency on mitochondrial metabolism and oxidative stress. Many studies have been undertaken in fibroblasts however there is a lack of studies assessing the biochemical consequences of CoQ_{10} deficiency at a neuronal level (Quinzii et al. 2012; Quinzii et al. 2013; Quinzii et al. 2010; Quinzii et al. 2008). A study by Quinzii et al., 2013 reported a kidney specific increase in oxidative stress and mitochondrial loss in *Pdss2* kd/kd mice the suggesting that the biochemical consequences of CoQ_{10} deficiency vary between organs. Furthermore, it has been suggested that there may be tissue specific isoenzymes in the CoQ_{10} biosynthetic pathway (Ogasahara et al. 1989). Therefore, the effect on a CoQ_{10} deficiency on fibroblast mitochondrial function and oxidative stress may not truly represent that of other cell types.

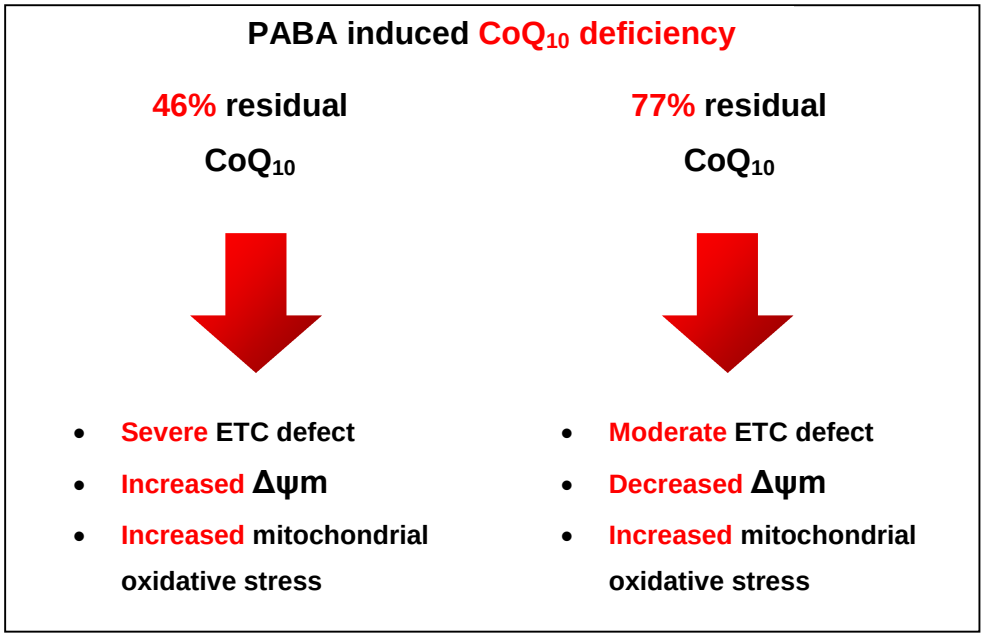

Figure 6.1 Diagrammatic Representation of SH-SY5Y Cell Model of CoQ_{10} Deficiency

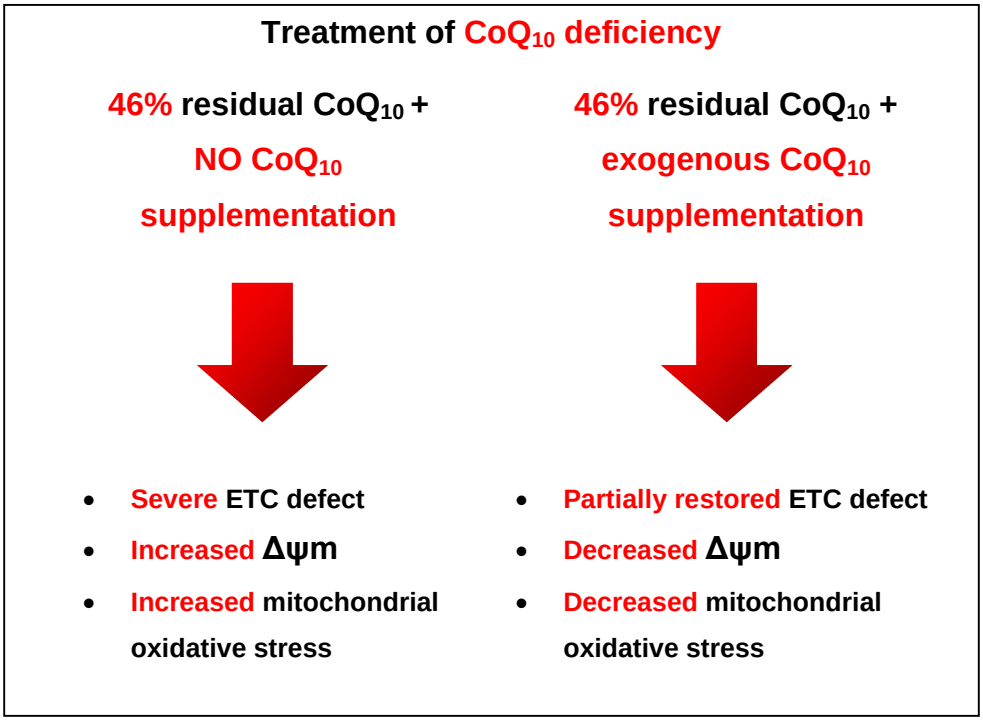

Figure 6.2 Diagrammatic Representation for the Results of CoQ_{10} Supplementation of the SH-SY5Y Cell Model of CoQ_{10} Deficiency

A marginal decrease in neuronal cell CoQ_{10} status (76% residual CoQ_{10}) appears sufficient to impair ETC function and increase oxidative stress, as well as decreasing Δψm to below normal levels (Figure 6.1). A more substantial decrease in CoQ_{10} (46% residual CoQ_{10}) resulted in further decreased ETC activities, an increase in Δψm (suggesting a reversal in Complex V activity) and an increase in oxidative stress (Figure 6.1).

The increase in Δψm observed in our CoQ_{10} deficient neuronal cell model is unique to this CoQ_{10} deficient model. The increase in Δψm in the presence of a concomitant decrease in ETC Complex I, II/III and IV activities indicates that a reversal of Complex V activity has occurred to maintain Δψm (Gandhi et al. 2009; Yao et al. 2012). Reversal of Complex V activity has been described in a limited number of mitochondrial diseases (Abramov et al. 2010; McKenzie et al. 2007); however this is the first study to report a reversal of Complex V activity in association with CoQ_{10} deficiency.

Mitochondrial oxidative stress is a common finding in a number of mitochondrial disorders including CoQ_{10} deficiency. Neuronal cells display mitochondrial oxidative stress at slightly higher residual CoQ_{10} levels than fibroblasts (neuronal cells: 76-46% of control CoQ_{10}; fibroblasts: 30-40% of control CoQ_{10}). Furthermore the ETC defect seen in the neuronal cell model is more severe. Inefficient transfer of electrons from ETC Complexes I, II and III, results in increased electron leak and enhanced production of the unstable semiquinone isoform of CoQ_{10}, a major site of ROS production.

It is interesting to note that the increased level of mitochondrial oxidative stress seen in our model is corrected after CoQ_{10} supplementation (Figure 6.2). This suggests that CoQ_{10} may be a good candidate therapy for mitochondrial disease, since secondary CoQ_{10} deficiency has been reported in MELAS and mtDNA depletion syndromes. Intriguingly, CoQ_{10} supplementation was found to reduce the level of mitochondrial oxidative stress below that of the control. Although ROS has been frequently associated with cellular damage, ROS are also important for cell signalling (Thannickal & Fanburg 2000). Thus a decrease in ROS below control levels may actually be detrimental to cellular function. Consequently decreased ROS signalling should be considered a potential drawback during CoQ_{10} supplementation.

However, CoQ_{10} supplementation was also partially effective at restoring mitochondrial ETC activity (Figure 6.2). In contrast Quinzii and colleagues found a complete restoration of ETC activity in CoQ_{10} deficient fibroblasts, demonstrated by ATP quantification (López et al. 2010). The inability to completely restore ETC activity following CoQ_{10} treatment in the CoQ_{10} deficient neuronal cells may be an indication of why neurological CoQ_{10} deficiency has been reported to be refractory to treatment (Emmanuele et al. 2012).

CoQ_{10} supplementation was also affective in restoring $\Delta\psi m$ to 90% of control levels (Figure 6.2), indicating that the reversal of ETC Complex V activity had been ameliorated, and Complex V activity was working in the forward direction.

MB has demonstrated efficacy in treating a number of neurodegenerative disorders including PD and AD (Lin et al. 2012). However MB was not effective at restoring the ETC deficiency associated with the perturbation in neuronal cell CoQ_{10} status. MB treatment induced a non-significant increase in Complex I activity, but was ineffective in restoring Complex II/III and Complex IV activity to control levels. Interestingly MB decreased the level of CoQ_{10} (not significant); implying that MB treatment of CoQ_{10} deficiency could further exacerbate the deficit in CoQ_{10} status.

CoQ_{10} supplementation in the treatment of neurodegenerative disease such as PD has to date proved ineffective in large scale clinical trials (Beale et al. 2011). In our study on supplementation we only see an adequate improvement of ETC activity after supplementation of 10µM CoQ_{10}. Previous studies have quoted that serum/plasma levels of CoQ_{10} only reach ~1-5µM regardless of the dose of CoQ_{10} prescribed (30-3000mg), highlighting issues of bioavailability in the treatment of neurological CoQ_{10} deficiency. There are many different formulations available and there is a great deal of variability in bioavailability between formulations. Newer more sophisticated formulations may be able to increase the plasma concentration in line with the 10µM target highlighted in this study.

The development of the tandem MS method for quantification of CoQ_{10} in CSF will allow us to monitor the CSF levels of CoQ_{10} following supplementation in patients. Following the results of our cellular supplementation study a target CSF level of 10µM could be aimed for successful CoQ_{10} therapy.

One of the most interesting applications of this method would be to investigate the terminal portion of the CoQ_{10} biosynthetic pathway. The biosynthetic pathway is best understood in lower organisms (*Escherichia coli, Saccharomyces cerevisiae, and Schizosaccharomyces pombe)* (Meganathan 2001; Kawamukai 2002). In contrast, very little is known about the human CoQ_{10} biosynthetic pathway. We currently know the function of two enzymes that are associated with human primary CoQ_{10} deficiency; COQ1 (*PDSS1/2*) and COQ2. However there are four other genes associated with the primary CoQ_{10} deficiency (*ADCK3, COQ4, COQ6, COQ9*). We know that these genes are involved in the terminal portion of the CoQ_{10} biosynthetic pathway but we have yet to elucidate their precise function.

The ability to assess CoQ_{10} levels in CSF will be of potential clinical utility for the diagnosis of patients with neurological CoQ_{10} deficiency, both primary and secondary. A recent literature review revealed that only 60% of patients with the cerebellar phenotype of CoQ_{10} deficiency have a decreased level in fibroblasts, and decrease in muscle CoQ_{10} status is not always significant (Emmanuele et al. 2012). The ability to assess CSF CoQ_{10} status will enable a direct evaluation of cerebral CoQ_{10} levels in patients with the cerebellar ataxic presentation of CoQ_{10} deficiency. This may improve the diagnostic yield of CoQ_{10} deficiency in this clinical phenotype since the possibility arises that the CoQ_{10} deficiency may not be expressed or to a lesser degree in fibroblasts or skeletal muscle.

6.1. Future Work

There are a number of further investigations that could be carried out to further the work done in this thesis.

6.1.1. Neuronal Cell Model

The cell model that has been developed for this thesis is the first human cell model of CoQ_{10} deficiency, however there is now the technology to develop a more sophisticated neuronal cell model of CoQ_{10} deficiency. Induced Pluripotency Stem (iPS) cell technology has allowed scientists to convert patient fibroblasts into functional neurones that, in theory have the same characteristics as those patients' neurones. There are a number of patient fibroblasts available for the various phenotypes and genotypes associated with CoQ_{10} deficiency. A comparative study of a predominantly neurological phenotype (ADCK3 gene mutation; Lagier-Tourenne et al. 2008; Horvath et al. 2012; Mollet et al. 2008) and a phenotype that has no neurological presentation (COQ6 gene mutation; Heeringa et al. 2011), would help us to understand more about the neurological features of CoQ_{10} deficiency.

6.1.2. Treatments

We have established that CoQ_{10} supplementation is effective at preventing mitochondrial superoxide production and restoring normal function of ETC Complex V, but ETC Complex I, II/III and IV were still compromised. Although the concentrations used are near to the level observed in plasma of treated patients, it would be interesting to investigate higher concentrations of CoQ_{10} to discover if ETC complex activities can be restored to normal levels.

To further strengthen this study oxygen electrode studies and ATP quantification could be carried out to assess the physiological functionality of the ETC. Additionally further investigation into the effect of CoQ_{10} supplementation on Complex V function would be of interest.

Regarding the MB treatment studies, we have established that MB treatment is not capable of restoring ETC complex activities, but not if MB treatment could prevent mitochondrial superoxide production and restore $\Delta\psi m$.

6.1.3. MS Method

In relation to the treatment and MS method chapters, it would be of interest to investigate the bioavailability of CoQ_{10} across the blood brain barrier. Previous studies have investigated plasma CoQ_{10} concentration after a 28 day treatment period with varying dosages (300 and 900mg; 2.27 and 6.62µg/ml above baseline). A comparative study of plasma versus CSF concentration could be done for different formulations of CoQ_{10} to determine which formulation crosses the blood brain barrier most effectively. Together with the results obtained in the treatment chapter, this will be extremely important in explaining why neurological CoQ_{10} deficiency may be refractory to treatment.

Another important application of the MS method will be to complete a screen of patients with ataxia of unknown cause. Following the discovery of several patients with adult onset ataxia caused by CoQ_{10} deficiency secondary to a mutation in the *ADCK3* gene (Horvath et al. 2012), there is a consensus in the scientific community that CoQ_{10} deficiency may be under diagnosed. Although a screen for the *ADCK3* gene mutation would potentially unearth new cases of CoQ_{10} deficiency, screening CSF for a CoQ_{10} deficiency would initially determine a deficiency, prompting a genetic screen in these patients. This would potentially allow the discovery of a new gene mutations associated with CoQ_{10} deficiency.

One of the most interesting adaptations of this method would be to look for intermediates in the CoQ_{10} biosynthetic pathway. Yeast studies have demonstrated the accumulation of a single product when any of the CoQ biosynthetic enzymes are mutated (coq1-9) (Tauche et al. 2008). It would be interesting to see if this phenomenon occurs in human CoQ deficiency.

6.2. References

Aberg, F., Appelkvist, E.L., Dallner, G. & Ernster, L., 1992. Distribution and redox state of ubiquinones in rat and human tissues. *Archives of biochemistry and biophysics*, 295(2), pp.230–4.

Abramov, A.Y., Smulders-Srinivasan, T.K., Kirby, D.M., Acin-Perez, R., Enriquez, J.A., Lightowlers, R.N., Duchen, M.R. & Turnbull, D.M., 2010. Mechanism of neurodegeneration of neurons with mitochondrial DNA mutations. *Brain*, 133(Pt 3), pp.797–807.

Ackrell, B.A., 2000. Progress in understanding structure-function relationships in respiratory chain complex II. *FEBS letters*, 466(1), pp.1–5.

Aeby, A., Sznajer, Y., Cavé, H., Rebuffat, E., Van Coster, R., Rigal, O. & Van Bogaert, P., 2007. Cardiofaciocutaneous (CFC) syndrome associated with muscular coenzyme Q10 deficiency. *Journal of inherited metabolic disease*, 30(5), p.827.

Alam, S.S., Nambidiri, A.M., Rudney, H. & Nambudiri, A.M., 1975. 4-Hydroxybenzoate: polyprenyl transferase and the prenylation of 4-aminobenzoate in mammalian tissues. *Archives of biochemistry and biophysics*, 171(1), pp.183–90.

Alberts, A.W., 1988. Discovery, biochemistry and biology of lovastatin. *The American journal of cardiology*, 62(15), p.10J–15J.

Alleva, R., Tomasetti, M., Battino, M., Curatola, G., Littarru, G.P. & Folkers, K., 1995. The roles of coenzyme Q10 and vitamin E on the peroxidation of human low density lipoprotein subfractions. *Proceedings of the National Academy of Sciences of the United States of America*, 92(20), pp.9388–91.

Almeida, A., Heales, S.J., Bolaños, J.P. & Medina, J.M., 1998. Glutamate neurotoxicity is associated with nitric oxide-mediated mitochondrial dysfunction and glutathione depletion. *Brain research*, 790(1-2), pp.209–16.

Anderson, M.E., 1985. Determination of Glutathione and Glutathione Disulphide in Biological Samples. *Annual review of biochemistry*, 113(70), pp.548–555.

Arroyo, A., Kagan, V., Tyurin, V.A., Burgess, J.R., Cabo, R.D.E., Navas, P. & Villalba, J.M., 2000. NADH and NADPH-Dependent Reduction of Coenzyme at the Plasma Membrane. *Antioxidants and redox signalling*, 2(2), pp.251–262.

Artuch, R., Brea-Calvo, G., Briones, P., Aracil, A., Galván, M., Espinós, C., Corral, J., Volpini, V., Ribes, A., Andreu, A.L., Palau, F., Sánchez-Alcázar, J. a, Navas, P. & Pineda, M., 2006. Cerebellar ataxia with coenzyme Q10 deficiency: diagnosis and follow-up after coenzyme Q10 supplementation. *Journal of the neurological sciences*, 246(1-2), pp.153–8.

Atamna, H., Nguyen, A., Schultz, C., Boyle, K., Newberry, J., Kato, H. & Ames, B.N., 2008. Methylene blue delays cellular senescence and enhances key mitochondrial biochemical pathways. *FASEB journal□: official publication of the Federation of American Societies for Experimental Biology*, 22(3), pp.703–12.

Auré, K., Benoist, J.F., Baulny, H.O. De, Romero, N.B. & Rigal, O., 2004. Progression despite replacement of a myopathic form of coenzyme Progression despite replacement of a myopathic form of coenzyme Q 10 defect. *Neurology*, 63(4), pp.727–9.

Von Ballmoos, C., Cook, G.M. & Dimroth, P., 2008. Unique rotary ATP synthase and its biological diversity. *Annual review of biophysics*, 37, pp.43–64.

Bartlett, K. & Eaton, S., 2004. Mitochondrial beta-oxidation. *European Journal of Biochemistry*, 271(3), pp.462–469.

Beale, Shoulson & Oakes, 2011. Statement of termination of QE3 study. *NINDS*. Available at: http://informahealthcare.com/doi/pdf/10.3109/00207454.2011.620194.

Belogrudov, G.I., Lee, P.T., Jonassen, T., Hsu, a Y., Gin, P. & Clarke, C.F., 2001. Yeast COQ4 encodes a mitochondrial protein required for coenzyme Q synthesis. *Archives of biochemistry and biophysics*, 392(1), pp.48–58.

Benzi G, Curti D, Pastoris O, Marzatico F, Villa RF, D.F., 1991. Sequential damage in mitochondrial complexes by peroxidative stress. *Neurochemical Research*, 16(12), pp.1295–302.

Le Ber, I., Dubourg, O., Benoist, J., Jardel, C., Mochel, F., Koenig, M., Brice, A., Lombès, A. & Dürr, A., 2007. Muscle coenzyme Q10 deficiencies in ataxia with oculomotor apraxia 1. *Neurology*, 68(4), pp.295–7.

Bhagavan, H.N. & Chopra, R.K., 2006. Coenzyme Q10: absorption, tissue uptake, metabolism and pharmacokinetics. *Free radical research*, 40(5), pp.445–53.

Bhuvaneswaran, C. & King, T.E., 1967. Succinate-dehydrogenating activity and cytochromes of hepatic microsomes. *Biochimica et biophysica acta*, 132(2), pp.282–289.

Biedler, J.L., Helson, L. & Spengler, B.A., 1973. Morphology and Growth , Tumorigenicity , and Cytogenetics of Human Neuroblastoma Cells in Continuous Culture Morphology and Growth , Tumorigenicity , and Cytogenetics of Human Neuroblastoma Cells in Continuous Culture. *Cancer Research*, pp.2643–2652.

Biedler, J.L., Roffler-tarlov, S., Schachner, M. & Freedman, L.S., 1978. Multiple Neurotransmitter Synthesis by Human Neuroblastoma Cell Lines and Clones Multiple Neurotransmitter Synthesis by Human Neuroblastoma Cell Lines and Clones. *Cancer Research*, 38, pp.3751–3757.

Boitier, E., Degoul, F., Desguerre, I., Charpentier, C., François, D., Ponsot, G., Diry, M., Rustin, P. & Marsac, C., 1998. A case of mitochondrial encephalomyopathy associated with a muscle coenzyme Q10 deficiency. *Journal of the neurological sciences*, 156(1), pp.41–6.

Bourgeron, T., Rustin, P., Chretien, D., Birch-Machin, M., Bourgeois, M., Viegas-Pequignot, E., Munnich, A. & Rotig, A., 1995. Mutation of a nuclear

succinate dehydrogenase gene results in mitochondrial respiratory chain deficiency. *Nature genetics*, 11, pp.144–9.

Boyer, P.D., 2002. A research journey with ATP synthase. *The Journal of biological chemistry*, 277(42), pp.39045–61.

Boyer, P.D., 1997. The ATP synthase--a splendid molecular machine. *Annual review of biochemistry*, 66, pp.717–49.

Bradford, M., 1976. A rapid and sensitive method for the quantitation of microgram quantities of protein utilizing the principle of protein-dye binding. *Analytical biochemistry*, 72, pp.248–254.

Braunstein, A., Horecker, B., Jacoby, W. & Karlson, P., 1975. Nomenclature of quinones with isoprenoid sidechains- Recommendations 1973. *Molecular and Cellular Biochemistry*, 8(3), pp.189–192.

Brightman, A.O., Wang, J., Miu, R.K., Sun, I.L., Barr, R., Crane, F.L. & Morré, D.J., 1992. A growth factor- and hormone-stimulated NADH oxidase from rat liver plasma membrane. *Biochimica et biophysica acta*, 1105(1), pp.109–17.

Brown, M.S. & Goldstein, J.L., 1986. A receptor-mediated pathway for cholesterol homeostasis. *Science*, 232(4746), pp.34–47.

Brzezinski, P. & Gennis, R.B., 2008. Cytochrome c oxidase: exciting progress and remaining mysteries. *Journal of bioenergetics and biomembranes*, 40(5), pp.521–31.

Burón, M., Rodriguez-Aguilera, J., Alcaín, F. & Navas, P., 1993. Transplasma membrane redox system in HL-60 cells is modulated during TPA-induced differentiation. *Biochemical and Biophysical Research Communications*, 192(2), pp.439–45.

Cadenas, E., Boveris, A., Ragan, C.I. & Stoppani, A.O., 1977. Production of Superoxide Radicals and Hydrogen Peroxide by NADH-Ubiquinone Reductase and Ubiquinol-Cytochrome c Reductase from Beef-Heart

Mitochondria. *Archives of Biochemistry and Biophysics*, 180(2), pp.248–257.

Cadenas, E. & Davies, K.J.A., 2000. Mitochondrial free radical generation, oxidative stress, and aging. *Free Radical Biology and Medicine*, 29(3-4), pp.222–230.

Casarin, A., Jimenez-Ortega, J.C., Trevisson, E., Pertegato, V., Doimo, M., Ferrero-Gomez, M.L., Abbadi, S., Artuch, R., Quinzii, C., Hirano, M., Basso, G., Ocaña, C.S., Navas, P. & Salviati, L., 2008. Functional characterization of human COQ4, a gene required for Coenzyme Q10 biosynthesis. *Biochemical and biophysical research communications*, 372(1), pp.35–9.

Cecchini, G., 2003. Function and structure of complex II of the respiratory chain. *Annual review of biochemistry*, 72, pp.77–109.

Cenens, J. & Schoonheydt, R.A., 1988. Visible spectroscopy of methylene blue on hectorite, laponite b and barasym in aqueous suspension. *Clay and Clay minerals*, 36(3), pp.214–224.

Chance, B. & Hollunger, G., 1961. The Interaction of Energy and Electron Transfer Reactions in Mitochondria I. General properties and nature of the products of succinate-linked reduction of pyridine nucleotide. *Journal of Biological Chemistry*, 236, pp.1534–1543.

Chance, B. & Williams, G.R., 1956. Respiratory enzymes in oxidative phosphorylation. VI. The effects of adenosine diphosphate on azide-treated mitochondria. *Journal of Biological Chemistry*, 221(1), pp.477–89.

Clinical Chemistry, 2012. Information to Authors. Available at: http://www.clinchem.org/site/info_ar/info_authors.xhtml#anal_meth.

Cooper, J.M., Korlipara, L.V.P., Hart, P.E., Bradley, J.L. & Schapira, A.H. V, 2008. Coenzyme Q10 and vitamin E deficiency in Friedreich's ataxia: predictor of efficacy of vitamin E and coenzyme Q10 therapy. *European journal of neurology*, 15(12), pp.1371–9.

Crane & Barr, 1967. Determination of ubiquinones [220]. In *Methods in Enzymology*. pp. 137–165.

Crane, F., Hatefi, Y., Lester, R. & Widmer, C., 1957. Isolation of a quinone from beef heart mitochondria. *Biochimica et biophysica acta.*, 25(1), pp.220–1.

Crane, F.L., 2001. Biochemical functions of coenzyme Q10. *Journal of the American College of Nutrition*, 20(6), pp.591–8.

Crane, F.L., Sun, I.L., Clark, M.G., Grebing, C. & Löw, H., 1985. Transplasma-membrane redox systems in growth and development. *Biochimica et biophysica acta*, 811(3), pp.233–64.

Crane, F.L., Sun, I.L., Crowe, R.A. & Alcaint, F.J., 1994. Coenzyme Q10 , Plasma Membrane Oxidase and Growth Control Growth Stimulation by Ligand-Activated Oxidase. *Molecular aspects of medicine*, 15, pp.1–11.

Crofts, A.R., 2004. The cytochrome bc1 complex: function in the context of structure. *Annual review of physiology*, 66, pp.689–733.

D'Arrigo, S., Riva, D., Bulgheroni, S., Chiapparini, L., Castellotti, B., Gellera, C. & Pantaleoni, C., 2008. Ataxia with oculomotor apraxia type 1 (AOA1): clinical and neuropsychological features in 2 new patients and differential diagnosis. *Journal of child neurology*, 23(8), pp.895–900.

Davey, G.P., Peuchen, S. & Clark, J.B., 1998. Energy Thresholds in Brain Mitochondria. *Biochemistry*, 273(21), pp.12753–12757.

Van Dijck, P.W., De Kruijff, B., Van Deenen, L.L., De Gier, J. & Demel, R.A., 1976. The preference of cholesterol for phosphatidylcholine in mixed phosphatidylcholine-phosphatidylethanolamine bilayers. *Biochimica et biophysica acta*, 455(2), pp.576–87.

Diomedi-Camassei, F., Di Giandomenico, S., Santorelli, F.M., Caridi, G., Piemonte, F., Montini, G., Ghiggeri, G.M., Murer, L., Barisoni, L., Pastore, A., Muda, A.O., Valente, M.L., Bertini, E. & Emma, F., 2007. COQ2 nephropathy: a newly described inherited mitochondriopathy with primary

renal involvement. *Journal of the American Society of Nephrology*, 18(10), pp.2773–80.

Duncan, A., Bitner-Glindzicz, M., Meunier, B., Costello, H., Hargreaves, I.P., López, L.C., Hirano, M., Quinzii, C.M., Sadowski, M.I., Hardy, J., Singleton, A., Clayton, P.T. & Rahman, S., 2009. A nonsense mutation in COQ9 causes autosomal-recessive neonatal-onset primary coenzyme Q10 deficiency: a potentially treatable form of mitochondrial disease. *American journal of human genetics*, 84(5), pp.558–66.

Duncan, A., Heales, S., Mills, K., Eaton, S., Land, J. & Hargreaves, I., 2005. Determination of coenzyme Q10 status in blood mononuclear cells, skeletal muscle, and plasma by HPLC with di-propoxy-coenzyme Q10 as an internal standard. *Clinical chemistry*, 51(12), pp.2380–2.

Düssmann, H., Kögel, D., Rehm, M. & Prehn, J.H.M., 2003. Mitochondrial membrane permeabilization and superoxide production during apoptosis. A single-cell analysis. *The Journal of biological chemistry*, 278(15), pp.12645–9.

Dutton, P.L., Moser, C.C., Sled, V.D., Daldal, F. & Ohnishi, T., 1998. A reductant-induced oxidation mechanism for complex I. *Biochimica et biophysica acta*, 1364(2), pp.245–57.

Eaton, S., Skinner, R., Hale, J.P., Pourfarzam, M., Roberts, A., Price, L. & Bartlett, K., 2000. Plasma coenzyme Q(10) in children and adolescents undergoing doxorubicin therapy. *Clinica chimica acta; international journal of clinical chemistry*, 302, pp.1–9.

Echtay, K.S., Winkler, E., Frischmuth, K. & Klingenberg, M., 2001. Uncoupling proteins 2 and 3 are highly active H(+) transporters and highly nucleotide sensitive when activated by coenzyme Q (ubiquinone). *Proceedings of the National Academy of Sciences of the United States of America*, 98(4), pp.1416–21.

Echtay, K.S., Winkler, E. & Klingenberg, M., 2000. Coenzyme Q is an obligatory cofactor for uncoupling protein function. *Nature*, 408(6812), pp.609–13.

Edlund, 1988. Determination of coenzyme Q10, α-tocopherol and cholesterol in biological samples by coupled-column liquid chromatography with coulometric and ultraviolet detection. *Journal of chromatography*, 425, pp.87–97.

Emmanuele, V., López, L.C., Berardo, A., Naini, A., Tadesse, S., Wen, B., D'Agostino, E., Solomon, M., DiMauro, S., Quinzii, C. & Hirano, M., 2012. Heterogeneity of coenzyme Q10 deficiency: patient study and literature review. *Archives of neurology*, 69(8), pp.978–83.

Ericsson, J. & Dallner, G., 1993. Distribution, biosynthesis, and function of mevalonate pathway lipids. *Subcellular Biochemistry*, 21, pp.229–72.

Ernster, L. & Dallner, G., 1995. Biochemical, physiological and medical aspects of ubiquinone function. *Biochimica et biophysica acta*, 1271(1), pp.195–204.

Ernster, L., Forsmark, P. & Nordenbrand, K., 1992. The mode of action of lipid-soluble antioxidants in biological membranes. Relationship between the effects of ubiquinol and vitamin E as inhibitors of lipid peroxidation in submitochondrial particles. *Journal of Nutritional Science and Vitaminology*, S-19-4, pp.548–551.

Ernster, L. & Forsmark-Andree, P., 1993. Ubiquinol: an endogenous antioxidant in aerobic organisms. *The Journal of clinical investigation*, 71, pp.60–65.

Ernster, L., Lee, I.Y., Norling, B. & Persson, B., 1969. Studies with ubiquinone-depleted submitochondrial particles. Essentiality of ubiquinone for the interaction of succinate dehydrogenase, NADH dehydrogenase, and cytochrome b. *European journal of biochemistry / FEBS*, 9(3), pp.299–310.

Fassone, E. & Rahman, S., 2012. Complex I deficiency: clinical features, biochemistry and molecular genetics. *Journal of medical genetics*, 49(9), pp.578–90.

Fenn, J.B., Mann, M., Meng, C.K., Wong, S.F., Craig, M., Meng, C.K.A.I., Mann, M. & Whitehouse, C.M., 1989. Electrospray Ionization of Large for Mass Spectrometry Biomolecules. *Science*, 246(4926), pp.64–71.

Festenstein, G.N., Heaton, F.W., Lowe, J.S. & Morton, R. a, 1955. A constituent of the unsaponifiable portion of animal tissue lipids (lambda max. 272 m mu). *The Biochemical journal*, 59(4), pp.558–66.

Floyd, R. a, Schneider, J.E. & Dittmer, D.P., 2004. Methylene blue photoinactivation of RNA viruses. *Antiviral research*, 61(3), pp.141–51.

Fontaine, E. & Bernardi, P., 1999. Progress on the mitochondrial permeability transition pore: regulation by complex I and ubiquinone analogs. *Journal of bioenergetics and biomembranes*, 31(4), pp.335–45.

Fontaine, E., Ichas, F. & Bernardi, P., 1998. A ubiquinone-binding site regulates the mitochondrial permeability transition pore. *The Journal of biological chemistry*, 273(40), pp.25734–40.

Frei, B., Kim, M.C. & Ames, B.N., 1990. Ubiquinol-10 is an effective lipid-soluble antioxidant at physiological concentrations. *Proceedings of the National Academy of Sciences of the United States of America*, 87(12), pp.4879–83.

Friedrich, T., Heek, P.V.A.N., Leif, H., Ohnishi, T., Forche, E., Kunze, B., Jansen, R., Trowitzsch-kienast, W., Hofle, G., Reichenbach, H. & Weiss, H., 1994. Two binding sites of inhibitors in NADH-ubiquinone oxidoreductase (complex I). *European Journal of Biochemistry*, 219, pp.691–698.

Galimberti, D. & Scarpini, E., 2011. Disease-modifying treatments for Alzheimer's disease. *Therapeutic advances in neurological disorders*, 4(4), pp.203–16.

Gandhi, S., Wood-Kaczmar, A., Yao, Z., Plun-favreau, H., Deas, E., Klupsch, K., Downward, J., Latchman, D.S., Tabrizi, S.J., Nicholas, W., Duchen, M.R. & Abramov, A.Y., 2009. PINK1-Associated Parkinson's Disease Is Caused by Neuronal Vulnerability to Calcium-Induced Cell Death. *Molecular Cell*, 33, pp.627–638.

Gegg, M.E., Beltran, B., Salas-Pino, S., Bolanos, J.P., Clark, J.B., Moncada, S. & Heales, S.J.R., 2004. Differential effect of nitric oxide on glutathione metabolism and mitochondrial function in astrocytes and neurones:

implications for neuroprotection/neurodegeneration? *Journal of Neurochemistry*, 86(1), pp.228–237.

Gempel, K., Topaloglu, H., Talim, B., Schneiderat, P., Schoser, B.G.H., Hans, V.H., Pálmafy, B., Kale, G., Tokatli, A., Quinzii, C., Hirano, M., Naini, A., DiMauro, S., Prokisch, H., Lochmüller, H., et al., 2007. The myopathic form of coenzyme Q10 deficiency is caused by mutations in the electron-transferring-flavoprotein dehydrogenase (ETFDH) gene. *Brain*, 130(Pt 8), pp.2037–44.

Gilbert, W., 1893. *De Magnete*,

Gille, L. & Nohl, H., 2000. The existence of a lysosomal redox chain and the role of ubiquinone. *Archives of biochemistry and biophysics*, 375(2), pp.347–54.

Gin, P. & Clarke, C.F., 2005. Genetic evidence for a multi-subunit complex in coenzyme Q biosynthesis in yeast and the role of the Coq1 hexaprenyl diphosphate synthase. *The Journal of biological chemistry*, 280(4), pp.2676–81.

Giovanni, S. Di, Mirabella, M. & Spinazzola, A., 2001. Coenzyme Q 10 reverses pathological phenotype and reduces apoptosis in familial CoQ 10 deficiency. *Neurology*, 57, p.515.

Gironi, M., Lamperti, C. & Nemni, R., 2004. Late-onset cerebellar ataxia with hypogonadism and muscle coenzyme Q10 deficiency. *Neurology*, 62, p.818.

Gómez-Díaz, C., Rodríguez-Aguilera, J.C., Barroso, M.P., Villalba, J.M., Navarro, F., Crane, F.L. & Navas, P., 1997. Antioxidant ascorbate is stabilized by NADH-coenzyme Q10 reductase in the plasma membrane. *Journal of bioenergetics and biomembranes*, 29(3), pp.251–7.

González-Aragón, D., Burón, M.I., López-Lluch, G., Hermán, M.D., Gómez-Díaz, C., Navas, P. & Villalba, J.M., 2005. Coenzyme Q and the regulation of intracellular steady-state levels of superoxide in HL-60 cells. *BioFactors (Oxford, England)*, 25(1-4), pp.31–41.

Green, D.E. & Tzagoloff, A., 1966. The mitochondrial electron transfer chain. *Archives of biochemistry and biophysics*, 116, pp.293–304.

Green, D.R. & Reed, J.C., 1998. Mitochondria and Apoptosis. *Science*, 281(5381), pp.1309–1312.

Greenberg, S. & Frishman, W., 1990. Co-enzyme Q10: a new drug for cardiovascular disease. *The journal of clinical pharmacology*, 30(7), pp.596–608.

Grune, T., Reinheckel, T. & Davies, K.J., 1997. Degradation of oxidized proteins in mammalian cells. *The FASEB journal*, 11(7), pp.526–34.

Grünler, J., Ericsson, J. & Dallner, G., 1994. Branch-point reactions in the biosynthesis of cholesterol, dolichol, ubiquinone and prenylated proteins. *Biochimica et biophysica acta*, 1212(3), pp.259–77.

Haas, D., Niklowitz, P., Hörster, F., Baumgartner, E.R., Prasad, C., Rodenburg, R.J., Hoffmann, G.F., Menke, T. & Okun, J.G., 2009. Coenzyme Q(10) is decreased in fibroblasts of patients with methylmalonic aciduria but not in mevalonic aciduria. *Journal of inherited metabolic disease*, 32(4), pp.570–5.

Hackenbrock, C.R., Chazotte, B. & Gupte, S.S., 1986. The random collision model and a critical assessment of diffusion and collision in mitochondrial electron transport. *Journal of bioenergetics and biomembranes*, 18(5), pp.331–68.

Hahn, S.H., Kerfoot, S. & Vasta, V., 2012. Assay to Measure Oxidized and Reduced Forms of CoQ by LC–MS/MS. In L.-J. C. Wong, Ph.D., ed. *Methods in molecular biology*. Totowa, NJ: Humana Press, pp. 169–179.

Halliwell, B. & Aruom, O.I., 1991. DNA damage by oxygen-derived species. Its mechanism and measurement in mammalian systems. *FEBS letters*, 281(1-2), pp.9–19.

Hamamura, K., Yamagishi, Y., Kijima, S., Suzuki, T., Mori, Y. & Nakamura, T., 2002. Synthesis of deuterium-labelled coenzyme Q10. *Journal of Labelled Compounds and Radiopharmaceuticals*, 45(10), pp.831–839.

Hamamura, K., Yamatsu, I., Minami, N., Yamagishi, Y., Inai, Y., Kijima, S. & Nakamura, T., 2002. Synthesis of [3'-14C] coenzyme Q10. *Journal of Labelled Compounds and Radiopharmaceuticals*, 45, pp.823–829.

Hargreaves, 2007. Coenzyme Q10 in phenylketonuria and mevalonic aciduria. *Mitochondrion*, 7 Suppl, pp.S175–80.

Hargreaves & Heales, 2002. Statins and myopathy. *The Lancet*, 359(9307), pp.711–712.

Hargreaves, Heales & Land, 1999. Mitochondrial respiratory chain defects are not accompanied by an increase in the activities of lactate dehydrogenase or manganese superoxide dismutase in paediatric skeletal muscle biopsies. *Journal of inherited metabolic disease*, 22(8), pp.925–31.

Hargreaves, I.P., Duncan, A.J., Heales, S.J.R. & Land, J.M., 2005. The effect of HMG-CoA reductase inhibitors on coenzyme Q10: possible biochemical/clinical implications. *Drug safety*, 28(8), pp.659–76.

Hargreaves, Lane & Sleiman, 2008. The coenzyme Q10 status of the brain regions of Parkinson's disease patients. *Neuroscience letters*, 447(1), pp.17–9.

Harper, C.R. & Jacobson, T.A., 2010. Evidence-based management of statin myopathy. *Current atherosclerosis reports*, 12(5), pp.322–30.

Harvey, D., 2009. The Vocabulary of Analytical Chemistry. *Analytical chemistry 2.0*. Available at: http://www.asdlib.org/onlineArticles/ecourseware/Analytical Chemistry 2.0/Text_Files_files/Chapter3.pdf.

Hassani, A., Horvath, R. & Chinnery, P.F., 2010. Mitochondrial myopathies: developments in treatment. *Current opinion in neurology*, 23(5), pp.459–65.

Heales SJ, Davies SE, Bates TE, C.J., 1995. Depletion of brain glutathione is accompanied by impaired mitochondrial function and decreased N-acetyl aspartate concentration. *Neurochemical Research*, 20(1), pp.31–8.

Heeringa, S.F., Chernin, G., Chaki, M., Zhou, W., Sloan, A.J., Ji, Z., Xie, L.X., Salviati, L., Hurd, T.W., Vega-warner, V., Killen, P.D., Raphael, Y., Ashraf, S., Ovunc, B., Schoeb, D.S., et al., 2011. COQ6 mutations in human patients produce nephrotic syndrome with sensorineural deafness. , 121(5), pp.2013–24.

Hinkle, P.C., Butow, R.A., Racker, E. & Chance, B., 1967. Partial resolution of the enzymes catalyzing oxidative phosphorylation. XV. Reverse electron transfer in the flavin-cytochrome β region of the respiratory chain of beef heart submitochondrial particles. *Journal of Biolgical Chemistry*, 242, pp.5169–5173.

Hirawake, H., Taniwaki, M., Tamura, A., Amino, H., Tomitsuka, E. & Kita, K., 1999. Characterization of the human SDHD gene encoding the small subunit of cytochrome b (cybS) in mitochondrial succinate-ubiquinone oxidoreductase. *Biochimica et biophysica acta*, 1412(3), pp.295–300.

Hirst, J., 2010. Towards the molecular mechanism of respiratory complex I. *The Biochemical journal*, 425(2), pp.327–39.

Holmgren, A. & Bjornstedt, M., 1995. Thioredoxin and thioredoxin reductase. *Methods*, 252, pp.199–208.

Holmsen, H., Holmsen, I. & Bernhardsen, A., 1966. Microdetermination of Adenosine Diphosphate and Adenosine Triphosphate in Plasma with the Firefly Luciferase System. *Analytical biochemistry*, 17(3), pp.456–473.

Horvath, R., Czermin, B., Gulati, S., Demuth, S., Houge, G., Pyle, A., Dineiger, C., Blakely, E.L., Hassani, A., Foley, C., Brodhun, M., Storm, K., Kirschner, J., Gorman, G.S., Lochmüller, H., et al., 2012. Adult-onset cerebellar ataxia due to mutations in CABC1/ADCK3. *Journal of neurology, neurosurgery, and psychiatry*, 83(2), pp.174–8.

Hosoe, K., Kitano, M., Kishida, H., Kubo, H., Fujii, K. & Kitahara, M., 2007. Study on safety and bioavailability of ubiquinol (Kaneka QH) after single and 4-week multiple oral administration to healthy volunteers. *Regulatory toxicology and pharmacology*, 47(1), pp.19–28.

Hsieh, E.J., Gin, P., Gulmezian, M., Tran, U.C., Saiki, R., Marbois, B.N. & Clarke, C.F., 2007. Saccharomyces cerevisiae Coq9 polypeptide is a subunit of the mitochondrial coenzyme Q biosynthetic complex. *Archives of biochemistry and biophysics*, 463(1), pp.19–26.

Hsu, Do, Lee & Clarke, 2000. Genetic evidence for a multi-subunit complex in the O-methyltransferase steps of coenzyme Q biosynthesis. *Biochimica et biophysica acta*, 1484(2-3), pp.287–97.

Huntsman, R.J., Lemire, E.G. & Dunham, C.P., 2009. Hypotonia and infantile spasms: a new phenotype of coenzyme Q10 deficiency? *The Canadian journal of neurological sciences. Le journal canadien des sciences neurologiques*, 36(1), pp.105–8.

Iiizumi, M., Arakawa, H. & Mori, T., 2002. Isolation of a Novel Gene , CABC1 , Encoding a Mitochondrial Protein That Is Highly Homologous to Yeast Activity of bc1 Complex Advances in Brief Highly Homologous to Yeast Activity of bc1 Complex 1. *Cancer Research*, pp.1246–1250.

Inui, M., Ooe, M., Fujii, K., Matsunaka, H., Yoshida, M. & Ichihashi, M., 2008. Mechanisms of inhibitory effects of CoQ10 on UVB-induced wrinkle formation in vitro and in vivo. *BioFactors (Oxford, England)*, 32(1-4), pp.237–43.

Isobe, C., Abe, T. & Terayama, Y., 2009. Increase in the oxidized/total coenzyme Q-10 ratio in the cerebrospinal fluid of Alzheimer's disease patients. *Dementia and geriatric cognitive disorders*, 28(5), pp.449–54.

Isobe, C., Abe, T. & Terayama, Y., 2010. Levels of reduced and oxidized coenzyme Q-10 and 8-hydroxy-2'-deoxyguanosine in the CSF of patients with Alzheimer's disease demonstrate that mitochondrial oxidative damage

and/or oxidative DNA damage contributes to the neurodegenerative process. *Journal of neurology*, 257(3), pp.399–404.

Iuchi, S. & Lin, E.C., 1991. Adaptation of Escherichia coli to respiratory conditions: Regulation of gene expression. *Cell*, 66(1), pp.5–7.

Johnson, A., Gin, P., Marbois, B.N., Hsieh, E.J., Wu, M., Barros, M.H., Clarke, C.F. & Tzagoloff, A., 2005. COQ9, a new gene required for the biosynthesis of coenzyme Q in Saccharomyces cerevisiae. *The Journal of biological chemistry*, 280(36), pp.31397–404.

Kawamukai, M., 2009. Biosynthesis and bioproduction of coenzyme Q10 by yeasts and other organisms. *Biotechnology and applied biochemistry*, 53(Pt 4), pp.217–26.

Kawamukai, M., 2002. Biosynthesis, bioproduction and novel roles of ubiquinone. *Journal of bioscience and engineering*, 94(6), pp.511–517.

Kebarle, P. & Verkerk, U.H., 2009. Electrospray: from ions in solution to ions in the gas phase, what we know now. *Mass spectrometry reviews*, 28(6), pp.898–917.

Kholodenko, B., Cascante, M. & Westerhoff, H., 1994. Control theory of metabolic channelling. *Molecular and Cellular Biochemistry*, 133-134, pp.313–331.

Kishi, T., Morré, D.M. & Morré, D.J., 1999. The plasma membrane NADH oxidase of HeLa cells has hydroquinone oxidase activity. *Biochimica et biophysica acta*, 1412(1), pp.66–77.

Kowaltowski & Vercesi, 1999. Mitochondrial damage induced by conditions of oxidative stress. *Free radical biology & medicine*, 26(3-4), pp.463–471.

Kröger, A. & Klingenberg, M., 1973. The kinetics of the redox reactions of ubiquinone related to the electron-transport activity in the respiratory chain. *European Journal of Biochemistry*, 34(2), pp.358–68.

Lagier-Tourenne, C., Tazir, M., López, L., Quinzii, C., Assoum, M., Drouot, N., Busso, C., Makri, S., Ali-Pacha, L., Benhassine, T., Anheim, M., Lynch, D., Thibault, C., Plewniak, F., Bianchetti, L., et al., 2008. ADCK3 , an Ancestral Kinase , Is Mutated in a Form of Recessive Ataxia Associated with Coenzyme Q 10 Deficiency. *Journal of Human Genetics*, (March), pp.661–672.

Lalani, S.R., Vladutiu, G.D., Plunkett, K., Lotze, T.E., Adesina, A.M. & Scaglia, F., 2005. Isolated mitochondrial myopathy associated with muscle coenzyme Q10 deficiency. *Archives of neurology*, 62(2), pp.317–20.

Lamperti, C., Naini, A., Hirano, M., Vivo, D.C. De, Bertini, E. & Servidei, S., 2003. Cerebellar ataxia and coenzyme Q10 deficiency. *Neurology*, 60(7), pp.1206–8.

Langsjoen, P. & Langsjoen, A., 1999. Overview of the use of CoQ10 in cardiovascular disease. *Biofactors*, 9(2-4), pp.273–84.

Larm, J.A., Vaillant, F., Linnane, A.W. & Lawen, A., 1994. Up-regulation of the plasma membrane oxidoreductase as a prerequisite for the viability of human Namalwa rho 0 cells. *The Journal of biological chemistry*, 269(48), pp.30097–100.

Li, L., Pabbisetty, D., Carvalho, P., Avery, M.A. & Avery, B.A., 2008. Analysis of CoQ10 in rat serum by ultra-performance liquid chromatography mass spectrometry after oral administration. *Journal of pharmaceutical and biomedical analysis*, 46(1), pp.137–42.

Lin, A.-L., Poteet, E., Du, F., Gourav, R.C., Liu, R., Wen, Y., Bresnen, A., Huang, S., Fox, P.T., Yang, S.-H. & Duong, T.Q., 2012. Methylene blue as a cerebral metabolic and hemodynamic enhancer. *PloS one*, 7(10), p.e46585.

Liu, Z. & Artmann, C., 2009. Relative bioavailability comparison of different Coenzyme Q10 formulations with a novel delivery system. *Alternative therapies*, 15(2), pp.42–46.

Lodi, R., Rajagopalan, B., Bradley, J.L., Taylor, D.J., Crilley, J.G., Hart, P.E., Blamire, A.M., Manners, D., Styles, P., Schapira, A.H.V. & Cooper, J.M., 2002. Mitochondrial Dysfunction in Friedreich's Ataxia: From Pathogenesis to Treatment Perspectives. *Free Radical Research*, 36(4), pp.461–466.

López, L.C., Quinzii, C.M., Area, E., Naini, A., Rahman, S., Schuelke, M., Salviati, L., Dimauro, S. & Hirano, M., 2010. Treatment of CoQ(10) deficient fibroblasts with ubiquinone, CoQ analogs, and vitamin C: time- and compound-dependent effects. *PloS one*, 5(7), p.e11897.

López, L.C., Schuelke, M., Quinzii, C.M., Kanki, T., Rodenburg, R.J.T., Naini, A., Dimauro, S. & Hirano, M., 2006. Leigh syndrome with nephropathy and CoQ10 deficiency due to decaprenyl diphosphate synthase subunit 2 (PDSS2) mutations. *American journal of human genetics*, 79(6), pp.1125–9.

López-Lluch, G., Barroso, M.P., Martín, S.F., Fernández-Ayala, D.J., Gómez-Díaz, C., Villalba, J.M. & Navas, P., 1999. Role of plasma membrane coenzyme Q on the regulation of apoptosis. *BioFactors (Oxford, England)*, 9(2-4), pp.171–7.

López-Martín, J.M., Salviati, L., Trevisson, E., Montini, G., DiMauro, S., Quinzii, C., Hirano, M., Rodriguez-Hernandez, A., Cordero, M.D., Sánchez-Alcázar, J. a, Santos-Ocaña, C. & Navas, P., 2007. Missense mutation of the COQ2 gene causes defects of bioenergetics and de novo pyrimidine synthesis. *Human molecular genetics*, 16(9), pp.1091–7.

Löw, P., Peterson, E., Edlund, C., Brunk, U. & Appelkvist, E., 1992. Nonmembrane associated dolichol in rat liver. *Lipids*, 27(1), pp.1–9.

Lowry, O., Rosebrough, N., Farr, A. & Randall, R., 1951. Protein measurement with the Folin phenol reagent. *The Journal of biological chemistry*, 193(1), pp.265–71.

Van Maldergem, L., Trijbels, F., DiMauro, S., Sindelar, P.J., Musumeci, O., Janssen, A., Delberghe, X., Martin, J.-J. & Gillerot, Y., 2002. Coenzyme Q-

responsive Leigh's encephalopathy in two sisters. *Annals of neurology*, 52(6), pp.750–4.

Malmquist, N.A., Gujjar, R., Rathod, P.K. & Phillips, M.A., 2008. Analysis of flavin oxidation and electron-transfer inhibition in Plasmodium falciparum dihydroorotate dehydrogenase. *Biochemistry*, 47(8), pp.2466–75.

Mancini, a, De Marinis, L., Littarru, G.P. & Balercia, G., 2005. An update of Coenzyme Q10 implications in male infertility: biochemical and therapeutic aspects. *BioFactors (Oxford, England)*, 25(1-4), pp.165–74.

Mandi, G., Witte, S., Meissner, P., Coulibaly, B., Mansmann, U., Rengelshausen, J., Schiek, W., Jahn, A., Sanon, M., Wüst, K., Walter-Sack, I., Mikus, G., Burhenne, J., Riedel, K.-D., Schirmer, H., et al., 2005. Safety of the combination of chloroquine and methylene blue in healthy adult men with G6PD deficiency from rural Burkina Faso. *Tropical medicine & international health : TM & IH*, 10(1), pp.32–8.

Marbois, B., Gin, P., Faull, K.F., Poon, W.W., Lee, P.T., Strahan, J., Shepherd, J.N. & Clarke, C.F., 2005. Coq3 and Coq4 define a polypeptide complex in yeast mitochondria for the biosynthesis of coenzyme Q. *The Journal of biological chemistry*, 280(21), pp.20231–8.

Marbois, B., Gina, P., Gulmeziana, M. & Clarke, C.F., 2009. The Yeast Coq4 Polypeptide Organizes a Mitochondrial Protein Complex Essential for Coenzyme Q Biosynthesis. *Biochimica et biophysica acta*, 1791(1), pp.69–75.

Marbois, B., Xia, Y., Lusis, A. & Clarke, C., 1994. Ubiquinone biosynthesis in eukaryotic cells: tissue distribution of mRNA encoding 3,4-dihydroxy-5-polyprenylbenzoate methyltransferase in the rat and mapping of the COQ3 gene to mouse chromosome 4. *Archives of biochemistry and biophysics*, 313(1), pp.83–8.

Matsuoka, T., Hiroko, M., Yu-ichi, G. & Ikuya, N., 1991. Muscle Coenzyme Q10 in mitochondrial encephalomyopathies. *Neuromuscular disorders*, 1(6), pp.443–447.

McKenzie, M., Liolitsa, D., Akinshina, N., Campanella, M., Sisodiya, S., Hargreaves, I., Nirmalananthan, N., Sweeney, M.G., Abou-Sleiman, P.M., Wood, N.W., Hanna, M.G. & Duchen, M.R., 2007. Mitochondrial ND5 gene variation associated with encephalomyopathy and mitochondrial ATP consumption. *The Journal of biological chemistry*, 282(51), pp.36845–52.

Meganathan, R., 2001. Ubiquinone biosynthesis in microorganisms. *FEMS microbiology letters*, 203(2), pp.131–9.

Meier, T., Perlman, S.L., Rummey, C., Coppard, N.J. & Lynch, D.R., 2012. Assessment of neurological efficacy of idebenone in pediatric patients with Friedreich's ataxia: data from a 6-month controlled study followed by a 12-month open-label extension study. *Journal of neurology*, 259(2), pp.284–91.

Meister, A. & Anderson, M.E., 1983. Glutathione. *Annual review of biochemistry*, 52, pp.711–60.

Miles, M. V, 2007. The uptake and distribution of coenzyme Q10. *Mitochondrion*, 7 Suppl, pp.S72–7.

Miles, M. V, Miles, L., Tang, P.H., Horn, P.S., Steele, P.E., DeGrauw, A.J., Wong, B.L. & Bove, K.E., 2008. Systematic evaluation of muscle coenzyme Q10 content in children with mitochondrial respiratory chain enzyme deficiencies. *Mitochondrion*, 8(2), pp.170–80.

Mitchell, P., 1966. Chemiosmotic coupling in oxidative and photosynthetic phosphorylation. *Biological reviews of the Cambridge Philosophical Society*, 41(3), pp.445–502.

Mitchell, P., 1961. Coupling of Phosphorylation to Electron and Hydrogen Transfer by a Chemi-Osmotic type of Mechanism. *Group*, 191, pp.144–148.

Mitchell, P., 1975. Protionmotive redox mechanism of the cytochrome b-c1 complex in the respiratory chain: protonmotive ubiquinone cycle. *FEBS letters*, 56(1), pp.1–6.

Mollet, J., Delahodde, A., Serre, V., Chretien, D., Schlemmer, D., Lombes, A., Boddaert, N., Desguerre, I., Lonlay, P. de, HO, de B., Munnich, A. & Rötig, A., 2008. CABC1 Gene Mutations Cause Ubiquinone Deficiency with Cerebellar Ataxia and Seizures. *Journal of Human Genetics*, 82, pp.623–630.

Mollet, J., Giurgea, I., Schlemmer, D., Dallner, G., Chretien, D., Delahodde, A., Bacq, D., Lonlay, P. De, Munnich, A. & Rötig, A., 2007. Prenyldiphosphate synthase, subunit 1 (PDSS1) and OH-benzoate polyprenyltransferase (COQ2) mutations in ubiquinone deficiency and oxidative phosphorylation disorders. *Journal of Clinical Investigation*, 117(3), pp.765–72.

Montero, R., Pineda, M., Aracil, A., Vilaseca, M.-A., Briones, P., Sánchez-Alcázar, J.-A., Navas, P. & Artuch, R., 2007. Clinical, biochemical and molecular aspects of cerebellar ataxia and Coenzyme Q10 deficiency. *Cerebellum*, 6(2), pp.118–22.

Moreira, M.C., Barbot, C., Tachi, N., Kozuka, N., Uchida, E., Gibson, T., Mendonça, P., Costa, M., Barros, J., Yanagisawa, T., Watanabe, M., Ikeda, Y., Aoki, M., Nagata, T., Coutinho, P., et al., 2001. The gene mutated in ataxia-ocular apraxia 1 encodes the new HIT/Zn-finger protein aprataxin. *Nature genetics*, 29(2), pp.189–93.

Morrison, J.D., McGilvery, D.C., Smith, D., Yost, R.A. & Enke, C.G., 1979. High efficiency collision induced dissociation in an rf only quadrupole. *International Journal or Mass Spectrometry and Ion Physics*, 30(2), pp.127–136.

Murata, T., Ohtsuka, C. & Terayama, Y., 2008. Increased mitochondrial oxidative damage and oxidative DNA damage contributes to the neurodegenerative process in sporadic amyotrophic lateral sclerosis. *Free radical research*, 42(3), pp.221–5.

Murphy, M.P., 2009. How mitochondria produce reactive oxygen species. *The Biochemical journal*, 417(1), pp.1–13.

Musumeci, O., Naini, A., Slonim, A.E., Skavin, N., Hadjigeorgiou, G.L., Krawiecki, N., Weissman, B.M., Tsao, C.Y., Mendell, J.R., Shanske, S., De Vivo, D.C., Hirano, M. & DiMauro, S., 2001. Familial cerebellar ataxia with muscle coenzyme Q10 deficiency. *Neurology*, 56(7), pp.849–55.

Navarro, F., Arroyo, a, Martín, S.F., Bello, R.I., de Cabo, R., Burgess, J.R., Navas, P. & Villalba, J.M., 1999. Protective role of ubiquinone in vitamin E and selenium-deficient plasma membranes. *BioFactors (Oxford, England)*, 9(2-4), pp.163–70.

Nicholls, D.G., 2006. Simultaneous monitoring of ionophore- and inhibitor-mediated plasma and mitochondrial membrane potential changes in cultured neurons. *The Journal of biological chemistry*, 281(21), pp.14864–74.

Nicholls, G. & Locke, R.M., 1984. Thermogenic mechanisms in brown fat. *Physiological reviews*, 64(1), pp.1–64.

Niki, E., 1987. Antioxidants in relation to lipid peroxidation. *Chemistry and Physics of Lipids*, 44, pp.227–253.

Ogasahara, S., Engel, A.G., Frens, D. & Mack, D., 1989. Muscle coenzyme Q deficiency in familial mitochondrial encephalomyopathy. *Proceedings of the National Academy of Sciences of the United States of America*, 86(7), pp.2379–82.

Onoue, S., Uchida, A., Kuriyama, K., Nakamura, T., Seto, Y., Kato, M., Hatanaka, J., Tanaka, T., Miyoshi, H. & Yamada, S., 2012. Novel solid self-emulsifying drug delivery system of coenzyme Q10 with improved photochemical and pharmacokinetic behaviors. *European journal of pharmaceutical sciences*, 46(5), pp.492–9.

Oz, M., Lorke, D.E. & Petroianu, G. a, 2009. Methylene blue and Alzheimer's disease. *Biochemical pharmacology*, 78(8), pp.927–32.

Ozawa, T., 1997. Genetic and functional changes in mitochondria associated with aging. *Physiological reviews*, 77(2), pp.425–64.

Papa, S. & Skulachev, V.P., 1997. Reactive oxygen species, mitochondria, apoptosis and aging. *Molecular and cellular biochemistry*, 174(1-2), pp.305–19.

Papucci, L., Schiavone, N., Witort, E., Donnini, M., Lapucci, A., Tempestini, A., Formigli, L., Zecchi-Orlandini, S., Orlandini, G., Carella, G., Brancato, R. & Capaccioli, S., 2003. Coenzyme q10 prevents apoptosis by inhibiting mitochondrial depolarization independently of its free radical scavenging property. *The Journal of biological chemistry*, 278(30), pp.28220–8.

Pecqueur, C., Couplan, E., Bouillaud, F. & Ricquier, D., 2001. Genetic and physiological analysis of the role of uncoupling proteins in human energy homeostasis. *Journal of Molecular Medicine*, 79(1), pp.48–56.

Pineda, M., Montero, R., Aracil, A., O'Callaghan, M.M., Mas, A., Espinos, C., Martinez-Rubio, D., Palau, F., Navas, P., Briones, P. & Artuch, R., 2010. Coenzyme Q(10)-responsive ataxia: 2-year-treatment follow-up. *Movement disorders: official journal of the Movement Disorder Society*, 25(9), pp.1262–8.

Poderoso, J.J., Lisdero, C., Schöpfer, F., Riobó, N., Carreras, M.C., Cadenas, E. & Boveris, a, 1999. The regulation of mitochondrial oxygen uptake by redox reactions involving nitric oxide and ubiquinol. *The Journal of biological chemistry*, 274(53), pp.37709–16.

Poderoso, J.J., Peralta, J.G., Lisdero, C.L., Carreras, M.C., Schöpfer, F., Cadenas, E., Boveris, A., Poderoso, J.J., Radisic, M., Scho, F., Juan, J. & Constanza, L., 1998. Nitric oxide regulates oxygen uptake and hydrogen peroxide release by the isolated beating rat heart. *American Journal of Physiology*, 274(1), pp.C112–C119.

Poon, W., Noelle, B. & Clarke, F.T., 1995. 3-hexaprenyl-4-hydroxybenzoic acid forms a predominant intermediate pool in ubiquinone biosynthesis in Saccharomyces cerevisiae. *Archives of biochemistry and biophysics*, 320, pp.305–314.

Poon, W.W., Do, T.Q., Marbois, B.N. & Clarke, C.F., 1997. Sensitivity to treatment with polyunsaturated fatty acids is a general characteristic of the ubiquinone-deficient yeast coq mutants. *Molecular aspects of medicine*, 18 Suppl, pp.S121–7.

Quinzii, C., Kattah, G., Naini, A., Akman, H., Mootha, V., DiMauro, S. & Hirano, M., 2005. Coenzyme Q deficiency and cerebellar ataxia associated with an aprataxin mutation. *Neurology*, 64(3), pp.539–41.

Quinzii, C., López, L.C., Gilkerson, R.W., Dorado, B., Coku, J., Naini, A.B., Lagier-Tourenne, C., Schuelke, M., Salviati, L., Carrozzo, R., Santorelli, F., Rahman, S., Tazir, M., Koenig, M., Dimauro, S., et al., 2010. Reactive oxygen species, oxidative stress, and cell death correlate with level of CoQ10 deficiency. *The FASEB journal*, 24, pp.3733–3743.

Quinzii, C., López, L.C., Von-Moltke, J., Naini, A., Krishna, S., Schuelke, M., Salviati, L., Navas, P., DiMauro, S. & Hirano, M., 2008. Respiratory chain dysfunction and oxidative stress correlate with severity of primary CoQ10 deficiency. *The FASEB journal*, 22(6), pp.1874–85.

Quinzii, C., Naini, A., Salviati, L., Trevisson, E., Navas, P., Dimauro, S. & Hirano, M., 2006. A mutation in para-hydroxybenzoate-polyprenyl transferase (COQ2) causes primary coenzyme Q10 deficiency. *American journal of human genetics*, 78(2), pp.345–9.

Quinzii, C.M., Garone, C., Emmanuele, V., Tadesse, S., Krishna, S., Dorado, B. & Hirano, M., 2013. Tissue-specific oxidative stress and loss of mitochondria in CoQ-deficient Pdss2 mutant mice. *FASEB journal*, 27(2), pp.612–21.

Quinzii, C.M., Tadesse, S., Naini, A. & Hirano, M., 2012. Effects of inhibiting CoQ10 biosynthesis with 4-nitrobenzoate in human fibroblasts. *PloS one*, 7(2), p.e30606.

Rahman, Hargreaves, Clayton & Heales, 2001. Neonatal presentation of coenzyme Q10 deficiency. *The Journal of pediatrics*, 139(3), pp.456–8.

Rahman, S., Clarke, C.F. & Hirano, M., 2012. 176th ENMC International Workshop: Diagnosis and treatment of coenzyme Q(10) deficiency. *Neuromuscular disorders*, 22(1), pp.76–86.

Ramamoorthy, S., Patel, S., Bradburn, E., Kadry, Z., Uemura, T., Janicki, P.K., Shah, R.A., Bezinover, D. & Description, C., 2013. Case Report Use of Methylene Blue for Treatment of Severe Sepsis in an Immunosuppressed Patient after Liver Transplantation. *Case reports in transplantation*, 2013, p.4 pages.

Reed, J.S. & Ragan, C.I., 1987. The effect of rate limitation by cytochrome c on the redox state of the ubiquinone pool in reconstituted NADH: cytochrome c reductase. *The Biochemical journal*, 247(3), pp.657–62.

Rice-Evans, C. & Burdon, R., 1993. Free radical-lipid interactions and their pathological consequences. *Progress in lipid research*, 32(1), pp.71–110.

Rich, P., 2003. The molecular machinery of Keilin's respiratory chain. *Biochemical Society Transactions*, 31, pp.1095–1105.

Riddle, C., Terrell, S., Menser, M., Aires, D. & Schweiger, E., 2009. A review of photodynamic therapy (PDT) for the treatment of acne vulgaris. *Journal of Drugs in Dermatology*, 8(11), pp.1010–1019.

Riederer, P., Sofic, E., Rausch, W.D., Schmidt, B., Reynolds, G.P., Jellinger, K. & Youdim, M.B., 1989. Transition metals, ferritin, glutathione, and ascorbic acid in parkinsonian brains. *Journal of neurochemistry*, 52(2), pp.515–20.

Rilling, H.C., 1985. Eukaryotic prenyltransferases. *Methods in Enzymology*, 110, pp.145–152.

Rodríguez-Hernández A, Cordero MD, Salviati L, Artuch R, Pineda M, Briones P, Gómez Izquierdo L, Cotán D, Navas P, S.-A.J., 2009. Coenzyme Q deficiency triggers mitochondria degradation by mitophagy. *Autophagy*, 5(1), pp.19–32.

Rolfe, D.F. & Brown, G.C., 1997. Cellular Energy Utilization of Standard Metabolic and Molecular Origin Rate in Mammals. *Physiological Reviews*, 77(3), pp.731–758.

Romagnoli, A., Oradei, A., Destito, C., Iacocagni, A., Marin, A.. & Littarru, G.P., 1994. Protective role in vivo of coenzyme Q10 during reperfusion of ischemic limbs. *Molecular aspects of medicine*, 15 Suppl, pp.s177–85.

Rötig, A., Appelkvist, E.L., Geromel, V., Chretien, D., Kadhom, N., Edery, P., Lebideau, M., Dallner, G., Munnich, A., Ernster, L. & Rustin, P., 2000. Quinone-responsive multiple respiratory-chain dysfunction due to widespread coenzyme Q10 deficiency. *Lancet*, 356(9227), pp.391–5.

Ruiz-Jiménez, J., Priego-Capote, F., Mata-Granados, J.M., Quesada, J.M. & Luque de Castro, M.D., 2007. Determination of the ubiquinol-10 and ubiquinone-10 (coenzyme Q10) in human serum by liquid chromatography tandem mass spectrometry to evaluate the oxidative stress. *Journal of chromatography. A*, 1175(2), pp.242–8.

Runquist, M., Parmryd, I., Thelin, a, Chojnacki, T. & Dallner, G., 1995. Distribution of branch point prenyltransferases in regions of bovine brain. *Journal of neurochemistry*, 65(5), pp.2299–306.

Sacconi, S., Trevisson, E., Salviati, L., Aymé, S., Rigal, O., Redondo, A.G., Mancuso, M., Siciliano, G., Tonin, P., Angelini, C., Auré, K., Lombès, A. & Desnuelle, C., 2010. Coenzyme Q10 is frequently reduced in muscle of patients with mitochondrial myopathy. *Neuromuscular disorders*, 20(1), pp.44–8.

Salah, M., Samy, N. & Fadel, M., 2009. Methylene blue mediated photodynamic therapy for resistant plaque psoriasis. *Journal of Drugs in Dermatology*, 8(1), pp.42–49.

Salviati, L., Trevisson, E., Rodriguez Hernandez, M.A., Casarin, A., Pertegato, V., Doimo, M., Cassina, M., Agosto, C., Desbats, M.A., Sartori, G., Sacconi, S., Memo, L., Zuffardi, O., Artuch, R., Quinzii, C., et al., 2012.

Haploinsufficiency of COQ4 causes coenzyme Q10 deficiency. *Journal of medical genetics*, 49(3), pp.187–91.

Schaefer, W.H., Lawrence, J.W., Loughlin, A.F., Stoffregen, D.A., Mixson, L.A., Dean, D.C., Raab, C.E., Yu, N.X., Lankas, G.R. & Frederick, C.B., 2004. Evaluation of ubiquinone concentration and mitochondrial function relative to cerivastatin-induced skeletal myopathy in rats. *Toxicology and Applied Pharmacology*, 194(1), pp.10–23.

Schägger, H. & Pfeiffer, K., 2000. Supercomplexes in the respiratory chains of yeast and mammalian mitochondria. *The EMBO journal*, 19(8), pp.1777–83.

Schneider, D. & Elstner, E.F., 2000. Coenzyme Q10 , Vitamin E , and Dihydrothioctic Acid Cooperatively Prevent Diene Conjugation in Isolated Low Density Lipoprotein. *Antioxidants and redox signalling*, 2(2), pp.327–333.

Shepherd, D. & Garland, P.B., 1969. The kinetic properties of citrate synthase from rat liver mitochondria. *The Biochemical journal*, 114(3), pp.597–610.

Shibanuma, M., Kuroki, T. & Nose, K., 1990. Stimulation by hydrogen peroxide of DNA synthesis, competence family gene expression and phosphorylation of a specific protein in quiescent Balb/3T3 cells. *Oncogene*, 5(7), pp.1025–1032.

Shults, C., Oakes, D., Kieburtz, K., Beal, F., Haas, R., Plumb, S., Juncos, J., Nutt, J., Shoulson, I., Carter, J., Kompoliti, K., Perlmutter, J., Reich, S., Stern, M., Watts, R., et al., 2002. Effects of Coenzyme Q 10 in Early Parkinson Disease. *Archives of Neurology*, 59(10), pp.1541–50.

Shults, C.W., Flint Beal, M., Song, D. & Fontaine, D., 2004. Pilot trial of high dosages of coenzyme Q10 in patients with Parkinson’s disease. *Experimental neurology*, 188(2), pp.491–4.

Shults, C.W., Haas, R.H., Passov, D. & Bed, M.F., 1997. Coenzyme Q10 Levels Correlate with the Activities of Complexes I and II/III in Mitochondria from

Parkinsonian and Nonparkinsonian Subjects. *Annals of Neurology*, 42, pp.261–264.

Siebert, M., Severin, K. & Heide, L., 1994. Formation of 4-hydroxybenzoate in Escherichia coli: characterization of the ubiC gene and its encoded enzyme chorismate pyruvate-lyase. *Microbiology*, (140), pp.897–904.

Skulachev, V.P., 2001. Mitochondrial filaments and clusters as intracellular power- transmitting cables. *Trends in biochemical sciences*, 26(1), pp.23–29.

Skulachev, V.P., 1998. Uncoupling: new approaches to an old problem of bioenergetics. *Biochimica et biophysica acta*, 1363(2), pp.100–24.

Sobreira, C., Hirano, M., Shanske, S., Keller, R., Haller, R., Davidson, E., Santorelli, F., Miranda, A., Bonilla, E., Mojon, D., Barreira, A., King, M. & DiMauro, S., 1997. Mitochondrial encephalomyopathy with coenzyme Q10 deficiency. *Neurology*, 48(5), pp.1238–43.

Soussi, B., Idström, J.P., Scherstén, T. & Bylund-Fellenius, a C., 1990. Cytochrome c oxidase and cardiolipin alterations in response to skeletal muscle ischaemia and reperfusion. *Acta physiologica Scandinavica*, 138(2), pp.107–14.

Spindler, M., Beal, M.F. & Henchcliffe, C., 2009. Coenzyme Q10 effects in neurodegenerative disease. *Neuropsychiatric disease and treatment*, 5, pp.597–610.

Stadtman, E.R., 1990. Metal ion-catalyzed oxidation of proteins: Biochemical mechanism and biological consequences. *Free radical biology & medicine*, 9, pp.315–325.

Stadtman, E.R. & Berlett, B.S., 1991. Fenton chemistry. Amino acid oxidation. *The Journal of biological chemistry*, 266(26), pp.17201–11.

Stirpe, F., 1991. Stimulation by xanthine oxidase of 3T3 Swiss fibroblasts and human lymphocytes. *Experimental Cell Research*, 192(2), pp.635–638.

Sugioka K, Nakano M, Totsune-Nakano H, Minakami H, Tero-Kubota S, I.Y., 1988. Mechanism of O2- generation in reduction and oxidation cycle of ubiquinones in a model of mitochondrial electron transport systems. *Biochimica et biophysica acta*, 936(3), pp.377–85.

Takahashi, T., Okamoto, T. & Kishi, T., 1996. Characterization of NADPH-dependent ubiquinone reductase activity in rat liver cytosol: effect of various factors on ubiquinone-reducing activity and discrimination from other quinone reductases. *Journal of biochemistry*, 119(2), pp.256–63.

Takamiya, S., Matsui, T., Taka, H., Murayama, K., Matsuda, M. & Aoki, T., 1999. Free-living nematodes Caenorhabditis elegans possess in their mitochondria an additional rhodoquinone, an essential component of the eukaryotic fumarate reductase system. *Archives of biochemistry and biophysics*, 371(2), pp.284–9.

Tauche, A., Krause-Buchholz, U. & Rödel, G., 2008. Ubiquinone biosynthesis in Saccharomyces cerevisiae: the molecular organization of O-methylase Coq3p depends on Abc1p/Coq8p. *FEMS yeast research*, 8(8), pp.1263–75.

Taylor, G., 1964. Disintegration of water drops in an electric field. In *Proceedings of the Royal Society of London. Series A, Mathematical and PhysicalSciences, Vol. 280, No. 1382*. pp. 383–397.

Terracciano, A., Renaldo, F., Zanni, G., D'Amico, A., Pastore, A., Barresi, S., Valente, E.M., Piemonte, F., Tozzi, G., Carrozzo, R., Valeriani, M., Boldrini, R., Mercuri, E., Santorelli, F.M. & Bertini, E., 2012. The use of muscle biopsy in the diagnosis of undefined ataxia with cerebellar atrophy in children. *European journal of paediatric neurology□: EJPN□: official journal of the European Paediatric Neurology Society*, 16(3), pp.248–56.

Teshima, K. & Kondo, T., 2005. Analytical method for ubiquinone-9 and ubiquinone-10 in rat tissues by liquid chromatography/turbo ion spray tandem mass spectrometry with 1-alkylamine as an additive to the mobile phase. *Analytical biochemistry*, 338(1), pp.12–9.

Thannickal, V.J. & Fanburg, B.L., 2000. Reactive oxygen species in cell signaling. *American journal of physiology. Lung cellular and molecular physiology*, 279(6), pp.L1005–28.

Thomas, S.R., Witting, P.K. & Stocker, R., 1999. A role for reduced coenzyme Q in atherosclerosis? *BioFactors (Oxford, England)*, 9(2-4), pp.207–24.

Tisdale, H., 1961. Preparation and properties of succinic-cytochrome c reductase (complex II-III). *Methods in Enzymology*, 10, pp.213–5.

Tran & Clarke, 2007. Endogenous synthesis of coenzyme Q in eukaryotes. *Mitochondrion*, 7, pp.S62–S71.

Tran, U.C., Marbois, B., Gin, P., Gulmezian, M., Jonassen, T. & Clarke, C.F., 2006. Complementation of Saccharomyces cerevisiae coq7 mutants by mitochondrial targeting of the Escherichia coli UbiF polypeptide: two functions of yeast Coq7 polypeptide in coenzyme Q biosynthesis. *The Journal of biological chemistry*, 281(24), pp.16401–9.

Turrens, Alexandre & Lehninger, 1985. Ubisemiquinone Is the Electron Donor for Superoxide by Complex III of Heart Mitochondria ' Formation. *Archives of Biochemistry and Biophysics*, 237(2), pp.408–414.

Turrens, J.F. & Boveris, A., 1980. Generation of superoxide anion by the NADH dehydrogenase of bovine heart mitochondria. *The Biochemical journal*, 191(2), pp.421–7.

Turunen, M., Olsson, J. & Dallner, G., 2004. Metabolism and function of coenzyme Q. *Biochimica et Biophysica Acta (BBA) - Biomembranes*, 1660(1-2), pp.171–199.

Tzagoloff, A. & Wharton, D.C., 1965. Studies on the electron transfer system-The reaction of cytochrome oxidase with carbon monoxide. *The Journal of biological chemistry*, 240(6), pp.2628–33.

Ullrich, O., Reinheckel, T., Sitte, N., Hass, R., Grune, T. & Davies, K.J., 1999. Poly-ADP ribose polymerase activates nuclear proteasome to degrade

oxidatively damaged histones. *Proceedings of the National Academy of Sciences of the United States of America*, 96(11), pp.6223–8.

Villalba, J.M. & Navas, P., 2000. Plasma Membrane Redox System in the Control of Apoptosis. *Antioxidants and redox signalling*, 2(2), pp.213–230.

Wallace, D.C., 2000. Mitochondrial defects in cardiomyopathy and neuromuscular disease. *American heart journal*, 139(2 Pt 3), pp.S70–85.

Walter, L., Miyoshi, H., Leverve, X., Bernardi, P. & Fontaine, E., 2002. Regulation of the Mitochondrial Permeability Transition Pore by Ubiquinone Analogs. A Progress Report. *Free Radical Research*, 36(4), pp.405–412.

Walter, L., Nogueira, V., Leverve, X., Heitz, M.P., Bernardi, P. & Fontaine, E., 2000. Three classes of ubiquinone analogs regulate the mitochondrial permeability transition pore through a common site. *The Journal of biological chemistry*, 275(38), pp.29521–7.

Wang, H. & Oster, G., 1998. Energy transduction in the F1 motor of ATP synthase. *Nature*, 396(6708), pp.279–82.

Ward, M.W., Rego, A.C., Frenguelli, B.G. & Nicholls, D.G., 2000. Mitochondrial membrane potential and glutamate excitotoxicity in cultured cerebellar granule cells. *The Journal of neuroscience*, 20(19), pp.7208–19.

Warner, G.J., Berry, M.J., Moustafa, M.E., Carlson, B. a, Hatfield, D.L. & Faust, J.R., 2000. Inhibition of selenoprotein synthesis by selenocysteine tRNA[Ser]Sec lacking isopentenyladenosine. *The Journal of biological chemistry*, 275(36), pp.28110–9.

Watmough, N.J. & Frerman, F.E., 2010. The electron transfer flavoprotein: ubiquinone oxidoreductases. *Biochimica et biophysica acta*, 1797(12), pp.1910–6.

Wen, Y., Li, W., Poteet, E.C., Xie, L., Tan, C., Yan, L.-J., Ju, X., Liu, R., Qian, H., Marvin, M. a, Goldberg, M.S., She, H., Mao, Z., Simpkins, J.W. & Yang, S.-H., 2011. Alternative mitochondrial electron transfer as a novel strategy

for neuroprotection. *The Journal of biological chemistry*, 286(18), pp.16504–15.

Wikstrom, 1977. Proton pump coupled to cytochrome c oxidase in mitochondria. *Nature*, 266, pp.271–3.

Wittig, I., Braun, H. & Schägger, H., 2006. Blue native PAGE. *Nature protocols*, 1(1), pp.418–28.

Wittig, I., Carrozzo, R., Santorelli, F.M. & Schägger, H., 2007. Functional assays in high-resolution clear native gels to quantify mitochondrial complexes in human biopsies and cell lines. *Electrophoresis*, 28(21), pp.3811–20.

Witting, P., Pettersson, K., Letters, J. & Stocker, R., 2000. Anti-atherogenic effect of coenzyme Q10 in apolipoprotein E gene knockout mice. *Science*, 29, pp.295–305.

Wolf, D.E., Hoffman, C.H., Trenner, N.R., Arison, B.H., Shunk, C.H., Linn, B.O., McPherson, J.F. & Folkers, K., 1958. Coenzyme Q. I. Structure Studies on the Coenzyme Q Group. *Journal of the American Chemical Society*, 80, p.4752.

Wood, R.D., 1996. DNA repair in eukaryotes. *Annual review of biochemistry*, 65, pp.135–67.

Wood, Z.A., Poole, L.B. & Karplus, A.P., 2003. Peroxiredoxin evolution and the regulation of hydrogen peroxide signaling. *Science*, 300(5619), pp.650–3.

Yankovskaya, V., Horsefield, R., Tornroth, S., Luna-Chevez, C. & Miyoshi, H., 2003. Architecture of Succinate Dehydrogenase and Reactive Oxygen Species. *Science*, 299, pp.700–704.

Yao, Z., Gandhi, S., Burchell, V.S., Plun-Favreau, H., Wood, N.W. & Abramov, A.Y., 2012. Cell metabolism affects selective vulnerability in PINK1-associated Parkinson's disease. *Journal of cell science*, 124, pp.4194–4202.

Zhang Y, Marcillat O, Giulivi C, Ernster L, D.K., 1990. The oxidative inactivation of mitochondrial electron transport chain components and ATPase. *Journal of Biological Chemistry*, 265(27), pp.16330–6.

Zhang, Y., Turunen, M. & Appelkvist, E.-L., 1996. Restricted Uptake of Dietary Coenzyme Q Is in Contrast to the unrestricted uptake of a-Tocopherol into Rat Organs and Cells. *The journal of nutrition*, (February), pp.2089–2097.

Zhu, H., Cao, Z., Zhang, L., Trush, M. a & Li, Y., 2007. Glutathione and glutathione-linked enzymes in normal human aortic smooth muscle cells: chemical inducibility and protection against reactive oxygen and nitrogen species-induced injury. *Molecular and cellular biochemistry*, 301(1-2), pp.47–59.

Zhu, H., Itoh, K., Yamamoto, M., Zweier, J.L. & Li, Y., 2005. Role of Nrf2 signaling in regulation of antioxidants and phase 2 enzymes in cardiac fibroblasts: protection against reactive oxygen and nitrogen species-induced cell injury. *FEBS letters*, 579(14), pp.3029–36.

Zierz, S., Jahns, G. & Jerusalem, F., 1989. Coenzyme Q in serum and muscle of 5 patients with Kearns-Sayre syndrome and 12 patients with ophthalmoplegia plus. *Journal of neurology*, 236(2), pp.97–101.